

Award Number: DAMD17-01-1-0129

TITLE: New Approaches for Early Detection of Breast Tumor  
Invasion or Progression

PRINCIPAL INVESTIGATOR: Yan-Gao Man, M.D., Ph.D.

CONTRACTING ORGANIZATION: American Registry of Pathology  
Washington, DC 20306

REPORT DATE: August 2004

TYPE OF REPORT: Annual Summary

PREPARED FOR: U.S. Army Medical Research and Materiel Command  
Fort Detrick, Maryland 21702-5012

DISTRIBUTION STATEMENT: Approved for Public Release;  
Distribution Unlimited

The views, opinions and/or findings contained in this report are those of the author(s) and should not be construed as an official Department of the Army position, policy or decision unless so designated by other documentation.

**BEST AVAILABLE COPY**

20050715 036

**REPORT DOCUMENTATION PAGE**Form Approved  
OMB No. 074-0188

Public reporting burden for this collection of information is estimated to average 1 hour per response, including the time for reviewing instructions, searching existing data sources, gathering and maintaining the data needed, and completing and reviewing this collection of information. Send comments regarding this burden estimate or any other aspect of this collection of information, including suggestions for reducing this burden to Washington Headquarters Services, Directorate for Information Operations and Reports, 1215 Jefferson Davis Highway, Suite 1204, Arlington, VA 22202-4302, and to the Office of Management and Budget, Paperwork Reduction Project (0704-0188), Washington, DC 20503

<b>1. AGENCY USE ONLY</b> (Leave blank)		<b>2. REPORT DATE</b> August 2004	<b>3. REPORT TYPE AND DATES COVERED</b> Annual Summary (23 Jul 2003 - 22 Jul 2004)	
<b>4. TITLE AND SUBTITLE</b> New Approaches for Early Detection of Breast Tumor Invasion or Progression			<b>5. FUNDING NUMBERS</b> DAMD17-01-1-0129	
<b>6. AUTHOR(S)</b> Yan-Gao Man, M.D., Ph.D.				
<b>7. PERFORMING ORGANIZATION NAME(S) AND ADDRESS(ES)</b> American Registry of Pathology Washington, DC 20306  <i>E-Mail:</i> man@afip.osd.mil			<b>8. PERFORMING ORGANIZATION REPORT NUMBER</b>	
<b>9. SPONSORING / MONITORING AGENCY NAME(S) AND ADDRESS(ES)</b> U.S. Army Medical Research and Materiel Command Fort Detrick, Maryland 21702-5012			<b>10. SPONSORING / MONITORING AGENCY REPORT NUMBER</b>	
<b>11. SUPPLEMENTARY NOTES</b> Original contains color plates: All DTIC reproductions will be in black and white.				
<b>12a. DISTRIBUTION / AVAILABILITY STATEMENT</b> Approved for Public Release; Distribution Unlimited			<b>12b. DISTRIBUTION CODE</b>	
<b>13. ABSTRACT (Maximum 200 Words)</b> The epithelium of normal and non-invasive human breast tumor tissues is physically separated from the stroma by the basement membrane and a layer of myoepithelial (ME) cells, whose degradation is a pre-requisite for tumor invasion. Our previous studies revealed that a subset of estrogen receptor (ER) positive in situ breast tumors contained focally disrupted ME cell layers, which were overlaid exclusively or preferentially by ER negative cell clusters. Our current studies further show that, compared to adjacent ER positive cells within the same duct, these cell clusters have several unique features: [1] a significantly higher proliferation rate; [2] a substantially different frequency and pattern of genetic alterations; [3] a significantly higher expression level and frequency of tumor progression and invasion related genes. Together, our findings suggest that these cell clusters may represent the direct precursor of invasive lesions, and the development of specific antibodies or chemical agents to target these cells might provide a more sensitive and less toxic approach to treat and prevent breast tumor invasion.				
<b>14. SUBJECT TERMS</b> Early detection of breast tumor invasion; estrogen receptor expression; myoepithelial cell layer disruptions;			<b>15. NUMBER OF PAGES</b> 203	
			<b>16. PRICE CODE</b>	
<b>17. SECURITY CLASSIFICATION OF REPORT</b> Unclassified	<b>18. SECURITY CLASSIFICATION OF THIS PAGE</b> Unclassified	<b>19. SECURITY CLASSIFICATION OF ABSTRACT</b> Unclassified	<b>20. LIMITATION OF ABSTRACT</b> Unlimited	

## Table of Contents

Cover.....	
SF 298.....	
Table of Contents.....	1
Introduction.....	2
Body.....	2
Key Research Accomplishments.....	3
Reportable Outcomes.....	3
Conclusions.....	4
References.....	4
Appendices.....	7

## **Introduction**

To assess interactions between epithelial (EP) and myoepithelial (ME) cells in association with breast tumor progression and invasion, a double immunostaining technique with antibodies to smooth muscle actin (SMA) and estrogen receptor (ER) was used to elucidate both the ME and EP cells in mammary tissues harboring ductal carcinoma in situ. Single or clusters of EP cells with a marked diminution or a total loss of ER expression were found immediately overlying focally disrupted ME cell layers, in contrast to the dominant population of ER (+) cells within the same duct that showed no associated ME cell layer disruptions. This study attempted to confirm our previous findings on a larger number of cases, and to compare the immunohistochemical and molecular biological profiles of the ER (-) cells overlying disrupted ME cell layers with those of adjacent ER (+) cells and surrounding stromal (ST) cells. Since ME cell layers are physical barriers protecting the microenvironment and integrity of EP cells, and the disruption of ME cell layers is an absolute pre-requisite for breast tumor invasion, the outcomes of this project could have significant values in early detection of breast tumor progression and/or invasion.

## **Body**

### **Statement of work**

A total of 7 tasks were listed in the Statement of Work of the original proposal:

Task 1. To repeat our previous studies and to identify epithelial (EP) cells overlying disrupted myoepithelial (ME) cell layers (months 1-6)

**Completed**

Task 2. To compare the biological behavior of cells overlying a disrupted ME cell layer with that of adjacent cells within the same duct (months 6-9)

**Completed**

Task 3. To microdissect phenotypically different EP cells and the surrounding ME and stromal (ST) cells for molecular biological analyses (months 9-12)

Task 4. To compare the frequency and pattern of loss of heterozygosity (LOH), and clonality among EP, ME, and ST cells (months 12-20)

**Completed**

Task 5. To assess the gene expression pattern in cells from frozen section sections with cDNA expression array technique, and to generate probes based on sequences exclusively or mainly expressed in cells overlying disrupted ME cell layers (months 20-24)

**Completed**

Task 6. To apply the probes to both paraffin and frozen sections, to identify the gene expressing cells and their morphologic features (months 24-32)

**Partially completed**

Task 7. To correlate the laboratory findings with that of clinical following-up data (months 32-36).

**Partially completed**



### **Experimental procedures:**

Consecutive sections were made from formalin-fixed, paraffin-embedded breast tissues from over 400 patients with various grades of ductal carcinoma in situ (DCIS), and double immunostained for ER and SMA. Cross sections of all ducts lined by  $\geq 40$  EP cells were examined for a focal ME cell layer disruption, defined as an absence of ME cells, resulting in a gap equal to or greater than the combined size of 3 EP or ME cells. A focal loss of ER expression was defined as marked diminution or a total loss of ER staining in cells immediately overlying a disrupted ME cell layer, in contrast to strong ER expression in adjacent cells within the same duct.

After immunostaining for ER and SMA, cells overlying disrupted ME cell layers, adjacent ER (+) cells within the same duct, adjacent stromal (ST) cells, and other controls were microdissected for DNA extraction and assessment for loss of heterozygosity (LOH) and microsatellite instability (MI), using PCR amplification with a panel of DNA markers at 6 chromosomes. The frequency and pattern of LOH and MI among samples were compared.

Consecutive sections were also prepared from frozen breast tissues of patients with DCIS and invasive ductal carcinomas (IDC), and were double immunostained for ER and SMA. Immunostained sections were examined for ER expression and focal ME cell layer disruptions. ER (-) cells overlying disrupted ME layers and adjacent (+) cells within the same duct in DCIS, along with morphologically and immunohistochemically similar cells in IDC, were microdissected for RNA extraction, using the RNA extraction kits from Arcturus Engineering, Inc (Mountain View, CA). The RNA extracts were subjected to RT PCR amplification. The gene expression profiles among samples were compared, using the software and reagents from Affymetrix, Inc (Santa Clara, CA) and SuperArray Bioscience Corporation (Frederick, MD).

A total of 7 biotin-labeled probes and detection kits from our collaborators, DAKO Corporation (Carpinteria, CA), and Sigma (St. Louis, MO) have been using in both paraffin-embedded and frozen sections from selected cases, to establish and optimize the in situ hybridization method that will be used with the new probes generated by our own study.

All above experimental procedures were carried out according to the methods described in the proposal without any major modifications. Also, all the laboratory efforts have been strictly adhered to address the issues listed in "Statement of Work".

### **Key research accomplishments**

All the laboratory procedures for Tasks 1 to 5 had been completed, and the outcomes have been reported and published (see below).

The laboratory protocols for Task 6 have been established and optimized. Preliminary studies in selected cases had been carried out before April 15, 2003, and the main experiments are in progress.

The clinical follow-up data for Task 7 for a portion of the selected cases have been collected, and the summarization of the data are in progress.

A total of 32 published, accepted, and submitted research articles were generated during 2003 and 2004 (see below).

### **Reportable outcomes**

During the year 2003 to 2004, a total of 31 research articles and a picture related to the project have been published, accepted, and submitted to national or international journals indexed by the National Library of Medicine (see the table below).

Category	Published	Accepted	Submitted	Total
Research papers	5	3	7	15
Research articles	16			16
Other	A picture for the cover of a Medline indexed journal			1
Total				32

## **Conclusions**

1. Tasks 1-5 listed in the proposal have been completed. The outcomes are in a total agreement with our hypotheses.
2. Tasks 6 and 7 have been partially completed. The preliminary results are also consistent with our hypotheses.
3. A total of 32 published, accepted, and submitted research articles were generated during 2003-2004.

## **References** (Published, accepted, and submitted papers and abstracts during 2003 to 2004)

1. Garayoa M, **Man YG**, Marinez A, Cuttitta F, Venzon DJ, Mulshine JL Down regulation of hRNP A2/B1 expression in tumor cells under prolonged hypoxia. Am J respir Cell Mol Biol 28: 80-85, 2003
2. Zhang R, **Man YG**, Vang RS, Saenger JS, Barner R, Wheeler D, Liang CY, Vinh TN, Bratthauer GL. A subset of morphologically distinct mammary myoepithelial cells lacks corresponding immunophenotypic markers. Breast Cancer Res 5: R151-156, 2003
3. **Man YG**, Tai L, Barner R, Vang R, Saenger JS, Shekitka KM, Bratthauer GL, Wheeler DT, Liang CL, Vinh TN, Strauss BL. Cell clusters overlying focally disrupted mammary myoepithelial cell layers and adjacent cells within the same duct display different immunohistochemical and genetic features: implications for tumor progression and invasion. Breast Cancer Res 5: R231-241, 2003
4. **Man YG**, Burgar A. An antigen unmasking protocol that satisfies both immunohistochemical and subsequent molecular biological assessments. Pathology-Research & Practice 199:815-825, 2003
5. Zhao YG, Xiao AZ, Park HI, Newcomer RG, Yan M, **Man YG**, Heffelfinger SC, Sang QX. Endometase in human breast carcinoma, selective activation of progelatinase B and inhibition by tissue inhibitors of metalloproteinases-2 and -4. Cancer Res 64: 590-598, 2004
6. **Man YG**, Zhang H, Vang R, Strauss B, Zhang L, Gao CL. Direct and repeat uses of tissue sections as templates for liquid phase pcr amplification: applications and implications. Applied Immunohistochemistry and Molecular morphology (AIMM), In press
7. **Man YG**, Magrane GG, Lininger RA, Shen T, Kuhls E, Bratthauer BL. Morphologically similar epithelial and stromal cells in primary bilateral breast tumors display different genetic profiles: implications for treatment. AIMM, In press
8. Yousefi M, Mattu R, Gao C, **Man YG**. Mammary ducts with and without focal myoepithelial cell layer disruptions show a different frequency of white blood cell infiltration and growth pattern: Implications for tumor progression and invasion. AIMM, In press

9. **Man YG**, Zhang Y, Shen T, Vinh TN, Zeng X, Tauler J, Mulshine JL, Strauss BL. cDNA expression profiling identifies elevated expressions of tumor progression and invasion related genes in cell clusters of in situ breast tumors. Breast Cancer Res Treat, In press
10. **Man YG**, Shen T, Zhao YG, Sang QX. Focal prostate basal cell layer disruptions and leukocyte infiltration are correlated events: A potential mechanism for basal cell layer disruptions and tumor invasion. Cancer Detect Prevent, Accepted with revision.
11. **Man YG**, Sang QXA. The significance of focal myoepithelial cell layer disruptions in breast tumor invasion: Implications from MMPI trials and our recent studies. Exp Cell Res, Accepted with revision.
12. Moinfar F, Kremser KL, **Man YG**, Lax K, Zatloukal K, Tavassoli FA, Denk H. Allelic imbalances in endometrial stromal neoplasms: A model for genetic alterations in tumor and microenvironmental tissues. Cancer Res. Pending acceptance (under revision)
13. **Man YG**, Fu SW, Pinzone JJ, Schwartz AM, Simmens SJ, Berg PE. Expression of BP1, a homobox gene, correlates with progression and invasion of mammary ductal Carcinoma. Submitted (under revision)
14. **Man YG**, Shen T, Sang QXA, Berg PE, Schwartz AM. Cell clusters in a subset of *in situ* breast tumors show an unusual growth pattern: Implications for invasion and metastasis. Submitted (under revision)
15. Weisz J, Shearer DA, Fraumeni JF, **Man YG**, McCaffery. Divergent effect of progression of breast cancer from the in situ to the invasive stage on the expression of the retinoic acid biosynthetic enzyme retinaldehyde dehydrogenase 2 (RALDH2): Implications for chemoprevention and treatment of breast cancer. Submitted (under revision)
16. **Man YG**, Saenger JS, Vang RS, Barner R, Wheeler D, Martinez A, Mulshine JL. Identification of invasive precursor cells in normal and hyperplastic breast tissue. Proceedings of the American Association for Cancer Research. Cancer Res, volume 44: 68, 357, 2003
17. **Man YG**, Vang RS, Saenger JS, Strauss BL, Barner R, Wheeler DT, Liang CY, Bratthauer GL, Mannion C. Development and progression of mammary ductal tumors appear to be mediated by surrounding myoepithelial cells. Mod Pathol 16(1): 39A-40A, 2003
18. Zhang R, **Man YG**, Strauss BL, Vang RS, Saenger JS, Barner R, Wheeler D, Liang CY. A subset of morphologically identifiable mammary myoepithelial cells lacks expression of corresponding phenotypic markers. Mod Pathol 16(1): 52A, 2003
19. **Man YG**, Mattu R, Zhang R, Yousefi M, Sang QXA, Shen T. A subset of normal and hyperplastic appearing mammary ductal cells display invasive features. Breast Cancer Res Treat 82 (supplement 1): S141, 2003
20. **Man YG**, Zhang R, Mattu R, Shen T, Sang QXA. A subset of mammary epithelial cells overlying focally disrupted myoepithelial cell layers shows an unusual immunostaining pattern for proliferation-related proteins. Breast Cancer Res Treat 82 (supplement 1): S163-164, 2003
21. Zhao YG, Xiao AZ, Park HI, Newcomer RG, Yan M, **Man YG**, Heffelfinger SC, Sang QXA. Endometase in human breast carcinomas, selective activation of progelatinase B and inhibition by tissue inhibitors of metalloproteinases-2 and -4. Breast Cancer Res Treat 82 (supplement 1): S64, 2003
22. Berg P, Fu SW, Pinzone JJ, **Man YG**. BP1 expression correlates with breast tumor aggressiveness. Platform presentation at the 26<sup>th</sup> San Antonio Breast Cancer Symposium (SABCS) at The Late Breaking News Section and published in the

SABCS' Website, 2003.

23. **Man YG**, Zeng X, Shen T, Vang R, Barner R, Wheeler DT, Vihn T, Liang CY, Strauss BL. Cell clusters overlying focally disrupted myoepithelial cell layers and their adjacent counterparts within the same duct display a different pattern of mRNA expression. *Mod Pathol* 17 (supplement1): 40-41a, 2004.
24. **Man YG**, Barner R, Vang R, Wheeler DT, Liang CY, Vihn T, Bratthauer GL, Strauss BL. Non-smooth muscle restricted proteins exclusively or preferentially expressed in mammary myoepithelial cells: a programmed or induced phenomenon? *Mod Pathol* 17 (supplement 1): 40a, 2004
25. Moinfar F, Kremser KL, **Man YG**, Lax K, Zatloukal K, Tavassoli FA, Denk H. Allelic imbalances in endometrial stromal neoplasms: A model for genetic alterations in tumor and microenviromental tissues. *Mod Pathol* 17 (supplement 1): 208a, 2004
26. **Man YG**, Shen T, Zhao YG, Sang QX. Focal prostate basal cell layer disruptions and leukocyte infiltration are correlated events: Implications for basal call layer degradation and tumor invasion. *Cancer Detection & Prevention, 2004 Symposium Issue S-51*: 15, 2004
27. **Man YG**, Strauss BL, Berg PE. Increasing BP1 expression correlates with progression and invasion of male breast and prostate tumors. *Cancer Detection & Prevention, 2004 Symposium Issue S-95*: 149, 2004
28. **Man YG**, Berg PE, Barner R, Vinh TN, Wheeler DT, Liang CY, Strauss BL. Morphologically similar normal and hyperplastic mammary ductal cells associated with and without malignant lesions have a different immunohistochemical profile. *Cancer Detection & Prevention, 2004 Symposium Issue S-137*: 282, 2004
29. Berg P, Fu SW, Pinzone JJ, **Man YG**. The Expression of BP1, a homeotic protein, increases with breast tumor progression. *Cancer Res*, in press (abstract)
30. **Man YG**, Yousefi M, Wheeler DT, Barner R, Vang R, Vinh T, Liang CY, Bratthauer GL, Strauss BL. Focal myoepithelial cell layer disruptions and white blood cell infiltration are related events: implications for breast tumor progression and invasion. *Cancer Res*, in press (abstract).
31. **Man YG**, Shen T, Zhao YG, Sang QX. Morphologically comparable prostate acini and ducts with and without a focal basal cell layer disruption have a different cell proliferation rate: Implications for tumor invasion. *FASEB* 18(5): A1193, 2004
32. **Man YG**, Bugar A. Triple immunohistochemical detection of Ki-67, ESA, and SMA in breast carcinoma. The cover-page for the entire 2004 issues. *Pathology-Research & Practice*, 200(2004).

## Research article

## Open Access

# Cell clusters overlying focally disrupted mammary myoepithelial cell layers and adjacent cells within the same duct display different immunohistochemical and genetic features: implications for tumor progression and invasion

Yan-gao Man, Lisa Tai, Ross Barner, Russell Vang, Jeffrey S Saenger, Kris M Shekitka, Gary L Brattbauer, Darren T Wheeler, Chang Y Liang, Tuyethoa N Vinh and Brian L Strauss

Department of Gynecologic and Breast Pathology, Armed Forces Institute of Pathology and American Registry of Pathology, Washington, DC, USA

Correspondence: Yan-gao Man (e-mail: [man@afip.osd.mil](mailto:man@afip.osd.mil))

Received: 11 Jul 2003 Revisions requested: 15 Aug 2003 Revisions received: 19 Aug 2003 Accepted: 28 Aug 2003 Published: 3 Oct 2003

*Breast Cancer Res* 2003, 5:R231-R241 (DOI 10.1186/bcr653)

© 2003 Man *et al.*, licensee BioMed Central Ltd (Print ISSN 1465-5411; Online ISSN 1465-542X). This is an Open Access article: verbatim copying and redistribution of this article are permitted in all media for any purpose, provided this notice is preserved along with the article's original URL.

## Abstract

**Introduction** Our previous studies detected focal disruptions in myoepithelial cell layers of several ducts with carcinoma *in situ*. The cell cluster overlying each of the myoepithelial disruptions showed a marked reduction in or a total loss of immunoreactivity for the estrogen receptor (ER). This is in contrast to the adjacent cells within the same duct, which were strongly immunoreactive for the ER. The current study attempts to confirm and expand previous observations on a larger scale.

**Methods** Paraffin sections from 220 patients with ER-positive intraductal breast tumors were double immunostained with the same protocol previously used. Cross-sections of ducts lined by  $\geq 40$  epithelial cells were examined for myoepithelial cell layer disruptions and for ER expression. In five selected cases, ER-negative cells overlying the disrupted myoepithelial cell layer and adjacent ER-positive cells within the same duct were separately microdissected and assessed for loss of heterozygosity and microsatellite instability.

**Results** Of the 220 cases with 5698 duct cross-sections examined, 94 showed disrupted myoepithelial cell layers with 405 focal disruptions. Of the 94 cases, 79 (84%) contained only ER-negative cell clusters, nine (9.6%) contained both ER-negative and ER-positive cell clusters, and six (6.4%) contained only ER-positive cell clusters overlying disrupted myoepithelial cell layers. Of the 405 disruptions, 350 (86.4%) were overlain by ER-negative cell clusters and 55 (13.6%) were overlain by ER-positive cell clusters ( $P < 0.01$ ). Microdissected ER-negative and ER-positive cells within the same duct from all five selected cases displayed a different frequency or pattern of loss of heterozygosity and/or microsatellite instability at 10 of the 15 DNA markers.

**Conclusions** Cells overlying focally disrupted myoepithelial layers and their adjacent counterparts within the same duct displayed different immunohistochemical and molecular features. These features potentially represent an early sign of the formation of a biologically more aggressive cell clone and the myoepithelial cell layer breakdown possibly associated with tumor progression or invasion.

**Keywords:** ductal carcinoma *in situ*, estrogen receptor, focal myoepithelial cell layer disruptions, tumor invasion, tumor progression

## Introduction

The epithelial component of normal and noninvasive breast tumor tissue is physically separated from the stroma by both the myoepithelial cells and the basement membrane (BM). Myoepithelial cells are joined by interme-

diate or gap junctions and a number of intercellular adhesion molecules, forming a continuous sheet or belt that encircles the epithelial cells (except at the terminal ductal-lobular unit, within which about 20% of the epithelial cells are reported to be in direct contact with the BM)

BM = basement membrane; DCIS = ductal carcinoma *in situ*; ER = estrogen receptor; H & E = hematoxylin and eosin; LOH = loss of heterozygosity; MI = microsatellite instability; PCR = polymerase chain reaction; SMA = smooth muscle actin.

[1–3]. The BM is composed of a group of fibrous proteins embedded in a hydrated polysaccharide gel, constituting a continuous lining surrounding and attaching to myoepithelial cells via hemidesmosomes and focal adhesion complexes [3–5]. Both the myoepithelial cell layer and the BM layer are permanent structural constituents, normally allowing only the passage of small molecules [1–5]. Due to this structural feature, most tumor epithelial cells have to first pass through the myoepithelial cell layer and then the BM in order to physically contact the stroma. In other words, the disruption of both the BM and the myoepithelial cell layer is an absolute prerequisite for breast tumor invasion.

Invasive and metastasized tumors, compared with *in situ* tumors, have a significantly higher mortality rate, accounting for a vast majority of breast cancer death [6]. This highlights the significance and the implications for the elucidation of the tumor invasion mechanism(s), which could potentially lead to vast benefits and advances in the field of breast cancer treatment and prevention. It has been generally accepted that an upregulated expression of proteolytic enzymes in tumor or stromal cells is the primary, if not the only, cause for BM disruptions and tumor invasion [6,7]. This theory, however, might not reflect the intrinsic mechanism(s) of myoepithelial layer disruptions for three main reasons. First, neither the normal cellular kinetics nor dynamic alterations of myoepithelial cells during tumor invasion have been well elucidated. Also, no conclusive evidence has shown that the host's own enzymes are capable of degrading its own myoepithelial cells. Finally, the results of proteolytic inhibitor-based human clinical trials for breast cancer treatment and prevention have been very disappointing [8].

While attempting to identify the early sign of myoepithelial disruptions and the precursor of invasion, we have carried out a number of studies focusing on the physical and functional correlation between epithelial and surrounding myoepithelial cells. In one of our previous studies, a double immunostaining method with antibodies to smooth muscle actin (SMA) and to the estrogen receptor (ER) was used to elucidate both epithelial cells and myoepithelial cells [9]. Several focal myoepithelial cell layer disruptions, defined as a total loss of SMA immunoreactivity and an absence of myoepithelial cells, resulting in a gap that is equal to or greater than the combined size of at least three epithelial or myoepithelial cells, were detected in several ducts that were classified as ductal carcinoma *in situ* (DCIS) based on examination on H&E stained slides. Each of the disruptions was exclusively overlain by a cluster of cells that showed either a complete loss of or a marked reduction of ER expression, in contrast to the adjacent nondisrupted myoepithelial cell layer within the same duct, which was overlain by cells with strong ER expression [9]. Those ER-negative cell clusters and focal myoepithelial disruptions, however, were generally small

and not easily identifiable on H&E stained sections [9]. Our subsequent studies further revealed that ducts with a disrupted myoepithelial cell layer had a significantly higher proliferation rate than ducts with an intact myoepithelial layer [10,11].

It has been documented that the disruption of the BM and myoepithelial cell layers is an absolute prerequisite for tumor invasion, that tumor epithelial cells and their surrounding stromal cells share a similar genetic profile [12,13], and that the progression of breast tumors is paralleled by a progressive hormonal independence [14–17]. Our findings therefore appear to have several clinical implications. First, those ER-negative cell clusters overlying the disrupted myoepithelial cell layer may represent a newly formed cell clone that is biologically more aggressive than the adjacent ER-positive cells within the same duct. Second, focal myoepithelial cell layer disruption might represent an initial or early sign of the BM and myoepithelial cell layer breakdown. Third, focal disruptions in the myoepithelial cell layer and the loss of ER expression in overlying cells might be correlated events, directly triggering or signifying tumor progression or potential invasion in some cases.

Based on these speculations, the present study attempted to confirm our previous observations in a larger number of cases, to determine whether focal disruptions of myoepithelial cell layers is a prevalent event, and whether all the cell clusters overlying focally disrupted myoepithelial cell layers have the same morphological and immunostaining feature. Also, we attempted to carry out a preliminary molecular study to compare the frequency and pattern of loss of heterozygosity (LOH) and microsatellite instability (MI) between ER-negative cells and the adjacent ER-positive cells within the same duct in selected cases.

## Materials and methods

Formalin-fixed, paraffin-embedded breast tissue blocks harboring various grades and subtypes of ER-positive, noninvasive breast lesions from 220 female patients were retrieved from the files of The Armed Forces Institute of Pathology. Serial sections of 5–7  $\mu$ m thickness were cut and placed on positively charged microscopic slides for immunohistochemical and morphologic assessment. Morphologic classifications were based on our published criteria [9]. Double immunohistochemical staining with antibodies to the ER (clone 6F11) and to SMA (clone asm-1) (Vector Laboratories, Burlingame, CA, USA) was carried out as previously described [9,18,19]. A micro-meter was inserted into the objective of a microscope to facilitate the reviewing of the whole section and the localization of a specific lesion [20].

Cross-sections of ducts lined by  $\geq 40$  epithelial cells were examined under a microscope for myoepithelial cell layer disruptions and for ER expression. A focal myoepithelial

layer disruption was defined as a total loss of SMA immunoreactivity and an absence of myoepithelial cells, resulting in a gap that is equal to or greater than the combined size of at least three epithelial or myoepithelial cells, or multiple such gaps in a given duct. A focal loss of ER expression was defined as a total loss or a marked reduction of ER immunostaining in cells overlying disrupted myoepithelial cell layers, compared with a strong ER immunostaining in their adjacent counterparts within the same duct overlying the nondisrupted myoepithelial cell layer. A focal positive ER expression was defined as the ER immunostaining in cells overlying focally disrupted myoepithelial cell layers being more intense than or comparable to that in their adjacent counterparts overlying the nondisrupted myoepithelial cell layer.

The profiles of ducts containing disrupted myoepithelial cell layers were photographed and reprints were made at a magnification of 400 $\times$ –800 $\times$  for immunohistochemical and morphological evaluation. The frequencies of myoepithelial cell layer disruptions associated with ER-negative and ER-positive cell clusters were statistically compared by the Student *t* test.

The adjacent sections from 20 cases with focal myoepithelial disruptions were immunostained with monoclonal antibodies to cytokeratins AE1/AE3 (clones AE1/AE3; Chemicon, Temecula, CA, USA), to cytokeratin 8 (clone TS1; Vector Laboratories), and to cytokeratin 19 (clone b170; Vector Laboratories) in order to assess whether cells overlying disrupted myoepithelial cell layers are epithelial in nature [21]. Also, the sections in selected cases were immunostained with antibodies to major constituents of the BM-collagen IV (clone CIV 22; Dako Corporation, Carpinteria, CA, USA) and laminin (code number Z0097; Dako Corporation; and clone Lam-89; Vector Laboratories) to assess the integrity of the BM underneath the disrupted myoepithelial cell layers.

For molecular analyses, paired ER-negative cells and adjacent ER-positive cells within the same duct, along with clear-cut normal epithelial or stromal cells, were microdissected from each of five selected cases, including one mild ductal hyperplasia and four DCIS or atypical intraductal hyperplasia. To obtain a sufficient number of cells, multiple consecutive sections were immunostained, and ER-negative cell clusters in different sections were microdissected and pooled. Microdissected cells were subjected to DNA extraction and assessed for LOH and for MI with 15 fluorescent-labeled DNA markers (Research Genetics, Huntsville, AL, USA) as previously described [22]. The DNA markers used and their main features are presented in Table 1. Amplified PCR products were subjected to electrophoresis, detection, and comparison with an automated 377 DNA sequencer (Perkin-Elmer, Foster City, CA, USA) as previously described [23,24].

**Table 1**

**DNA markers used for comparison of genetic alterations in estrogen receptor-negative cells and estrogen receptor-positive cells**

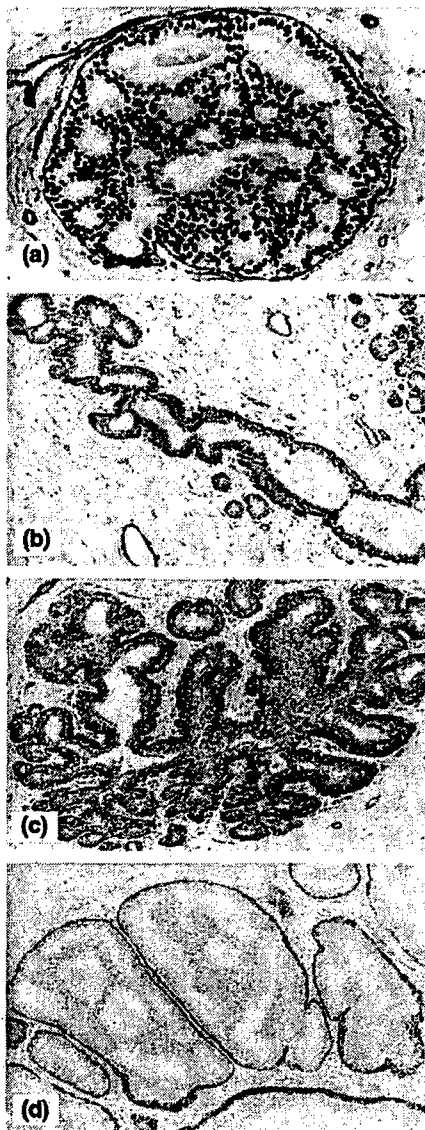
Marker	Name	Chromosomal location	Harbored gene	Size (base pairs)
1	D3S1300	3p21.1–p14.2	FHIT	217–241
2	D3S1481	3p14.2	FHIT	104
3	D3S1581	3p21.2–p14.2	FHIT	78–102
4	D11S902	11p15–p13	?	145–163
5	D11S904	11p14–p13	Wilms' tumor 1	185–201
6	D11S907	11p13	Wilms' tumor 1	163–173
7	D11S914	11p13–p12	Wilms' tumor 1	275–285
8	D13S119	13q14.3–q22	?	124–140
9	D13S173	13q32–q34	?	166–178
10	D13S219	13q12.3–q13	?	117–127
11	D13S263	13q14.1–q14.2	?	145–165
12	D16S518	16q23.1–q24.2	CDH 1 (adjacent to it)	272–290
13	D16S402	16q24.2	CDH 1 (adjacent to it)	161–187
14	D17S791	17q	BRCA 1	165–199
15	TP53	17p13	P53	104

FHIT, fragile histidine triad.

## Results

Of the 220 cases, 14 (6.4%) contained less than three profiles and 206 (93.6%) contained more than three profiles of duct cross-sections, with a total of 5698 profiles available for assessment. Of the total cases and cross-sections examined, 94 (42.7%) cases contained a disrupted myoepithelial cell layer with a total of 405 (7.1%) focal disruptions. Of the 94 cases, 61 (65%) contained one to four disruptions, and 33 (35%) contained five or more disruptions. Disruptions occurred in two forms: a cell-free gap between the two ends of the myoepithelial cell layer, and/or a gap filled with bud-like protrusions of epithelial cells. The size of disruptions varied substantially among ducts, ranging from the combined size of three to more than 30 myoepithelial cells. The frequency of disruptions also varied substantially among cases. In two cases that contained 129 and 130 profiles of duct cross-sections, respectively, no disruption was seen. In another two cases, two of two profiles and five of the seven profiles demonstrated focal myoepithelial layer disruptions. The form, size, or frequency of disruptions seemed to be independent of the size, length, architecture, and overall ER negativity of the ducts, and also of the histological grade of the lesions (Fig. 1).

Figure 1



Disruptions of myoepithelial cell layers are independent of the size, length, architecture, and overall estrogen receptor (ER) negativity of the ducts. Paraffin-embedded breast tissue sections were double immunostained with antibodies to ER and smooth muscle actin, and were developed with 3,3'-diaminobenzidine (DAB; black or brown) and 3-amino-9-ethylcarbazole (AEC; red) chromogens, respectively. Distinct myoepithelial cell layers are seen in the following structures: (a) a large duct with ductal carcinoma *in situ* (DCIS), 100x; (b) a long normal duct, 40x; (c) a duct with intraductal hyperplasia, 100x; (d) intermediate grade ER-negative DCIS, 100x.

The frequency and pattern of myoepithelial cell layer disruptions, however, were closely associated with the ER expression status in overlying cells. Of the 94 cases, 79 (84%) contained only ER-negative cell clusters, nine (9.6%) contained both ER-negative and ER-positive cell clusters, and six (6.4%) contained only ER-positive cell clusters overlying the disrupted myoepithelial cell layers. Of the 405 disruptions, 350 (86.4%) were overlain by ER-negative cell clusters and 55 (13.6%) were overlain by ER-positive cell clusters (Table 2). The frequency of myoepithelial cell layer disruptions associated with ER-negative cells was significantly higher ( $P < 0.01$ ) than that associated with ER-positive cells. The number of ER-negative cells overlying the disrupted myoepithelial cell layer varied markedly, ranging from three to more than 100 cells. These cells were generally distributed as clusters, and cells of the same cluster were morphologically similar. A vast majority (>90%) of the ER-negative cell clusters were small (<15 cells) and not easily appreciable on H&E stained sections (Fig. 2). The ER-negative cells in some of the larger clusters (>15 cells), however, showed noticeable alterations in shape and density, morphologically distinct from their adjacent ER-positive counterparts within the same duct (Fig. 3). More than 95% of the ducts contained only one or two disruptions, while a few of the ducts displayed multiple disruptions in the myoepithelial cell layer (Fig. 4). The stromal tissues surrounding ducts with myoepithelial cell layer disruptions were often more vascular and contained more leukocyte aggregates, compared with stromal tissues surrounding ducts with an intact myoepithelial cell layer (data not shown).

Although more than 86% of the myoepithelial cell layer disruptions were overlain by ER-negative cell clusters, nearly 14% of the disruptions were subjacent to ER-positive cell clusters. These ER-positive clusters were generally distinct from ER-negative cell clusters in three aspects: most of the clusters occurred in ducts with markedly attenuated myoepithelial cell layers, they usually showed no alterations in cell shape, density, or polarity, and the surrounding stromal tissues displayed no distinct morphological alterations (Fig. 5).

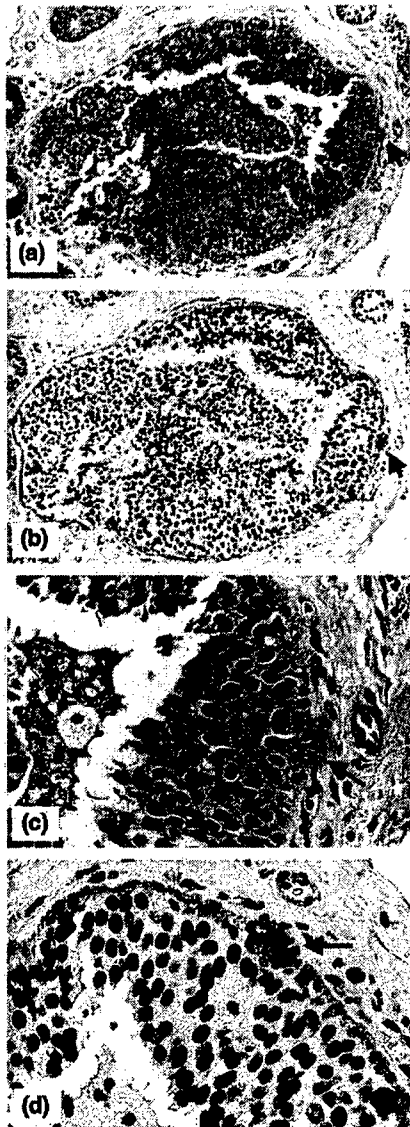
The myoepithelial cell layer disruptions and their associated ER-negative cell clusters occurred in ducts with DCIS or atypical intraductal hyperplasia in 90.6% of the cases. In 9.4% of the cases, however, myoepithelial cell layer disruptions and associated ER-negative cell clusters

Table 2

## Frequency of myoepithelial cell layer disruptions and the status of estrogen receptor expression

Total cross-sections	Total disruptions	Focal loss of estrogen receptor	Estrogen receptor-positive	P
5698	405 (7.1%)	350 (86.4%)	55 (13.6%)	< 0.01



**Figure 2**

Myoepithelial cell layer disruptions and overlying small estrogen receptor (ER)-negative cell clusters (<15 cells) in ER-positive ductal carcinoma *in situ* (DCIS). (a) H & E staining of a large duct with DCIS, 100 $\times$ ; (b) the adjacent section of (a) immunostained, 100 $\times$ ; (c) a higher magnification of (a); (d) a higher magnification of (b). The myoepithelial cell layer disruption and the overlying ER-negative cells are identified with an arrow.

were seen in hyperplastic, and even normal appearing, ducts (Fig. 6).

All the ER-negative cell clusters overlying the disrupted myoepithelial cell layer and their adjacent ER-positive counterparts in all 20 cases showed distinct immunoreactivity to cytokeratin 8, cytokeratin 19, and cytokeratins AE1/AE3, suggesting that they are epithelial in nature (data not shown). Immunostaining with antibodies to colla-

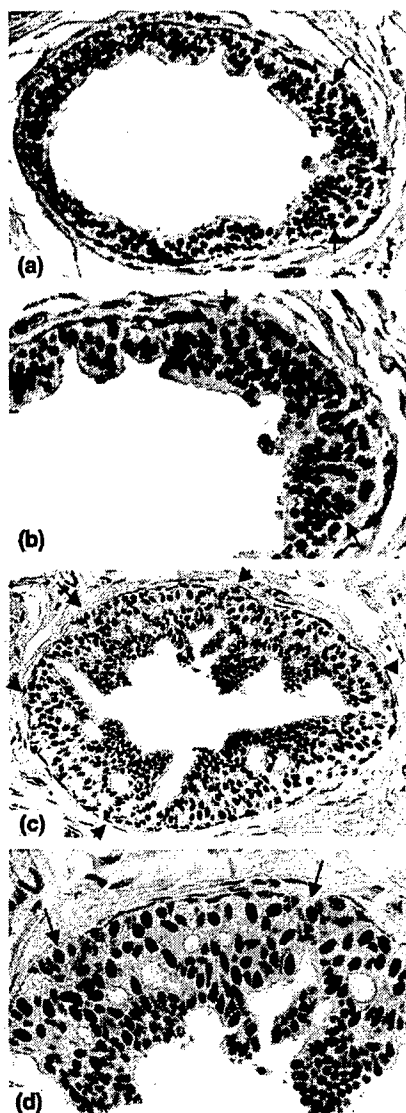
**Figure 3**

Myoepithelial cell layer disruptions and overlying larger estrogen receptor (ER)-negative cell clusters (>15 cells) in ER-positive neoplastic and hyperplastic ducts. All sections were immunostained for ER (brown) and smooth muscle actin (red). (a) Ductal carcinoma *in situ*, 100 $\times$ ; (b) two small ducts with atypical intraductal hyperplasia, 100 $\times$ ; (c) a hyperplastic duct, 100 $\times$ ; (d) two hyperplastic ducts, 200 $\times$ . Myoepithelial cell layer disruptions and ER-negative cell clusters are identified with arrows.

gen IV and laminin revealed no distinct immunoreactivity surrounding disrupted myoepithelial cell layers, suggesting that the basement membrane was also disrupted (data not shown). The ER-negative cell clusters were either in or protruded from the epithelial component.

Molecular analyses on microdissected cells from the five selected cases revealed distinct LOH and MI in both ER-negative cells and adjacent ER-positive cells within the

Figure 4



Multiple myoepithelial cell layer disruptions and overlying estrogen receptor (ER)-negative cell clusters in ductal carcinoma *in situ*. (a) A paraffin section immunostained for ER (brown) and smooth muscle actin (SMA) (red), 200 $\times$ ; (b) a higher magnification of (a), 400 $\times$ ; (c) a paraffin section immunostained for ER (brown) and SMA (red), 200 $\times$ ; (d) a higher magnification of (c), 400 $\times$ . Myoepithelial cell layer disruptions and ER-negative cell clusters are identified with arrows.

same duct at each of the 15 DNA markers. The frequency of LOH and MI among the DNA markers, however, varied from 12% to more than 70%. The ER-negative and ER-positive cells showed a different frequency or pattern of LOH and MI at 10 of the 15 markers, including those at chromosomes 3p, 11p, 13q, and 16q. Figure 7 shows examples of the LOH pattern in ER-negative cells and adjacent ER-positive cells from a selected case. Subsequently, and currently, additional cases with ER-negative cell clusters overlying disrupted myoepithelial cell layers

were selected for a larger scale comparison at a wider spectrum. The preliminary results are in agreement with those seen in the five previously selected cases. The detailed findings in all these cases will be pooled and reported separately.

### Discussion

The myoepithelial cell layer has been traditionally regarded as a structural barrier for separating mammary epithelial cells from the surrounding stroma and for contracting ductal and lobular spaces assisting milk secretion [25,26]. Recent studies, however, have revealed several lines of evidence suggesting that myoepithelial cells may play active roles in preventing *in situ* tumors from invasion, and in regulating the functions of the epithelial cells.

First, normal myoepithelial cells secrete several cell growth inhibitors, including maspin, which inhibit tumor cell growth in both tissue cultures and in animal models [27–29]. Second, normal myoepithelial cells can convert precursor hormones into active steroid hormones within the mammary epithelial tissue [30]. Third, the protein of a tumor suppressor gene, Wilms' tumor 1, is colocalized with maspin exclusively in myoepithelial cells, and the expression of these two proteins is linearly decreased with tumor progression in a vast majority of the cases assessed [10,11]. The loss of maspin and Wilms' tumor 1 expression or the disruption of myoepithelial cell layers leads to a significantly higher epithelial cell proliferation [10,11].

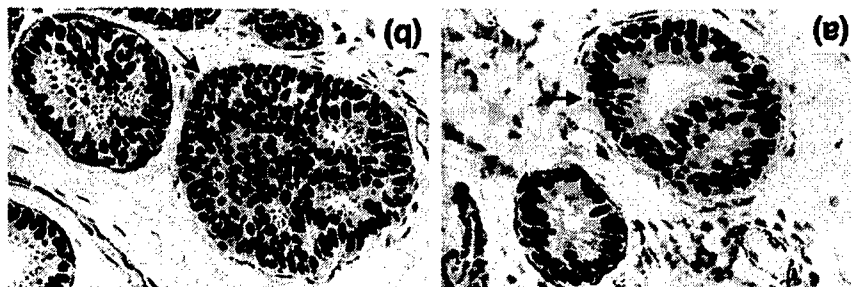
On the other hand, recent studies have suggested that myoepithelial cells could be the specific target of external and internal insults and could be subject to a variety of normal and pathologic changes. The exposure to lambda carrageenan could specifically result in the filament disassembly and loss of the mammary myoepithelial cells, whereas exposure to oxytocin could markedly enhance the myoepithelial cell differentiation and proliferation [31,32].

Our recent study has further demonstrated a subset of myoepithelial cells that are morphologically distinct on H&E sections, but are devoid of expression of nine phenotypic markers that are supposed to be exclusively or preferentially expressed in myoepithelial cells [33].

Despite this recent progress in myoepithelial cell research, the cell kinetics of myoepithelial cells has not been elucidated, and the mechanism of myoepithelial cell layer disruptions remains elusive.

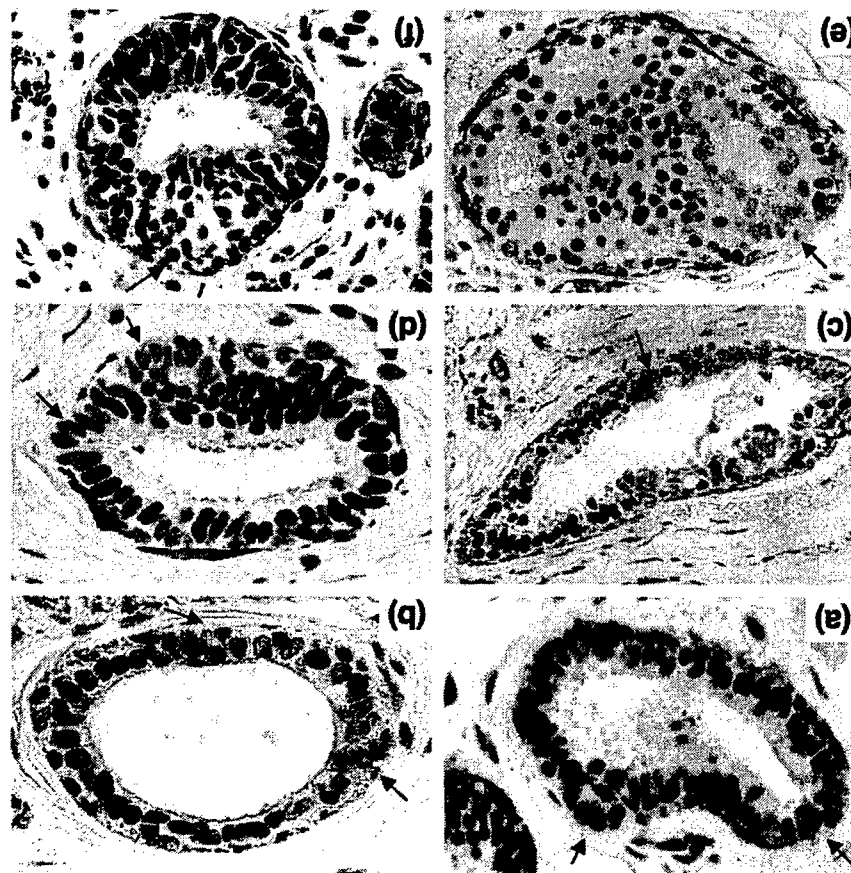
Based on our recent findings, we hypothesize that disruptions of the BM and myoepithelial cell layers and tumor invasion may be initiated or mediated by myoepithelial cells. Our hypothesized mechanism and the involved processes are as follows. Normal myoepithelial cells frequently undergo proliferation and differentiation to replace

**Figure 5**



Myoepithelial cell layer disruptions and associated estrogen receptor (ER)-positive cells in hyperplastic ducts. All sections were immunostained for ER (brown) and smooth muscle actin (red). (a), (b) Two ER-positive hyperplastic ducts showing attenuated and disrupted myoepithelial cell layers, 200 $\times$ . The disruptions are identified with arrows.

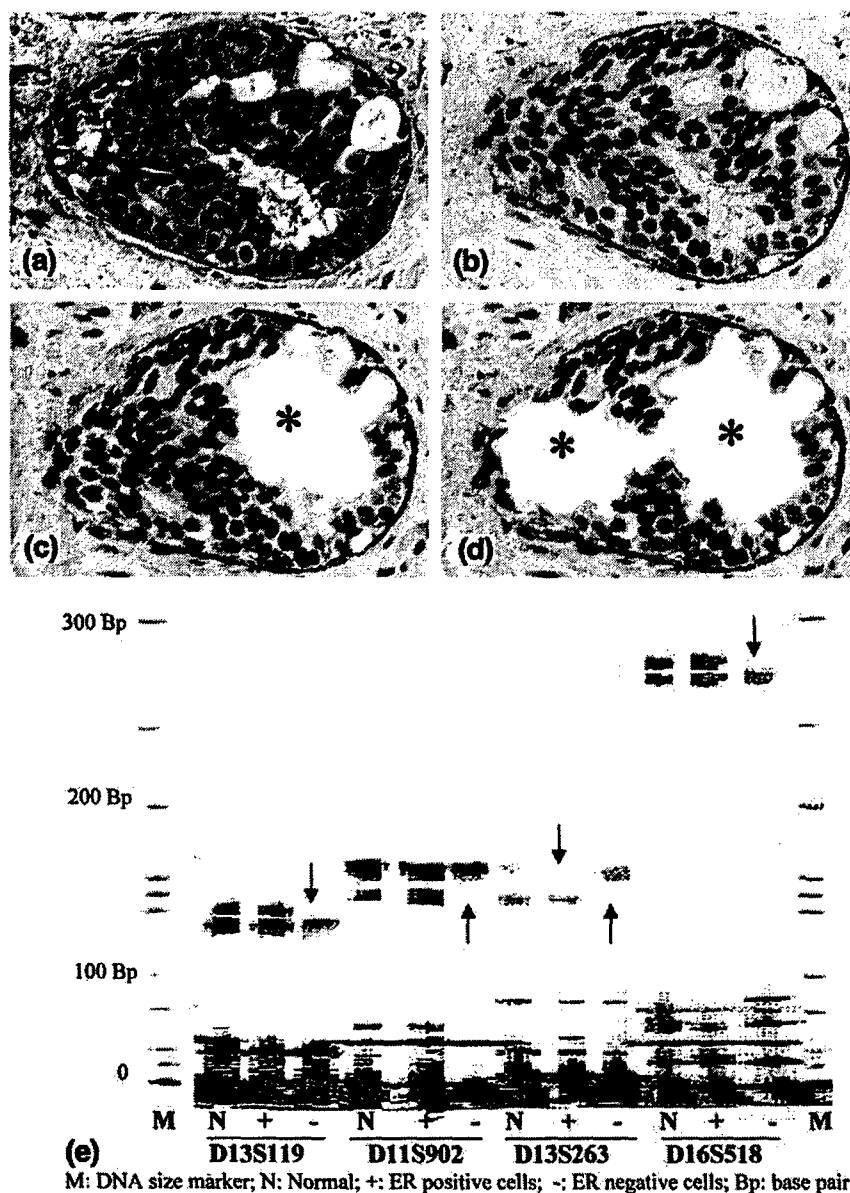
**Figure 6**



Myoepithelial cell layer disruptions and overlying estrogen receptor (ER)-negative cell clusters in normal and hyperplastic appearing ducts. All sections were immunostained for ER (brown) and smooth muscle actin (red). (a)-(c) Normal appearing ducts, 400 $\times$ ; (d)-(f) hyperplastic ducts, 400 $\times$ . Myoepithelial cell layer disruptions and ER-negative cell clusters are identified with arrows.

aged or injured cells. An external or internal insult then disrupts the normal replacement process, resulting in a cluster of dying myoepithelial cells. Following this, degraded products of dead myoepithelial cells attract lymphocyte infiltration that physically disrupts the BM. A focal disruption in the myoepithelial cell layer and the BM layer then results in an increased permeability for metabolism- and growth-related molecules. The altered micro-environment results in the changes of the gene expression pattern and the behavior of the adjacent epithelial cells, R237

### Figure 7



**Comparison of the loss of heterozygosity (LOH) pattern in estrogen receptor (ER)-negative cells and adjacent ER-positive cells within the same duct. (a)** H & E staining of a duct with atypical intraductal hyperplasia, 200 $\times$ ; **(b)** the adjacent section of (a) immunostained (before microdissection), 200 $\times$ ; **(c)** microdissection of ER-positive cells; **(d)** microdissection of ER-negative cells; **(e)** LOH at four selected DNA markers. Asterisks indicate the ER-negative cells and the ER-positive cells removed; arrows identify LOH.

facilitating the formation of a biologically more aggressive cell clone. Epithelial cells overlying disrupted myoepithelial cell layers then undergo a localized epithelial cell proliferation, which may occur in two forms: stem cell mediated proliferation that gives rise to ER-negative cell clusters, and differentiated cell mediated proliferation that produces ER-positive cells. Finally, cells overlying disrupted myoepithelial cell layers undergo cytodifferentiation, releasing stage-restricted and invasion-associated molecules, which trigger angiogenesis, tissue remodeling, and increasing

production of growth factors in the stroma, providing a favorable environment for epithelial cell growth [34–36]. These interactive changes between epithelial and stromal cells lead to further degradation of the BM and myoepithelial cell layers, and a clonal expansion and stromal invasion of cells overlying disrupted myoepithelial cell layers.

Our hypotheses appear to be supported by the results of two recent studies showing that the frequency of white blood cell infiltration into the tumor tissues seems to lin-

early increase with tumor progression [37,38]. Our hypotheses are also in an agreement with the results of our most recent study, which reveals that ducts with focally disrupted myoepithelial cell layers have a significantly higher rate of white blood cell infiltration and more clusters of multiple proliferating cells compared with morphologically comparable ducts without myoepithelial disruptions (unpublished data). It is not known, however, whether or to what extent our hypothesis reflects the intrinsic mechanism of the BM and myoepithelial cell layer disruptions. However, given the fact that the disruption of the BM and myoepithelial cell layers is an absolute prerequisite for tumor invasion, and that progression of breast tumors is paralleled by a progressive hormonal independence [14–17], our hypothesized model might open a new window for exploring these issues.

The mechanism for the loss or diminution of ER expression in cells overlying a disrupted myoepithelial cell layer is unknown, but could result from several reasons. First, these cells might be in the status of actively proliferating. A previous immunohistochemical study in human breasts has shown that none of the epithelial cells with ER expression and progesterone receptor expression was proliferating, and none of the proliferating cells showed either ER or progesterone receptor expression [39]. Second, the ER gene in these cells might have been inactivated by methylation during tumor progression. Previous studies have shown that the progression of breast tumors is paralleled by a progressive hormonal independence [14–17]. Third, these cells might express a different type of ER, including variants of the  $\beta$ -ER. A recent study has revealed that  $\alpha$ -ER and  $\beta$ -ER are separately localized in a subset of breast tumors and appear to have different functions [40]. Fourth, these cells might be derived from the myoepithelial lineage. A number of previous studies have shown that myoepithelial cells can express partial myodifferentiation in human breast cancer [41–43]. Finally, these cells are newly formed through a stem cell mediated clonal proliferation and are not mature enough to express the ER protein. Previous studies have demonstrated that the ER expression status is related to the age or differentiation status of the cells [25,44].

While each of these five assumptions could partially explain the loss of ER expression in cell clusters overlying disrupted myoepithelial cell layers, a stem cell mediated clonal proliferation appears to be a more reasonable interpretation, as our most recent studies on the same tissues used in the current study have further revealed several new features of these ER-negative clusters: negativity to p-cadherin, a newly introduced specific myoepithelial cell marker; strong immunoreactivities to epithelial-specific antigen; lost or markedly reduced expression of p27, a cell growth inhibitor; and a unique rate and pattern of cell proliferation-related proteins [45,46]. It is also possible,

however, that these ER-negative clusters represent the intermediate cells of a myoepithelial lineage, as our previous study has revealed that a subset of morphologically distinct myoepithelial cells is devoid of the ER and also a total of nine markers that are supposed to be exclusively or preferentially expressed in myoepithelial cells [33]. In any case, the loss or reduction of the ER, along with a different pattern of genetic alterations, suggests that the ER-negative clusters and their adjacent ER-positive counterparts may have substantially different genetic and biochemical profiles. Consequently, comparisons of these two cell populations at DNA, RNA, and protein levels may lead to identification of very specific biomolecules that are exclusively associated with myoepithelial cell layer disruptions and tumor invasion. These molecules might be used for development of vaccine or biomarkers for early detection, treatment, and prevention of breast cancer [47].

## Conclusions

A total of 405 focal disruptions in the myoepithelial cell layers were detected from 5698 duct cross-sections of 94 patients with DCIS. Of the 405 disruptions, 350 (86.4%) were overlain by ER-negative cell clusters and 55 (13.6%) were overlain by ER-positive cell clusters ( $P < 0.01$ ).

The microdissected ER-negative and ER-positive cells within the same duct from all five selected cases showed a different frequency or pattern of LOH and/or MI at 10 of 15 markers.

The loss or reduction of ER expression, along with a different pattern of genetic alterations, suggests that the ER-negative cell clusters and their adjacent ER-positive counterparts might have substantially different genetic and biochemical profiles.

## Competing interests

None declared.

## Acknowledgements

The opinions and assertions contained herein represent the personal views of the authors and are not to be construed as official or as representing the views of the Department of the Army or the Department of Defense. The authors are grateful to Doug Landry and James A Nola of the Armed Forces Institute of Pathology exhibition section for their technical assistance in preparing the figures. This study was supported by The Congressionally Directed Medical Programs, grants DAMD 17-01-0129 and DAMD17-01-0130 (to Y-gM).

## References

1. Tsubura A, Shikata N, Inui T, Morii S, Hatano T, Oikawa T: **Immunohistochemical localization of myoepithelial cells and basement membrane in normal, benign and malignant human breast lesions.** *Virchows Arch* 1988, **413**:133-139.
2. Jolicoeur F, Seemayer TA, Gabbiani G, Robidoux A, Gaboury L, Oligny LL, Schurch W: **Multifocal, nascent, and invasive myoepithelial carcinoma (malignant myoepithelioma) of the breast: an immunohistochemical and ultrastructural study.** *Int J Surg Pathol* 2002, **10**:281-291.
3. Slade MJ, Coope RC, Gomm JJ, Coombes RC: **The human mammary gland basement membrane is integral to the polarity of luminal epithelial cells.** *Exp Cell Res* 1999, **247**:267-278.

4. Miosge N: The ultrastructural composition of basement membrane in vivo. *Histol Histopathol* 2001, 16:1239-1248.
5. Nerlich A: Morphology of basement membrane and associated matrix proteins in normal and pathological tissues. *Veroff Pathol* 1995, 145:1-139.
6. Pasqualini JR: *Breast Cancer—Prognosis, Treatment, and Prevention*. New York: Marcel Dekker; 2002.
7. Goldfarb RH, Liotta LA: Proteolytic enzymes in cancer invasion and metastasis. *Semin Thromb Hemost* 1986, 12:294-307.
8. Coussens LM, Fingleton B, Matrisian LM: Matrix metalloproteinase inhibitors and cancer: trial and tribulations. *Science* 2002, 295:2387-2392.
9. Tavassoli FA, Man YG: Morphofunctional features of intraductal hyperplasia, atypical hyperplasia, and various grades of intraductal carcinoma. *Breast J* 1995, 1:155-162.
10. Man YG, Saenger JS, Strauss BL, Vang RS, Bratthauer GL, Chen PY, Tavassoli FA: Focal alterations of p27 expression and sub-jacent myoepithelial cell layer disruptions are correlated events in ER(-) ductal intraepithelial neoplasia. In *Proceedings of Department of Defense Breast Cancer Research Program Meeting: September 25-28 2002; Orlando, FL*, vol. 1. Fort Detrick, MD: US Army Medical Research and Material Command; 2002: Poster section 9:14.
11. Man YG, Vang RS, Saenger JS, Strauss BL, Bratthauer GL, Chen PY, Tavassoli FA: Co-expression of maspin and Wilms' tumor 1 proteins in mammary myoepithelial cells: Implication for tumor progression and invasion. In *Proceedings of Department of Defense Breast Cancer Research Program Meeting: September 25-28 2002; Orlando, FL*, vol. 1. Fort Detrick, MD: US Army Medical Research and Material Command; 2002: Poster section 9:16.
12. Moinfar F, Man YG, Arnould L, Bratthauer GL, Ratschek M, Tavassoli FA: Concurrent and independent genetic alterations in the stromal and epithelial cells of mammary carcinoma: Implications for tumorigenesis. *Cancer Res* 2000, 60:2562-2566.
13. Man YG, Mannion C, Albores-Saavedra J, Bratthauer GL, Kuhls E, Tavassoli FA: Allelic losses at 3p and 11p are detected in both epithelial and stromal components of cervical small cell neuroendocrine carcinoma. *Appl Immunohistochem Mol Morphology* 2001, 9:340-345.
14. Schmitt FC: Multistep progression from an oestrogen-dependent growth towards an autonomous growth in breast carcinogenesis. *Eur J Cancer* 1995, 31A:2049-2052.
15. Clarke R, Brunner N, Katzenellenbogen BS: Progression of human breast cancer cells from hormone-dependent to hormone-independent growth both in vitro and in vivo. *Proc Natl Acad Sci USA* 1989, 86:3649-3653.
16. Murphy LC: Mechanism of hormone independence in human breast cancer. *In vivo* 1998, 2:95-106.
17. Sheikh MS, Garcia M, Pujol P, Fontana JA, Rochefort H: Why are estrogen receptor negative breast cancers more aggressive than the estrogen receptor positive breast cancers? *Invasion Metastasis* 1994-95, 14:329-336.
18. Man YG, Tavassoli FA: A simple epitope retrieval method without the use of microwave oven or enzyme digestion. *Appl Immunohistochem* 1996, 4:139-141.
19. Man YG, Ball WD, Culp AJ, Hand AR, Moreira JE: Persistence of a perinatal cellular phenotype in the ducts of adult glands. *J Histochem Cytochem* 1995, 43:1203-1215.
20. Man YG, Schammel DP, Tavassoli FA: Detection of telomerase activity in microdissected breast lesions [abstract]. *Cell Vision* 1998, 5:84-85.
21. Moinfar F, Man YG, Lininger RA, Tavassoli FA: Use of keratin 34βE12 as an adjunct in the diagnosis of mammary intraepithelial neoplasia—duct type (benign and malignant intraductal proliferations of the breast). *Am J Surg Pathol* 1999, 23:1048-1058.
22. Man YG, Moinfar F, Bratthauer GL, Kuhls E, Tavassoli FA: An improved method for DNA extraction from paraffin sections. *Pathol Res Pract* 2001, 197:635-642.
23. Man YG, Moinfar F, Bratthauer GL, Tavassoli FA: Five useful approaches for generating more valid gel images for LOH and clonality analysis with an automated DNA sequencer. *Diag Mol Pathol* 2000, 9:84-90.
24. Man YG, Kuhls E, Bratthauer GL, Moinfar F, Tavassoli FA: Multiple use of slab gels in sequencing apparatus for separation of polymerase chain reaction products. *Electrophoresis* 2001, 22: 1915-1919.
25. Robinson GW, McKnight RA, Smith GH, Hennighausen L: Mammary epithelial cells undergo secretory differentiation in cycling virgins but require pregnancy for the establishment of terminal differentiation. *Development (Camb)* 1995, 121:2079-2090.
26. Chodosh LA, Cruz CMD, Gardner HP: Mammary gland development, reproductive history, and breast cancer risk. *Cancer Res* 1999, 59:1765s-1772s.
27. Sternlight MD, Barsky SH: The myoepithelial defense: a host defense against cancer. *Med Hypotheses* 1997, 48:37-46.
28. Sternlight MD, Safarians S, Rivera SP, Barsky SH: Characterization of the extracellular matrix and proteinase inhibitor content of human myoepithelial tumors. *Lab Invest* 1996, 74: 781-796.
29. Shao ZM, Nguyen M, Alpaugh ML, O'Connell JT, Barsky SH: The human myoepithelial cells exerts antiproliferative effects on breast carcinoma cells characterized by p21WAF1/CIP1 induction, G2M arrest, and apoptosis. *Exp Cell Res* 1998, 241:394-403.
30. Tobacman JK, Hinkhouse M, Khalkhali-Ellis Z: Steroid sulfatase activity and expression in mammary myoepithelial cells. *J Steroid Biochem Mol Biol* 2002, 81:65-68.
31. Tobacman JK: Filament disassembly and loss of mammary myoepithelial cells after exposure to lambda-carrageenan. *Cancer Res* 1997, 57:2823-2826.
32. Sapino A, Macri L, Tonda L, Bussolati G: Oxytocin enhances myoepithelial cell differentiation and proliferation in the mouse mammary gland. *Endocrinology* 1993, 133:838-842.
33. Zhang R, Man YG, Vang RS, Saenger JS, Barner R, Wheeler DT, Liang CY, Vinh TN, Bratthauer GL: A subset of morphologically identifiable mammary myoepithelial cells lacks expression of corresponding phenotypic markers. *Breast Cancer Res* 2003, 5:R151-R156.
34. Bissell MJ, Radisky DC, Rizki A, Weaver VM, Petersen OW: The organizing principle: microenvironmental influences in the normal and malignant breast. *Differentiation* 2002, 70:537-546.
35. Muschler J, Levy D, Boudreau R, Henry M, Campbell K, Bissell MJ: A role for dystroglycan in epithelial polarization: loss of function in breast tumor cells. *Cancer Res* 2002, 62:7102-7109.
36. Gudjonsson T, Ronnov-Jessen L, Villadsen R, Rank F, Bissell MJ, Petersen OW: Normal and tumor-derived myoepithelial cells differ in their ability to interact with luminal breast epithelial cells for polarity and basement membrane deposition. *J Cell Sci* 2002, 115:39-50.
37. Ben-Hur H, Cohen O, Schneider D, Gyrevich P, Halperin R, Bala U, Mozes M, Zusman I: The role of lymphocytes and macrophages in human breast tumorigenesis: an immunohistochemical and morphometric study. *Anticancer Res* 2002, 22: 1231-1238.
38. Gannot G, Gannot I, Vered H, Buchner A, Keisari Y: Increase in immune cell infiltration with progression of oral epithelium from hyperkeratosis to dysplasia and carcinoma. *Br J Cancer* 2002, 86:1444-1448.
39. Russo J, Ao X, Grill C, Russo IH: Pattern of distribution of cells positive for estrogen receptor alpha and progesterone receptor in relation to proliferating cells in the mammary gland. *Breast Cancer Res Treat* 1999, 53:217-227.
40. Fuqua SA, Schiff R, Parra I, Moore JT, Mohsin SK, Osborne CK, Clark GM, Allred DC: Estrogen receptor beta protein in human breast cancer: correlation with clinical tumor parameters. *Cancer Res* 2003, 63:2434-2439.
41. Malzahn K, Mitze M, Thoenes M, Moll R: Biological and prognostic significance of stratified epithelial cytokeratins in infiltrating ductal breast carcinomas. *Virch Arch* 1998, 433:119-129.
42. Petersen OW, Nielsen HL, Gudjonsson T, Villadsen, Ronnov-Jessen L, Bissell MJ: The plasticity of human breast carcinoma cells is more than epithelial to mesenchymal conversion. *Breast Cancer Res* 2001, 3:213-217.
43. Petersen OW, Hoyer PE, van Deurs B: Frequency and distribution of estrogen receptor-positive cells in normal, nonlactating human breast tissue. *Cancer Res* 1987, 47:5748-5751.
44. Chen CM, Martin LA, Johnston SR, Ali S, Dowsett M: Molecular changes associated with the acquisition of oestrogen hypersensitivity in MCF-7 breast cancer cells on long-term oestrogen deprivation. *J Steroid Biochem Mol Biol* 2002, 81:333-341.
45. Man YG, Mattu R, Zhang R, Yousefi M, Sang QXA, Shen T: A subset of normal and hyperplastic appearing mammary

- ductal cells display invasive features [abstract]. *Breast Cancer Res Treat* 2003, in press.
46. Man YG, Zhang R, Mattu R, Shen T, Sang QXA: **A subset of mammary epithelial cells overlying focally disrupted myo-epithelial cell layers shows an unusual immunostaining pattern for proliferation-related proteins [abstract].** *Breast Cancer Res Treat* 2003, in press.
47. Ponder BA: **Cancer genetics.** *Nature* 2001, 411:336-341.

### Correspondence

Yan-gao Man, MD, PhD, Department of Gynecologic and Breast Pathology, Armed Forces Institute of Pathology and American Registry of Pathology, 6825 16th Street, NW, Washington, DC 20306-6000, USA. Tel: +1 202 782 1612; fax: +1 202 782 3939; e-mail: [man@afip.osd.mil](mailto:man@afip.osd.mil)

## Open Access

## Research article

**A subset of morphologically distinct mammary myoepithelial cells lacks corresponding immunophenotypic markers**

Roy R Zhang, Yan-Gao Man, Russell Vang, Jeffrey S Saenger, Ross Barner, Darren T Wheeler, Chang Y Liang, Tuyethoa N Vinh and Gary L Bratthauer

Department of Gynecologic and Breast Pathology, Armed Forces Institute of Pathology, Washington, DC, USA

Corresponding author: Yan-Gao Man (e-mail: [man@afip.osd.mil](mailto:man@afip.osd.mil))

Received: 6 Jun 2003 Revisions requested: 30 Jun 2003 Revisions received: 4 Jul 2003 Accepted: 7 Jul 2003 Published: 24 Jul 2003

*Breast Cancer Res* 2003, **5**:R151-R156 (DOI 10.1186/bcr635)© 2003 Zhang *et al.*, licensee BioMed Central Ltd (Print ISSN 1465-5411; Online ISSN 1465-542X). This is an Open Access article: verbatim copying and redistribution of this article are permitted in all media for any purpose, provided this notice is preserved along with the article's original URL.**Abstract**

**Introduction:** Immunostaining for smooth muscle actin (SMA) is commonly used to elucidate mammary myoepithelial (ME) cells, whose presence or absence is a reliable criterion for differentiating *in situ* and invasive carcinomas. However, some morphologically distinct ME cells fail to stain for SMA. This study intended to assess whether these SMA-negative cells also lack the expression of other ME cell markers.

**Methods:** Hematoxylin/eosin and SMA immunostained sections from 175 breast cancer patients were examined. Three cases were found to harbor ducts that showed morphologically distinct ME cell layers, but showed no SMA immunostaining in at least one-third of the layer or the entire layer. Eight additional consecutive sections from each case were stained for SMA, using a black chromogen, and each was then re-stained for one of eight additional markers supposed to exclusively or preferentially stain ME cells, using a red

chromogen. SMA-negative ME cells were re-examined for the expression of other markers.

**Results:** SMA-negative ME cells in two cases also failed to display immunoreactivity for other markers, including calponin, CD10, smooth muscle myosin heavy chain, protease inhibitor 5 (maspin), Wilms' tumor-1, and cytokeratins 5, 14, and 17 (CK5, CK14, and CK17). However, in one case SMA-negative ME cells displayed immunoreactivities for maspin, CK5, CK14, and CK17. The distribution of these ME cells is independent of ductal size, length, and architecture.

**Conclusions:** A subset of morphologically identifiable ME cells lack the expression of nine corresponding immunophenotypic markers, suggesting that ME cells might also be subject to different normal and pathological alterations.

**Keywords:** double immunohistochemical staining; myoepithelial cell layer; myoepithelial cell markers; myoepithelial-epithelial cell interaction

**Introduction**

The epithelial component of normal and non-invasive breast tissues is normally surrounded by a layer of myoepithelial (ME) cells, whose absence or disruption is an absolute prerequisite for tumor invasion and metastasis [1]. ME cells are not easily identifiable in hematoxylin/eosin (H&E)-stained breast tissue sections, as they are often indistinguishable from subjacent myofibroblastic cells in the stroma. Immunohistochemical staining for smooth muscle actin (SMA) has been routinely used to assist in the identification of ME cells [2]. However, we and others have repeatedly noted that about 4–6% of morphologically rec-

ognizable ME cells in H&E-stained sections fail to display SMA immunoreactivity [3,4]. We attempted to assess whether these SMA-negative cells also lack the expression of eight additional markers that are supposed to present exclusively or preferentially at ME cells.

**Materials and methods****Case selection**

Formalin-fixed, paraffin-embedded tissue blocks from female patients with breast lesions were retrieved from files of the Armed Forces Institute of Pathology. Consecutive sections at 4–5 µm thickness were cut and placed on



Table 1

**Antibodies used in this study**

Antibody	Company	Clone	Titer	Staining pattern
Alpha-smooth muscle actin	Novocastra	$\alpha$ sm-1	1:50	Cytoplasmic
Maspin	Novocastra	EAW24	1:25	Cytoplasmic and nuclear
Calponin	Novocastra	CLAP	1:25	Cytoplasmic
Smooth muscle myosin heavy chain	Dako	SMMS-1	1:100	Cytoplasmic
'Wilms' tumor protein	Cell Marque	6F-H2	1:10	Cytoplasmic
CD10	Novocastra	56C6	1:80	Cytoplasmic
Cytokeratin 5	Novocastra	XM26	1:100	Cytoplasmic
Cytokeratin 14	Novocastra	LL002	1:20	Cytoplasmic
Cytokeratin 17	Novocastra	E3	1:20	Cytoplasmic

positively charged microscopic slides. A total of 175 cases with distinct ME cells, defined as a continuous layer of spindle- or cuboid-shaped cells that overlie the basement membrane and encircle epithelial cells, were selected for this study. Among the 175 cases, all contained non-invasive lesions, including ductal and lobular carcinoma *in situ* and sclerosing adenosis, and a few cases had invasive components.

**Markers and reagents**

Nine antibodies reported to present exclusively or preferentially at ME cells were selected for this study [5–25] (Table 1); these included antibodies against SMA, smooth muscle myosin heavy chain (SM-MHC), CD10, calponin, protease inhibitor 5 (maspin), Wilms' tumor-1 (WT-1), and cytokeratins 5, 14, and 17 (CK5, CK4, and CK17). Other reagents, including the secondary antibody, detection kits, and chromogen kits, were purchased from Vector Laboratories, Inc (Burlingame, CA). Digestion enzymes recommended for antigen retrieval were bought from Sigma (St Louis, MO). A microwave oven and pressure cooker designated for antigen retrieval, along with retrieval solutions, were purchased from Biocare Medical (Walnut Creek, CA).

**Immunohistochemical staining**

A preliminary study was performed to optimize the immunostaining condition for all antibodies selected. First, each of the nine antibodies was tested strictly in accordance with the manufacturer's recommended protocol, including the methods of antigen retrieval and the length of the primary antibody incubation time. Then, each antibody was tested with our published protocol, which involves an overnight incubation of deparaffinized sections at 70°C in the retrieval solution and an incubation for 3–4 hours or overnight of the primary antibody at about 25°C [26]. Two adjacent sections stained by using our

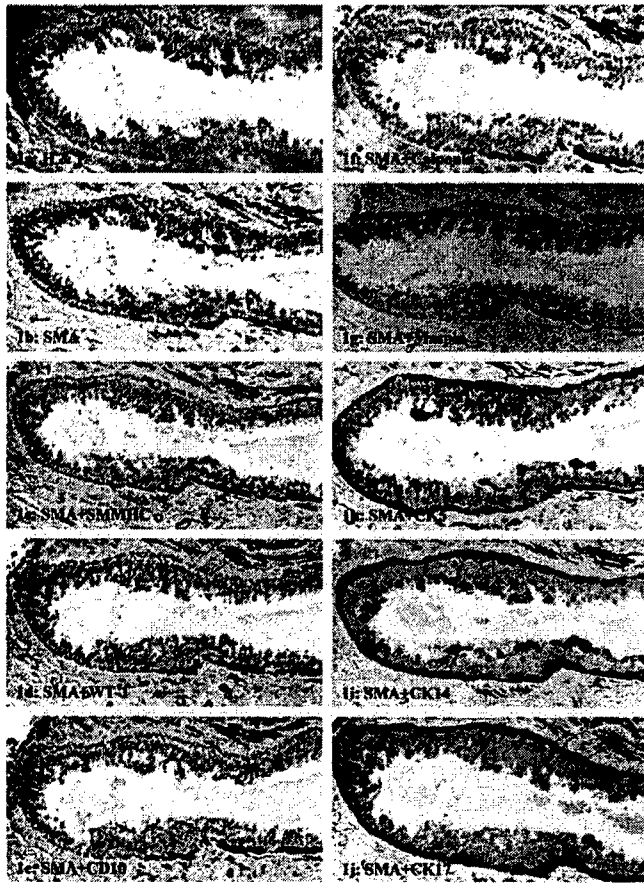
protocol and the manufacturer's recommended protocols were compared for specificity and sensitivity. As our protocol consistently yielded stronger and more distinct staining for all the antibodies, the final staining for all the 175 cases with SMA and a double immunostaining with additional markers in selected cases (see below) were performed with our published protocol [26].

**Double immunohistochemical staining**

All H&E-stained and immunostained sections were reviewed independently by at least two investigators. All ducts lined by at least 50 epithelial cells were examined, and three cases were found to contain ducts that displayed morphologically distinct ME cell layers in H&E-stained sections, but ME cells in at least one-third of the layer or the entire layer were devoid of SMA staining. Eight consecutive sections from each of the three selected cases were used for a double immunostaining with our published protocols [26,27]. In brief, all eight sections were first immunostained for SMA with a black chromogen. Each section was then stained for one of the eight additional ME markers with a red chromogen. The same ducts with SMA-negative ME cells were examined for the expression of other markers. In addition, sections from all three cases were immunostained for estrogen receptor (ER) and CK8 to exclude the possibility that these SMA-negative cells might be epithelial in nature.

**Results and discussion**

Results showed that all three cases spanned a morphologic spectrum ranging from columnar cell hyperplasia to ductal carcinoma *in situ*. Case 1 (columnar cell hyperplasia) contained two ducts of interest lined by about 500 epithelial cells surrounded by morphologically distinct ME cell layers on the H&E-stained section (Fig. 1a). The ME cells in about two-thirds of the ME layer showed distinct and strong SMA immunostaining, whereas the cells

**Figure 1**

Immunostaining pattern of ME cells in columnar hyperplasia (case 1). (a) H&E staining; (b) immunostaining for SMA; (c-f) double immunostaining of SMA with SM-MHC, WT-1, CD10, and calponin, respectively, and the segment of the ME layer is negative for all antibodies; (g-j) double immunostaining of SMA with maspin, CK5, CK14, and CK17, respectively, and the segment of the ME layer is positive for all antibodies.

in about one-third of the layer were devoid of SMA immunostaining (Fig. 1b). The SMA-positive and SMA-negative cells were morphologically indistinguishable on H&E-stained sections. In double immunostained sections, these SMA-negative cells were also negative for SM-MHC, WT-1, CD10, and calponin (Fig. 1c-f). However, these SMA-negative cells were positive for maspin, CK5, CK14, and CK17 (Fig. 1g-j).

Cases 2 and 3 contained ductal carcinoma *in situ*, of intermediate grade and low grade, respectively. The ducts were surrounded by morphologically distinct ME cell layers in H&E-stained sections (Fig. 2a). These ME cell layers were attenuated, consisting of elongated spindle cells with dark and compressed nuclei. The entire ME cell layer was devoid of SMA immunostaining (Fig. 2b). In double immunostained sections, these SMA-negative cells

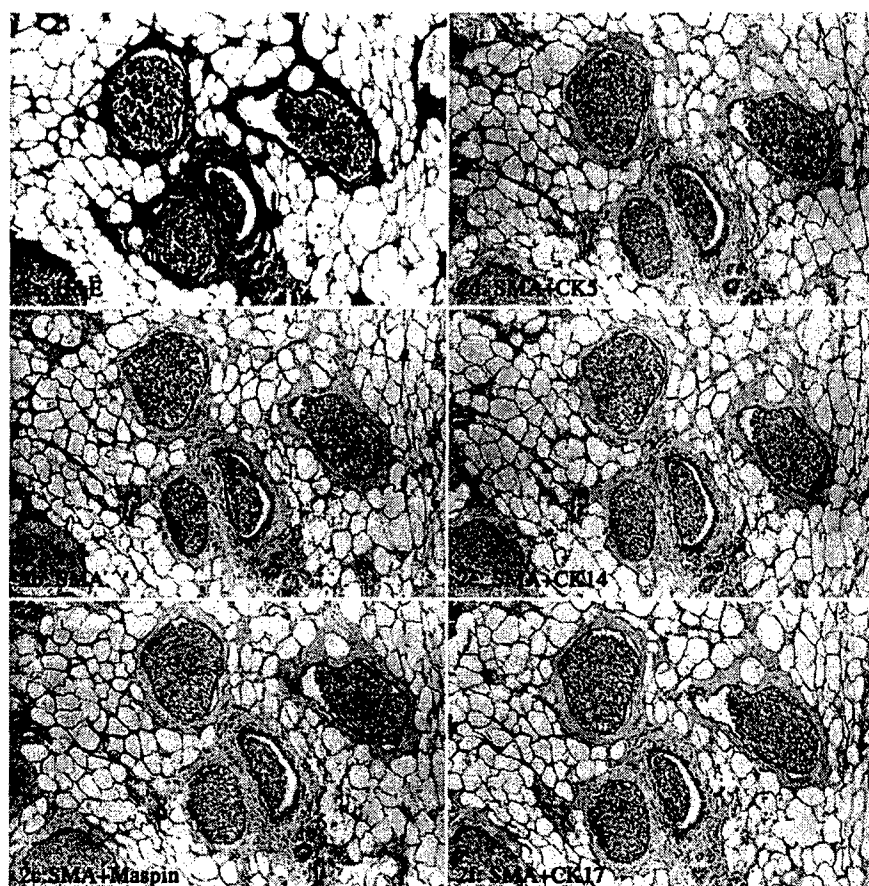
were also devoid of distinct immunostaining for any of the additional eight markers (Fig. 2c-f).

The SMA-negative cells in all three cases showed distinct negativity to ER and CK8, in sharp contrast with the overlying epithelial cells that showed strong ER and CK8 positivities (data not shown). The distribution of these SMA-negative ME cells seemed to be independent of the ductal size, length, and architecture.

Our findings are consistent with those of a recent study showing that a vast majority of the ME cells in both normal and ductal carcinoma *in situ* displayed distinct immunostaining to p63, SM-MHC, and calponin, whereas a single or a cluster of a few ME cells in some ducts failed to show immunoreactivity to all these three markers [28]. However, our study differs from this study [28] and previous studies [3,4] in four aspects: first, the SMA-negative cells were segmented, accounting for at least one-third or all of the ME cells in involved ducts; second, we tested for more ME cell markers; third, the SMA-negative cells assessed were morphologically similar to their adjacent SMA-positive neighbors on H&E-stained sections; fourth, our focus is directed toward the elucidation of the detailed immunohistochemical profile of these SMA-negative cells identified in 3 of 175 examined cases. The distribution of different ME markers among normal, benign, and malignant breast lesions in the remaining cases will be presented separately. In our study, p63 was replaced with WT-1 for three main reasons: first, p63 is a nuclear protein, which is not easily identifiable in attenuated or compressed ME cells; second, previous studies have shown that this protein is also expressed in ME-cell-derived neoplasms and tumors with squamous cell differentiation [29]; third, our preliminary study had showed that WT-1 had the same subcellular localization but seemed to be more specific for ME cells, compared with p63 [12].

The mechanism of the loss of myoepithelial markers in some of the ME cells is unknown, but could result from the dynamic and reciprocal interactions between epithelial and ME cells. It has been documented that a variety of proteolytic enzymes produced by malignant epithelial cells could have substantial impacts on the physical integrity or functions of the subjacent ME cells and the basement membrane [30-32]. In contrast, ME cells could influence the biological behavior of subjacent epithelial cells. Our recent studies have revealed the co-localization of maspin and WT-1 exclusively in mammary ME cells [12]. In a vast majority of cases, the expression of these two proteins decreases linearly with tumor progression, and the loss of these proteins or focal disruptions in the ME cell layers leads to a significantly higher cell proliferation in the subjacent epithelial cells [12,33]. In addition, these changes in ME cells could result from effects of certain chemical compounds.

Figure 2



Immunostaining pattern of ME cells in ductal carcinoma *in situ* (case 2). (a) H&E staining; (b) immunostaining for SMA; (c-f) double immunostaining of SMA with maspin, CK5, CK14, and CK17, respectively, and the entire ME cell layer is negative for these antibodies in some ducts and is also negative for SM-MHC, WT-1, CD10, and calponin (not shown).

It has been reported that the exposure to lambda-carrageenan could specifically result in filament disassembly and loss of ME cells [34]. In contrast, exposure to oxytocin could substantially enhance ME cell differentiation and proliferation in mouse breasts [35]. In addition, these SMA-negative ME cells might be newly formed through stem-cell-mediated proliferation and are in the transition to a terminally differentiated status. Our previous studies on animal models have shown that intercalated duct cells in adult rat submandibular glands are the common progenitor for both the acinar and granular duct cells [27,36]. A recent study in human breast has revealed that CK5-positive cells are capable of giving rise to both glandular and ME cell lineages [21]. In both cases the intermediate cells showed an unusual immunostaining pattern for several proteins [21,36].

The total loss of all nine ME cell immunophenotypic markers suggests that these ME cells have genetic and biochemical properties differing from their SMA-positive counterparts. The significance and consequence of these

changes in ME cells are unknown. However, given that the disruption of the ME cell layer and basement membrane is an absolute prerequisite for tumor invasion and metastasis, these alterations in ME cells might affect the biological behavior of the epithelial cells, making them prone to progression. Our assumption is in agreement with our previous findings, which have revealed that focal disruptions of ME cell layers could lead to a significantly higher proliferation rate in subjacent epithelial cells [12,33]. Our assumption is also supported by a recent study showing that normal and tumor-derived ME cells differ substantially in their ability to interact with luminal breast epithelial cells for polarity and basement membrane deposition [37]. Further studies are currently in progress to elucidate the biological behavior and genetic profile of epithelial cells immediately subjacent to these SMA-negative ME cells.

## Conclusions

A subset of morphologically identifiable ME cells lacks the expression of nine corresponding immunophenotypic markers, suggesting that, like the epithelial cells, ME cells

might also be subject to different normal and pathological alterations, and that alterations in ME cells might significantly affect the functions and biological behavior of the adjacent epithelial cells.

## Competing interests

None declared.

## Acknowledgments

The authors are indebted to Mr Doug Landry and James A Nola of the AFIP exhibition section and Mr Kenneth J Vrtacnik of the AFIP Photography Lab for their assistance in preparation of the figures. This study was supported in part by grants DAMD17-01-1-0129 and DAMD17-01-1-0130 from Congressionally Directed Medical Research Programs to YM. The opinions and assertions contained herein are the private viewpoints of the authors and do not reflect the official views of The Department of Defense or The Army.

## References

1. Sternlicht MD, Barsky SH: **The myoepithelial defense: a host defense against cancer.** *Med Hypotheses* 1997, **48**:37-46.
2. Masood S, Sim SJ, Lu L: **Immunohistochemical differentiation of atypical hyperplasia vs. carcinoma in situ of the breast.** *Cancer Detect Prev* 1992, **16**:225-235.
3. Bose S, Derosa CM, Ozzello L: **Immunostaining of type IV collagen and smooth muscle actin as an aid in the diagnosis of breast lesions.** *Breast J* 1999, **5**:194-201.
4. Joshi MG, Lee AK, Pedersen CA, Schnitt S, Camus MG, Hughes KS: **The role of immunocytochemical markers in the differential diagnosis of proliferative and neoplastic lesions of the breast.** *Mod Pathol* 1996, **9**:57-62.
5. Blacque OE, Worrall DM: **Evidence of a direct interaction between the tumorsuppressor serpin, maspin, and types I and III collagen.** *J Biol Chem* 2002, **277**:10783-10788.
6. Maass N, Hojo T, Zhang M, Sager R, Jonat W, Nagasaki K: **Maspin - a novel protease inhibitor with tumor suppressing activity in breast cancer.** *Acta Oncol* 2000, **39**:931-934.
7. Zou Z, Zhang W, Young D, Gleave MG, Rennie P, Connell T, Connolly R, Moul J, Srivastava S, Sesterhenn I: **Maspin expression profile in human prostate cancer (CaP) and in vitro induction of Maspin expression by androgen ablation.** *Clin Cancer Res* 2002, **8**:1172-1177.
8. Reis-Filho JS, Milanezi F, Silva P, Schmitt FC: **Maspin expression in myoepithelial tumors of the breast.** *Pathol Res Pract* 2001, **197**:817-821.
9. Schamhorst V, van der Eb AJ, Jochemsen AG: **WT1 proteins: functions in growth and differentiation.** *Gene* 2001, **273**:141-161.
10. Fabre A, McCabb AH, O'Shea D, Broderick D, Keating G, Tobin B, Gorey T, Dervan PA: **Loss of heterozygosity of the Wilms' tumor suppressor gene (WT-1) in in-situ and invasive breast carcinoma.** *Hum Pathol* 1999, **30**:661-665.
11. Zapata-Benavides P, Tuna M, Lopez-Berestein G, Tari AM: **Down-regulation of Wilms' tumor 1 protein inhibits breast cancer proliferation.** *Biochem Biophys Res Commun* 2002, **295**:784-790.
12. Man YG, Vang RS, Saenger JS, Strauss B, Brattthauer GL, Chen PY, Tavassoli FA: **Co-expression of maspin and Wilms' tumor 1 proteins in mammary myoepithelial cells - Implication for tumor progression and invasion.** In *Proceedings of Department of Defense Breast Cancer Research Program Meeting: September 25-28, 2002; Orlando, Florida.* Edited by US Army Medical Research and Material Command. Fort Detrick, Maryland, USA: Office of the Commanding General; 2002: vol 1 9,16.
13. Mahendran R, McIlhinney R, O'Hare M, Monaghan P, Gusterson B: **Expression of the common acute lymphoblastic leukaemia antigen (CALLA) in the human breast.** *Mol Cell Probes* 1989, **3**:39-44.
14. Iwaya K, Ogawa H, Izumi M, Kuroda M, Mukai K: **Stromal expression of CD10 in invasive breast carcinoma: a new predictor of clinical outcome.** *Virchows Arch* 2002, **440**:589-593.
15. Moritani S, Kushima R, Sugihara H, Bamba M, Kobayashi T, Hattori T: **Availability of CD10 immunohistochemistry as a marker of breast myoepithelial cells on paraffin sections.** *Mod Pathol* 2002, **15**:397-405.
16. Yaziji H, Gown AM, Sniege N: **Detection of stromal invasion in breast cancer: the myoepithelial markers.** *Adv Anat Pathol* 2000, **7**:100-109.
17. Damiani S, Ludvikova M, Tomasic G, Bianchi S, Gown AM, Eusebi V: **Myoepithelial cells and basal lamina in poorly differentiated in situ duct carcinoma of the breast. An immunocytochemical study.** *Virchows Arch* 1999, **434**:227-234.
18. Dabbs DJ, Gown AM: **Distribution of calponin and smooth muscle myosin heavy chain in fine-needle aspiration biopsies of the breast.** *Diag Cytopathol* 1999, **20**:203-207.
19. Ohyabu I, Takasaki T, Akiba S, Nomura S, Enokizono N, Sagara Y, Hiroi J, Nagai R, Yoshida H: **Immunohistochemical studies on expression of human vascular smooth muscle myosin heavy chain isoforms in normal mammary glands, benign mammary disorders and mammary carcinomas.** *Pathol Int* 1998, **48**:433-439.
20. Moll R, Franke WW, Schiller DL, Geiger B, Krepler R: **The catalog of human cytokeratins: patterns of expression in normal epithelia, tumors and cultured cells.** *Cell* 1982, **31**:11-24.
21. Bocker W, Moll R, Poremba C, Holland R, van Diest PJ, Dervan P, Burger H, Wai D, Diallo RI, Brandt B, Herbst H, Schmidt A, Lerch MM, Buchwallow IB: **Common adult stem cells in the human breast give rise to glandular and myoepithelial cell lineages: a new cell biological concept.** *Lab Invest* 2002, **82**:737-746.
22. Bocker W, Moll R, Dervan P, Buerger H, Poremba C, Diallo R, Herbst H, Schmidt A, Lerch MM, Buchwallow IB: **Usual ductal hyperplasia of the breast is a committed stem (progenitor) cell lesion distinct from atypical ductal hyperplasia and ductal carcinoma in situ.** *J Pathol* 2002, **198**:458-467.
23. Wetzels RH, Kuijpers HJ, Lane EB, Leigh IM, Troyanovsky SM, Holland R, Van Haelst UJ, Ramaekers FC: **Basal cell-specific and hyperproliferation-related keratins in human breast cancer.** *Am J Pathol* 1991, **138**:751-763.
24. Wetzels RH, Holland R, Van Haelst UJ, Lane EB, Leigh IM, Ramaekers FC: **Detection of basement membrane components and basal cell keratin 14 in noninvasive and invasive carcinomas of the breast.** *Am J Pathol* 1989, **134**:571-579.
25. McGowan KM, Coulombe PA: **Onset of keratin 17 expression coincides with the definition of major epithelial lineages during skin development.** *J Cell Biol* 1998, **143**:469-486.
26. Man YG, Tavassoli FA: **A simple epitope retrieval method without the use of microwave oven or enzyme digestion.** *Appl Immunohistochem* 1996, **4**:139-141.
27. Man YG, Ball WD, Culp AJ, Hand AR, Moreira JE: **Persistence of a perinatal cellular phenotype in the ducts of adult glands.** *J Histochem Cytochem* 1995, **43**:1203-1215.
28. Werling RW, Hwang H, Yaziji H, Gown AM: **Immunohistochemical distinction of invasive from noninvasive breast lesions: a comparative study of p63 versus calponin and smooth muscle myosin heavy chain.** *Am J Surg Pathol* 2003, **27**:82-90.
29. Barbareschi M, Pecciarini L, Cangi MG, Macri E, Rizzo A, Viale G, Dogliani C: **p63, a p53 homologue, is a selective nuclear marker of myoepithelial cells of the human breast.** *Am J Surg Pathol* 2001, **25**:1054-1060.
30. Goldfarb RH, Liotta LA: **Proteolytic enzymes in cancer invasion and metastasis.** *Semin Thromb Hemost* 1986, **12**:294-307.
31. Mignatti P, Robbins E, Rifkin DB: **Tumor invasion through the human amniotic membrane: requirement for a proteinase cascade.** *Cell* 1986, **47**:487-498.
32. Wang F, Weaver VM, Petersen OW, Larabell CA, Dedhar S, Briand P, Lupu R, Bissell MJ: **Reciprocal interactions between  $\beta$ 1-integrin and epidermal growth factor receptor in three-dimensional basement membrane breast cultures: a different perspective in epithelial biology.** *Proc Natl Acad Sci USA* 1998, **95**:14821-14826.
33. Man YG, Saenger JS, Strauss B, Vang RS, Brattthauer GL, Chen PY, Tavassoli FA: **Focal alterations of p27 expression and sub-jacent myoepithelial cell layer disruptions are correlated events in ER<sup>+</sup> ductal intraepithelial neoplasia.** In *Proceedings of Department of Defense Breast Cancer Research Program Meeting: September 25-28, 2002; Orlando, Florida.* Edited by US Army Medical Research and Material Command. Fort Detrick, Maryland, USA: Office of the Commanding General; 2002: vol 1 9,14.

34. Tobacman JK: **Filament disassembly and loss of mammary myoepithelial cells after exposure to lambda-carrageenan.** *Cancer Res* 1997, **57**:2823-2826.
35. Sapino A, Macri L, Tonda L, Bussolati G: **Oxytocin enhances myoepithelial cell differentiation and proliferation in the mouse mammary gland.** *Endocrinology* 1993, **133**:838-842.
36. Man YG, Ball WD, Marchetti L, Hand AR: **Contributions of intercalated duct cells to the normal parenchyma of submandibular glands of adult rats.** *Anat Rec* 2001, **263**:202-214.
37. Gudjonsson T, Ronnov-Jessen L, Villadsen R, Rank F, Bissell MJ, Petersen OW: **Normal and tumor-derived myoepithelial cells differ in their ability to interact with luminal breast epithelial cells for polarity and basement membrane deposition.** *J Cell Sci* 2002, **115**:39-50.

### Correspondence

Yan-Gao Man MD PhD, Department of Gynecologic and Breast Pathology, Armed Forces Institute of Pathology, 6825 16th Street, NW, Washington, DC 20306, USA. Tel: +1 202 782 1612; fax: +1 202 782 -3939; e-mail: man@afip.osd.mil

## An Antigen Unmasking Protocol that Satisfies both Immunohistochemistry and Subsequent PCR Amplification\*

Yan-Gao Man and Ana Bugar

Department of Gynecologic and Breast Pathology, Armed Forces Institute of Pathology (AFIP) and American Registry of Pathology (ARP), Washington, USA

### Summary

Immunohistochemical elucidation of many proteins in formalin-fixed, paraffin-embedded tissues requires a prior antigen unmasking treatment, which often damages both the morphology and genetic materials, making subsequent assessments difficult or impossible. This study attempted to develop a method that satisfies both immunohistochemical and genetic analyses. Consecutive sections were made from formalin-fixed, paraffin-embedded breast and other tissues, and a set of four adjacent sections from each case were treated with (1) routine H & E staining; (2) our unmasking protocol; (3) microwave oven irradiation; (4) pressure cooker incubation. After immunohistochemical staining, the tissue in each section was scraped off, or the same cell clusters in four sections were separately microdissected for DNA extraction and PCR amplification. Compared to microwave and pressure cooker methods, our protocol showed the following advantages: (1) a better preservation of the morphology; (2) a substantial reduction of tissue detachment from slides; (3) effectiveness on all antibodies tested, including those requiring enzyme digestion or no prior unmasking; (4) higher PCR yields; (5) larger (higher molecular weight) amplified PCR products. Compared to the routine method on untreated tissues, our method consistently produced a comparable quality and quantity of PCR products. Our protocol, however, takes a longer time to yield results.

\* The opinions and assertions contained herein represent the personal views of the authors and are not to be construed as official or as representing the views of the Department of the Army or the Department of Defense.

**Key words:** Histotechniques – Antigen unmasking protocol – Immunohistochemical and molecular correlation – Polymerase chain reaction (PCR) – Microdissection

### Introduction

Genetic alterations determine the scope and extent of, and also precede, biochemical abnormalities, whereas the latter is the direct cause for a vast majority of human diseases and pathological processes [6, 21]. Therefore, the assessment of the correlation between genetic and biochemical events holds significant promises in assisting clinical diagnosis and treatment. The introduction of several novel protocols has made it possible to correlate the immunohistochemical and molecular events in frozen and ethanol-fixed, paraffin-embedded tissues [2–4]. The assessment in formalin-fixed, paraffin-embedded tissues, however, has been hampered by the lack of a reliable protocol that satisfies both immunohistochemical and subsequent molecular procedures. Because of the “cross-links” induced by the formalin fixation, the immunohistochemical elucidation of a wide variety of gene products, including p53 and most oncoproteins, growth factors and their receptors, different

**Address for correspondence:** Yan-Gao Man, Gynecologic and Breast Research Laboratory, Department of Gynecologic and Breast Pathology, Armed Forces Institute of Pathology and American Registry of Pathology, 6825 16<sup>th</sup> Street, NW, Washington, DC 20306-6000, USA.  
Phone: 202-782-0507, Fax: 202-782-3939.  
E-mail: [man@afip.osd.mil](mailto:man@afip.osd.mil)

hormone receptors, as well as most cell proliferation related molecules, requires a prior antigen unmasking treatment using a proteolytic enzyme or high temperature [8, 18, 22]. The application of these antigen unmasking methods, however, is often a difficult task, as an under-treatment could yield false negative results, whereas an overtreatment could damage the morphology and genetic materials, making further analyses difficult or impossible [1, 7, 19]. In a recent study, DNA extracts from formalin-fixed, paraffin-embedded tissue sections pretreated with trypsin or heating in a pressure cooker or a microwave oven were subjected to PCR amplification for a 110-bp portion of the beta-globin gene [20]. The PCR efficiency was evaluated by two parameters: (1) the cycle count in which the first visible band was obtained ( $CYCLE_{min}$ ) and (2) the maximum amount of PCR products ( $CONC_{max}$ ). The study found that the trypsin treatment significantly prolonged the  $CYCLE_{min}$  ( $p < 0.01$ ), and PCR amplification did not reach the "plateau" level with a maximum of 60 cycles. The PCR efficiency was worse in microwave or pressure cooker treatment, with neither  $CYCLE_{min}$  nor  $CONC_{max}$  being obtained [20]. The authors concluded that "A successful PCR amplification may not be expected in sections that are pretreated in a microwave oven or pressure cooker" [20].

Attempting to reduce the destructive effects of antigen unmasking methods on tissues, we had previously developed an antigen unmasking protocol which involves a 30–60 minute incubation of paraffin sections at 80 °C and an overnight incubation of deparaffinized sections in a regular oven at 70 to 80 °C in 10 mM citrate buffer [9]. With this protocol, a variety of cytoplasmic and nuclear antigens known to require microwave irradiation or enzymatic digestion for their optimal detection could be clearly demonstrated with better preservation of the morphology, less background, and more uniform immunoreactivities. Our subsequent study further revealed that this protocol not only facilitated the immunohistochemical detection of estrogen receptor (ER) proteins, but also facilitated the detection of ER mRNA with *in situ* hybridization and *in situ* RT PCR techniques [10], suggesting that this protocol might be able to satisfy both immunohistochemical and subsequent molecular biological assessments. This study intended to confirm previous findings by comparing the PCR efficiencies among immunostained tissues that were pre-treated with our protocol or under a high temperature using a microwave oven or a pressure cooker.

## Materials and Methods

### Reagents and instrument

Xylene, ethanol, and hematoxylin were obtained from Fisher Scientific (Pittsburgh, PA). Positively charged

microscope slides were purchased from CMS (Houston, TX). A pressure cooker designated for the antigen retrieval procedure along with the antigen retrieval solution were purchased from Biocare Medical (Walnut Creek, CA). A microwave was commercially purchased and inspected by a certified technician of our institute. Immunohistochemical staining reagents were from Vector Laboratories (Burlingame, CA). DNA extraction-related reagents were obtained from Sigma (St. Louis, MO). An automated 377 DNA sequencer along with the software and the User's Manual, PCR amplification kits, and the DNA size standard, were from Perkin-Elmer (Foster City, CA). A total of 15 fluorescent dye-labeled primer sets were purchased from Research Genetics (Huntsville, AL), and the DNA sequence for each primer set is available at public data bases. Electrophoresis reagents, including 40% polyacrylamide gel solution, ammonium persulfate, and TEMED, were from Bio-Rad (Forster City, CA).

### Tissue samples

Formalin-fixed, paraffin-embedded breast and other tissues (including lung, cervix, and prostate) were retrieved from the files of Armed Forces Institute of Pathology. Consecutive sections of 4–5  $\mu$ m thickness were cut and placed on positively charged microscope slides. To minimize contamination or carrying over that may interfere with a subsequent molecular analysis, a "clear" cutting method was used, which involves the use of distilled water, gloves, and a new blade for each case.

### Antigen retrieval procedure

A set of four consecutive sections containing the same tissue structures were prepared from each of selected breast ( $n = 45$ ), cervical ( $n = 25$ ), lung ( $n = 18$ ), and prostate ( $n = 5$ ) tumors, and sections were treated as follows:

#### *Routine H & E stain*

Sections were routinely deparaffinized with xylene cleaned in ethanol and water, and processed for DNA extraction, as described previously [11].

#### *Our antigen unmasking protocol*

Sections were first incubated in a regular oven at 80 °C for 30 minutes and were deparaffinized with xylene and cleaned in ethanol and water. Deparaffinized sections were incubated overnight with 1X antigen retrieval solution or with home-made 10 mM sodium citrate buffer [9] in a regular oven at 65–80 °C and then processed for immunostaining.

#### *Microwave oven irradiation*

Sections were routinely deparaffinized with xylene and cleaned in ethanol and water. Antigen unmasking was

carried out according to a commonly practiced protocol [22], which involves a 10 minute (2 × 5 minutes) irradiation of deparaffinized sections in 10 mM citrate buffer. After the microwave irradiation, sections were cooled at room temperature and processed for immunostaining.

#### *Pressure cooker incubation*

Sections were routinely deparaffinized with xylene and cleaned in ethanol and water. Antigen unmasking was carried out according to the protocol provided by the manufacturer. Briefly, the deparaffinized sections were

placed in warm 1X antigen retrieval solution and heated in the pressure cooker for 3 minutes. After heating, sections were transferred to fresh 1X antigen retrieval solution and heated under the same condition for 10 minutes. Then, sections were cooled at room temperature for 10 minutes and processed for immunostaining.

#### **Immunohistochemical staining**

The antibodies tested and manufacturers' recommendations for the prior treatment are listed in Table 1. Im-

**Table 1.** Antibodies tested and manufacturer's recommendation for pretreatment

No	Antibody	Manufacturer	Manufacturers recommend pretreatment
1	AR	Vector	Microwave oven or pressure cooker
2	Bcl-2	Vector	Same as above
3	CD10	Vector	Same as above
4	CD31	Vector	Same as above
5	CD44	Vector	Same as above
6	CD117	Vector	Same as above
7	c-erbB 2	Vector	Same as above
8	CK5	Vector	Same as above
9	CK8	Vector	Same as above
10	CK 34βE12	Vector	Same as above
11	CK AE1/AE3	Vector	Same as above
12	Collagen 4	Dako	Same as above
13	Cyclin A	Vector	Same as above
14	Cyclin D3	Vector	Same as above
15	E-Cadherin	Vector	Same as above
16	EGFR	Vector	Same as above
17	ER	Vector	Same as above
18	Ets-1	Vector	Same as above
19	Ki-67	Dako	Same as above
20	Maspin	Vector	Same as above
21	P16	NeoMarkers	Same as above
22	P21	Dako	Same as above
23	P24	Vector	Same as above
24	P27	Vector	Same as above
25	P53	Dako	Same as above
26	PR	Vector	Same as above
27	Topoisomerase IIα	Vector	Same as above
28	WT-1	Cell Marque	Same as above
29	Vimentin	Vector	Same as above
30	Calponin	Vector	Trypsin digestion (TD)
31	CD34	Vector	TD
32	CK10	Vector	TD
33	CK19	Vector	TD
34	ESA	Vector	TD
35	Fibronectin	Vector	TD
36	Tenancy	Vector	TD
37	SMA	Vector	TD or None
38	PAP	Vector	None
39	PCNA	Vector	None
40	PS2	Vector	None
41	PSA	Vector	None
42	S100	Vector	None
43	EMA	Vector	None



munohistochemical staining was carried out as described previously [9, 12]. Briefly, differently treated tissue sections were incubated in 0.3% H<sub>2</sub>O<sub>2</sub> in methanol for 30 minutes to block endogenous peroxidase activity and in 10% normal serum in PBS to eliminate nonspecific binding.

Then, sections were incubated with primary antibody or control solution for 1–3 hours at room temperature or overnight at 4 °C. After incubation, sections were washed with PBS and sequentially incubated with biotinylated secondary antibody, avidin-peroxidase or avidin-alkaline phosphatase solution, and finally with a chromogen. For double or triple immunostaining, the stained sections were first incubated in PBS in 80 °C for 5 minutes to inactivate possible enzyme residuals, then with a new antibody, as described above.

#### Microdissection and DNA extraction

After immunohistochemical staining, the tissue in each of the sections was scraped off the slide and placed in a separate PCR tube for DNA extraction. Since tissue detachments were often seen in sections treated with the microwave oven or pressure cooker method, microdissection was used to obtain a comparable number of cells from the same and well-preserved areas in different sections of the same case. Microdissection was carried out manually under a microscope for large and easily separable tissues or with a computer-based laser capture microdissection machine for small samples. Microdissected cells from each of the four sections in the same case were identically treated for DNA extraction and subsequent PCR amplification and detection to further ensure that the comparison among the samples was carried out under the same conditions (except the prior treatment).

#### PCR amplification, electrophoresis, and gel image analysis

A panel of 15 DNA markers at 6 different chromosomes was used for the comparison of the PCR efficiencies among different samples. The expected sizes of amplified PCR products among DNA markers varied from 95 to 290 base pairs (bp). The main features of the DNA markers are listed in Table 2. An equal amount of DNA extract (1.0–1.5 µl) from each sample was mixed with 10 µl of PCR solution containing a pair of fluorescence labeled primers. The mixture was covered with 40 µl of mineral oil. PCR amplification was carried out in a programmable thermal cycler (Perkin-Elmer, Forster City,

**Table 2.** DNA markers used for comparison of PCR efficiencies among samples

#	Name	Chromosomal location	Size (base pairs)
1	D3S1067	3p21.1–14.3	95
2	D13S219	13q12.3–q13	117–127
3	D13S119	13q14.3–q22	120–140
4	D3S1311	3q27–qter	134–152
5	D8S137	8p21.3–p11.1	150–162
6	D11S29	11q23.3	143–163
7	D13S263	13q14.1–14.2	145–165
8	D16S402	16q24.2	161–187
9	D17S791	17q	165–199
10	D11S904	11p14–p13	185–201
11	D17S785	17q11–q23	181–207
12	D8S505	8p	203–213
13	D3S1300	3p21.1–p14.2	217–241
14	D11S914	11p13–p12	275–285
15	D16S518	16q23.1–q24.2	272–290

CA) at the following settings: after a denaturation at 94 °C for 10 min, samples were amplified for 35–40 cycles at 94 °C, 55 °C, and 72 °C, each for 1 min with a final extension at 72 °C for 10 min. After amplification, an equal volume of the PCR product from each sample was mixed with the loading buffer, and the same amount of mixtures from each sample was subjected to electrophoresis in 5–6% polyacrylamide gels. The amplified PCR products were detected with a 377 DNA sequencer (Perkin-Elmer, Forster City, CA), and the gel images were produced in accordance with the manufacturer's specifications and with our recently developed protocols [13, 14]. The specific PCR products were located, and the intensity of the DNA bands and the height of the peaks in different samples were compared [15].

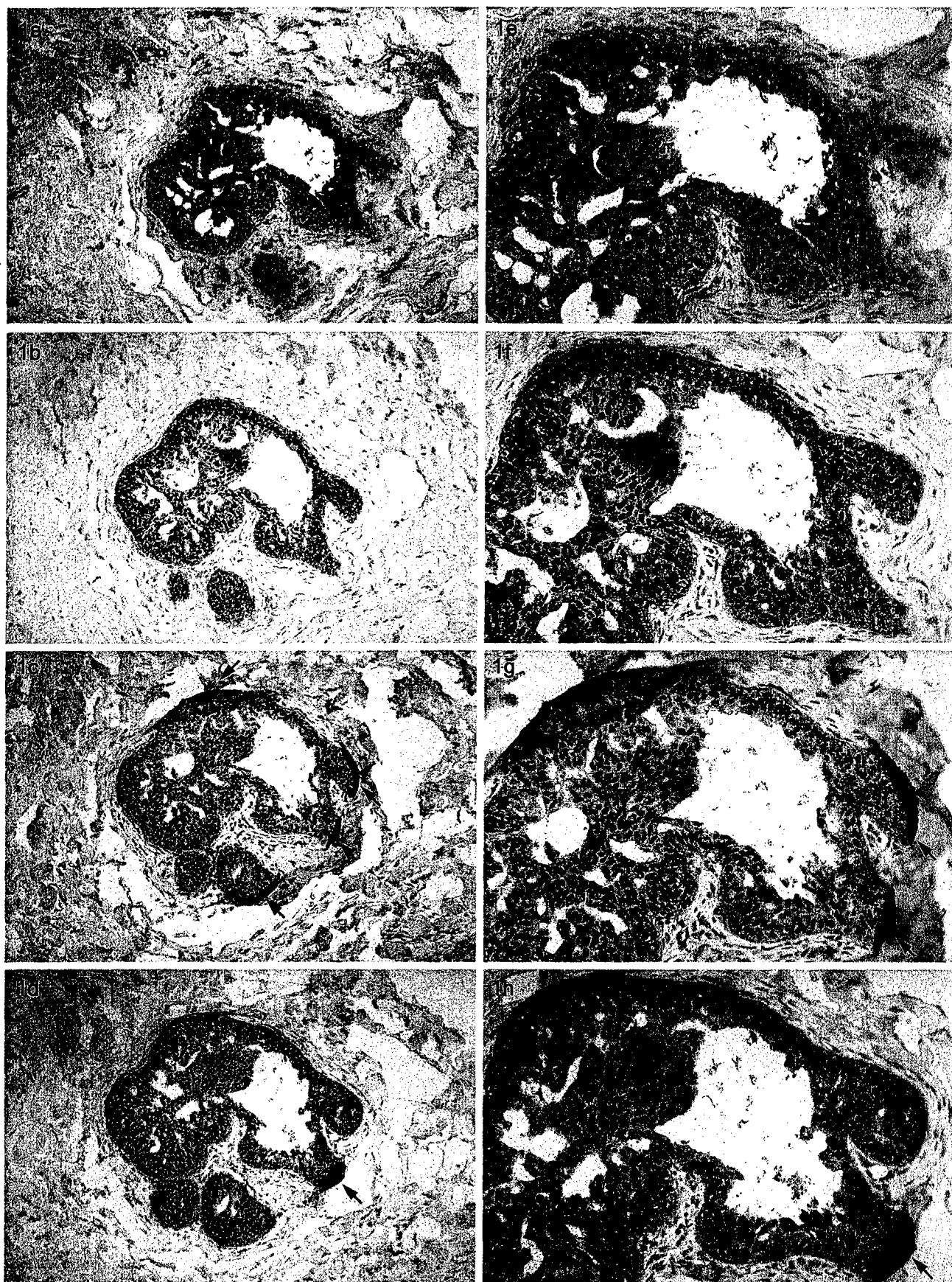
## Results

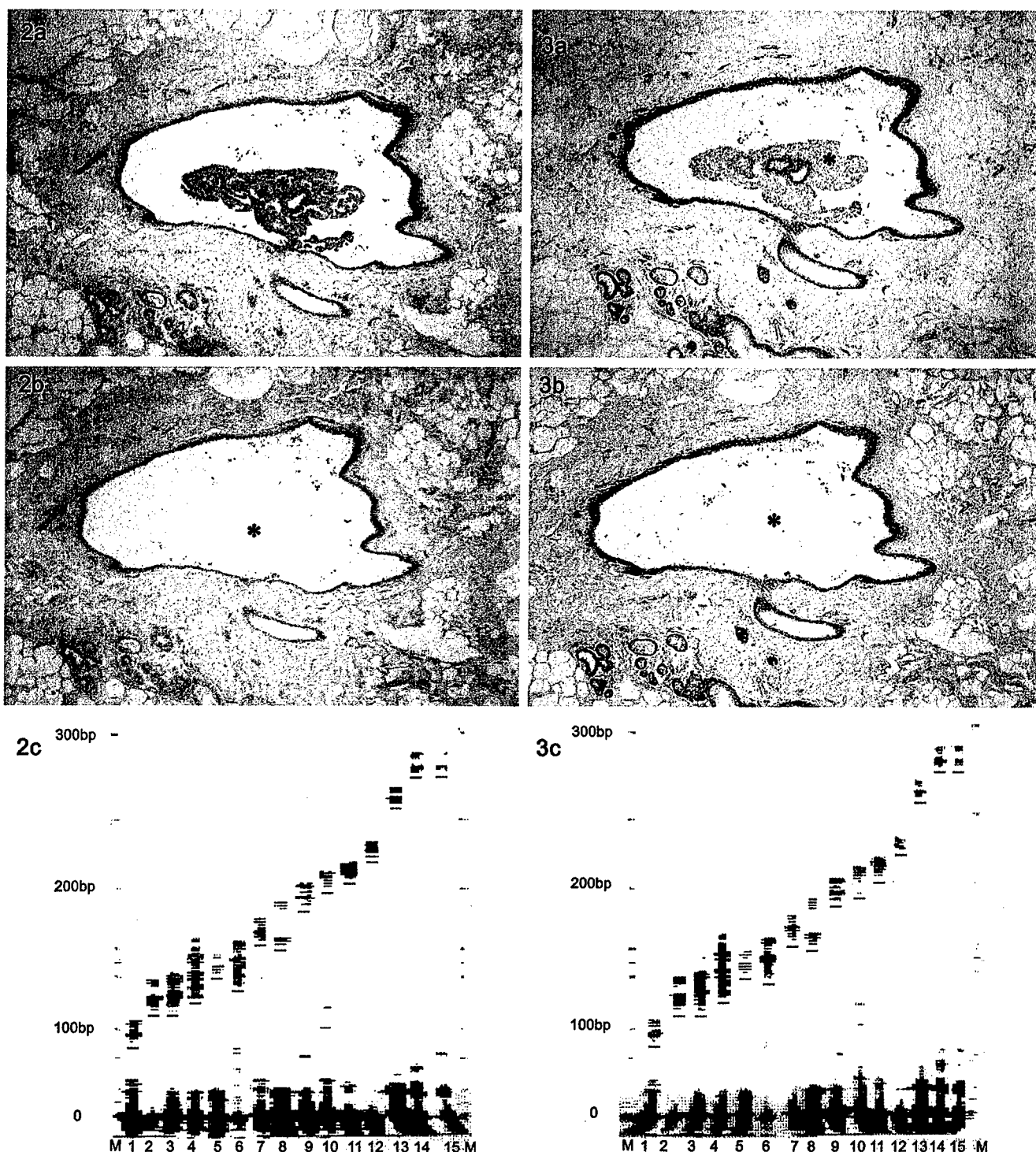
According to the manufacturers, 29 of the 43 antibodies listed in Table 1 require microwave irradiation or pressure cooker incubation, 8 require enzymatic digestion, and 6 require no special treatment for the optimal demonstration of the corresponding antigens. However, using our protocol of an overnight incubation at 65–80 °C, distinct immunostaining was readily appreciable for each of the 43 antibodies. Compared to other

**Figs. 1a–1h.** Immunohistochemical staining for ER (brown) and ESA (red) in pretreated sections with different antigen unmasking methods. ▶

**1a.** Routine H & E staining; **1b.** Our protocol; **1c.** Microwave oven; **1d.** Pressure cooker. 1e, 1f, 1g, and 1h are the higher magnification of 1a, 1b, 1c, and 1d, respectively.

Arrows identify tissue detachment.

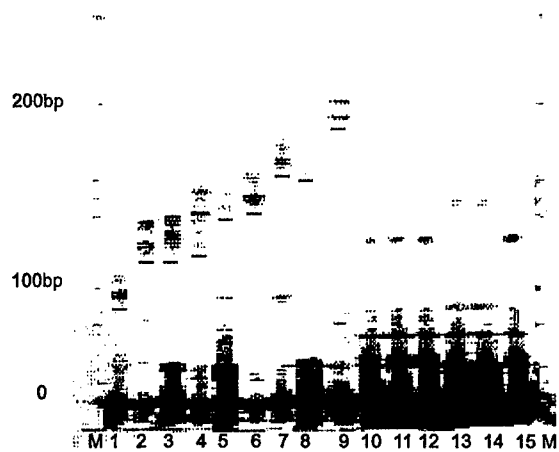




**Figs. 2-5.** Comparison of the PCR efficiencies among cells microdissected from pretreated and immunostained sections. ▲ ► The amplified PCR products of all samples were subject to electrophoresis at an equal volume, and the specific PCR products of each DNA marker were detected with an automated DNA sequencer and underlined with a red line.  
**Fig. 2.** Routine H&E staining; **Fig. 3.** Our protocol; **Fig. 4.** Microwave oven; **Fig. 5.** Pressure cooker.  
**a.** before microdissection; **b.** after microdissection; **c.** amplified PCR products.  
Arrows identify tissue detachments; Asterisks indicate tissues removed for DNA extraction and PCR amplification; M = DNA size marker; 1-15: DNA markers listed in Table 2.

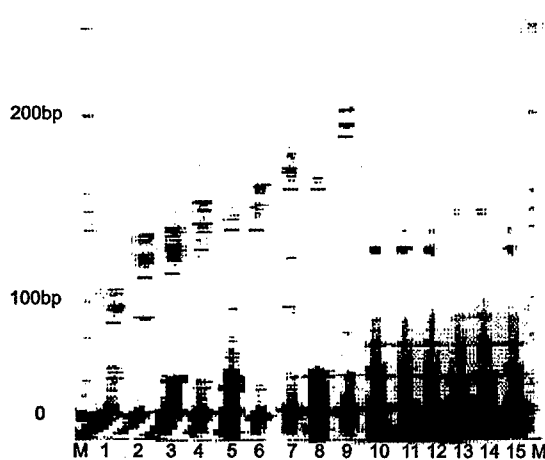


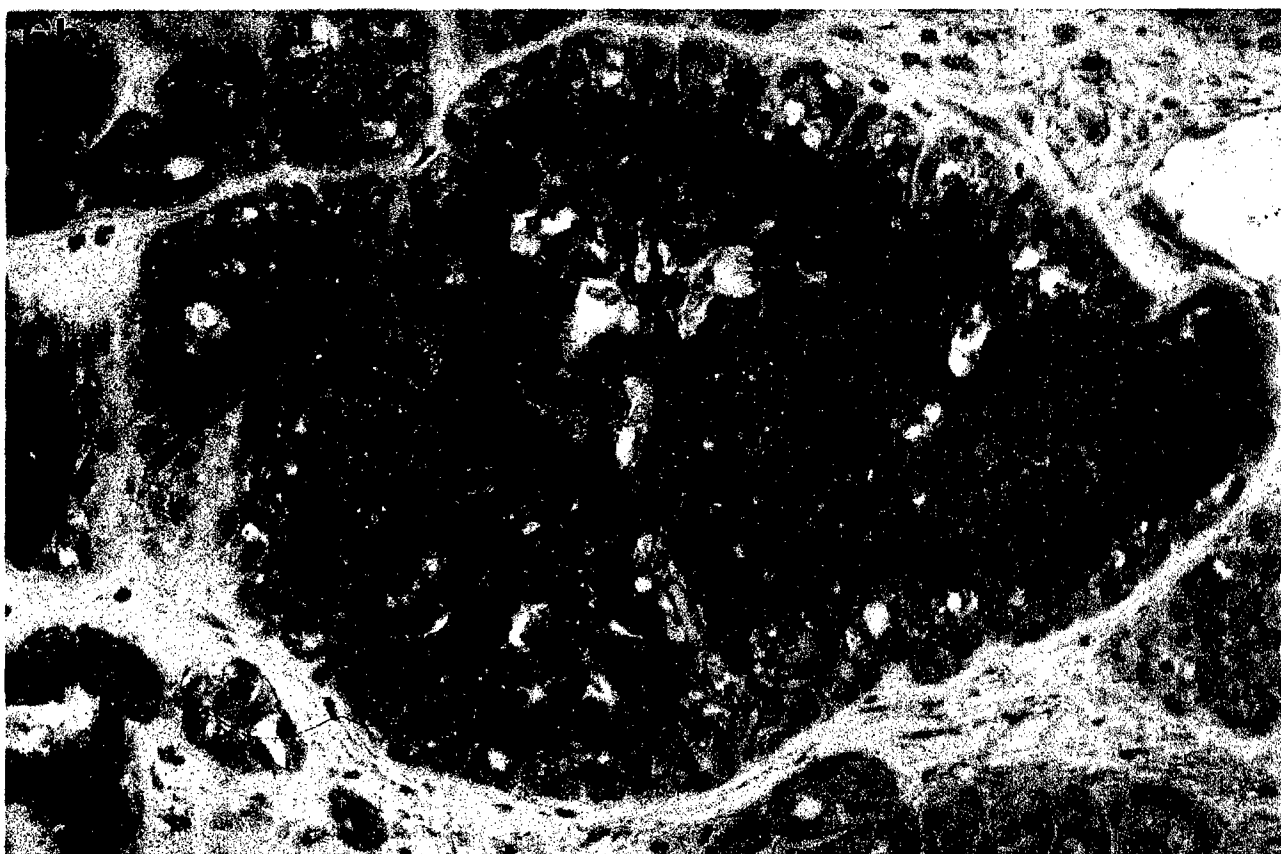
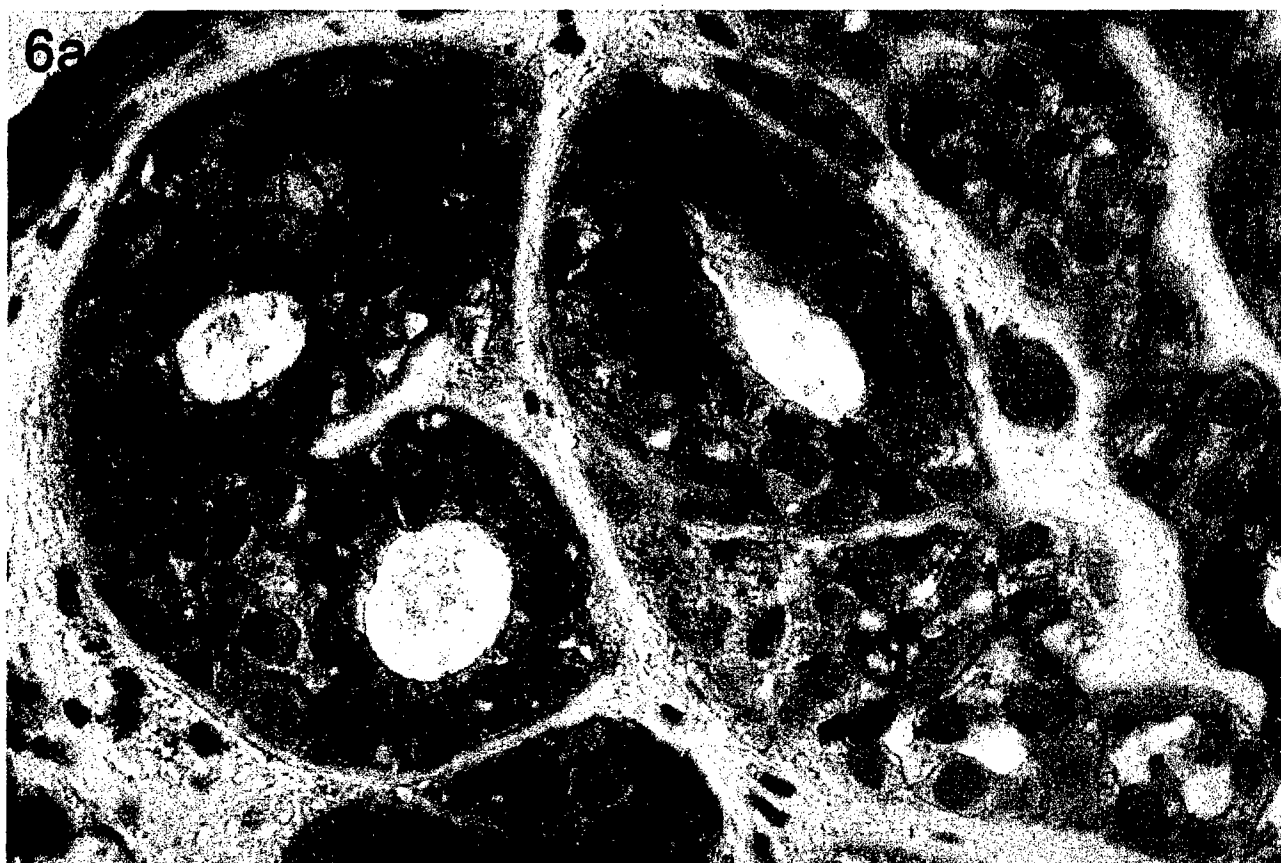
4c 300bp



5c

300bp







antigen unmasking treatments on the adjacent sections, our protocol also possesses the following advantages: (1) a better preservation of the morphological detail; (2) a substantial reduction of tissue detachments from slides. Figures 1a to 1h show such comparisons in four adjacent sections pretreated with different methods.

Under the same volume and PCR conditions, DNA extracts from tissues scraped off or microdissected from sections pretreated with our protocol consistently generated higher PCR yields and also produced PCR products with higher molecular weights, compared to DNA extracts from tissue sections pretreated with microwave oven irradiation or pressure cooker incubation. DNA extracts from tissues scraped off or microdissected from sections pretreated with our protocol consistently generated a similar quality and quantity of PCR products, compared to DNA extracts from routine H&E-stained sections. Figures 2 to 5 show tissues microdissected from each of the four adjacent sections and the comparisons of the resultant PCR products.

Our protocol is also effective for antigens that require enzyme digestion or no pretreatment for their optimal elucidation. Figures 6a and 6b show triple immunohistochemical staining in the same section pretreated with our protocol for three different antigens, Ki-67, epithelial-specific antigen, and smooth muscle actin, which require three different treatments for their optimal detection.

## Discussion

Antigen unmasking methods, using either microwave oven or pressure cooker under a high temperature, or proteolytic digestion with different enzymes, have been routinely used in clinical and research laboratories for the optimal detection of a wide variety of antigens in formalin-fixed, paraffin-embedded tissues [8, 18, 22]. These methods, however, are not easy to use, since an over-treatment could result in the destruction of the morphology and detachment of the tissues, while an under-treatment may yield false-negative results [1,7,19]. Unfortunately, there are no objective criteria available to monitor the unmasking process, or to assess the unmasking effects before the completion of the entire immunostaining process. Therefore, a series of pre-tests have to be conducted to identify the optimal condition. A number of studies have shown that the optimal condition for different antigens varies substantially; also, the optimal condition for the same antigen changes with the type of the tissues, length of the fixation, and

thickness of the sections [1, 7, 19]. Consequently, the identification of the optimal condition for multiple antigens could be a time- and reagent-consuming process or is impossible to achieve if there are only limited sections available. In contrast, our protocol is easy and safe to use, as it only involves an overnight incubation of the deparaffinized sections in a regular oven in antigen unmasking solution. The incubation time and temperature are very flexible, ranging from 65 °C to 80 °C and from less than 10 to over 30 hours, respectively. Also, a variety of solutions could be used to produce a similar or even better result. A recent study [5] has shown that an overnight incubation at 70–80 °C in Tris-HCL buffer (pH 9) could produce more distinct and stronger signals for estrogen receptor, compared to an overnight incubation at the same temperature in sodium citrate buffer (pH 6). Our method is also effective on all the tissues tested, including lung, ovary, cervix, and prostate, and is effective on tissues received from different institutes or different countries. In addition, our recent study obtained distinct immunohistochemical staining for androgen receptor and cytokeratin 34βE12 from rat submandibular glands that were fixed in formalin for over 20 days.

Our preference for an overnight incubation at  $\approx 70$  °C in sodium citrate buffer is based on three reasons or assumptions: (1) this temperature is higher than the melting point temperature of all subtypes of paraffin, such that it could dissolve and wash off any possible paraffin residue that repels water-based solutions, preventing the physical contact between tissues and reagents; (2) this temperature is lower than the denaturing temperature of DNA, RNA, and many proteins, such that it may have less destructive effects on these molecules, preventing tissue loss or detachment from the slides; (3) the citrate buffer is acidic (pH 6), which might be able to gradually disrupt the masking proteins and "cross-links" induced by formalin fixation, increasing the accessibility of probes or antibodies to their targets. Consistent with our assumptions, our previous study has shown that our protocol not only facilitates immunohistochemical detection of estrogen receptor (ER) proteins, but also facilitates the detection of ER mRNA with the *in situ* hybridization and *in situ* RT PCR techniques [10]. In our current study, the quality and quantity of amplified PCR products are consistently better and higher in DNA extracts from tissues pretreated with our unmasking method than those from tissues pretreated with a microwave oven or pressure cooker and are very comparable to those from the adjacent untreated control tissues, further supporting our assumptions.

◀ **Figs. 6a–6b.** Triple immunohistochemical staining in a section pretreated with our protocol.

1. Ki-67 (black) recommended for a pretreatment with microwave oven or pressure cooker; 2. ESA (brown) recommended for a pretreatment with trypsin digestion; 3. SMA (red), pretreatment is not needed.

Our assumptions were additionally supported by the results of a most recent study [23], which compared the DNA yields and PCR efficiencies among 33 serial sections of formalin-fixed, paraffin-embedded tissues that were inserted into 33 microtubes and subjected to antigen retrieval under three temperatures (80, 100, and 120 °C) and 11 variable pH values [2–12]. The study revealed that the incubation of tissues at a higher temperature and at pH 6–9 gave higher yields of DNA, and that the PCR products of these DNA extracts were comparable to those of the control sample subjected to the standard, non-heating, enzymatic DNA extraction method [23].

Taken together, these results suggest that our antigen unmasking protocol could satisfy both the immunohistochemical and subsequent molecular analyses in formalin-fixed, paraffin-embedded tissues. With our protocol, we have recently revealed a subset of morphologically comparable tumor cells, within the same duct, that display substantially different immunoreactivities to estrogen receptor and also showed a different genetic profile [16, 17]. These findings suggest that our protocol may have both scientific and clinical values in assisting the assessment of the correlation between genetic and biochemical events in cells with antigens that could not be elucidated without a pre-antigen unmasking treatment. The drawback of our protocol, however, is that a significantly longer time is needed to complete the experimental procedure.

**Acknowledgement.** The authors are grateful to Doug Landry and Jomie Nola of AFIP Exhibition Section and Kenneth J. Vitacnik of AFIP Photography Lab for their technical assistance in preparing some of the figures.

This study was supported in part by The Congressional Directed Medical Research Programs, grants DAMD 17-01-0129 and DAMD17-01-0130 to Yan-gao Man, M.D., Ph.D.

## References

1. Dookham DB, Kovatich AJ, Miettinen M (1993) Non-enzymatic antigen retrieval in immunohistochemistry: Comparison between different antigen retrieval modalities and proteolytic digestion. *Appl Immunohistochem* 1: 149–155
2. Ehrig T, Abdulkadir SA, Dintzis SM, Milbrandt J, Watson MA (2001) Quantitative amplification of genomic DNA from histological tissue sections after staining with nuclear dyes and laser capture microdissection. *J Mol Diagn* 3: 22–25
3. Heinmoller E, Liu Q, Sun Y, Schlake G, Hill KA, Weiss LM, Sommer SS (2002) Toward efficient analysis of mutations in single cells from ethanol-fixed, paraffin-embedded, and immunohistochemically stained tissues. *Lab Invest* 82: 443–453
4. Hirose Y, Aldape K, Takahashi M, Berger MS, Feuerstein BG (2001) Tissue microdissection and degenerate oligonucleotide primed-polymerase chain reaction (DOP-PCR) is an effective method to analyze genetic aberrations in invasive tumors. *J Mol Diagn* 3: 62–67
5. Koopal SA, Coma MI, Tiebosh ATMG, Suurmeijer AJI (1998) Low temperature heating overnight in Tris-HCl buffer (pH9) is a good alternative for antigen retrieval in formalin-fixed paraffin-embedded tissue. *Appl Immunohistochem* 6: 228–233
6. Lengauer C, Kinzler KW, Vogelstein B (1998) Genetic instabilities in human cancers. *Nature* 369: 643–649
7. Leong ASY, Milios J (1993) An assessment of the efficiency of the microwave antigen-retrieval procedure on a range of tissue antigens. *Appl Immunohistochem* 1: 267–274
8. Magi-Galluzzi C, Montironi R, Prete E, Kwan PW, DeLellis RA (1996) Effect of microwave oven heating times on androgen receptor antigen retrieval from paraffin-embedded prostatic adenocarcinoma. *Anticancer Res* 16: 2931–2936
9. Man YG, Tavassoli FA (1996) A simple epitope retrieval method without the use of microwave Oven or enzyme digestion. *Appl Immunohistochem* 4: 139–141
10. Man YG, Zhaung ZP, Bratthauer GL, Bagasra O, Tavassoli FA (1996) Detailed RT-PCR protocol For preserving morphology and confining PCR products in routinely processed paraffin Sections. *Cell Vision* 3: 389–396
11. Man YG, Moinfar F, Bratthauer GL, Kuhls EA, Tavassoli FA (2001) An Improved Method for DNA extraction from Paraffin Sections. *Pathol. Res. Pract* 197: 635–642
12. Man YG, Ball WD, Culp DJ, Hand AR, Moreira JE (1995) Persistence of a perinatal cellular phenotype in submandibular glands of the adult rat. *J Histochem Cytochem* 43: 1203–1215
13. Man YG, Moinfar F, Bratthauer GL, Tavassoli FA (2000) Five useful approaches for generating more valid gel images of LOH and clonality analysis with an automated 377 DNA sequencer. *Diagn Mol Pathol* 9: 84–90
14. Man YG, Kuhls EA, Bratthauer GL, Moinfar F, Tavassoli FA (2001) Multiple use of stab gels in sequencing apparatus for separation of polymerase chain reaction products. *Electrophoresis* 22: 1915–1919
15. Man YG, Martinez A, Avis IM, Hong SH, Cuttitta F, Venzon DJ, Mulshine JL (2000) Phenotypically different respiratory epithelial cells with hnRNP A2/B1 over-expression display similar genetic alterations. *Am J Respir Cell Mol Biol* 23: 636–645
16. Man YG, Tai L, Barner R, Vang R, Saenger JS, Shekitka KM, Bratthauer GL, Wheeler DT, Liang CL, Vinh TN, Strauss BL (2003) Cell clusters overlying focally disrupted mammary myoepithelial cell layers and adjacent cells within the same duct display different immunohistochemical and genetic features: implications for tumor progression and invasion. *Breast Cancer Res*, In press
17. Man YG, Strauss BL, Saenger JS, Vang RS, Barner R, Wheeler D, Martinez A, Mulshine JL (2003) Identification of invasive precursor cells in normal and hyperplastic appearing breast tissues. *Proceedings of the American Association for Cancer Research* 44: 68 (Abstract)
18. Momose H, Mehta P, Battifora H (1993) Antigen retrieval by microwave irradiation in lead thiocyanate: comparison with protease digestion retrieval. *Appl Immunohistochem* 1: 77–82

19. Munakata S, Hendricks JB (1993) Effect of fixation time and microwave oven heating time on retrieval of the Ki-67 antigen from paraffin-embedded tissue. *J Histochem Cytochem* 41: 1241–1246
20. Murase T, Inagaki H, Eimoto T (2000) Influence of histochemical and immunohistochemical stains on polymerase chain reaction. *Mod Pathol* 13: 147–151
21. Offringa R, van der Burg SH, Ossendorp F, Toes REM, Melief CJM (2000) Design and evaluation of antigen vaccination strategies against cancer. *Curr Opin Immunol* 12: 576–582
22. Shi SR, Key ME, Kalra KL (1991) Antigen retrieval in formalin-fixed, paraffin-embedded tissues: an enhancement method for immunohistochemical staining based on microwave oven heating of tissue sections. *J Histochem Cytochem* 39: 741–748
23. Shi SR, Cote RJ, Wu L, Liu C, Shi Y, Liu D, Lim H, Taylor CR (2002) DNA extraction from archival formalin-fixed, paraffin-embedded tissue sections based on the antigen retrieval principle: heating under the influence of pH. *J Histochem Cytochem* 50: 1005–1011

Received: April 7, 2003

Accepted in revised version: November 27, 2003



OK

# Morphologically Similar Epithelial and Stromal Cells in Primary Bilateral Breast Tumors Display Different Genetic Profiles

## Implications for Treatment

Yan-gao Man, MD, PhD,\* Gregg G. Magrane, PhD,† Ruth A. Lininger, MD,\* Ting Shen, MD, PhD,\* Elizabeth Kuhls, MD,\* Gary L. Brattbauer, MS, MT\*

**Abstract:** The morphologic features of primary bilateral breast carcinoma have been well elucidated, but it is not known whether tumors at two sides share a common genetic profile and undergo the same clinical course. To address this issue, morphologically comparable epithelial and stromal cells in 18 paired primary bilateral breast tumors were microdissected and subjected to comparisons for the frequency and pattern of loss of heterozygosity (LOH) and microsatellite instability (MI), as well as the profiles of comparative genomic hybridization. Of 18 paired bilateral epithelial samples assessed with 10 DNA markers at five chromosomes, 78 altered loci were found; of these, 23 (29.5%) displayed concurrent and 55 (70.5%) showed independent LOH, MI, or both. Of 18 paired bilateral stromal samples assessed with the same markers, 70 altered loci were seen; of these, 9 (12.9%) displayed concurrent and 61 (87.1%) showed independent LOH, MI, or both. Collectively, all the markers and 30 (83.3%) of 36 paired bilateral epithelial and stromal cells displayed significantly more ( $P < 0.01$ ) independent than concurrent LOH, MI, or both. In contrast, the epithelial cells of a pulmonary small cell carcinoma me-

tastasized to both breasts displayed concurrent LOH at each of the four altered loci. Of seven selected cases for comparative genomic hybridization, six (86%) displayed chromosomal changes, but none showed an identical pattern and frequency of changes in both breasts. The significantly higher rate of independent genetic alterations in morphologically comparable cells of paired bilateral primary breast tumors supports the notion that the development and clinical course of tumors in two sides differ substantially; consequently, different interventions might be needed for the optimal management of bilateral breast tumors.

**Key Words:** bilateral primary breast tumor, comparative genomic hybridization, loss of heterozygosity, microsatellite instability, stromal-epithelial interaction

(*Appl Immunohistochem Mol Morphol* 2004;00:000-000)

AU2

Manuscript received; accepted.

From the \*Department of Gynecologic and Breast Pathology, Armed Forces Institute of Pathology and American Registry of Pathology, Washington, DC; †Cancer Center and Department of Laboratory Medicine, University of California, San Francisco, California. Dr. Lininger's current address is Department of Pathology and Laboratory Medicine, University of North Carolina School of Medicine, Chapel Hill, NC; Dr. Shen's current address is Department of Pathology and Laboratory Medicine, Temple University Hospital, Philadelphia, Pennsylvania.

This study was supported in part by grants to Dr. Lininger from American Registry of Pathology (1006-7011) and to Dr. Man from Congressionally Directed Medical Research Programs (DAMD17-01-1-0129 and DAMD17-01-1-0130).

Reprints: Yan-gao Man, MD, PhD, Director of Gynecologic and Breast Research Laboratory, Department of Gynecologic & Breast Pathology, The Armed Forces Institute of Pathology and American Registry of Pathology, 6825 16<sup>th</sup> Street, NW, Washington, DC 20306-6000 (man@afip.osd.mil).

The opinions and assertions contained herein are the private viewpoints of the authors and do not reflect the official views of the Department of Defense or Department of the Army.

Copyright © 2004 by Lippincott Williams & Wilkins

Clinically detected female bilateral primary breast cancers that represent either two independent primary lesions or one primary lesion with metastasis account for 3% to 9% of the total breast malignancies.<sup>1-3</sup> Occult or asymptomatic bilateral cancers, however, have been reported in 34% to 50% of contralateral mastectomy specimens prophylactically removed from patients with a primary breast cancer, in 21% to 68% of autopsy specimens from patients with a history of breast cancer, and in about 10% of mastectomy specimens removed for benign disease.<sup>4-13</sup> The substantially higher incidence of bilateral breast cancers in autopsy and mastectomy specimen than in clinical reports raises several questions: Why are so many contralateral cancers occult or asymptomatic? Will occult or asymptomatic cancers manifest as clinically evident cancers if the patient's life span increases? How could we accurately identify specific individuals with occult or asymptomatic cancer? More importantly, the discrepancy of the incidence of bilateral breast cancers between autopsy and mastectomy specimens and clinical reports suggests that the clinical course of bilateral tumors and the molecular mechanism of tumor pro-

gression in the left and right breast differ substantially, and some of the bilateral carcinomas in one side might either regress or become latent during the patient's lifetime. Consequently, comparisons of the genetic profiles of cells in bilateral breast cancers, especially those with progressive cancer in one side and with a regressive or latent lesion in the other, might lead to identification of specific factors that either promote development and progression or promote regression and latency. The use of the factors that promote regression or latency might provide a novel approach for treatment and prevention of breast cancer.

Based on the above findings and speculations, we hypothesized that the genetic profiles of cells in primary bilateral tumors differ substantially, explaining the discrepancy in the bilateral breast cancer incidence between autopsy and mastectomy specimens and clinical reports. In this study we attempted to test our hypothesis by comparing the frequency and pattern of loss of heterozygosity (LOH) and microsatellite instability (MI) as well as the profiles of comparative genomic hybridization (CGH) in both the epithelial and stromal cells of morphologically similar primary bilateral breast lesions. This study was directed more toward verifying the concept than identifying specific alterations. More selective comparisons will be carried out in patients with a progressive tumor in one side and with a regressive or latent one in the other side, if substantial differences are identified in the paired samples of our current study.

## MATERIALS AND METHODS

### Collection and Classification of Tissue Samples

Formalin-fixed, paraffin-embedded biopsy samples or unstained sections from 18 females with primary bilateral breast tumors were retrieved from the files of Armed Forces Institute of Pathology. Of the 18 patients, 16 were older than 40 years and the other 2 were 17 and 27 years old. Of the 18 paired tumors, 16 occurred synchronously and 2 metachronously. In metachronous tumors, the interval between the first and second tumor was 36 months. Of the 18 paired epithelial lesions, 15 were noninvasive, 2 were invasive, and 1 was metastatic (pulmonary small cell carcinoma with simultaneous metastasis to both breasts). The morphologic classification of the lesions was based on published criteria,<sup>14-16</sup> and the main lesions are listed in Table 1. Breast tissues obtained during bilateral reduction mammoplasty from 10 women who had no clinical, radiologic, or histologic abnormalities were included in the study as external controls.

### Microdissection and DNA Extraction

Serial sections of 5 to 7  $\mu$ m thickness were prepared and processed for morphologic assessment. Morphologically similar epithelial and stromal cells in the left and right breast of each case were manually microdissected under a standard microscope, placed in different tubes, and subjected to DNA ex-

TABLE 1. Age of Patients and Principal Types of Lesions

Case #	Age	Left (year)	Right (year)
1	73	Inf W/lob; <b>DCIS (G2)</b> ; LN 3 (1998)	Inf W/lob; <b>DCIS (G2)</b> ; LN 3 (1998)
2	54	<b>DCIS</b> (1989)	<b>DCIS</b> (1989)
3	63	<b>IDC</b> (G3) (1994)	<b>IDC</b> (G3) (1994)
4	58	<b>DCIS (G1)</b> (1998)	Inv tubular; <b>DCIS (G1)</b> (1998)
5	45	<b>IDC; DCIS (G2)</b> (1999)	<b>IDC (G2); DCIS (G2)</b> (1999)
6	55	<b>DCIS (G1); LN 2</b> (1999)	<b>LN 2; IDH</b> (1999)
7	41	<b>IDC</b> (1989)	<b>IDC</b> (1989)
8	17	<b>AIDH</b> (1997)	<b>AIDH</b> (1997)
9	69	<b>IDC; DCIS</b> (1997)	<b>IDC; DCIS</b> (1997)
10	42	<b>Inf small cell Ca (metastasis)</b> (1989)	<b>Inf small cell Ca (metastasis)</b> (1989)
11	44	<b>AIDH; DCIS (G3); LN 3</b> (1998)	<b>DCIS (G3); IDH</b> (1998)
12	58	Inv lob; <b>LN 2</b> (1999)	<b>IDC (G3); LN 2</b> (1999)
13	63	<b>DCIS (G1)</b> (1999)	<b>IDC; DCIS (G1)</b> (1999)
14	62	Inf lob; <b>LN 2; DCIS</b> (2000)	Inf lob & duct; <b>LN 2</b> (2000)
15	86	<b>DCIS; IDH</b> (1997)	<b>DCIS; IDH</b> (1997)
16	54	<b>DCIS; LN 1</b> (1996)	<b>IDC; DCIS</b> (1996)
17	44	<b>IDC; DCIS (G2); IDH</b> (1995)	<b>LN 2; IDH</b> (1998)
18	27	<b>IDH</b> (2000)	<b>IDC; IDH</b> (1997)

The microdissected samples from each paired lesions are highlighted.

traction as previously described.<sup>17-20</sup> The tumor cells microdissected from each case are listed in Table 1.

The number of microdissected cells from the left and right breast was similar in each of the 18 cases. The histologic type of microdissected cells from the two breasts was homogeneous in each of the 18 cases (see Table 1). Clear-cut normal epithelial and stromal cells at least 1 cm away from the lesions and from the tissues of 10 normal controls were also microdissected and used as internal and external controls.

### Assessment for LOH and MI

Fluorescent dye-labeled polymorphic DNA markers were purchased from Research Genetics (Huntsville, AL). A panel of 10 markers reported to show a high frequency of LOH and MI in a wide variety of mammary carcinomas<sup>17,18</sup> was selected for the LOH and MI assessment (Table 2). Gene Amp PCR kits, Taq gold DNA polymerase, gel loading buffer, and the DNA size standard were purchased from Perkin-Elmer (Foster City, CA). Polymerase chain reaction (PCR) amplification was carried out as previously described.<sup>17-20</sup> After amplification, 2 to 3  $\mu$ L PCR solution was mixed with 6 to 8  $\mu$ L gel loading buffer, and 1.0 to 1.5  $\mu$ L of the mixture was subjected to electrophoresis in 6% polyacrylamide gels. The signal was detected with a 377 DNA sequencer (Perkin-Elmer, Foster City, CA) as previously described.<sup>17-20</sup> All tissue samples amplified with each of the 10 DNA markers were examined for LOH and MI, defined as "the complete absence or at least a 75% reduction of one allele" and as "an addition or deletion of one or more repeat units that result in a shift of micro-satellite alleles," respectively.<sup>17-20</sup> A concurrent LOH was defined as "the loss of an identical allele in cells from both sides for a given marker." An independent LOH was defined as "the loss of an allele in cells from one side, or the loss in cells from two sides at different alleles for a given marker." The samples that failed to produce distinct PCR products after three attempts or showed homozygosity were considered non-

informative. Gel images of LOH in our recently published protocol<sup>23</sup> independent and concurrent LOH, epithelial and stromal samples that were independently statistically compared with the

### CGH

Seven cases (cases 4, 6, 7, 8, 9, 10, and 11) were selected for CGH. Sufficient DNA extracts were selected for CGH according to the protocol of the manufacturer.<sup>23,24</sup> PCR-amplified DNA from the tumor and the normal reference samples were labeled with biotin-14-dATP and fluorescein-12-dUTP (Du Pont NEN, Boston, MA), respectively. The DNA was then hybridized to a CGH array (Gibco BRL, Gaithersburg, MD) containing 500 to 1,000 ng of each labeled DNA. The array was then hybridized to metaphase spreads prepared from normal cells. The slides were washed and processed for CGH as previously described.<sup>23,24</sup> The CGH profiles of each chromosome subregions of each chromosome were analyzed and described.<sup>23,24</sup>

### RESULTS

The left and right breast in all cases were morphologically similar epithelial and stromal cells were generally distributed as described. The acquisition of a relatively uniform LOH and MI in the epithelial and stromal cells from two different

The frequencies and patterns of LOH and MI detected among different DNA markers for LOH, MI, or both were seen in the epithelial and stromal cells with

TABLE 2. DNA Markers Used for Comparison of Genetic Alterations in Paired Bilateral Breast Lesions

Case #	Name	Chromosomal Location	Harbored Gene
1	D3S1300	3p21.1-p14.2	FHIT
2	D3S1481	3p14.2	FHIT
3	D11S904	11p14-p13	Wilms' tumor 1
4	D11S914	11p13-p12	Wilms' tumor 1
5	D13S219	13q12.3-q13	?
6	D13S765	13	?
7	D16S518	16q23.1-q24.2	CDH 1 (adjacent to)
8	D16S402	16q24.2	CDH 1 (adjacent to)
9	D17S791	17q	BRCA 1
10	TP53	17p13	p53

traction as previously described.<sup>17–20</sup> The tumor cells microdissected from each case are listed in Table 1.

The number of microdissected cells from the left and right breast was similar in each of the 18 cases. The histologic type of microdissected cells from the two breasts was homogeneous in each of the 18 cases (see Table 1). Clear-cut normal epithelial and stromal cells at least 1 cm away from the lesions and from the tissues of 10 normal controls were also microdissected and used as internal and external controls.

### Assessment for LOH and MI

Fluorescent dye-labeled polymorphic DNA markers were purchased from Research Genetics (Huntsville, AL). A panel of 10 markers reported to show a high frequency of LOH and MI in a wide variety of mammary carcinomas<sup>17,18</sup> was selected for the LOH and MI assessment (Table 2). Gene Amp PCR kits, Taq gold DNA polymerase, gel loading buffer, and the DNA size standard were purchased from Perkin-Elmer (Foster City, CA). Polymerase chain reaction (PCR) amplification was carried out as previously described.<sup>17–20</sup> After amplification, 2 to 3  $\mu$ L PCR solution was mixed with 6 to 8  $\mu$ L gel loading buffer, and 1.0 to 1.5  $\mu$ L of the mixture was subjected to electrophoresis in 6% polyacrylamide gels. The signal was detected with a 377 DNA sequencer (Perkin-Elmer, Foster City, CA) as previously described.<sup>17–20</sup> All tissue samples amplified with each of the 10 DNA markers were examined for LOH and MI, defined as “the complete absence or at least a 75% reduction of one allele” and as “an addition or deletion of one or more repeat units that result in a shift of micro-satellite alleles,” respectively.<sup>17–20</sup> A concurrent LOH was defined as “the loss of an identical allele in cells from both sides for a given marker.” An independent LOH was defined as “the loss of an allele in cells from one side, or the loss in cells from two sides at different alleles for a given marker.” The samples that failed to produce distinct PCR products after three attempts or showed homozygosity were considered non-

informative. Gel images of LOH and MI were prepared using our recently published protocols.<sup>21,22</sup> The frequencies of independent and concurrent LOH, MI, or both in paired epithelial and stromal samples that were informative at both breasts were statistically compared with the Student *t* test.

### CGH

Seven cases (cases 4, 6, 8, 11, 13, 14, and 15) with sufficient DNA extracts were selected for CGH analysis, which was carried out according to previously published protocols.<sup>23,24</sup> PCR-amplified DNA products from seven selected cases and the normal reference DNA from normal females were labeled with biotin-14-deoxyadenosine triphosphate (14-dATP) and fluorescein-12-deoxyuridine triphosphate (dUTP) (Du Pont NEN, Boston, MA), respectively, using a Bionick kit (Gibco BRL, Gaithersburg, MD). DNA mixtures containing 500 to 1,000 ng of each labeled DNA and 50  $\mu$ g Cot 1 DNA (Gibco BRL) at a total volume of 6 to 8  $\mu$ L were hybridized to metaphase spreads prepared from normal human male lymphocytes for 48 to 72 hours at 37°C. After hybridization, slides were washed and processed for image analysis as previously described.<sup>23,24</sup> The CGH profile was analyzed and changes at subregions of each chromosome were identified as previously described.<sup>23,24</sup>

### RESULTS

The left and right breast in each of the 18 cases contained morphologically similar epithelial and stromal cells, which were generally distributed as distinct cell clusters, facilitating the acquisition of a relatively uniform cell population by microdissection. Figures 1 and 2 show microdissected epithelial and stromal cells from two different cases.

The frequencies and patterns of LOH, MI, or both detected among different DNA markers are listed in Table 3. Distinct LOH, MI, or both were seen among the 36 paired bilateral epithelial and stromal cells with each of the 10 DNA markers,

TABLE 2. DNA Markers Used for Comparison of Genetic Alterations in Paired Bilateral Breast Lesions

Case #	Name	Chromosomal Location	Harbored Gene	Size (Base Pair)
1	D3S1300	3p21.1–p14.2	FHIT	217–241
2	D3S1481	3p14.2	FHIT	104
3	D11S904	11p14–p13	Wilms' tumor 1	185–201
4	D11S914	11p13–p12	Wilms' tumor 1	275–285
5	D13S219	13q12.3–q13	?	117–127
6	D13S765	13	?	193
7	D16S518	16q23.1–q24.2	CDH 1 (adjacent to it)	272–290
8	D16S402	16q24.2	CDH 1 (adjacent to it)	161–187
9	D17S791	17q	BRCA 1	165–199
10	TP53	17p13	p53	104

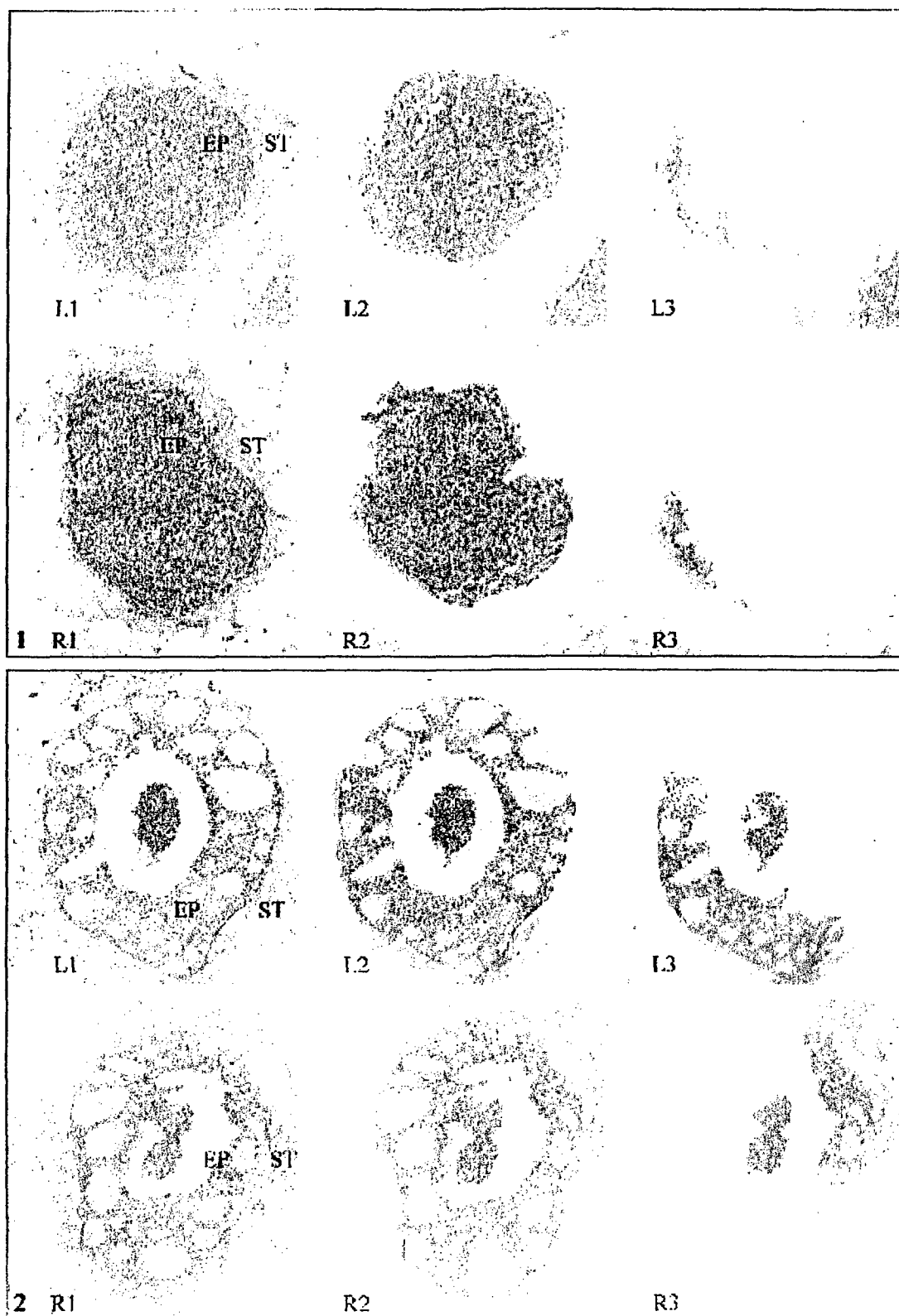


FIGURE 1. Legend on facing page.

while the frequencies varied substantially among markers, ranging from 17.9% (D11S914) to 40.3% (D13S219) in informative loci.

Of 18 paired bilateral epithelial samples assessed with 10 DNA markers at five chromosomes, 78 altered loci were found; of these, 23 (29.5%) showed concurrent and 55 (70.5%) showed independent LOH, MI, or both (see Table 3). Of 18 paired bilateral stromal samples assessed with the same markers, 70 altered loci were seen; of these, 9 (12.9%) showed concurrent and 61 (87.1%) showed independent LOH, MI, or both (see Table 3). Collectively, of the 36 paired samples, 30 (83.3%) showed more independent, 3 (8.3%) showed an equal, and only 3 (8.3%) showed more concurrent LOH, MI, or both (see Table 3). The rate of independent LOH, MI, or both was significantly higher ( $P < 0.01$ ) than that of concurrent LOH and MI in both epithelial and stromal cells (Table 4). The case of pulmonary small cell carcinoma (case 10) with simultaneous metastasis to both breasts, however, showed concurrent LOH at each of the four DNA markers (see Table 3). Figure 3 shows examples of LOH and MI in these paired bilateral epithelial and stromal samples. No distinct LOH or MI was seen in either the epithelial or stromal cells of the 10 bilateral reduction mammoplasty specimens from women having no clinical, histopathologic, or radiologic abnormalities in their breasts.

Results of the CGH assessment are summarized in Table 5. Of the seven selected cases, chromosomal changes (gain or loss of DNA copy numbers) were found in the epithelial component in one side of three cases, in both sides of three cases, and also in the stromal component of two cases. The total CGH changes were distributed in five left and four right breasts. The most common change was a loss of 16q, which was seen in five epithelial components of four cases, followed by a loss of 11q, which was seen in the epithelial and stromal components of three cases. None of the cases that displayed CGH changes, however, showed an identical frequency and pattern of changes in the epithelial component of both breasts (see Table 5). On the other hand, an identical CGH change, a loss of 13q, was detected in both the epithelial and stromal cells of the right breast of one case (case 4). Figure 4 shows the CGH change in each case.

## DISCUSSION

Our findings of LOH and MI assessments were similar to those of another recent study.<sup>25</sup> In that study, tissue sections

from 31 young (age <50) patients with breast cancers were subjected to mutation analysis of tumor susceptibility genes 1 and 2 (BRCA1 and BRCA2) by assessment with six DNA markers. In the 31 (100%) right samples, 3 showed no LOH, and the rest of the 28 paired samples showed LOH at one or more paired chromosomal loci. Of the 28 paired samples, 15 displayed more independent than concurrent LOH. Of the 77 LOH, 44 (57%) were in the left and 34 (44%) in the right breast. Of the 77 LOH, 44 (57%) showed unilateral and 33 (43%) showed bilateral LOH. Also, five of six DNA markers showed independent LOH. In our study, of the 36 paired samples assessed with 10 DNA markers, 78 altered loci were found, of which 23 (29.5%) showed concurrent and 55 (70.5%) showed independent LOH, MI, or both. Of the 18 paired bilateral stromal samples assessed with the same markers, 70 altered loci were found, of which 9 (12.9%) showed concurrent and 61 (87.1%) showed independent LOH, MI, or both. Collectively, all 10 paired bilateral epithelial and stromal samples showed independent LOH, MI, or both. The results of our report<sup>25</sup> are statistically similar to those of a wider age range, the use of more DNA markers.

By CGH, gains or losses were found in one breast in three cases, in both breasts in three cases. The most common change was a loss of 16q, which was seen in five epithelial components of four breasts. A loss of 11q was detected in two epithelial components of four breasts. None of the cases displayed an identical pattern of changes in the epithelial components of both breasts. The epithelial components of both breasts present bilaterally in one woman. An identical CGH change was seen in both the epithelial and stromal components of one breast in one case. To our knowledge, this study reveals the loss of DNA copy numbers by CGH technique. This finding is similar to the results of assessments of our previous study of breast carcinomas, which have revealed

**FIGURE 1.** Examples of microdissection of morphologically similar epithelial and stromal cells from solid tumors. L1: left, before microdissection; L2: microdissection of left stromal (ST) cells; L3: microdissection of left epithelial (EP) cells. R1: right, before microdissection; R2: microdissection of right stromal (ST) cells; R3: microdissection of right epithelial (EP) cells. (Magnification, 100×)

**FIGURE 2.** Examples of microdissection of morphologically similar epithelial and stromal cells from ductal carcinoma in situ. L1: left, before microdissection; L2: microdissection of left stromal (ST) cells; L3: microdissection of left epithelial (EP) cells. R1: right, before microdissection; R2: microdissection of right stromal (ST) cells; R3: microdissection of right epithelial (EP) cells. (Magnification, 100×)

while the frequencies varied substantially among markers, ranging from 17.9% (D11S914) to 40.3% (D13S219) in informative loci.

Of 18 paired bilateral epithelial samples assessed with 10 DNA markers at five chromosomes, 78 altered loci were found; of these, 23 (29.5%) showed concurrent and 55 (70.5%) showed independent LOH, MI, or both (see Table 3). Of 18 paired bilateral stromal samples assessed with the same markers, 70 altered loci were seen; of these, 9 (12.9%) showed concurrent and 61 (87.1%) showed independent LOH, MI, or both (see Table 3). Collectively, of the 36 paired samples, 30 (83.3%) showed more independent, 3 (8.3%) showed an equal, and only 3 (8.3%) showed more concurrent LOH, MI, or both (see Table 3). The rate of independent LOH, MI, or both was significantly higher ( $P < 0.01$ ) than that of concurrent LOH and MI in both epithelial and stromal cells (Table 4). The case of pulmonary small cell carcinoma (case 10) with simultaneous metastasis to both breasts, however, showed concurrent LOH at each of the four DNA markers (see Table 3). Figure 3 shows examples of LOH and MI in these paired bilateral epithelial and stromal samples. No distinct LOH or MI was seen in either the epithelial or stromal cells of the 10 bilateral reduction mammoplasty specimens from women having no clinical, histopathologic, or radiologic abnormalities in their breasts.

Results of the CGH assessment are summarized in Table 5. Of the seven selected cases, chromosomal changes (gain or loss of DNA copy numbers) were found in the epithelial component in one side of three cases, in both sides of three cases, and also in the stromal component of two cases. The total CGH changes were distributed in five left and four right breasts. The most common change was a loss of 16q, which was seen in five epithelial components of four cases, followed by a loss of 11q, which was seen in the epithelial and stromal components of three cases. None of the cases that displayed CGH changes, however, showed an identical frequency and pattern of changes in the epithelial component of both breasts (see Table 5). On the other hand, an identical CGH change, a loss of 13q, was detected in both the epithelial and stromal cells of the right breast of one case (case 4). Figure 4 shows the CGH change in each case.

## DISCUSSION

Our findings of LOH and MI assessments were similar to those of another recent study.<sup>25</sup> In that study, tissue sections

from 31 young (age <50) patients with bilateral primary breast cancers were subjected to mutation analyses for breast cancer susceptibility genes 1 and 2 (BRCA 1 and 2) and to LOH assessment with six DNA markers. Of the 31 paired (left and right) samples, 3 showed no LOH on all six DNA markers. The rest of the 28 paired samples contained a total of 77 LOH at 58 paired chromosomal loci. Of the 28 paired samples, 17 (61%) displayed more independent and 6 (21%) showed more concurrent LOH. Of the 77 LOH, 43 (56%) were distributed in the left and 34 (44%) in the right breast. Of the 58 paired loci, 39 (67%) showed unilateral and 19 (33%) displayed bilateral LOH. Also, five of six DNA markers displayed more independent LOH. In our study, of the 18 paired bilateral epithelial samples assessed with 10 DNA markers at five chromosomes, 78 altered loci were found, of which 23 (29.5%) showed concurrent and 55 (70.5%) showed independent LOH, MI, or both. Of the 18 paired bilateral stromal samples assessed with the same markers, 70 altered loci were seen, of which 9 (12.9%) showed concurrent and 61 (87.1%) showed independent LOH, MI, or both. Collectively, all 10 markers and 30 (83.3%) of 36 paired bilateral epithelial and stromal samples showed more independent whereas only 3 (8.3%) showed more concurrent LOH, MI, or both. The results of our study and the previous report<sup>25</sup> are statistically similar. The slightly higher frequency of independent LOH seen in our study may result from the wider age range, the use of microdissected cells, and more DNA markers.

By CGH, gains or losses of DNA copy numbers were found in one breast in three cases and in both breasts in three cases. The most common change was a loss of 16q, which was seen in five epithelial components of five breasts from four women (three of them were lobular neoplasia lesions). A loss of 11q was detected in two epithelial and two stromal components of four breasts. None of the cases with CGH changes displayed an identical pattern of chromosomal alterations in the epithelial components of both breasts, though 16q loss was present bilaterally in one woman with bilateral lobular neoplasia. An identical CGH change, a loss of 13q, however, was seen in both the epithelial and stromal components of the right breast in one case. To our knowledge, this is the first study that reveals the loss of DNA copy numbers in stromal cells with the CGH technique. This finding is in agreement with LOH assessments of our previous studies on both breast and cervical carcinomas, which have revealed that the epithelial and the

**FIGURE 1.** Examples of microdissection of morphologically similar epithelial and stromal cells from the left and right breast with solid tumors. L1: left, before microdissection; L2: microdissection of left stromal (ST) cells; L3: microdissection of left epithelial (EP) cells. R1: right, before microdissection; R2: microdissection of right stromal (ST) cells; R3: microdissection of right epithelial (EP) cells. (Magnification, 100×)

**FIGURE 2.** Examples of microdissection of morphologically similar epithelial and stromal cells from the left and right breast with ductal carcinoma in situ. L1: left, before microdissection; L2: microdissection of left stromal (ST) cells; L3: microdissection of left epithelial (EP) cells. R1: right, before microdissection; R2: microdissection of right stromal (ST) cells; R3: microdissection of right epithelial (EP) cells. (Magnification, 100×)

TABLE 3. Comparison of Frequency and Pattern of LOH and MI in Paired EP and ST Cells

Case #	Cell Type	Marker								
		1	2	3	4	5	6	7	8	9
1	EP	Ø		Ø	Ind	Ind		Co		Ø
	ST	Ø		Ø	Ind	Co				
2	EP	Ind	Ind				Ø		Ø	
	ST	Ind					Ø		Ø	
3	EP	Ind	Ind		Ø		Ind	Co	Ind	CC
	ST	Ind	Ind	Ind	Ind	Ind		Ind	Ind	In
4	EP	Ind		Ø		Ø		Co	Co	CC
	ST			Ø		Ø			Ind	In
5	EP	Ind	Co		Ø	Co	Co	Ø		In
	ST		Ind		Ø	Ind	Ind			In
6	EP		Ind	Ø		Ø		Ø	Ind	
	ST			Ø		Ø	Ind		Ind	CC
7	EP	Ind	Ind				Co		Ind	
	ST	Ind				Ind	Ind		Co	
8	EP	Ind	Ind	Ø			Co			
	ST	Ind					Ind			In
9	EP	Ind	Ind	Ind	Ind	Ind	Ind			
	ST	Co	Ind	Co	Ind					
10	EP	Co	Co	Ø		Ø	Co		Co	
	ST	Ind		Ø		Co	Ind		Ind	
11	EP	Ind	Ind			Ind				Ø
	ST		Co	Ind		Ind				
12	EP		Co	Ind				Ind	Ind	Ø
	ST			Ind	Ø	Ind	Ø	Ind		Ø
13	EP	Ø		Ind		Ind	Ø	Ind	Ind	
	ST	Ø		Ind		Ind	Ø	Ind	Ind	
14	EP		Ind		Co	Ind	Ø			In
	ST	Ind	Ind	Ind			Ø	Co		In
15	EP		Ind				Ind	Ø	Co	In
	ST								Ind	
16	EP		Ind	Ø	Ø	Ind		Ind	Co	Ø
	ST			Ø	Ø	Co		Ind	Ind	Ø
17	EP	Ø	Ø	Ind	Ind	Ind	Ind			Ø
	ST	Ø	Ø	Ind	Ind	Ind	Ø		Ind	Ø
18	EP		Ø	Ind	Ø	Ind	Ind	Ø	Ø	
	ST		Ø	Ind	Ø	Ind	Ind	Ø	Ø	
Co pair		2	4	0	2	4	4	4	5	3
Ind pair		14	13	13	6	17	11	7	13	8

LOH was defined as the complete absence or at least 75% reduction of one allele, and MI was defined as an addition or deletion resulting in a shift of microsatellite alleles. A concurrent LOH was defined as "loss of an allele for a given marker in cells from one breast." Empty space was defined as "loss of an allele only in cells from one breast, or cells in two breasts show LOH at different allele." Empty space = concurrent alteration; Ind, independent alteration; ST, stromal cells; EP, epithelial cells.

surrounding stromal cells share the same genetic profile of a majority of the DNA markers assessed.<sup>17,19</sup> Together, these findings suggest that stromal cells may be concurrently involved or may even play initiative roles in the development and progression of breast tumors.

The consistent detection of LOH in stromal cells is in concordance with the traditional concept that the development of breast cancer is a multistep process consisting of multiple cellular and biofunctionally different alterations. The detection of LOH in a given stromal cell type



TABLE 3. Comparison of Frequency and Pattern of LOH and MI in Paired EP and ST Cells

Case #	Cell Type	Marker										Co Pair	Ind Pair
		1	2	3	4	5	6	7	8	9	10		
1	EP	Ø		Ø	Ind	Ind		Co		Ø	Ind	1	3
	ST	Ø		Ø	Ind	Co						1	1
2	EP	Ind	Ind				Ø		Ø				2
	ST	Ind					Ø		Ø				2
3	EP	Ind	Ind		Ø		Ind	Co	Ind	Co	Ind	2	5
	ST	Ind	Ind	Ind	Ind	Ind		Ind	Ind	Ind	Ind	0	9
4	EP	Ind		Ø		Ø		Co	Co	Co	Ind	3	2
	ST			Ø		Ø			Ind	Ind	Ind	0	3
5	EP	Ind	Co		Ø	Co	Co	Ø		Ind	Co	4	2
	ST		Ind		Ø	Ind	Ind			Ind	Ind	0	5
6	EP		Ind	Ø		Ø		Ø	Ind			0	2
	ST			Ø		Ø	Ind		Ind	Co	Ind	1	3
7	EP	Ind	Ind				Co		Ind		Ind	1	4
	ST	Ind				Ind	Ind		Co			1	3
8	EP	Ind	Ind	Ø			Co				Co	2	2
	ST	Ind					Ind			Ind	Ind	0	4
9	EP	Ind	Ind	Ind	Ind	Ind	Ind				Ø	0	6
	ST	Co	Ind	Co	Ind						Ø	2	2
10	EP	Co	Co	Ø		Ø	Co		Co		Ø	4	0
	ST	Ind		Ø		Co	Ind		Ind			1	3
11	EP	Ind	Ind			Ind				Ø		0	3
	ST		Co	Ind		Ind					Ind	1	3
12	EP		Co	Ind				Ind	Ind	Ø	Co	2	3
	ST			Ind	Ø	Ind	Ø	Ind		Ø	Ind	0	4
13	EP	Ø		Ind		Ind	Ø	Ind	Ind			0	4
	ST	Ø		Ind		Ind	Ø	Ind	Ind			0	4
14	EP		Ind		Co	Ind	Ø			Ind	Ind	1	4
	ST	Ind	Ind	Ind			Ø	Co		Ind	Ø	1	4
15	EP		Ind				Ind	Ø	Co	Ind		1	3
	ST								Ind		Ind	0	2
16	EP		Ind	Ø	Ø	Ind		Ind	Co	Ø		1	3
	ST			Ø	Ø	Co		Ind	Ind	Ø		1	2
17	EP	Ø	Ø	Ind	Ind	Ind	Ind			Ø	Co	1	4
	ST	Ø	Ø	Ind	Ind	Ind	Ø		Ind	Ø	Ø	0	4
18	EP		Ø	Ind	Ø	Ind	Ind	Ø	Ø		Ø	0	3
	ST		Ø	Ind	Ø	Ind	Ind	Ø	Ø		Ø	0	3
Co pair		2	4	0	2	4	4	4	5	3	4	32	
Ind pair		14	13	13	6	17	11	7	13	8	14		116

LOH was defined as the complete absence or at least 75% reduction of one allele, and MI was defined as an addition or deletion of one or more repeat units resulting in a shift of microsatellite alleles. A concurrent LOH was defined as "loss of an allele for a given marker in cells from both breasts." An independent LOH was defined as "loss of an allele only in cells from one breast, or cells in two breasts show LOH at different allele." Empty space, no loss; Ø, not informative; Co, concurrent alteration; Ind, independent alteration; ST, stromal cells; EP, epithelial cells.

surrounding stromal cells share the same genetic profile of a majority of the DNA markers assessed.<sup>17,19</sup> Together, these findings suggest that stromal cells may be concurrently involved or may even play initiative roles in the development and progression of breast tumors.

The consistent detection of LOH in stromal cells is hard to reconcile with the traditional belief that the stromal component consists of multiple cellular phenotypes that are genetically and biofunctionally different,<sup>26,27</sup> which could mask LOH in a given stromal cell type. There are two potential

**TABLE 4.** Comparison of Frequencies of Concurrent and Independent LOH and MI in Paired Bilateral EP and ST Samples

Cell Type	Sample #	Informative Foci	Altered Foci	Con-Altered Foci	Ind-Altered Foci	P
EP	18	147	78	23 (29.5%)	55 (70.5%)	<0.05
ST	18	149	70	9 (12.9%)	61 (87.1%)	<0.05
Total	36	296	148	32 (21.6%)	116 (78.4%)	<0.05

Morphologically comparable epithelial (EP) and surrounding stromal (ST) cells in two sides of primary bilateral breast tumor lesions were microdissected and subjected to assessments for LOH and MI with 10 DNA markers in a 377 DNA sequencer. The rates of independent and concurrent LOH and MI were obtained by dividing the number of foci that showed independent and concurrent LOH and MI by the total number of altered foci, and the rates between these two categories were statistically compared with the Student *t* test.

Con, concurrent; Ind, independent.

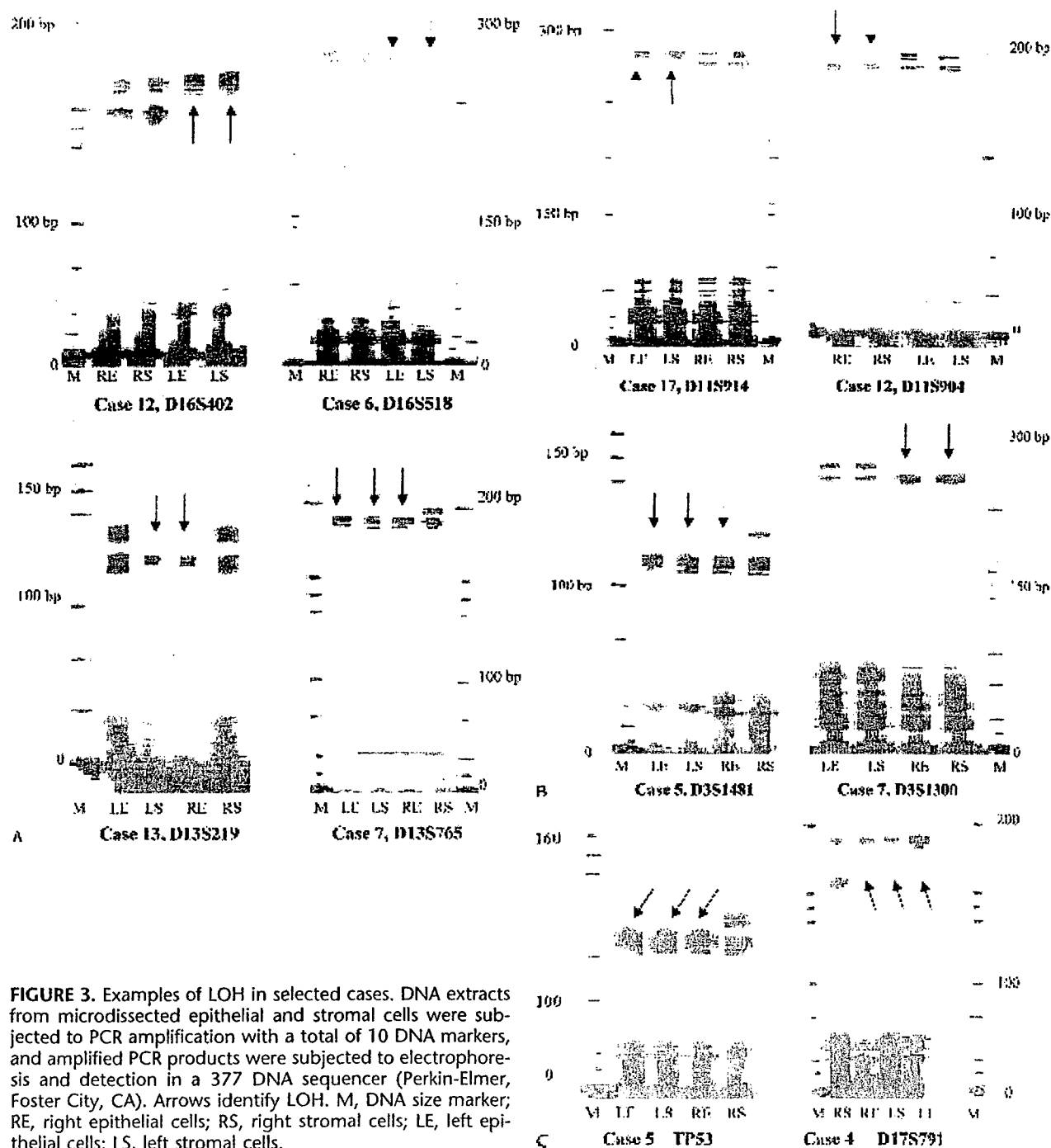


**FIGURE 3.** Examples of LOH in selected cases. DNA extracts from microdissected epithelial and stromal cells were subjected to PCR amplification with a total of 10 DNA markers, and amplified PCR products were subjected to electrophoresis and detection in a 377 DNA sequencer (Perkin-Elmer, Foster City, CA). Arrows identify LOH. M, DNA size marker; RE, right epithelial cells; RS, right stromal cells; LE, left epithelial cells; LS, left stromal cells.

TABLE 5. CGH Profiles of Seven Selected Bilateral Breast Lesions

Case Number*	EP Lesions in Both Breasts	Cell Type	Chromosomal Changes	
			Left Breast	Right Breast
1 (4)	DCIS (G1)	EP	Loss: 16q	Losses: 6q; 11q; 16q
		ST	No change	No change
2 (6)	LN 2	EP	No change	No change
		ST	No change	No change
3 (8)	AIDH	EP	Gain: 1q Losses: 9p; 11q; 16q	No change
		ST	No change	No change
4 (11)	DCIS (G3)	EP	Gain: 1q	Loss: 13q
		ST	Loss: 11q	Loss: 13q
5 (13)	DCIS (G1)	EP	No change	Loss: 4p
		ST	No change	Not informative
6 (14)	LN 2	EP	Gains: 1q; 8q; 16p Losses: 16q; 17p	Gains: 3p, 5q Losses: 4p; 5p
		ST	No change	Losses: 3p; 8p (very small)
7 (15)	DCIS	EP	Gains: 6p; 12p; 14q Losses: 16p; 16q	No change
		ST	No change	No change

Morphologically comparable tumor epithelial (EP) and surrounding normal appearing stromal (ST) tissues in two sides of primary bilateral breast tumor lesions were microdissected and subjected to analysis with the comparative genomic hybridization (CGH) technique, using published protocols.<sup>23,24</sup>

\*Both the newly assigned and the original (see Table 1) case numbers are given.

mechanisms, however, that could result in the detection of LOH in a given stromal cell type. First, a single genetically altered stromal cell type could acquire growth advantages and undergo a localized clonal expansion, forming a genetically similar cell cluster. Consistent with this is that the stromal component of some breast carcinosarcomas shares the same clonality with the epithelial component.<sup>28</sup> Second, a genetically mutated multipotential stem cell could give rise to different stromal cells that contain the same genetic defect. Previous studies have well demonstrated that maturation arrest of stem cells is a common pathway for the cellular origin of both teratocarcinomas and malignant epithelial tumors, and that an entire functional mammary gland may be regenerated from a single cell.<sup>29-31</sup>

The high frequency of LOH in stromal cells is also hard to reconcile with the reportedly low incidence of malignancies in stromal cells.<sup>32</sup> There are several possible explanations. First, genetically altered stromal cells have more disadvantages for progression, for two main reasons: they are subjected to more immunologic surveillance because of their direct association with leukocytes that are generally absent in the normal epithelial component, and a constant remodeling and replacement of the extracellular matrix and stromal tissues may disfavor the accumulation of genetic abnormalities in stromal cells.<sup>33-37</sup> Second, the progression of stromal tumors may require more internal assaults and additional steps due to the potential interactions among stromal cells. Third, genetic or biochemical alterations in the stromal component might have more impacts on the epithelial component than on itself, be-

cause (1) the normal epithelial component is devoid of blood and lymph vessels and totally relies on the stromal component for its basic needs, and (2) a number of stroma-derived biomolecules, including proteinases, matrix metalloproteinases, and growth factors, are key factors for normal morphogenesis, differentiation, and wound healing of the epithelial cells, and also for tumor invasion and metastasis.<sup>33-37</sup>

The substantial differences in LOH and MI frequencies and CGH profiles in both epithelial and stromal cells favor two independent molecular mechanisms for the development or progression of bilateral breast tumors. No definitive conclusions, however, could be drawn at present for several reasons. First, the high degree of heterogeneity of LOH and CGH profiles among cases and the high frequencies of genetic abnormalities at multiple chromosomal loci suggest that the genetic alteration in each individual might be unique, or multiple molecular mechanisms are involved. Second, the presence of a high degree of heterogeneity of LOH and CGH profiles among cases may simply result from different cell clones, or the same clone at differently differentiated states.<sup>38</sup> Third, the small sample size may not be representative of the general population. However, given that genetic alterations determine the scope and extent of, and also precede, the biochemical and morphologic abnormalities, our findings appear to have several potential implications. First, they suggest that the biologic behavior and clinical course of the bilateral tumors in two breasts may differ substantially. Consequently, different treatment regimens might be needed for the optimal management of patients with bilateral breast tumors. Second, the consistent

comprehensive and selective analysis in patients with a progressive tumor in one side and with a regressive or latent one in the other side might lead to the identification of factors that promote progression or promote regression. The manipulation of these factors might be more effective for the treatment and prevention of breast tumors.

### ACKNOWLEDGMENTS

The authors thank Dr. Fattaneh A. Tavassoli, the former chairperson, for her support in initiation of this study, her assistance in the selection and morphologic classification of breast tissues used in this study, and her constructive suggestions on the manuscript. The authors also thank Dr. Frederic M. Waldman, Mr. Bob Flemon, and Ms. Susan Cender of the Cancer Center and Department of Laboratory Medicine, University of California San Francisco for their major roles in performing the CGH and in analyzing the CGH data. The authors are indebted to Mr. Doug Landry of the AFIP exhibition section and Mr. Kenneth J. Vrtacnik of the AFIP Photography Lab for their assistance in preparation of the figures.

### REFERENCES

1. Fisher ER, Fisher B, Sass R, et al. and collaborating NSABP investigators. Pathologic findings from the National Surgical Adjuvant Breast and Bowel Project (Protocol No. 4). XI. Bilateral breast cancer. *Cancer*. 1984;54:3002-3011.
2. Kollias J, Ellis IO, Elston CW, et al. Prognostic significance of synchronous and metachronous bilateral breast cancer. *World J Surg*. 2001;25:1117-1124.
3. Donovan AJ. Bilateral breast cancer. *Surg Clin North Am*. 1990;70:1141-1149.
4. Hoffman E. The contralateral breast biopsy in ipsilateral carcinoma. *South Med J*. 1990;83:1009-1015.
5. Ringberg A, Palmer B, Linell F, et al. Bilateral and multifocal breast carcinoma. A clinical and autopsy study with special emphasis on carcinoma in situ. *Eur J Surg Oncol*. 1991;17:20-29.
6. Nielsen M, Christensen L, Andersen J. Contralateral cancerous breast lesions in women with clinical invasive breast carcinoma. *Cancer*. 1986;57:897-903.
7. Lawson R. Mammary cancer: the other breast. *Can Med Assoc J*. 1955;73:676-677.
8. Masood S. Occult breast lesions and aspiration biopsy: a new challenge. *Diagn Cytopathol*. 1993;9:613-614.
9. Barton FE Jr. Breast cancer, subcutaneous mastectomy, breast reconstruction. *Selected Readings Plastic Surg*. 1986;3:1-23.
10. Ronnov-Jessen L, Petersen OW, Bissell MJ. Cellular changes involved in conversion of normal to malignant breast: importance of the stromal reaction. *Physiol Rev*. 1996;76:69-125.
11. Fracchia AA, Robinson D, Legaspi A, et al. Survival in bilateral breast cancer. *Cancer*. 1985;55:1414-1421.
12. Staren ED, Robinson DA, Wir TR, et al. Synchronous, bilateral mastectomy. *J Surg Oncol*. 1995;59:75-79.
13. Healey EA, Cook EF, Orav EJ, et al. Contralateral breast cancer: clinical characteristics and impact on prognosis. *J Clin Oncol*. 1993;11:1545-1552.
14. Sterns EE, Fletcher WA. Bilateral cancer of the breast: a review of clinical, histologic and immunohistologic characteristics. *Surgery*. 1991;110:617-622.
15. Hungness ES, Safa M, Shaughnessy EA, et al. Bilateral synchronous breast cancer: mode of detection and comparison of histologic features between the 2 breasts. *Surgery*. 2000;128:702-707.
16. Dawson LA, Chow E, Goss PE. Evolving perspectives in contralateral breast cancer. *Eur J Cancer*. 1998;34:2000-2009.
17. Moirfar F, Man YG, Arnould A, et al. Concurrent and independent genetic alterations in the stromal and epithelial cells of mammary carcinoma: implications for tumorigenesis. *Cancer Res*. 2000;60:2562-2566.
18. Moirfar F, Man YG, Brathauer GL, et al. Genetic abnormalities in mammary ductal intraepithelial neoplasia-flat type (clinging ductal carcinoma in situ): a simulator of normal mammary epithelium. *Cancer*. 2000;88:2072-2081.
19. Man YG, Mannion C, Kuhls E, et al. Allelic losses at 3p and 11p are detected in both epithelial and stromal components of cervical small-cell neuroendocrine carcinoma. *Appl Immunohistochem Mol Morphol*. 2001;9:340-345.
20. Man YG, Moirfar F, Brathauer GL, et al. An improved method for DNA extraction from paraffin sections. *Pathol Res Pract*. 2001;197:635-642.
21. Man YG, Moirfar F, Brathauer GL, et al. Five useful hits for making more valid gel images of loss of heterozygosity and clonality analysis with a 377 DNA sequencer. *Diagn Mol Pathol*. 2000;9:84-90.
22. Man YG, Kuhls EA, Brathauer GL, et al. Multiple use of slab gels in sequencing apparatus for separation of PCR products. *Electrophoresis*. 2001;22:1915-1919.
23. Kallioniemi A, Kallioniemi OP, Sudar D, et al. Comparative genomic hybridization for molecular cytogenetic analysis of solid tumors. *Science*. 1992;258:818-821.
24. Ried T, Just KE, Holtgreve-Grez H, et al. Comparative genomic hybridization of formalin-fixed, paraffin-embedded breast tumors reveals different patterns of chromosomal gains and losses in fibroadenomas and diploid and aneuploid carcinomas. *Cancer Res*. 1995;55:5415-5423.
25. Kollias J, Man S, Marafie M, et al. Loss of heterozygosity in bilateral breast cancer. *Breast Cancer Res Treat*. 2000;64:241-251.
26. Simian M, Hirai Y, Navre M, et al. The interplay of matrix metalloproteinases, morphogens and growth factors is necessary for branching of mammary epithelial cells. *Development*. 2001;128:3117-3131.
27. Bissell MJ, Radisky DC, Rizki A, et al. The organizing principle: microenvironmental influences in the normal and malignant breast. *Differentiation*. 2002;70:537-546.
28. Zhaung Z, Lininger RA, Man YG, et al. Identical clonality of both components of mammary carcinomas with differential loss of heterozygosity. *Mod Pathol*. 1997;10:354-362.
29. Sell S, Pierce GB. Maturation arrest of stem cells is a common pathway for the cellular origin of teratocarcinomas and epithelial cancers. *Lab Invest*. 1994;70:6-22.
30. Kordon EC, Smith GH. An entire functional mammary gland may comprise the progeny from a single cell. *Development*. 1998;125:1921-1930.
31. Drummond R. The malignant stem cells. *Med Hypotheses*. 1994;43:157-159.
32. Wingo PA, Ries LA, Rosenberg HM, et al. Cancer incidence and mortality, 1973-1995: a report card for the U.S. *Cancer*. 1998;82:1197-1207.
33. Schedin P, Strange R, Mitrenga T. Fibronectin fragments induce MM activity in mouse mammary epithelial cells: evidence for a role in mammary tissue remodeling. *J Cell Sci*. 1995;113:795-806.
34. Werb Z, Ashkenas J, MacAuley A, et al. Extracellular matrix remodeling as a regulator of stromal-epithelial interactions during mammary gland development, involution and carcinogenesis. *Braz J Med Biol Res*. 1996;29:1087-1097.
35. McCawley LJ, Matrisian LM. Matrix metalloproteinases: multifunctional contributors to tumor progression. *Mol Med Today*. 2000;6:149-156.
36. Hansen RK, Bissell MJ. Tissue architecture and breast cancer: the role of extracellular matrix and steroid hormones. *Endocr Relat Cancer*. 2000;7:95-113.
37. Nelson AR, Fingleton B, Rothenberg ML, et al. Matrix metalloproteinases: biologic activity and clinical implications. *J Clin Oncol*. 2000;18:1135-1149.
38. Lininger RA, Fujii H, Man YG, et al. Comparison of loss heterozygosity in primary and recurrent ductal carcinoma in situ of the breast. *Mod Pathol*. 1998;11:1151-1159.
39. Cooper M, Pinkus H. Intrauterine transplantation of rat basal cell carcinoma as a model for reversion of malignant to benign growth. *Cancer Res*. 1977;37:2544-2552.
40. Fibach E, Landau T, Sachs L. Normal differentiation of myeloid leukaemic cells induced by a differentiation-inducing protein. *Nat New Biol*. 1972;237:276-278.

# Mammary Ducts With and Without Focal Myoepithelial Cell Layer Disruptions Show a Different Frequency of White Blood Cell Infiltration and Growth Pattern: Implications for Tumor Progression and Invasion

AU2

Morvarid Yousefi,\* Rubina Mattu,\* Chunling Gao,† and Yan-gao Man, MD, PhD\*

**Abstract:** The authors' previous studies revealed that a subset of ductal carcinoma in situ (DCIS) contained focally disrupted myoepithelial (ME) cell layers and basement membrane (BM). As the disruption of these two structures is a prerequisite for tumor invasion, and white blood cells (WBCs) contain digestive enzymes capable of degrading both the BM and damaged host cells, this study was designed to assess the possible roles of WBC in ME cell layer disruptions and tumor invasion. A total of 23 DCIS containing ducts with focally disrupted ME cell layers were selected from 94 such cases identified in the authors' previous studies. Two consecutive sections from each case were double immunostained, one with leukocyte common antigen (LCA) plus smooth muscle actin (SMA) and the other with Ki-67 plus SMA. Ducts lined by at least 50 epithelial cells and distinct ME cell layers were examined. A total of 191 duct cross-sections were found to contain focal ME cell layer disruptions; of these, 186 (97.4%) were with and 5 (2.6%) were without WBC infiltration. Of 207 morphologically similar sections without ME disruptions, 46 (22.2%) were with and 161 (77.8%) were without WBC infiltration. Ki-67-positive cells in ducts with focally disrupted ME cell layers were generally subjacent to ME cell layers, and more than 30 clusters of multiple proliferating cells were seen directly overlying or near focally disrupted ME cell layers. In contrast, Ki-67-positive cells in ducts without ME disruptions were scattered over the entire epithelial compartment. The significantly different frequency of

WBC infiltration and clusters of multiple proliferating cells in ducts with and without ME disruptions suggests that WBCs might play important roles in ME disruption and tumor invasion.

**Key Words:** tumor progression and invasion, myoepithelial cell layer disruption, white blood cell infiltration, epithelial-stromal interactions, cell growth pattern

(*Appl Immunohistochem Mol Morphol* 2004;00:000-000)

The epithelial component of normal and noninvasive human breast tissue is physically separated from the stroma by both myoepithelial (ME) cells and the basement membrane (BM).<sup>1-3</sup> ME cells are joined by a number of intercellular adhesion molecules and intermediate junctions, forming a continuous sheet or belt that encircles the epithelial cells (except at the terminal ductal-lobular unit, within which about 20% of the epithelial cells are in direct contact with the BM).<sup>1-3</sup> The BM is composed of a group of fibrous proteins embedded in a hydrated polysaccharide gel, constituting a continuous lining surrounding and attaching to the ME cells via hemidesmosomes and focal adhesion complexes.<sup>4,5</sup> Both the ME cell layer and basement membrane (BM) are permanent structural constituents that normally allow only the passage of water, oxygen, and other small molecules.<sup>1-5</sup> Due to the interposition of the BM and ME cell layer between the stroma and the epithelium, the tumor cells must first pass through the ME cell layer, followed by the BM, to physically contact the stroma. Hence, the disruption of both the BM and the ME cell layer is a prerequisite for tumor invasion and metastasis.

Compared with in situ tumors, invasive and metastasized tumors have a significantly higher mortality rate, accounting for a vast majority of breast cancer deaths. This fact highlights the significance and implications for the identification of tumor invasion mechanism(s), potentially leading directly to vast benefits and advances in breast cancer treatment or prevention. A generally accepted theory for the cause of BM disruptions and tumor invasion has been attributed primarily, if not solely, to an upregulated expression of proteolytic en-

AU3 Received for publication; accepted.

From the \*Department of Gynecologic and Breast Pathology, Armed Forces Institute of Pathology and American Registry of Pathology, Washington DC; and the †Center for Prostate Disease Research, Department of Surgery, Uniformed Service University of Health Science, Bethesda, Maryland.

This study was supported in part by grants DAMD17-01-1-0129 and DAMD17-01-1-0130 from Congressionally Directed Medical Research Programs to Yan-gao Man, MD, PhD.

Reprints: Yan-gao Man, MD, PhD, Dept. of Gynecologic & Breast Pathology The Armed Forces Institute of Pathology and American Registry of Pathology, 6825 16<sup>th</sup> Street, NW, Washington, DC 20306-6000 (man@afip.osd.mil).

The opinions and assertions contained herein are the private viewpoints of the authors and do not reflect the official views of the Department of Defense or Department of the Army or the Navy.

Copyright © 2004 by Lippincott Williams & Wilkins

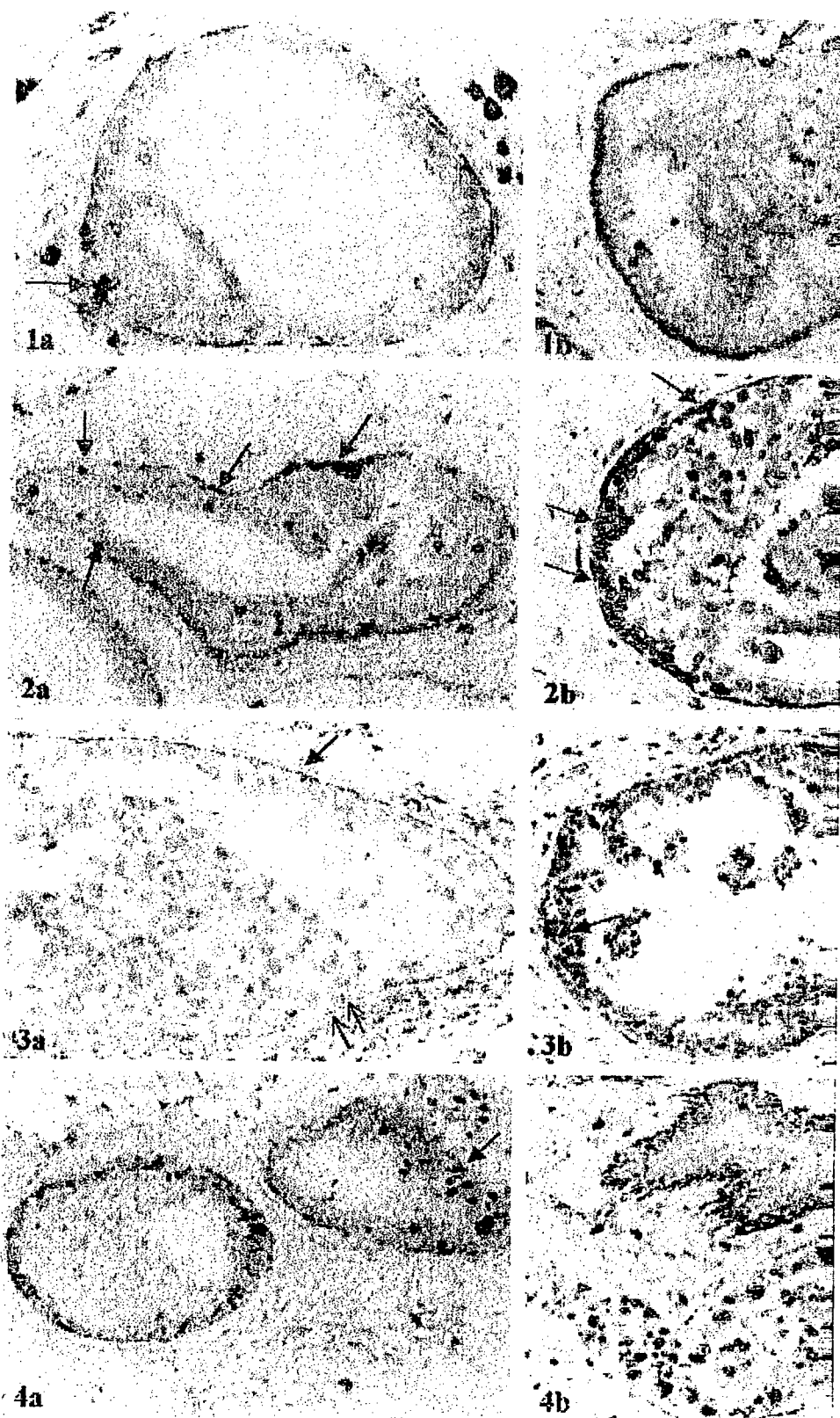


FIGURE 1. (Legend continues on facing page).

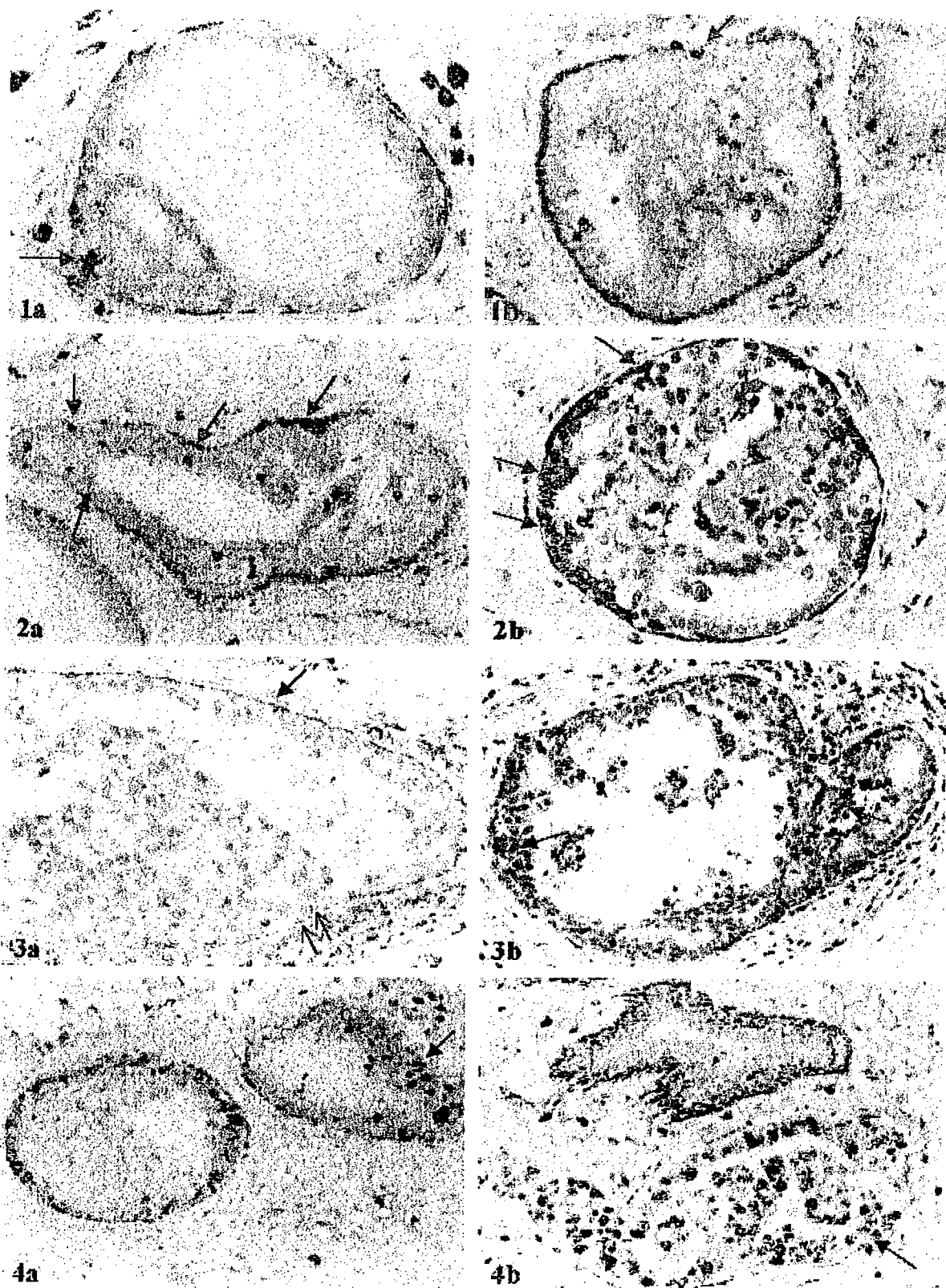


FIGURE 1. (Legend continues on facing page).

zymes in tumor or stromal cells.<sup>6</sup> This theory, however, may not reflect the intrinsic mechanism of these events for two main reasons: first, neither the normal cellular kinetics nor dynamic alterations of ME cells during tumor invasion have been well elucidated; and second, results of proteolytic inhibitor-based clinical trials have been disappointing.<sup>7</sup>

In an attempt to elucidate the intrinsic mechanism(s) of ME cell layer disruptions and tumor invasion, we carried out several studies focusing on the correlation between the physical and functional integrity of the ME cell layer and the immunohistochemical and genetic profiles in adjacent epithelial cells. In 5,698 duct cross-sections from 220 patients with estrogen receptor-positive, noninvasive breast tumors, we detected a total of 405 focal ME cell layer disruptions, defined as the absence of ME cells resulting in a gap equal to or greater than the combined size of 3 ME or epithelial cells.<sup>8</sup> Of the 405 disruptions, 350 (86.4%) were overlain by clusters of cells with no or substantially reduced estrogen receptor expression, in sharp contrast to their adjacent cells within the same duct, which overlaid nondisrupted ME cell layer and displayed strong estrogen receptor immunoreactivity.<sup>8</sup> Compared with their neighbors, those estrogen receptor-negative cell clusters overlying focally disrupted ME cell layers also displayed the following unique features: (1) a significantly higher cell proliferation rate, 18.2% versus 3.6% and 19.9% versus 4.4% in two separate studies<sup>9,10</sup>; (2) a total loss or marked reduction of p27, a cell growth inhibitor<sup>9</sup>; and (3) a substantially higher or different pattern of genetic alterations.<sup>11,12</sup> As it has been well documented that the disruption of ME and BM layers is a prerequisite for tumor invasion and metastasis, and that progression of breast tumors is paralleled by a progressive hormonal independence,<sup>13–15</sup> our findings appear to represent an early sign of ME and BM layer breakdown and the formation of a biologically more aggressive cell clone that is in the process of invasion. Our subsequent studies revealed that 3 of 175 patients with noninvasive breast tumors contained ducts that showed morphologically distinct ME cells in H&E-stained sections, whereas one third of, or the entire, ME cell layer was devoid of expression of nine phenotypic markers that supposedly were exclusively or preferentially present in ME cells.<sup>16</sup> Our studies also revealed that the stromal tissues surrounding

ducts with ME cell layer disruptions were often more vascular and contained more white blood cell (WBC) aggregates compared with stromal tissues around ducts with an intact ME cell layer.<sup>17</sup>

As previous studies have well documented that (1) WBCs contain a number of digestive enzymes capable of degrading both the BM and altered host cells in vivo and in vitro<sup>18,19</sup>; (2) WBCs are capable of freely crossing over the ME cell and BM layers<sup>20,21</sup>; and (3) tumors with and without WBC infiltration have a substantially different clinical course and prognosis,<sup>22,23</sup> this study attempted to assess the potential correlation between WBCs and ME cell layer disruptions during tumor progression and invasion. As the first step, we attempted to determine whether ducts with focally disrupted ME cell layers have a higher frequency of WBC infiltration and more clusters of multiple proliferating cells, which are likely to represent clonal or stem cell-mediated proliferation and have a greater potential for invasion.<sup>24,25</sup>

## MATERIALS AND METHODS

A total of 23 cases with focally disrupted ME cell layers were selected from the 94 cases identified in our previous studies.<sup>8,17</sup> Consecutive sections at 4 to 5  $\mu$ m thickness were cut and placed on positively charged microscope slides for morphologic and immunohistochemical assessment. Morphologic classification was based on our previously published criteria.<sup>26</sup> All of the lesions were noninvasive, including atypical intraductal hyperplasia (AIDH) and ductal carcinoma in situ (DCIS;  $n = 20$ ), as well as intraductal hyperplasia (IDH;  $n = 3$ ). All of the cases contained at least two ducts with focally disrupted ME cell layers.

Monoclonal antibodies to human leukocyte common antigen (LCA), smooth muscle actin (SMA), and Ki-67 were purchased from Dako (Carpinteria, CA). The biotinylated secondary antibody, ABC detection kits, and 3, 3'-diaminobenzidine (DAB) substrate kit were obtained from Vector Laboratories, Inc. (Burlingame, CA). The AP-red substrate kit was purchased from Zymed Laboratories, Inc. (South San Francisco, CA). The antigen retrieval solution (10 $\times$ ) was purchased from Biocare Medical Inc. (Walnut Creek, CA).

**FIGURE 1.** WBC infiltration associated with a single focal ME cell layer disruption Sections were double immunostained for LCA (brown) and SMA (red). Arrows identify WBCs and ME disruptions. (a, 400 $\times$ ; b, 200 $\times$ )

**FIGURE 2.** WBC infiltration associated with multiple focal ME cell layer disruptions Sections were double immunostained for LCA (brown) and SMA (red). Arrows identify WBCs and ME disruptions. (a, 200 $\times$ ; b, 400 $\times$ )

**FIGURE 3.** a: WBC aggregates associated with ME cell layer attenuation and disruptions Sections were double immunostained for LCA (brown) and SMA (red). Double arrows identify attenuated and disrupted ME cell layer lined by WBC aggregates; the single arrow identifies the normal ME cell layer. (300 $\times$ ) b: WBC infiltration within the epithelial component of a duct without a focal ME disruption Sections were double immunostained for LCA (brown) and SMA (red). Arrows identify selected WBCs within the epithelial component. (200 $\times$ )

**FIGURE 4.** Comparison of the epithelial cell proliferation rates in ducts with and without ME disruptions. Sections were double immunostained for Ki-67 (black) and SMA (red). Arrows identify focal ME disruptions (200 $\times$ ).



Immunohistochemical staining was carried out as previously described.<sup>27,28</sup> Briefly, two immediately adjacent sections from each case were incubated at 70°C for about 30 minutes, deparaffinized with three changes of xylene, and washed in descending concentrations of ethanol and water. Deparaffinized sections were incubated at about 70°C overnight in 1× antigen retrieval solution, washed in warm tap water, and incubated with H<sub>2</sub>O<sub>2</sub> blocking solution and normal serum. Then one section was sequentially immunostained with antibodies to LCA and SMA, and the other was sequentially stained with antibodies to Ki-67 and SMA, and developed with the DAB and AP-red substrates, respectively.

Each H&E-stained or immunostained section was examined under a microscope with attention to cross-section profiles of ducts that were lined by at least 50 epithelial cells and morphologically distinct ME cell layers. A focal disruption of the ME cell layer was defined as a total loss of SMA immunoreactivity and absence of ME cells, resulting in a gap equal to or greater than the combined size of at least three epithelial or ME cells, or multiple such gaps in a given duct. WBC infiltration was defined as the distribution of a single or a group of LCA-positive cells within the epithelial compartment or the direct physical contact between WBCs and epithelial cells near the ME and BM layers.

The ME cell layer disruptions and WBC infiltration were evaluated in two ways. First, the physical status (with or without ME cell layer disruptions and WBC infiltration) of each duct cross-section was recorded and photographed with 35-mm slide film. Then, the developed slide films were reviewed under a slide projector by at least two investigators. The interpretation of the physical status of each duct was based on the uniform conclusion of all the reviewers. Disagreements were settled by either excluding the section or repeating the immunostaining on a new slide. The rate and distribution of proliferating cells in ducts with and without ME cell layer disruptions were similarly evaluated as above, focusing on the clusters of multiple proliferating cells, defined as a group of at least four Ki-67-positive epithelial cells immediately overlying or near the ME cell layer.

**TABLE 1.** Frequencies of White Blood Cell Infiltration in Mammary Ducts With and Without Focal Myoepithelial Cell Layer Disruptions

	Section Number	With WBC	Without WBC	P
Disrupted	191	186 (97.4%)	5 (2.6%)	<0.01
Nondisrupted	207	46 (22.6%)	161 (77.4%)	

## RESULTS

Cells with distinct LCA immunoreactivity were identifiable in each of the tissue sections, while the number and distributions of LCA-positive cells among cases differed substantially. The WBC infiltration into the epithelial component occurred in four forms: (1) a single or a few WBCs interpositioning the center of a focal ME disruption (Fig. 1); (2) multiple WBCs lined along the ME layer with multiple ME disruptions (Fig. 2); (3) a sheet- or belt-like WBC aggregate partially surrounding a duct, in which the ME cell layer near the WBCs was markedly attenuated or disrupted, while the ME cell layer away from the WBCs was distinct and intact (Fig. 3a); and (4) multiple WBCs scattered among tumor cells of the duct without distinct ME disruptions (see Fig. 3b). The frequency of each form appeared to be not statistically different.

The frequencies of WBC infiltration in ducts with and without focal ME cell layer disruptions are summarized in Table 1. A total of 191 profiles of duct cross-sections were found to contain focal ME cell layer disruptions. Of these, 186 (97.4%) were with and 5 (2.6%) were without WBC infiltration. A total of 207 profiles of ductal cross-sections were found to contain no ME cell layer disruptions. Of these, 46 (22.2%) were with and 161 (77.8%) were without WBC infiltration. The frequency of WBC infiltration in ducts with focally disrupted ME cell layers was significantly higher ( $P < 0.01$ ) compared with that in their morphologically similar counterparts without ME cell layer disruptions.

Distinct Ki-67-positive cells were seen in ducts with and without focal ME cell layer disruptions. However, ducts with a

**FIGURE 5.** Clusters of multiple proliferating cells associated with focal ME disruptions. a: The section was double immunostained for LCA (brown) and SMA (red), and the adjacent section (b) was double immunostained for Ki-67 (black) and SMA (red). Arrows identify WBCs and clusters of multiple proliferating cells (200×).

**FIGURE 6.** Clusters of multiple proliferating cells associated with focal ME disruptions. a: The section was double immunostained for LCA (brown) and SMA (red), and the adjacent section (b) was double immunostained for Ki-67 (black) and SMA (red). Arrows identify WBCs and clusters of multiple proliferating cells (200×).

**FIGURE 7.** WBC infiltration and epithelial cell proliferation associated with no ME disruptions. a: The section was double immunostained for LCA (brown) and SMA (red), and (b) the adjacent section was double immunostained for Ki-67 (black) and SMA. Arrows identify selected WBCs and Ki-67-positive cells (200×).

**FIGURE 8.** WBC aggregates associated with no infiltration. Sections were double immunostained for LCA (brown) and SMA (red). WBC aggregates are subjacent to or surround the tumor nests, while there are no infiltration or ME disruptions (a, 400×; b, 200×).

focally disrupted ME cell layer displayed a substantially higher proliferation rate compared with their morphologically comparable (the same lesion type and histologic grade, and similar size and architecture) counterparts (Fig. 4). Also, Ki-67-positive cells in ducts with focally disrupted ME cell layers were generally subjacent to ME cell layers, and more than 30 distinct clusters of multiple proliferating cells were seen directly overlying or near focally disrupted ME cell layers (Figs. 5 and 6). In contrast, Ki-67-positive cells in ducts without ME cell layer disruptions were generally scattered over the entire epithelial component (Fig. 7).

Focal ME cell layer disruptions and WBC infiltration appeared to be independent of the lesion type and histologic grade, as many high-grade DCIS specimens with necrosis showed distinct ME cell layers and no WBC infiltration (Fig. 8a). Focal ME layer disruptions and WBC infiltration also appeared to be independent of the number of WBCs, as no distinct ME cell layer disruptions or WBC infiltration were found in ducts that were completely or partially surrounded by WBCs (see Fig. 8b).

## DISCUSSION

In this study, we found that mammary ducts with focally disrupted ME cell layers had a significantly higher ( $P < 0.01$ ) frequency of WBC infiltration than their histologically comparable counterparts without ME cell disruptions, and that WBCs were often located at or near the center of the ME layer disruptions (see Table 1 and Figs. 1 and 2). Also, the proliferating cells in ducts with ME disruptions were generally subjacent to the ME layers, often forming clusters near or overlying the focal ME disruptions (see Figs. 5b and 6b), a sign of clonal or stem cell-mediated cell proliferation.<sup>24,25</sup> In contrast, proliferating cells in ducts without focal ME disruptions were distributed in a scattered manner over the entire epithelial component, and no basally located clusters of multiple proliferating cells were seen (see Fig. 7b). These findings suggest that WBCs might have a direct or indirect impact on the structural integrity of the ME cell layers and the growth pattern of adjacent tumor cells, potentially leading to more aggressive behavior or stromal invasion. Our speculation is supported by a previous report showing that patients with lymphocyte infiltration at the tumor edge have a noticeable poorer short-term prognosis compared with those with lymphocyte infiltration in other locations.<sup>23</sup> Our speculation is also supported by several lines of experimental and clinical follow-up data. It has been well documented that WBC infiltration into tumor tissues is common and that the number of WBCs within the tumor tissues increases linearly with tumor progression.<sup>29-31</sup> The increase in WBCs is particularly evident during the progression of DCIS to infiltrating carcinoma, in which up to a fourfold increase in lymphoid infiltration has been reported.<sup>29-31</sup> The extent of the increased macrophages in breast tumor tissues has been found

to inversely correlate with a worse prognosis and a significantly higher mortality rate.<sup>30</sup>

Despite these findings, the impact of WBCs on tumor progression and invasion has been a subject of long debate and much controversy, and the intrinsic mechanism and significance of WBC infiltration are elusive. Based on our findings and published data, we propose that direct physical and functional interactions between WBCs and ME cells are a triggering factor for ME cell layer disruptions and tumor invasion. We believe that the main processes are as follows: (1) ME cells normally undergo proliferation to replace aged or injured ME cells; (2) an external or internal insult disrupts the normal replacement process or directly affects the ME cell layer, resulting in a cluster of dying ME cells; (3) degraded products of dying ME cells attract WBC infiltration and activate the functions of WBCs, disrupting the physical integrity of the ME cell and BM layers; (4) a focal disruption in the ME cell and BM layers results in an increased permeability for growth and metabolism-related molecules; (5) the altered microenvironment results in changes of the gene expression pattern and behavior of the adjacent epithelial cells, facilitating the formation of a biologically more aggressive clone; (6) epithelial cells overlying disrupted ME cell layers undergo a localized epithelial cell proliferation, which may occur in two forms: stem cell-mediated proliferation that gives rise to clusters of multiple proliferating cells, and differentiated cell-mediated proliferation that gives rise to proliferating cells randomly distributed within the epithelial compartment; and (7) cells overlying disrupted ME cell layers undergo cytodifferentiation, releasing stage-restricted and invasion-associated molecules, which trigger angiogenesis, tissue remodeling, and increasing production of growth factors in the stroma, providing a favorable environment for epithelial cell growth. These interactive changes between epithelial and stromal cells lead to further degradation of BM and ME cell layers and a clonal expansion and stromal invasion of cells overlying disrupted ME cell layers.

Our hypotheses are far-fetched due to the lack of direct experimental evidence and the small sample size, which might not reflect the real status in the general population. However, given that (1) the results of human clinical trials<sup>7</sup> have disproved the traditional belief that overproduction of proteolytic enzymes is the sole cause for BM and ME layer disruptions, and (2) our study has revealed a significant correlation between WBC infiltration and an increased rate of ME disruptions and cell proliferation, which has been considered a direct cause for tumor progression,<sup>32,33</sup> our hypothesis appears to have important scientific and clinical implications. In the scientific field, our hypothesis may open a new window for the exploration of the mechanism of ME cell layer disruptions and tumor invasion. In the clinical field, our hypothesis might be beneficial for the early detection and treatment of breast cancer. Double immunostainings with antibodies to LCA plus

SMA or Ki-67 plus SMA might be a more sensitive approach to identify patients who are at a higher risk of developing invasive or metastatic tumors. The development of specific antibodies or chemical reagents to target WBCs or degenerated ME cells might provide a more effective and less toxic means of blocking tumor invasion at a very early stage. In addition, our hypothesis might be useful in reconciling the conflicting reports regarding the impacts of WBCs on tumor cells, as our findings have suggested that those conflicts are likely to result from differences in the location of the WBC infiltration and the cell growth patterns, and the presence or absence of ME layer disruptions.

It is possible, however, that other factors, including altered expression of the surface proteins, "sequestered" or self-antigens, and abnormal expression of hyaluronidases in tumor cells, might also play important roles in ME cell layer disruptions and tumor invasion.<sup>34,35</sup> On the other hand, it is unlikely that the WBC is a bystander or a secondary response with no impact on the adjacent cells. Studies on a larger number of cases are in progress to explore the issues that were not addressed in this study. The main goals of our current studies are to compare the proliferation rate and apoptotic index in ME cells at different stages during tumor progression, to identify the specific types of WBCs and proteins associated with ME disruptions, and to assess the gene expression pattern in cells overlying focally disrupted ME cell layers associated with WBC infiltration. The preliminary results of our studies appear to be in a total agreement with our hypothesis.<sup>36,37</sup>

#### ACKNOWLEDGMENTS

The authors thank Doug Landry and James A. Nola of the AFIP Exhibition Section for their technical assistance in preparation of the figures.

#### REFERENCES

1. Tsubura A, Shikata N, Inui T, et al. Immunohistochemical localization of myoepithelial cells and basement membrane in normal, benign and malignant human breast lesions. *Virchows Arch*. 1988;413:133-139.
2. Jolicoeur F, Seemayer TA, Gabbiani G, et al. Multifocal, nascent, and invasive myoepithelial carcinoma (malignant myoepithelioma) of the breast: an immunohistochemical and ultrastructural study. *Int J Surg Pathol*. 2002;10:281-291.
3. Slade MJ, Coope RC, Gomm JJ, et al. The human mammary gland basement membrane is integral to the polarity of luminal epithelial cells. *Exp Cell Res*. 1999;247:267-278.
4. Miosge N. The ultrastructural composition of basement membrane in vivo. *Histol Histopathol*. 2001;16:1239-1248.
5. Nerlich A. Morphology of basement membrane and associated matrix proteins in normal and pathological tissues. *Feroff Pathol*. 1995;145:1-139.
6. Goldfarb RH, Liotta LA. Proteolytic enzymes in cancer invasion and metastasis. *Semin Thromb Hemost*. 1986;12:294-307.
7. Coussens LM, Fingleton B, Matrisian LM. Matrix metalloproteinase inhibitors and cancer: trial and tribulations. *Science*. 2002;295:2387-2392.
8. Man YG, Tai L, Barner R, et al. Focal losses of ER expression in epithelial cells and disruptions of subjacent myoepithelial cell layers are correlated events in ER (+) ductal intracipithelial neoplasia. *Proceedings of Department of Defense Breast Cancer Research Program Meeting*. Vol. 1, 2002;9, 17. Edited by Congressionally Directed Medical Research Programs, US Army Medical Research and Materiel Command, Fort Detrick, MD.
9. Man YG, Saenger JS, Strauss BL, et al. Focal alterations of p27 expression and subjacent myoepithelial cell layer disruptions are correlated events in ER (-) ductal intracipithelial neoplasia. *Proceedings of Department of Defense Breast Cancer Research Program Meeting*. Vol. 1, 2002;9, 14. Edited by Congressionally Directed Medical Research Programs, US Army Medical Research and Materiel Command, Fort Detrick, MD.
10. Man YG, Vang RS, Saenger JS, et al. Co-expression of maspin and Wilms' tumor 1 proteins in mammary myoepithelial cells: Implication for tumor progression and invasion. *Proceedings of Department of Defense Breast Cancer Research Program Meeting*. Vol. 1: 2002, 9, 16. Edited by Congressionally Directed Medical Research Programs, US Army Medical Research and Materiel Command, Fort Detrick, MD.
11. Man YG, Shekitka KM, Brathauer GL, et al. Immunohistochemical and genetic alterations in mammary epithelial cells overlying focally disrupted myoepithelial cell layers. *Breast Cancer Res Treat*. 2002;76:S143, S69.
12. Man YG, Saenger JS, Vang RS, et al. Identification of invasive precursor cells in normal appearing and hyperplastic breast tissue. *Proceedings of the American Association for Cancer Research*. 2003;44:68, 357.
13. Clarke R, Brunner N, Katzenellenbogen BS. Progression of human breast cancer cells from hormone-dependent to hormone-independent growth both in vitro and in vivo. *Proc Natl Acad Sci USA*. 1989;86:3649-3653.
14. Murphy LC. Mechanism of hormone independence in human breast cancer. *In Vivo*. 1998;2:95-106.
15. Sheikh MS, Garcia M, Pujol P, et al. Why are estrogen receptor-negative breast cancers more aggressive than the estrogen receptor-positive breast cancers? *Invasion Metastasis*. 1994-95;14:329-336.
16. Zhang R, Man YG, Vang RS, et al. A subset of morphologically identifiable mammary myoepithelial cells lacks expression of corresponding phenotypic markers. *Breast Can Res*. 2003;5:R151-R156.
17. Man YG, Tai L, Barner R, et al. Cell clusters overlying focally disrupted mammary myoepithelial cell layers and adjacent cells within the same duct display different immunohistochemical and genetic features: implications for tumor progression and invasion. *Breast Cancer Res*. 2003;5: R231-R241.
18. Yakirevich E, Izhak OB, Remert G, et al. Cytotoxic phenotype of tumor infiltrating lymphocytes in medullary carcinoma of the breast. *Mod Pathol*. 1999;12:1050-1056.
19. Zhang XD, Schiller GD, Gill PG, et al. Lymphoid cell infiltration during cancer growth: a syngenic rat model. *Immunol Cell Biol*. 1998;76:550-555.
20. Corca I, Plunkett T, Vlad A, et al. Form and pattern of MUC1 expression on T cells activated in vivo or in vitro suggests a function in T-cell migration. *Immunology*. 2003;108:32-41.
21. Chen SY, Yang AG, Chen JD, et al. Potent antitumor activity of a new class of tumour-specific killer cells. *Nature*. 1997;385:78-80.
22. Manard S, Tomasic G, Casalini P, et al. Lymphoid infiltration as a prognostic variable for early-onset breast carcinomas. *Clin Cancer Res*. 1997; 3:817-819.
23. Hartveit F. Breast cancer: poor short-term prognosis in cases with moderate lymphocyte infiltration at the tumor edge: a preliminary report. *Oncol Rep*. 1998;5:423-426.
24. Nowell PC. The clonal evolution of tumor cell populations. *Science*. 1976;194:23-28.
25. Man YG, Ball WD, Marchetti L, et al. Contributions of intercalated duct cells to the normal parenchyma of submandibular glands of adult rats. *Anat Rec*. 2001;263:202-214.
26. Tavassoli FA, Man YG. Morphofunctional features of intraductal hyperplasia, atypical hyperplasia, and various grades of intraductal carcinoma. *Breast J*. 1995;1:155-162.
27. Man YG, Tavassoli FA. A simple epitope retrieval method without the use of microwave oven or enzyme digestion. *Appl Immunohistochem*. 1996; 4:139-141.
28. Man YG, Ball WD, Culp AJ, et al. Persistence of a perinatal cellular phe-

- notype in the ducts of adult glands. *J Histochem Cytochem*. 1995;43:1203-1215.
29. Ben-Hur H, Mordechay E, Halperin R, et al. Apoptosis-related proteins (Fas, Fas ligand, bcl-2 and p53) in different types of human breast tumors. *Oncol Rep*. 2002;9:977-980.
30. Ben-Hur H, Cohen O, Schneider D, et al. The role of lymphocytes and macrophages in human breast tumorigenesis: an immunohistochemical and morphometric study. *Anticancer Res*. 2002;22:1231-1238.
31. Harney JH, Dimitriadis E, Kay E, et al. Regulation of macrophage production of vascular endothelial growth factor (VEGF) by hypoxia and transforming growth factor beta-1. *Ann Surg Oncol*. 1998;5:271-278.
32. Pan H, Yin C, Van Dyke T. Apoptosis and cancer mechanism. *Cancer Surv*. 1997;29:305-327.
33. Pierce GB, Speers WC. Tumors as caricatures of the process of tissue renewal: prospects for therapy by directing differentiation. *Cancer Res*. 1996;48:1990-2004.
34. Madan AK, Yu K, Dhurandhar N, et al. Association of hyaluronidase adenocarcinoma invasiveness. *Oncol Rep*. 1999;6:607-609.
35. Victor R, Chauzy C, Girard N, et al. Human breast cancer metastasis formation in a nude-mouse model: studies of hyaluronidase, hyaluronan and hyaluronan-binding sites in metastatic cells. *Int J Cancer*. 1999;82:77-83.
36. Man YG, Zeng X, Shen T, et al. Cell clusters overlying focally disrupted myoepithelial cell layers and their adjacent counterparts within the same duct display a different pattern of mRNA expression. *Mod Pathol*. (abstract) (in press)
37. Man YG, Barner R, Vang R, et al. Differential expression of non-structure restricted proteins in mammary myoepithelial cells: a programmed or induced phenomenon? [abstract] *Mod Pathol*. (in press).

[CANCER RESEARCH 64, 590-598, January 15, 2004]

# Endometase/Matrilysin-2 in Human Breast Ductal Carcinoma *in Situ* and Its Inhibition by Tissue Inhibitors of Metalloproteinases-2 and -4: A Putative Role in the Initiation of Breast Cancer Invasion

Yun-Ge Zhao,<sup>1</sup> Ai-Zhen Xiao,<sup>1</sup> Hyun I. Park,<sup>1</sup> Robert G. Newcomer,<sup>1</sup> Mei Yan,<sup>2</sup> Yan-Gao Man,<sup>3</sup> Sue C. Heffelfinger,<sup>2</sup> and Qing-Xiang Amy Sang<sup>1</sup>

<sup>1</sup>Department of Chemistry and Biochemistry and Institute of Molecular Biophysics, Florida State University, Tallahassee, Florida; <sup>2</sup>Department of Pathology and Laboratory of Medicine, University of Cincinnati College of Medicine, Cincinnati, Ohio; and <sup>3</sup>Department of Gynecology and Breast Pathology, The Armed Forces Institute of Pathology, Washington, D.C.

## ABSTRACT

Local disruption of the integrity of both the myoepithelial cell layer and the basement membrane is an indispensable prerequisite for the initiation of invasion and the conversion of human breast ductal carcinoma *in situ* (DCIS) to infiltrating ductal carcinoma (IDC). We previously reported that human endometase/matrilysin-2/matrix metalloproteinase (MMP) 26-mediated pro-gelatinase B (MMP-9) activation promoted invasion of human prostate carcinoma cells by dissolving basement membrane proteins (Y. G. Zhao *et al.*, *J. Biol. Chem.*, 278: 15056-15064, 2003). Here we report that tissue inhibitor of metalloproteinases (TIMP)-2 and TIMP-4 are potent inhibitors of MMP-26, with apparent  $K_i$  values of 1.6 and 0.62 nM, respectively. TIMP-2 and TIMP-4 also inhibited the activation of pro-MMP-9 by MMP-26 *in vitro*. The expression levels of MMP-26, MMP-9, TIMP-2, and TIMP-4 proteins in DCIS were significantly higher than those in IDC, atypical intraductal hyperplasia, and normal breast epithelia adjacent to DCIS and IDC by immunohistochemistry and integrated morphometry analysis. Double immunofluorescence labeling and confocal laser scanning microscopy revealed that MMP-26 was colocalized with MMP-9, TIMP-2, and TIMP-4 in DCIS cells. Higher levels of MMP-26 mRNA were also detected in DCIS cells by *in situ* hybridization.

## INTRODUCTION

Matrix metalloproteinases (MMPs) are known to be associated with cancer cell invasion, growth, angiogenesis, inflammation, and metastasis (1, 2). MMP-26 is a novel enzyme that was recently cloned and characterized by our group (3) and others (4-6). It has several structural features characteristic of MMPs, including a signal peptide, a propeptide domain, and a catalytic domain with a conserved zinc-binding motif, but it lacks the hemopexin-like domain (3-6). A unique "cysteine switch" sequence in the prodomain, PHCGVPD as opposed to the conserved PRGXXD sequence found in many other MMPs, keeps the enzyme latent.

MMP-26 mRNA is primarily expressed in cancers of epithelial origin, such as endometrial carcinomas (3, 7), prostate carcinomas (7), lung carcinomas (7), and their corresponding cell lines (3-6), and in a small number of normal adult tissues, such as the uterus (3, 5), placenta (4, 5), and kidney (6). Some parallels exist with MMP-7, which is also expressed epithelially and also lacks the hemopexin-like domain. We have also reported that the levels of *MMP-26 gene* and

protein expression are higher in a malignant choriocarcinoma cell line (JEG-3) than in normal human cytotrophoblast cells (8). Recently, we found that the levels of MMP-26 protein in human prostate carcinomas from multiple patients were significantly higher than those in prostatitis, benign prostate hyperplasia, and normal prostate tissues (9). MMP-26 is capable of activating pro-MMP-9 by cleavage at the Ala<sup>91</sup>-Met<sup>94</sup> site of the pro-enzyme, and this activation facilitates the efficient cleavage of fibronectin (FN), promoting the invasion of highly invasive and metastatic androgen-repressed prostate cancer cells through FN or type IV collagen (9). The activation is prolonged but persistent, which is consistent with the process of tumor cell invasion. These findings indicate that MMP-26-mediated pro-MMP-9 activation may be one biochemical mechanism contributing to human carcinoma cell invasion *in vivo*.

MMP activities are inhibited by endogenous tissue inhibitors of metalloproteinases (TIMPs). Four mammalian TIMPs have been identified: (a) TIMP-1 (10); (b) TIMP-2 (11); (c) TIMP-3 (12); and (d) TIMP-4 (13). The hydrolytic activity of MMP-26 against synthetic peptides is blocked by TIMP-1, TIMP-2, and TIMP-4 (5, 6, 8), but the inhibitory potential of TIMP-1 is lower than that of TIMP-2 and TIMP-4 (5). TIMP-1 and TIMP-2 also inhibit the cleavage of denatured type I collagen (gelatin) by MMP-26 (6). TIMPs are expressed in human breast cancer cells (14-16). Here, we continue to explore the possible roles of MMP-26 and the coordination of MMP-26 with MMP-9, TIMP-2, and TIMP-4 in human breast carcinoma invasion.

In the present study, we showed that TIMP-2 and TIMP-4 completely inhibited the activation of pro-MMP-9 by MMP-26. The expressions of MMP-26, MMP-9, TIMP-2, and TIMP-4 proteins in human breast ductal carcinomas *in situ* (DCIS) were significantly higher than those in infiltrating ductal carcinoma (IDC), atypical intraductal hyperplasia (AIDH), and normal breast epithelia around the DCIS and IDC. Furthermore, MMP-26 was colocalized with MMP-9, TIMP-2, and TIMP-4 in human breast DCIS.

## MATERIALS AND METHODS

**Inhibition Assays of MMP-26 by TIMP-2 and TIMP-4.** The quenched fluorescence peptide substrates, *Mca-Pro-Leu-Ala-Nva-Dpa-Ala-Arg-NH<sub>2</sub>* and *Mca-Arg-Pro-Lys-Pro-Val-Glu-Nva-Trp-Arg-Lys(Dnp)-NH<sub>2</sub>* were purchased from Calbiochem. The MMP-26 used in this experiment is recombinant and partially active. Briefly, MMP-26 was expressed in the form of inclusion bodies from transformed *Escherichia coli* cells as described previously (3). The inclusion bodies were isolated and purified using B-PER bacterial protein extraction reagent according to the manufacturer's instructions. The insoluble protein was dissolved in 8 M urea to ~5 mg/ml. The protein solution was diluted to ~100 µg/ml in 8 M urea and 10 mM DTT for 1 h; dialyzed in 4 M urea, 1 mM DTT, and 50 mM HEPES (pH 7.5) for at least 1 h; and then folded by dialysis in 1× HEPES buffer [50 mM HEPES, 0.2 M NaCl, 10 mM CaCl<sub>2</sub>, and 0.01% Brij-35 (pH 7.5)] with 20 µM ZnSO<sub>4</sub> for 16 h. To enhance the activity of MMP-26, the folded enzyme was dialyzed twice for 24 h at 4°C in the folding buffer without Zn<sup>2+</sup> ions. The total enzyme concentration was measured by UV absorption using  $\epsilon_{280} = 57,130 \text{ M}^{-1} \text{ cm}^{-1}$ , which was

Received 6/30/03; revised 10/29/03; accepted 11/7/03.

Grant support: Department of Defense Congressionally Directed Medical Research Programs Grant DAMD17-02-1-0238, NIH Grant CA78646, American Cancer Society grant, Florida Division Grant F01FSU-1 (to Q.-X. A. S.), Florida State University Research Foundation grant (to Q.-X. A. S. and Y.-G. Z.), and Department of Defense Congressionally Directed Medical Research Programs Grants DAMD17-01-0129 and DAMD17-01-0130 (to Y.-G. M.).

The costs of publication of this article were defrayed in part by the payment of page charges. This article must therefore be hereby marked advertisement in accordance with 18 U.S.C. Section 1734 solely to indicate this fact.

Requests for reprints: Qing-Xiang Amy Sang, Department of Chemistry and Biochemistry, Florida State University, Chemistry Research Building D1C, Room 203, Tallahassee, Florida 32306-4390. Phone: (850) 644-8683; Fax: (850) 644-8281; E-mail: sang@chem.fsu.edu.

## MATRIX METALLOPROTEINASE 26 IN HUMAN BREAST CANCER

calculated using Genetics Computer Group software. The concentration of active MMP-26 was determined by active site titration with the tight-binding inhibitor GM-6001 as described previously (17). GM-6001 was the most potent inhibitor of MMP-26 tested, with a  $K_i^{app}$  of 0.36 nM (17). Because TIMPs are tight-binding and slow-binding inhibitors of MMPs, MMP-26 was incubated for 4 h with human TIMP-2 and TIMP-4 before the measurement of substrate hydrolysis to allow the enzyme and inhibitor to reach their binding equilibrium. Human fibroblast TIMP-2 was provided by Dr. L. Jack Windsor (Indiana University, Indianapolis, IN). Recombinant human TIMP-4 was purchased from R&D Systems (Minneapolis, MN). The concentrations of TIMPs ranged from 0.2 to 60 nM. The assay was initiated by the addition of a substrate stock solution (4  $\mu$ l) prepared in 1:1 water and DMSO to an enzyme-inhibitor assay buffer (196  $\mu$ l) for a final concentration of 1  $\mu$ M. The release of the fluorogenic cleavage product was monitored by measuring fluorescence (excitation and emission wavelengths at 328 and 393 nm, respectively) with a Perkin-Elmer Luminescence Spectrophotometer LS 50B connected to a water bath with a temperature control. All kinetic experiments were conducted in 1 $\times$  HEPES buffer. Fluorogenic peptide substrate assays were performed following the procedures we reported previously (17). To assess inhibition potency, the apparent inhibition constants (apparent  $K_i$  values) were determined by fitting the two trial data sets to the Morrison equation below (18) with nonlinear regression. In this equation,  $\nu_i$  is the initial rate of MMP-26 catalysis in the presence of inhibitor, and  $\nu_o$  is the initial rate without inhibitor. [E] and [I] are the initial enzyme and inhibitor concentrations, respectively, and  $K_i^{app}$  is the apparent inhibition constant.

$$\frac{\nu_i}{\nu_o} = 1 - \frac{([E] + [I] + K_i^{app}) - \sqrt{([E] + [I] + K_i^{app})^2 - 4[E][I]}}{2[E]}$$

**Pro-MMP-9 Activation by MMP-26 and Inhibition of the Activation by TIMP-2 and TIMP-4.** Zymography and silver staining were performed as reported previously (3, 7, 19, 20). MMP-26, pro-MMP-9, and active MMP-9 were purified in our laboratory (3, 21). The molar concentration ratios of TIMPs, MMP-26, and pro-MMP-9 were 10:1:4. Two metal chelators/metalloproteinase inhibitors, 1, 10-phenanthroline and EDTA, were used as controls. Briefly, MMP-26 was incubated in the presence or absence of different inhibitors (TIMPs, 1,10-phenanthroline, and EDTA) in 30  $\mu$ l of 1 $\times$  HEPES buffer at room temperature (25°C) for 4 h. Pro-MMP-9 was then added and incubated at 37°C for 20 h. For zymography, aliquots of the reaction solution were removed and treated with a nonreducing sample buffer. MMP-9 activity was analyzed by zymography on 9% SDS-polyacrylamide gels containing 1% gelatin (22). For silver staining, aliquots were removed and treated with a

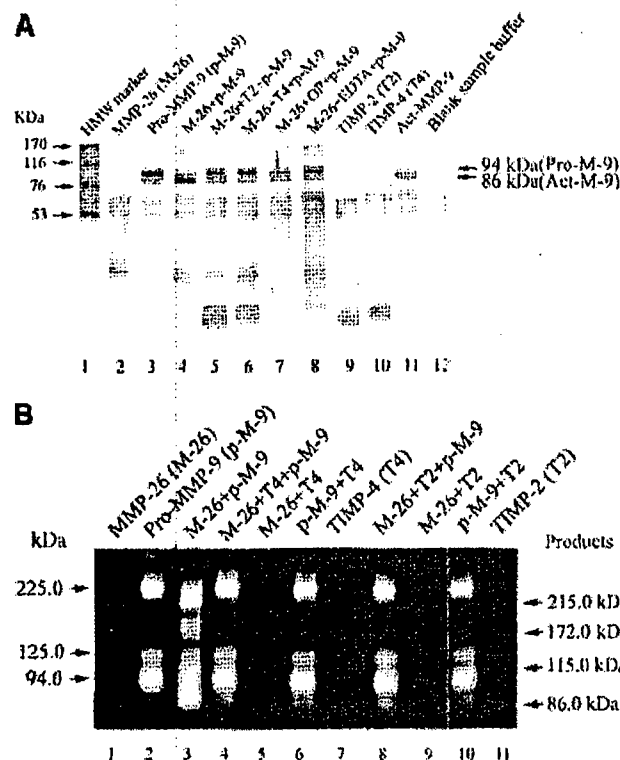


Fig. 2. Tissue inhibitor of metalloproteinases (TIMP)-2 and TIMP-4 inhibit pro-matrix metalloproteinase (MMP)-9 activation by MMP-26. **A**, pro-MMP-9 activation by MMP-26 was inhibited by both TIMP-2 and TIMP-4 (electrophoresis samples were treated under reducing conditions). MMP-26 activates pro-MMP-9, enhancing the 86-kDa band (Lane 4). This activation was completely blocked by adding TIMP-2 (Lane 5) or TIMP-4 (Lane 6). The inhibition by TIMP-2 and TIMP-4 is comparable with that of two broad-spectrum metal chelators/metalloproteinase inhibitors, 1,10-phenanthroline (OP) and EDTA (Lanes 7 and 8). **B**, zymogram assay of MMP-9 activation by MMP-26 and inhibition by TIMP-2 and TIMP-4 (electrophoresis samples under nonreducing conditions). The 225-kDa band is a homodimer of pro-MMP-9, the 125-kDa band is a heterodimer of pro-MMP-9 and neutrophil gelatinase-associated lipocalin, and the 94-kDa band is a monomer of pro-MMP-9. MMP-26 activates pro-MMP-9 to generate new 215-, 172-, 115-, and 86-kDa active fragments (Lane 3). This activation was completely blocked by adding TIMP-4 (Lane 4) or TIMP-2 (Lane 8).

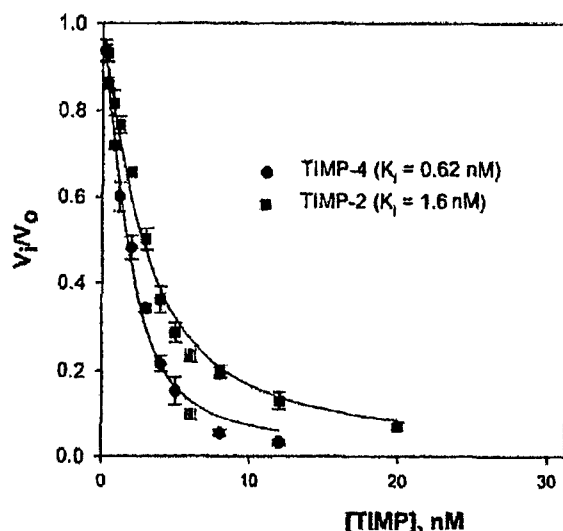


Fig. 1. Inhibition kinetics of matrix metalloproteinase 26 by tissue inhibitor of metalloproteinases (TIMP)-2 and TIMP-4. Matrix metalloproteinase 26 (2 nM) was incubated for 4 h in the presence of TIMP-2 or TIMP-4 at concentrations of 0.2–60 nM. The substrate hydrolysis assay was initiated by the addition of substrate stock solution. The data were fitted to the Morrison equation to calculate the apparent  $K_i$  values.

reducing sample buffer and boiled for 5 min. After electrophoresis on 9% SDS-polyacrylamide gels, the protein bands were visualized by silver staining (19).

**FN Cleavage Assay.** MMP-26, pro-MMP-9, MMP-26-activated MMP-9, and TIMPs were prepared as described above. Active MMP-9, purified from human neutrophils (21), was used as a positive control. FN was incubated with MMP-26, pro-MMP-9, active MMP-9, or MMP-26 plus pro-MMP-9 in the presence or absence of TIMP-2 or TIMP-4 in 1 $\times$  HEPES buffer at 37°C for 18 h. The molar concentration ratio of MMP-26:pro-MMP-9:FN:TIMP was approximately 1:4:10:10. Aliquots were removed and treated with a reducing sample buffer and boiled for 5 min. Samples were then loaded onto 9% polyacrylamide gels in the presence of SDS, electrophoresed, and subjected to silver staining (19).

**In Situ Hybridization.** The DCIS samples were classified according to our previous reports (23, 24). Briefly, the formalin-fixed, paraffin-embedded samples were sectioned to 5- $\mu$ m thickness and fixed onto slides. The full-length MMP-26 sense cDNA and antisense cDNA were amplified in pCR 3.1 and purified as described in our previous report (9). The sense and antisense plasmids were linearized with *Xho*I and *Xba*I, respectively. The sense and antisense digoxigenin-labeled RNA probes were generated by *in vitro* transcription with T7 polymerase. *In situ* hybridization was performed as per our previous report (22). Briefly, the paraffin-embedded sections (5  $\mu$ m) were deparaffinized with xylene and treated with proteinase K solution [50  $\mu$ g/ml in 0.2 M Tris-HCl (pH 7.5), 2 mM  $MgCl_2$ ] for 15 min at room temperature. After prehybridization, the sections were hybridized to digoxigenin-labeled MMP-26 antisense cRNA probes for 18 h at 45°C and 100% humidity. The

## MATRIX METALLOPROTEINASE 26 IN HUMAN BREAST CANCER

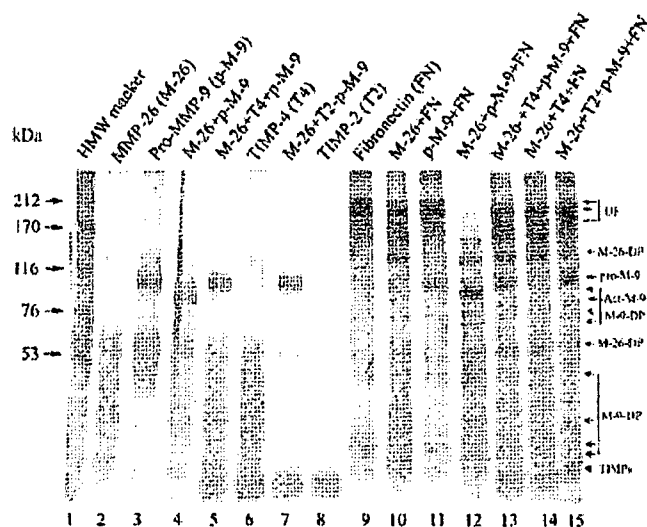


Fig. 3. Cleavage of fibronectin (FN) by matrix metalloproteinase (MMP)-9 and MMP-26. MMP-26 cleaved FN weakly, generating 125- and 58-kDa bands (Lane 10). pro-MMP-9 did not cleave FN (Lane 11), and MMP-26-activated MMP-9 (Lane 4) cleaved FN efficiently (Lane 12). Tissue inhibitor of metalloproteinases (TIMP)-4 weakly blocked FN cleavage by MMP-26 (Lane 14). Both TIMP-4 and TIMP-2 blocked pro-MMP-9 activation by MMP-26 (Lanes 5 and 7), which significantly diminished FN cleavage (Lanes 13 and 15). UF, uncleaved fibronectin; M-26-DP, MMP-26-degraded FN products; M-9-DP, MMP-9-degraded FN products; pro-M-9, pro-MMP-9; Act-M-9, activated MMP-9.

MMP-26 sense RNA probe was used under the same hybridization conditions as the control. After hybridization, the slides were washed with saline sodium citrate buffer and blocked [1% blocking reagents in Tris-buffered saline (pH 7.5)] for 30 min. The slides were then covered with anti-digoxigenin-alkaline phosphatase Fab fragments (1:400) for 2 h. Then the slides were stained with nitroblue tetrazolium/5-bromo-4-chloro-3-indolyl phosphate (Roche Applied Science, Mannheim, Germany). The expression signals were photographed under a microscope.

**Immunohistochemistry.** The human breast DCIS, IDC, and hyperplasia tissue samples were classified according to our reports (23–26). Immunohistochemistry was performed on consecutive sections according to our previous report (9). Briefly, the formalin-fixed, paraffin-embedded samples were sectioned to 5- $\mu$ m thickness and fixed onto slides. After dewaxing and rehydrating, the slides were blocked with 3% BSA/Tris-buffered saline for 1 h at room temperature before incubation with affinity-purified, polyclonal rabbit antihuman MMP-26, MMP-9, TIMP-2, and TIMP-4 antibodies (all 25  $\mu$ g/ml) at room temperature for 90 min. Sections were then incubated with alkaline phosphatase-conjugated secondary antirabbit antibody (1:500; Jackson ImmunoResearch, West Grove, PA) for 1 h at room temperature. The signals were detected with Fast-red (Sigma, St. Louis, MO). Purified preimmune IgGs from the same animal were used as negative controls.

**Double Immunofluorescence and Confocal Laser Scanning Microscopy.** Double immunofluorescence staining was performed as per our previous description (9). Briefly, the slides were incubated with a rabbit antihuman MMP-26 IgG (25  $\mu$ g/ml) and a goat antihuman MMP-9 antibody (1:200 dilution; R&D Systems) or a mouse antihuman MMP-26 IgG (25  $\mu$ g/ml; R&D Systems) and a rabbit antihuman TIMP-4 (25  $\mu$ g/ml) or a rabbit antihuman TIMP-2 antibody (30  $\mu$ g/ml) overnight at 4°C. The slides were then incubated with a goat antimouse-IgG IgG for 30 min at room temperature. Secondary Rhodamine Red-X-conjugated donkey antirabbit IgG and FITC-conjugated donkey antigiant IgG (Jackson ImmunoResearch) were subsequently applied at a 1:50 dilution for 30 min at room temperature. Slow Fade mounting medium was added to the slides, and fluorescence was analyzed using a Zeiss LSM510 Laser Scanning Confocal Microscope (Carl Zeiss, Heidelberg, Germany) equipped with a multi-photon laser. Images were processed for reproduction using Photoshop software version 6.0 (Adobe Systems, Mountainview, CA). Purified preimmune IgG and normal goat serum were used as negative controls.

**Densitometric and Statistical Analysis.** Four to 16 pictures were taken from the glandular epithelia after immunostaining by each of the four antibodies and the two preimmune IgGs in the DCIS, IDC, AIDH, and normal glands around the DCIS and IDC. Quantification of the immunostaining signals was performed using the Metamorph System (version 4.6r8; Universal Imaging Corp., Inc., West Chester, PA) according to our previous description (9). Briefly, an appropriate color threshold was determined (color model, HSI; hue, 230–255; saturation and intensity, full spectrum). The glandular epithelia

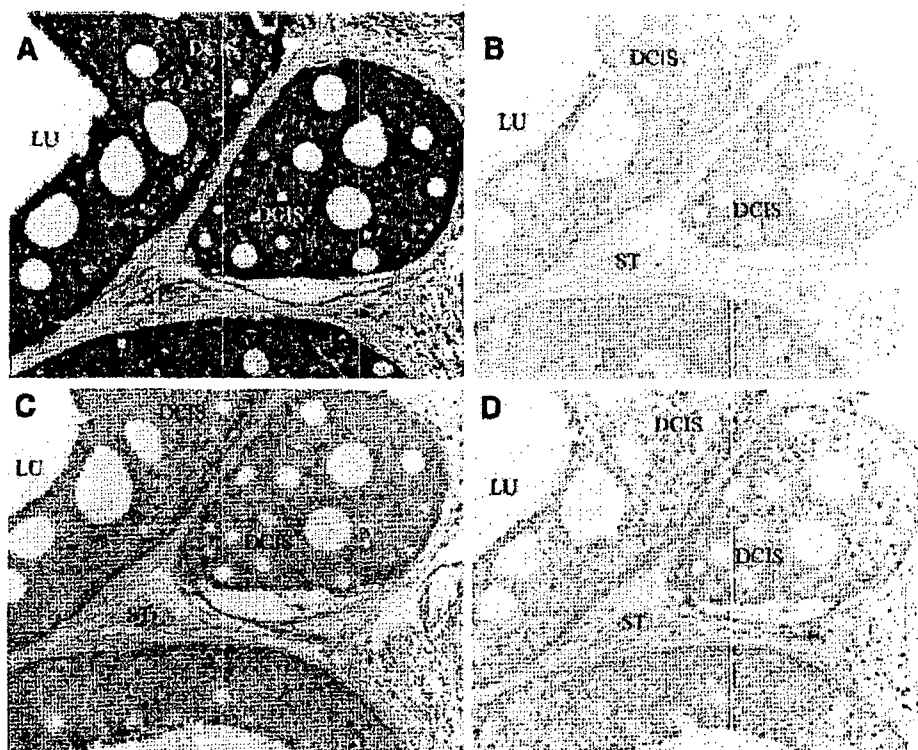


Fig. 4. Matrix metalloproteinase (MMP)-26 mRNA and protein expression in human mammary tissues. A and B are *in situ* hybridization to detect MMP-26 mRNA expression, and C and D are immunohistochemical staining to detect MMP-26 protein expression. A, MMP-26 antisense probe; B, MMP-26 sense probe; C, rabbit antihuman MMP-26 metallo domain IgG; D, pre-immune IgG. Blue indicates MMP-26 mRNA signals, and red indicates MMP-26 protein expression. Cells were counterstained lightly with hematoxylin for viewing of negatively stained epithelial and stromal cells in C and D. DCIS, ductal carcinoma *in situ*; ST, stroma; LU, lumen.



## MATRIX METALLOPROTEINASE 26 IN HUMAN BREAST CANCER

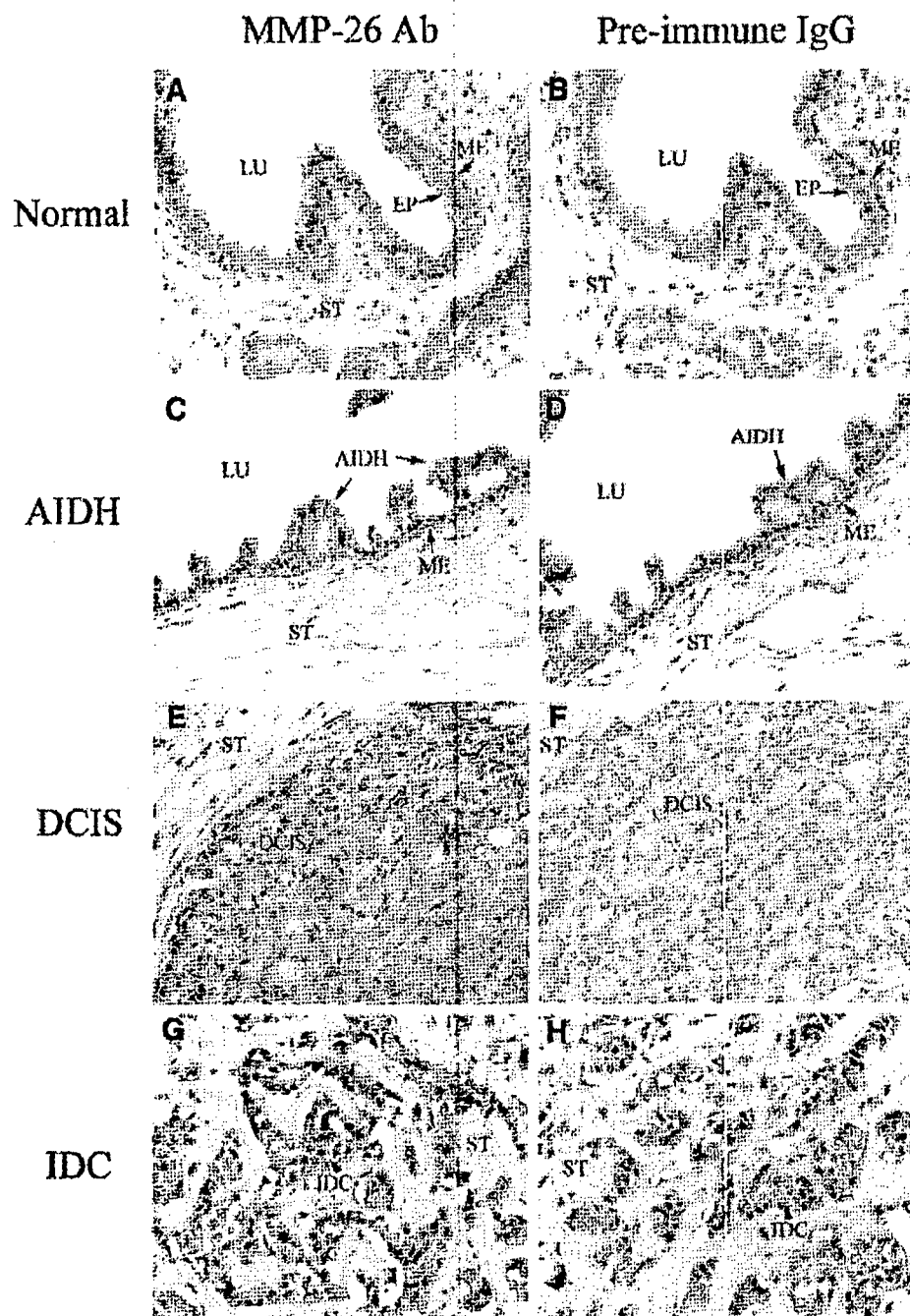


Fig. 5. Expression of matrix metalloproteinase (MMP)-26 protein in human mammary gland. Cells stained red indicate MMP-26 protein expression. All sections were counterstained lightly with hematoxylin for viewing negatively stained epithelial and stromal cells. A, C, E, and G are stained with anti-MMP-26 antibody, and B, D, F, and H are stained with pre-immune IgG. A and B, normal breast tissues; C and D, atypical intraductal hyperplasia (AIDH); E and F, breast ductal carcinoma *in situ* (DCIS); G and H, breast infiltrating ductal carcinoma (IDC). All figures are  $\times 200$  magnifications. LU, lumen; EP, epithelial cells; ST, stroma; ME, myoepithelial cells.

from each image were isolated into closed regions, and the signal areas and intensities of staining in compliance with the chosen parameters were measured by integrated morphometry analysis. The selected epithelial area was obtained by region measurement. The signal intensities were expressed as integrated absorbance (IOD, the sum of the optical densities of all pixels that make up the object). The ratio of the IOD to the selected epithelial area was determined, and the average ratios from each case were then calculated and used for statistical analysis. Statistical analysis of all samples was performed with the least significant difference correction of ANOVA for multiple comparisons. Data represent the mean  $\pm$  SE, and  $P < 0.05$  was considered significant.

## RESULTS

**Determination of the Apparent Inhibition Constants of TIMP-2 and TIMP-4 against MMP-26.** The apparent  $K_i$  values of MMP-26 were measured and calculated to be 1.6 and 0.62 nM for TIMP-2 and

TIMP-4, respectively (Fig. 1), using the Morrison equation (18). The apparent  $K_i$  values show that TIMP-4 is a slightly more potent inhibitor of MMP-26 than TIMP-2.

**Activation of Pro-MMP-9 by MMP-26 and Inhibition of the Activation by TIMP-2 and TIMP-4.** To explore the inhibition of MMP-26-mediated MMP-9 activation by TIMP-2 and TIMP-4, purified pro-MMP-9 and MMP-26 were incubated with these TIMPs, and the samples were subsequently analyzed by SDS-PAGE. MMP-26 cleaved pro-MMP-9 (94 kDa) to yield an enhanced active form 86-kDa band on a silver-stained gel under reducing conditions as per our recent report (Ref. 9; Fig. 2A, Lane 4). Zymography revealed that pro-MMP-9 presented as 225-, 125-, and 94-kDa gelatinolytic bands under nonreducing conditions. The 225-kDa band is a homodimer of pro-MMP-9, the 125-kDa band is a heterodimer of pro-MMP-9 and neutrophil gelatinase-associated lipocalin, and the 94-kDa band is a



## MATRIX METALLOPROTEINASE 26 IN HUMAN BREAST CANCER

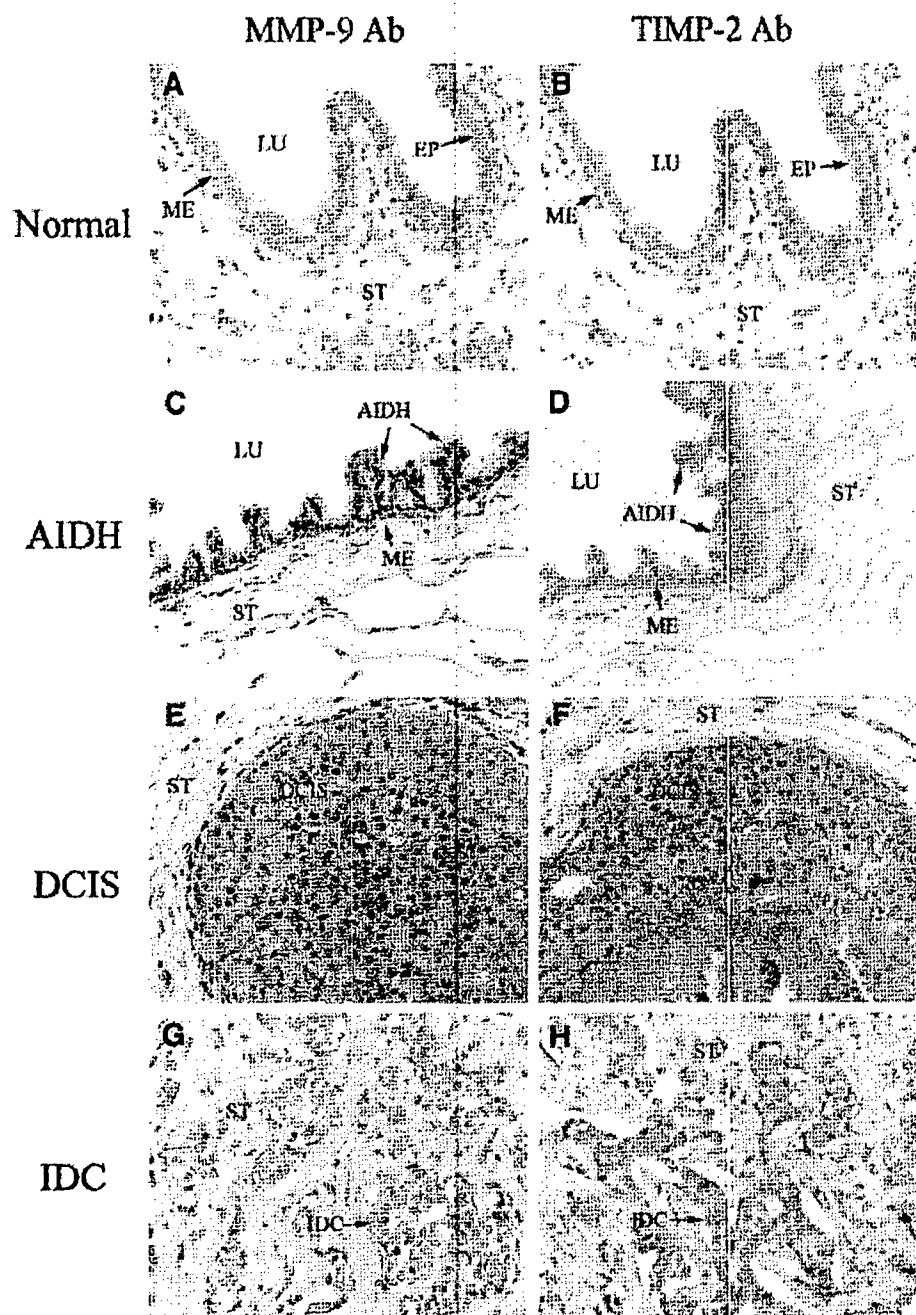


Fig. 6. Expression of matrix metalloproteinase (MMP)-9 and tissue inhibitor of metalloproteinases (TIMP)-2 proteins in human mammary gland. Cells stained red indicate MMP-9 or TIMP-2 protein expression. All sections were counterstained lightly with hematoxylin for viewing negatively stained epithelial and stromal cells. A, C, E, and G are stained with anti-MMP-9 antibody. B, D, F, and H are stained with TIMP-2 antibody. A and B, normal breast tissues; C and D, atypical intraductal hyperplasia (AIDH); E and F, ductal carcinoma in situ (DCIS); G and H, infiltrating ductal carcinoma (IDC). All figures are  $\times 200$  magnifications. LU, lumen; EP, epithelial cells; ST, stroma; ME, myo-epithelial cells.

monomer of pro-MMP-9 (21, 27, 28). The new active 215-, 172-, 115-, and 86-kDa bands were generated after incubation with MMP-26 (Fig. 2B, Lane 3). The 215-, 115-, and 86-kDa bands are the active forms of the 225-, 125-, and 94-kDa forms, respectively. The 172-kDa band is a dimer of the 86-kDa forms. The activation of pro-MMP-9 by MMP-26 was completely inhibited by recombinant TIMP-2 and TIMP-4 (Fig. 2A, Lanes 5 and 6; Fig. 2B, Lanes 4 and 8). The blocking efficiencies of TIMP-2 and TIMP-4 were comparable with those of two broad-spectrum metal chelators/metalloproteinase inhibitors, 1,10-phenanthroline and EDTA (Fig. 2A, Lanes 7 and 8).

To further confirm the inhibition of MMP-26-mediated pro-MMP-9 activation by TIMP-2 and TIMP-4, *in vitro* FN cleavage assays were performed. MMP-26 slowly cleaved FN to generate 125- and 58-kDa bands (Fig. 3, Lane 10), whereas pro-MMP-9 did not cleave FN (Fig. 3, Lane 11). However, MMP-26-activated MMP-9 cleaved FN com-

pletely, generating at least seven new bands (Fig. 3, Lane 12). Both TIMP-2 and TIMP-4 completely blocked the activation of pro-MMP-9 by MMP-26, which subsequently resulted in inhibition of FN cleavage (Fig. 3, Lanes 13 and 15).

**Expression of MMP-26 mRNA in Human Breast Tissues.** *In situ* hybridization showed that MMP-26 mRNA was localized in human breast DCIS (Fig. 4A). On a serial section of the same tissue, MMP-26 protein was also detected in human breast DCIS (Fig. 4C). The MMP-26 sense probe and pre-immune IgG from the same animal as the MMP-26 antibody were used as controls (Fig. 4, B and D).

**Expressions of MMP-26, MMP-9, TIMP-2, and TIMP-4 Proteins in Human Breast Tissues.** MMP-26, MMP-9, TIMP-2, and TIMP-4 proteins were detected in human breast epithelia (Figs. 5-7). The expressions of the four proteins were extremely high in human breast DCIS (20 cases) cells (Fig. 5E; Fig. 6, E and F; Fig. 7E) but

## MATRIX METALLOPROTEINASE 26 IN HUMAN BREAST CANCER

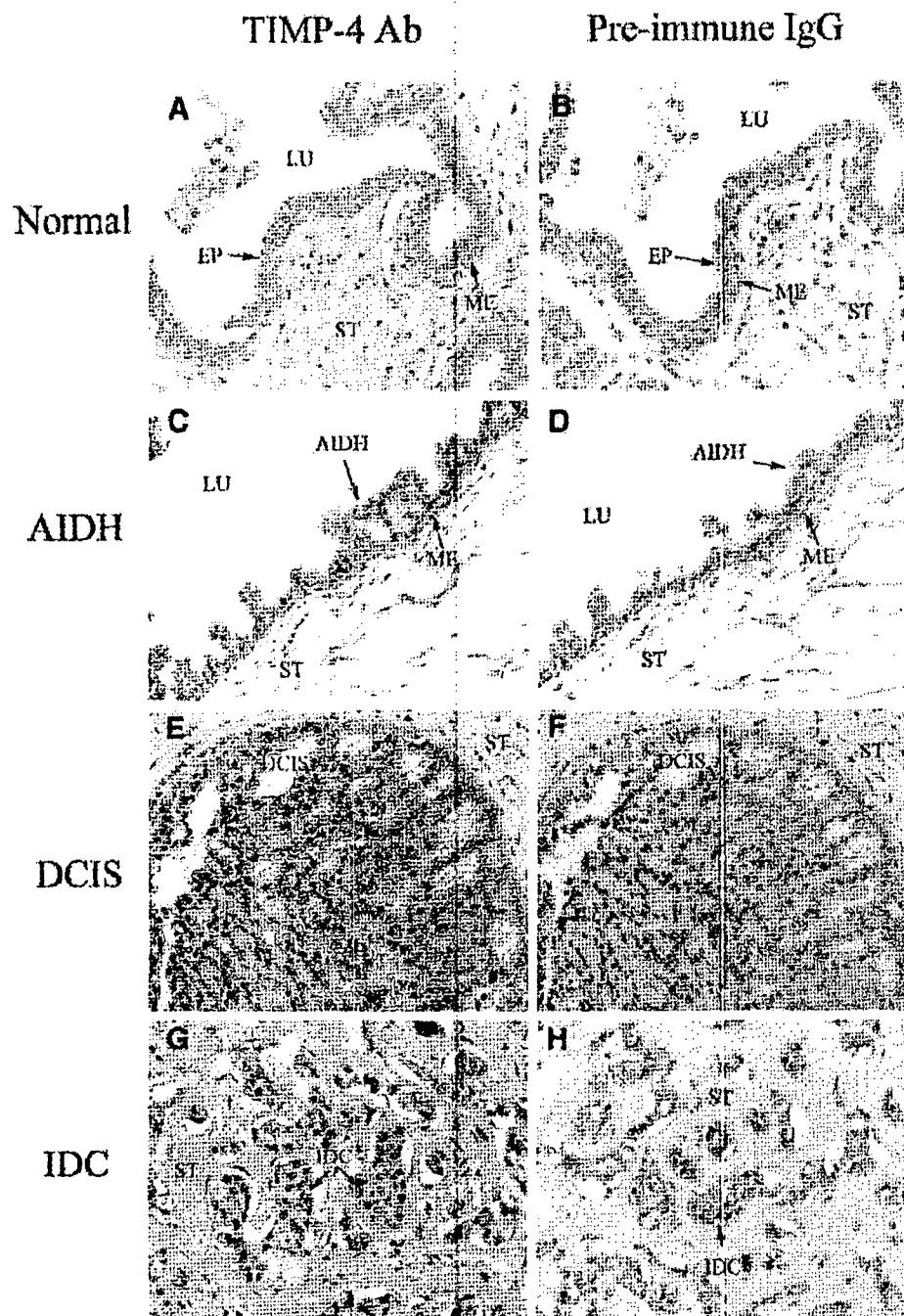


Fig. 7. Expression of tissue inhibitor of metalloproteinases (TIMP)-4 protein in human mammary gland. Cells stained red indicate TIMP-4 protein expression. All sections were counterstained lightly with hematoxylin for viewing negatively stained epithelial and stromal cells. A, C, E, and G are stained with antihuman TIMP-4 antibody. B, D, F, and H are stained with pre-immune IgG. A and B, normal breast tissues; C and D, atypical intra-ductal hyperplasia (AIDH); E and F, ductal carcinoma in situ (DCIS); G and H, infiltrating ductal carcinoma (IDC). All figures are  $\times 200$  magnifications. LU, lumen; EP, epithelial cells; ST, stroma; ME, myoepithelial cells.

very low in the normal glandular epithelial cells (25 cases) around DCIS and IDC (Fig. 5A; Fig. 6, A and B; Fig. 7A) and also in AIDH [15 cases (Fig. 5C; Fig. 6, C and D; Fig. 7C)]. Their expressions were substantially decreased in IDC [23 cases (Fig. 5G; Fig. 6, G and H; Fig. 7G)]. Statistical analysis revealed that the signal intensities of MMP-26, MMP-9, TIMP-2, and TIMP-4 proteins in DCIS were significantly higher than those in IDC, AIDH, and normal epithelia around the DCIS and IDC ( $P < 0.05$  or  $P < 0.01$ ; Fig. 8). There was no significant difference for the signals of MMP-26, MMP-9, TIMP-2, and TIMP-4 proteins among the normal epithelia around the DCIS and IDC, or in the AIDH and IDC samples ( $P > 0.05$ ; Fig. 8). Pre-immune IgGs from the same animals as the MMP-26 or TIMP-4 antibodies were used as controls (Fig. 5, B, D, F, and H; Fig. 7, B, D, F, and H). There was no significant difference ( $P > 0.05$ ) for the

pre-immune IgG signals among the normal, AIDH, DCIS, and IDC samples.

**Coexpression of MMP-26 and MMP-9 in Human Breast Carcinoma.** To confirm the distributions of MMP-26, MMP-9, TIMP-2, and TIMP-4 within carcinoma cells, double immunofluorescence staining assays were performed in human breast DCIS samples. MMP-26 protein was localized mainly in the cytoplasm of the cancerous cells (Fig. 9A, red; Fig. 9B, green), which is consistent with our previous report (9). MMP-9 was localized both in the cytoplasm of the cancerous cells and at the cell surface, mainly on the cell membrane (Fig. 9C, green). The merged picture shows that MMP-26 and MMP-9 were coexpressed in the cytoplasm of the cancerous cells (Fig. 9E, yellow). The high magnification pictures in Fig. 9, A, C, and E, clearly demonstrate MMP-26 and MMP-9 colocalization (indicated by ar-

## MATRIX METALLOPROTEINASE 26 IN HUMAN BREAST CANCER

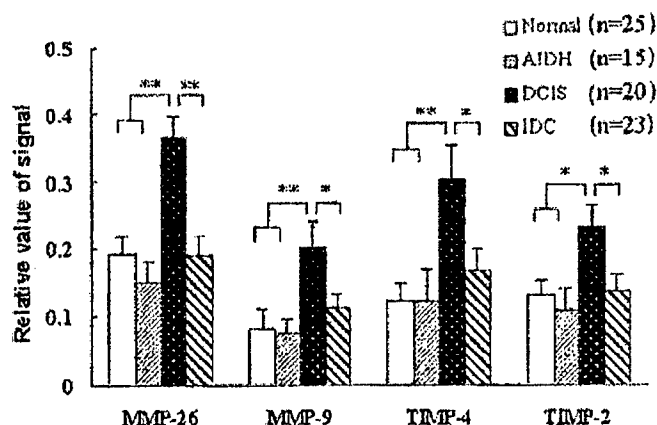


Fig. 8. Densitometric quantification analyses of matrix metalloproteinase 26, matrix metalloproteinase 9, tissue inhibitor of metalloproteinases 2, and tissue inhibitor of metalloproteinases 4 protein expression. The quantification analysis was described in "Materials and Methods." The epithelial regions were isolated, and the staining area and total selected area were obtained by Integrated Morphometry Analysis (IMA) and analyzed by one-way ANOVA with least significant difference (LSD) correction. Each value represents the mean  $\pm$  SE. \*,  $P < 0.05$ ; \*\*,  $P < 0.01$ . Normal, normal breast tissue; AIDH, atypical intraductal hyperplasia; DCIS, ductal carcinoma *in situ*; IDC, infiltrating ductal carcinoma; n, the number of cases.

rowheads). TIMP-4 is shown in Fig. 9D (red). MMP-26 and TIMP-4 were also coexpressed in the cytoplasm of the cancerous cells (Fig. 9F, yellow). MMP-26 and TIMP-2 were also colocalized in cancer cells, and minimal signals were detected in control tissues using purified pre-immune rabbit IgG and nonimmune goat sera (data not shown).

## DISCUSSION

The epithelial component of the normal and noninvasive human breast is physically separated from the stroma by myoepithelial cells and the basement membrane, which is composed of a group of fibrous proteins, including type IV collagen, FN, laminin, and proteoglycans. The disruption of both the myoepithelial cell layer and the basement membrane is an essential prerequisite for the invasion of DCIS. In this present investigation, we found that the levels of MMP-26 and MMP-9 proteins in human breast DCIS were significantly higher than those in human breast IDC, normal mammary glands, and AIDH. MMP-26 and MMP-9 were colocalized in human breast DCIS cells. MMP-9 is a powerful enzyme associated with human breast cancer development and invasion (29, 30). Scorilas *et al.* (29) and Soini *et al.* (31) demonstrated that *MMP-9 mRNA* and protein were highly expressed in human breast carcinoma cells. MMP-9 protein is also expressed in the breast carcinoma cell lines MCF-7 (32, 33), SKBR-3 (34), MDA-MB-231 (35, 36), and MCF10A (36) and in normal breast epithelial cell lines HMT-3522 and T4-2 (32, 37). Our recent study (9) demonstrated that the level of MMP-26 protein in human prostate carcinomas is also significantly higher than those in prostatitis, benign prostate hyperplasia, and normal prostate tissues. MMP-26 and MMP-9 are not only coexpressed in human prostate carcinomas and in androgen-repressed prostate cancer cells, but they also promoted the invasion of androgen-repressed prostate cancer cells across FN or type IV collagen via MMP-26-mediated pro-MMP-9 activation.

Nguyen *et al.* (38) showed that active MMP-9 accumulates in the cytosol of human endothelial cells, where it is eventually used by invading pseudopodia, and it is possible that endogenous, self-activated MMP-26 serves as an activator for intracellular pro-MMP-9. The active form of MMP-9 may then be stored inside the cell, ready for rapid release when it is required to initiate invasion of human

breast DCIS cells. Although DCIS is not invasive cancer, it may have the potential to develop into IDC, given time. The localization of *MMP-26 mRNA* and protein in carcinomas was confirmed by *in situ* hybridization and immunohistochemistry, providing evidence that MMP-26 is an epithelial cell-derived enzyme (3–6).

We demonstrated that the hydrolysis of synthetic peptides by MMP-26 is inhibited by TIMP-2 and TIMP-4, which is consistent with previous reports (5, 6, 8). TIMP-2 and TIMP-4 were also able to completely block MMP-9 activation by MMP-26, as well as the cleavage of FN by MMP-26-activated MMP-9. Therefore, one consequential function of TIMP-2 and TIMP-4 may be their inhibition of MMP-9 activation by MMP-26. TIMP-2 and TIMP-4 possess several distinct cellular functions, but their most widely appreciated biological functions are their roles in the inhibition of cell invasion *in vitro* (39–42) and their *in vivo* contributions to tumorigenesis (43, 44) and growth and metastasis (44–47). The underlying molecular mechanism for the tumor-suppressing activities of the TIMPs is thought to be dependent on their anti-MMP activities.

In our experiments, the expressions of TIMP-2 and TIMP-4 were all increased significantly in human breast DCIS but decreased in IDC, mimicking the expression of MMP-26 and MMP-9 in DCIS and IDC, which indicates that these four proteins are highly coordinated during human breast carcinoma development and progression. It may also suggest that remodeling of the extracellular matrix by MMP-26 and MMP-9 stimulates the expression of TIMP-2 and TIMP-4, implying self-regulation through a negative feedback loop. The consistently high expression of TIMP-2 and TIMP-4 proteins in human breast DCIS is in agreement with reports that the expression of TIMP-2 and TIMP-4 in human breast carcinomas is increased (14, 16,

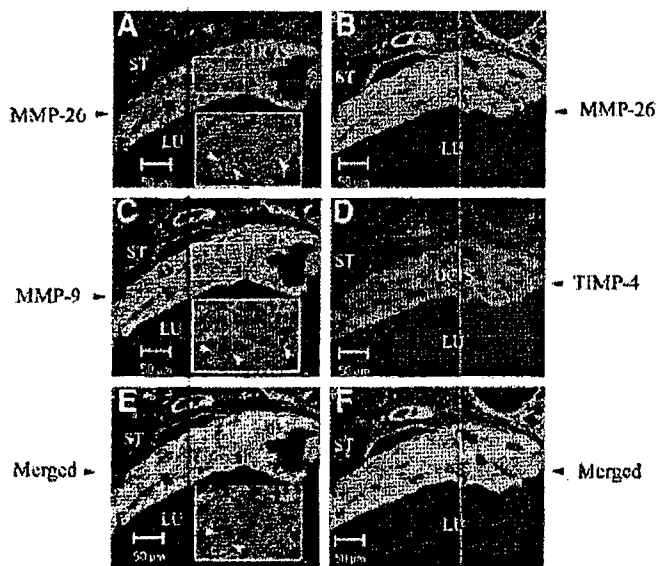


Fig. 9. Coexpression of matrix metalloproteinase (MMP)-26 with MMP-9 or tissue inhibitor of metalloproteinases (TIMP)-4 in human breast ductal carcinoma *in situ* (DCIS). In A, C, and E, the primary antibodies are rabbit anti-human MMP-26 IgG and goat anti-human MMP-9 IgG, the secondary antibodies are Rhodamine Red-X-conjugated donkey anti-rabbit IgG and FITC-conjugated donkey anti-goat IgG. A, red indicates MMP-26 protein staining, which is localized mainly in the cytoplasm of DCIS cells. C, green indicates MMP-9 protein staining, which is localized mainly on the cell surface of the cancerous cells. E, merged images show a color shift to orange-yellow, indicating colocalization between MMP-26 and MMP-9 proteins in DCIS. In B, D, and F, the primary antibodies are mouse anti-human MMP-26 IgG and rabbit anti-human TIMP-4 IgG. After incubation with primary antibodies, the slides were incubated with goat anti-mouse IgG IgG. The secondary antibodies are the same as those described in A, C, and E. B, green indicates MMP-26 protein staining, which is localized mainly in the cytoplasm of DCIS cells. D, red indicates TIMP-4 protein staining. F, merged images show a color shift to orange-yellow, indicating colocalization between MMP-26 and TIMP-4 proteins in DCIS. Scale bars, 50  $\mu$ m. ST, stroma; LU, lumen.

39, 48). This may represent a compensatory response to the increased MMP-26- and MMP-9-mediated remodeling stimuli in DCIS in an attempt to reach a new balance between MMP-26/MMP-9 and TIMP-2/TIMP-4 to regulate degradation of the extracellular matrix and to suppress tumor progression by impeding MMP-26, MMP-9, and MMP-26-mediated MMP-9 activation. TIMP-2 and TIMP-4 may play multiple roles in human breast cancer in addition to inhibiting MMPs, including antiapoptotic activity and tumor-stimulating effects when administered systemically (16). The new paradigms concerning the potential roles of TIMPs in suppressing or promoting tumor progression have been discussed previously (49).

The decreased MMP-26 and MMP-9 expression levels in IDC suggest that these two enzymes may play a role in the very early stages of DCIS invasion, but once the basement membrane has been breached, cancer cells become less dependent on the activities of MMP-26 and MMP-9. Nielsen *et al.* (50) demonstrated that MMP-9 immunostaining or *in situ* hybridization signals were not detected in human breast ductal carcinoma cells but were seen in tumor-infiltrating stromal cells including macrophages, neutrophils, and vascular pericytes. This indicates that MMP-9 may be transiently expressed in cells during the early stages of human breast carcinoma (DCIS), but not in the later stages of breast carcinoma (IDC). The controversy surrounding the expression of MMP-9 found in the literature (29, 31, 50), inclusive of our current findings, might also suggest that these different expression patterns arise from DCIS and IDC representing genetically distinct disease forms, raising the possibility that DCIS does not simply designate a transitory disease state that invariably leads to IDC.

Down-regulation of TIMPs contributed significantly to the tumorigenic and invasive potentials of cancer cells (43, 44). Decreased production of TIMP-2 resulted in increased MMP activity, leading to increased invasiveness by cancer cells (39). Therefore, maintenance of the balance between MMPs and TIMPs appears critical for the suppression of cancer cell invasion and metastasis. Once the balance between MMP-26/MMP-9 and TIMP-2/TIMP-4 in DCIS is destroyed, the inhibition by TIMP-2 and TIMP-4 may be inadequate to block the degradation of extracellular matrix components by MMP-26 and MMP-9 in DCIS, resulting in degradation of basement membrane components and initiation of the invasive processes of DCIS cells. MMP-26, MMP-9, TIMP-2, and TIMP-4 may be spatially and temporally expressed in the very early stages of DCIS invasion, whereas other enzymes/inhibitors are responsible for the late-stage invasion of IDC cells. Further investigations will provide a more complete understanding of the functions of MMP-26, MMP-9, and TIMPs in human breast cancer progression.

## ACKNOWLEDGMENTS

We thank Dr. L. Jack Windsor of Indiana University for kindly providing us with TIMP-2 protein and the polyclonal anti-TIMP-2 antibody, Dr. Weiping Jiang of R&D Systems for the monoclonal anti-MMP-26 antibody, Dr. Jianzhou Wang of University of Oklahoma College of Medicine for critical review of the manuscript, and Sara C. Monroe at our laboratory at Florida State University for editorial assistance with manuscript preparation. We are also grateful to Kimberly Riddle and Jon Ekman at the Department of Biological Sciences Imaging Resources at Florida State University for their excellent assistance with confocal microscopy and integrated morphometry analysis.

## REFERENCES

1. Sternlicht, M. D., and Werb, Z. How matrix metalloproteinases regulate cell behavior. *Annu. Rev. Cell Dev. Biol.*, 17: 463-516, 2001.
2. Egeblad, M., and Werb, Z. New functions for the matrix metalloproteinases in cancer progression. *Nat. Rev. Cancer*, 2: 163-176, 2002.
3. Paik, H. I., Ni, J., Gerkema, F. E., Liu, D., Belozertv, V. E., and Sang, Q. X. Identification and characterization of human endonuclease (matrix metalloproteinase-26) from endometrial tumor. *J. Biol. Chem.*, 275: 20549-20544, 2000.
4. de Coignac, A. B., Elson, G., Delneste, Y., Magistrelli, G., Jeannin, P., Aubry, J. P., Berthier, O., Schmitz, D., Bonnefoy, J. Y., and Gauchat, J. F. Cloning of MMP-26. A novel matrilysin-like proteinase. *Eur. J. Biochem.*, 267: 3323-3329, 2000.
5. Uriá, J. A., and López-Otin, C. Matrilysin-2, a new matrix metalloproteinase expressed in human tumors and showing the minimal domain organization required for secretion, latency, and activity. *Cancer Res.*, 60: 4745-4751, 2000.
6. Marchenko, G. N., Ratnikov, B. I., Rozanov, D. V., Godzik, A., Deryugina, E. I., and Strongin, A. Y. Characterization of matrix metalloproteinase-26, a novel metalloproteinase widely expressed in cancer cells of epithelial origin. *Biochem. J.*, 356: 705-718, 2001.
7. Marchenko, G. N., Marchenko, N. D., Leng, J., and Strongin, A. Y. Promoter characterization of the novel human matrix metalloproteinase-26 gene: regulation by the T-cell factor-4 implies specific expression of the gene in cancer cells of epithelial origin. *Biochem. J.*, 363: 253-262, 2002.
8. Zhang, J., Cao, Y. J., Zhao, Y. G., Sang, Q. X., and Duan, E. K. Expression of matrix metalloproteinase-26 and tissue inhibitor of metalloproteinase-4 in human normal cytotrophoblast cells and a choriocarcinoma cell line, JEG-3. *Mol. Hum. Reprod.*, 8: 659-666, 2002.
9. Zhuo, Y. G., Xiao, A. Z., Newcomer, R. G., Park, H. J., Kang, T., Chung, L. W., Swanson, M. G., Zhou, H. E., Kuchanewicz, J., and Sang, Q. X. Activation of pro-gelatinase B by endonuclease/matrilysin-2 promotes invasion of human prostate cancer cells. *J. Biol. Chem.*, 278: 15056-15064, 2003.
10. Carrichuel, D. F., Sommer, A., Thompson, R. C., Anderson, D. C., Smith, C. G., Welgus, H. G., and Stiecklin, G. P. Primary structure and cDNA cloning of human fibroblast collagenase inhibitor. *Proc. Natl. Acad. Sci. USA*, 83: 2407-2411, 1986.
11. Stetler-Stevenson, W. G., Brown, P. D., Onisto, M., Levy, A. T., and Liotta, L. A. Tissue inhibitor of metalloproteinases-2 (TIMP-2) mRNA expression in tumor cell lines and human tumor tissues. *J. Biol. Chem.*, 265: 13933-13938, 1990.
12. Uriá, J. A., Ferrando, A. A., Velasco, G., Freije, J. M., and Lopez-Otin, C. Structure and expression in breast tumors of human TIMP-3, a new member of the metalloproteinase inhibitor family. *Cancer Res.*, 54: 2091-2094, 1994.
13. Greene, J., Wang, M., Liu, Y. E., Raymond, L. A., Rosen, C., and Shi, Y. E. Molecular cloning and characterization of human tissue inhibitor of metalloproteinase 4. *J. Biol. Chem.*, 271: 30375-30380, 1996.
14. Remacle, A., McCarthy, K., Noel, A., Maguire, T., McDermott, E., O'Higgins, N., Foidart, J. M., and Duffy, M. J. High levels of TIMP-2 correlate with adverse prognosis in breast cancer. *Int. J. Cancer*, 20: 118-121, 2000.
15. Hurst, D. R., Li, H., Xu, X., Badisa, V. L., Shi, Y. E., and Sang, Q. X. Development and characterization of a new polyclonal antibody specifically against tissue inhibitor of metalloproteinases 4 in human breast cancer. *Biochem. Biophys. Res. Commun.*, 281: 166-171, 2001.
16. Jiang, Y., Wang, M., Celiker, M. Y., Liu, Y. E., Sang, Q. X., Goldberg, I. D., and Shi, Y. E. Stimulation of mammary tumorigenesis by systemic tissue inhibitor of matrix metalloproteinase 4 gene delivery. *Cancer Res.*, 61: 2365-2370, 2001.
17. Park, H. I., Turk, B. E., Gerkema, F. E., Cantley, L. C., and Sang, Q. X. Peptide substrate specificities and protein cleavage sites of human endonuclease/matrilysin-2/matrix metalloproteinase-26. *J. Biol. Chem.*, 277: 35168-35175, 2002.
18. Morrison, J. F. Kinetics of the reversible inhibition of enzyme-catalysed reactions by tight-binding inhibitors. *Biochim. Biophys. Acta*, 165: 269-286, 1969.
19. Zhan, Y. G., Wei, P., and Sang, Q. X. Inhibitory antibodies against endopeptidase activity of human adamalysin 19. *Biochem. Biophys. Res. Commun.*, 289: 288-294, 2001.
20. Patterson, B. C., and Sang, Q. A. Angiostatin-converting enzyme activities of human matrilysin (MMP-7) and gelatinase B/type IV collagenase (MMP-9). *J. Biol. Chem.*, 272: 28823-28825, 1997.
21. Sang, Q. X., Birkedal-Hansen, H., and Van Wart, H. E. Proteolytic and non-proteolytic activation of human neutrophil gelatinase B. *Biochim. Biophys. Acta*, 1251: 99-108, 1995.
22. Zhao, Y. G., Xiao, A. Z., Cao, X. M., and Zhu, C. Expression of matrix metalloproteinase-2, -9 and tissue inhibitors of metalloproteinase-1, -2, -3 mRNAs in rat uterus during early pregnancy. *Mol. Reprod. Dev.*, 62: 149-153, 2002.
23. Heffelfinger, S. C., Yassin, R., Miller, M. A., and Lower, E. Vascularity of proliferative breast disease and carcinoma *in situ* correlates with histological features. *Clin. Cancer Res.*, 2: 1873-1878, 1996.
24. Heffelfinger, S. C., Yassin, R., Miller, M. A., and Lower, E. E. Cyclin D1, retinoblastoma, p53, and Her2/neu protein expression in preinvasive breast pathologies: correlation with vascularity. *Pathobiology*, 68: 129-136, 2000.
25. Moinsfar, F., Man, Y. G., Lininger, R. A., Bodian, C., Tavassoli, F. A. Use of keratin 15/βE12 as an adjunct in the diagnosis of mammary intraepithelial neoplasia-ductal type-benign and malignant intraductal proliferations. *Am. J. Surg. Pathol.*, 23: 1048-1058, 1999.
26. Brattthauer, G. L., Moinsfar, F., Stamatakis, M. D., Mezzetti, T. P., Shekitka, K. M., Man, Y. G., and Tavassoli, F. A. Combined E-cadherin and high molecular weight cytokeratin immunoprofile differentiates lobular, ductal, and hybrid mammary intraepithelial neoplasias. *Hum. Pathol.*, 33: 620-627, 2002.
27. Tschesche, H., Zolzer, V., Triebel, S., and Bartsch, S. The human neutrophil lipocalin supports the allosteric activation of matrix metalloproteinases. *Eur. J. Biochem.*, 268: 1918-1928, 2001.
28. Yan, L., Borregaard, N., Kjeldsen, L., and Moses, M. A. The high molecular weight urinary matrix metalloproteinase (MMP) activity is a complex of gelatinase B/MMP-9 and neutrophil gelatinase-associated lipocalin (NGAL). Modulation of MMP-9 activity by NGAL. *J. Biol. Chem.*, 276: 37258-37265, 2001.

## MATRIX METALLOPROTEINASE 26 IN HUMAN BREAST CANCER

29. Scorilas, A., Karameris, A., Amogiannaki, N., Aravanis, A., Bassilopoulos, P., Trangas, T., and Tiliari, M. Overexpression of matrix-metalloproteinase-9 in human breast cancer: a potential favourable indicator in node-negative patients. *Br. J. Cancer*, **84**: 1488-1496, 2001.
30. Rolli, M., Fransvea, E., Pilch, J., Saven, A., Felding-Habermann, B. Activated integrin  $\alpha_5\beta_1$  cooperates with metalloproteinase MMP-9 in regulating migration of metastatic breast cancer cells. *Proc. Natl. Acad. Sci. USA*, **100**: 9482-9487, 2003.
31. Soini, Y., Hurskainen, T., Hoyhtya, M., Oikarinen, A., Antio-Harjainen, H. 72 KD and 92 KD type IV collagenase, type IV collagen, and laminin mRNAs in breast cancer: a study by *in situ* hybridization. *J. Histochem. Cytochem.*, **42**: 945-951, 1994.
32. Morgan, M. P., Cooke, M. M., Christopherson, P. A., Westfall, P. R., and McCarthy, G. M. Calcium hydroxyapatite promotes mitogenesis and matrix metalloproteinase expression in human breast cancer cell lines. *Mol. Carcinog.*, **32**: 111-117, 2001.
33. Hazan, R. B., Phillips, G. R., Qiao, R. F., Norton, L., and Aaronson, S. A. Exogenous expression of N-cadherin in breast cancer cells induces cell migration, invasion, and metastasis. *J. Cell Biol.*, **148**: 779-790, 2000.
34. Reddy, K. B., Krueger, J. S., Kondapaka, S. B., and Diglio, C. A. Mitogen-activated protein kinase (MAPK) regulates the expression of progelatinase B (MMP-9) in breast epithelial cells. *Int. J. Cancer*, **82**: 268-273, 1999.
35. Duivenvoorden, W. C., Hirte, H. W., and Singh, G. Transforming growth factor  $\beta 1$  acts as an inducer of matrix metalloproteinase expression and activity in human bone-metastasizing cancer cells. *Clin. Exp. Metastasis*, **17**: 27-34, 1999.
36. Tolh, M., Sudo, Y., Ninomiya, Y., and Fridman, R. Biosynthesis of  $\alpha 2(\text{IV})$  and  $\alpha 1(\text{IV})$  chains of collagen IV and interactions with matrix metalloproteinase-9. *J. Cell. Physiol.*, **180**: 131-139, 1999.
37. Price, D. J., Avraham, S., Feuerstein, J., Fu, Y., and Avraham, H. K. The invasive phenotype in HMT-3522 cells requires increased EGF receptor signaling through both PI 3-kinase and ERK 1,2 pathways. *Cell Commun. Adhes.*, **9**: 87-102, 2002.
38. Nguyen, M., Arkell, J., and Jackson, C. J. Active and tissue inhibitor of matrix metalloproteinase-free gelatinase B accumulates within human microvascular endothelial vesicles. *J. Biol. Chem.*, **273**: 5400-5404, 1998.
39. Poulson, R., Hanby, A. M., Pignatelli, M., Jeffery, R. E., Longcroft, J. M., Rogers, L., and Stamp, G. W. Expression of gelatinase A and TIMP-2 mRNAs in desmoplastic fibroblasts in both mammary carcinomas and basal cell carcinomas of the skin. *J. Clin. Pathol.*, **46**: 429-436, 1993.
40. Albini, A., Melchiori, A., Santi, L., Liotta, L. A., Brown, P. D., and Stetler-Stevenson, W. G. Tumor cell invasion inhibited by TIMP-2. *J. Natl. Cancer Inst.* (Bethesda), **83**: 775-779, 1991.
41. Inoue, S., Kohn, D. B., Shimada, H., Blavier, L., and DeClerck, Y. A. Overexpression of tissue inhibitor of metalloproteinases-2 retroviral-mediated gene transfer *in vivo* inhibits tumor growth and invasion. *Cancer Res.*, **56**: 2891-2895, 1996.
42. Liu, Y. E., Wang, M., Greene, J., Su, J., Ulrich, S., Li, H., Sheng, S., Alexander, P., Sang, Q. A., and Shi, Y. E. Preparation and characterization of recombinant tissue inhibitor of metalloproteinase 4 (TIMP-4). *J. Biol. Chem.*, **272**: 20479-20483, 1997.
43. Khokha, R., Waterhouse, P., Yagel, S., Lala, P. K., Overall, C. M., Norton, G., and Denhardt, D. T. Antisense RNA-induced reduction in murine TIMP levels confers oncogenicity on Swiss 3T3 cells. *Science (Wash. DC)*, **243**: 947-950, 1989.
44. Mohanam, S., Wang, S. W., Rayford, A., Yamamoto, M., Sawaya, R., Nakajima, M., Liotta, L. A., Nicolson, G. L., Stetler-Stevenson, W. G., and Rao, J. S. Expression of tissue inhibitors of metalloproteinases: negative regulators of human glioblastoma invasion *in vivo*. *Clin. Exp. Metastasis*, **13**: 57-62, 1995.
45. DeClerck, Y. A., Perez, N., Shimada, H., Boone, T. C., Langley, K. E., and Taylor, S. M. Inhibition of invasion and metastasis in cells transfected with an inhibitor of metalloproteinases. *Cancer Res.*, **52**: 701-708, 1992.
46. Wang, M., Liu, Y. E., Greene, J., Sheng, S., Fuchs, A., Rosen, E. M., and Shi, Y. E. Inhibition of tumor growth and metastasis of human breast cancer cells transfected with tissue inhibitor of metalloproteinase 4. *Oncogene*, **14**: 2767-2774, 1997.
47. Celiker, M. Y., Wang, M., Atsidaftos, E., Liu, X., Liu, Y. E., Jiang, Y., Valderrama, E., Goldberg, I. D., and Shi, Y. E. Inhibition of Wilms' tumor growth by intramuscular administration of tissue inhibitor of metalloproteinases-4 plasmid DNA. *Oncogene*, **20**: 4337-4343, 2001.
48. Ree, A. H., Flores, V. A., Berg, J. P., Maelandsmo, G. M., Nestlond, J. M., and Fodstad, O. High levels of messenger RNAs for tissue inhibitors of metalloproteinases (TIMP-1 and TIMP-2) in primary breast carcinomas are associated with development of distant metastases. *Clin. Cancer Res.*, **3**: 1621-1628, 1997.
49. Jiang, Y., Goldberg, I. D., and Shi, Y. E. Complex roles of tissue inhibitors of metalloproteinases in cancer. *Oncogene*, **21**: 2245-2252, 2002.
50. Nielsen, B. S., Sehested, M., Kjeldsen, L., Borregaard, N., Rygaard, J., and Dano, K. Expression of matrix metalloproteinase-9 in vascular pericytes in human breast cancer. *Lab. Invest.*, **77**: 345-355, 1997.





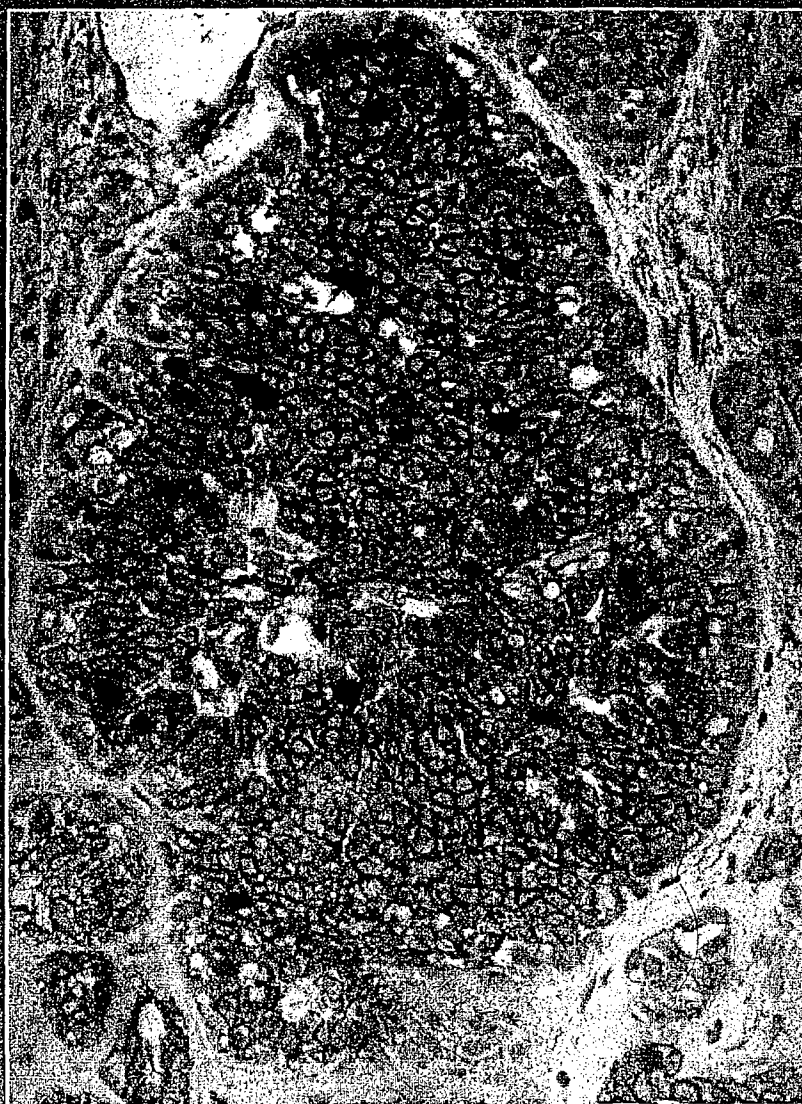
# PATHOLOGY

## RESEARCH AND PRACTICE



Co-sponsored by the American Registry of Pathology  
Co-sponsored by the Canadian Association of Pathologists  
Co-sponsored by the Japanese Society of Pathology

# 200/1



**Executive Editors:**  
Albert Rosenblatt (Chairman)  
Margarita G. Ghera  
Rikuo Maehara  
Takao Tanabe  
Klaus H. P. Dittler  
Hiroshi Iwama  
Klaus H. P. Dittler  
Takao Tanabe  
Hiroshi Iwama  
Klaus H. P. Dittler  
Hiroshi Iwama

ISSN 0844-0368  
Pathol. Res. Pract.  
200 (2004) 1  
pp. 1-66

[www.elsevier.com](http://www.elsevier.com)

## IMPRESSUM

**Publisher:** Elsevier GmbH, Office Jena, P.O. Box 100537, 07705 Jena, Germany.

Phone: +49(0)3641/62 63, Fax: +49(0)3641/62 65 00, E-mail: journals@elsevier.com

**Advertisement Department:** Elsevier GmbH, Office Jena, Attn.: Sabine Schröter, Lößdergraben 14a, 07743 Jena, Germany. Phone: +49(0)3641/62 64 45, Fax: +49(0)3641/62 64 21; E-mail: s.schroeter@elsevier.com

**Advertising rates:** The price list of January 1, 2004 is effective at present.

**Terms of delivery (2004):** Volume 200 (1 volume consisting of 12 issues).

**Subscription rate\*** including online access (2004):

Region	Institutional	Personal	Single issue
D, A, CH <sup>#</sup>	1,123.00 EUR	448.00 EUR	113.00 EUR
Rest of Europe	1,270.00 EUR	505.00 EUR	113.00 EUR
Japan	168,000.00 YEN	62,700.00 YEN	14,300.00 YEN
USA/Rest of the world	1,364.00 USD	495.00 USD	132.00 USD

<sup>#</sup>Germany, Austria, Switzerland

\* All prices are suggested list prices and may be subject to change without notice. Prices include postage by surface mail and exclude VAT. VAT is effective according to international tax regulations as valid on the day of invoicing. Special airmail rates are available on request. Customers in EU countries are requested to state their VAT identification number if applicable.

Subscription orders at a personal rate must be addressed directly to the publisher and must include the recipient's name and residential address. An institutional or business address is only acceptable, if the institute or company has a subscription as well. Payment of personal subscribers has to be made by personal cheque or by credit card (Eurocard/Mastercard, VISA or American Express; please note card-No. and expiry date).

The publisher reserves the right to issue additional volumes during the course of the year.

Supplements and/or cumulative indexes are included in the subscription rates.

**Termination of subscriptions:** Subscriptions not entered specifically for one year only will be renewed automatically unless cancelled by October 31.

**Subscriptions:** Please send your order to Elsevier GmbH, Office Jena, Subscription Service, P.O. Box 100537, 07705 Jena, Germany. Phone: +49(0)3641/62 64 47, Fax: +49(0)3641/62 64 43, E-mail: k.ernst@elsevier.com

### Bank Accounts:

Deutsche Bank Jena, Account No. 390 7656 00 (BLZ 820 700 00);

IBAN: DE76 8207 0000 0390 7656 00; BIC/SWIFT: DEUTDE8E

or

Postbank Leipzig, Account No. 0 149 249 903 (BLZ 860 100 90);

IBAN: DE48 8601 0090 0149 2499 03; BIC/SWIFT: PBNKDEFF

Full details must accompany the payment.

**Copyright:** The articles published in this journal are protected by copyright. All rights are reserved. No part of the journal may be reproduced in any form without written permission of the publisher. This includes digitisation and any further electronic computing, like saving, copying, printing or electronic transmission of digitised material from this journal (online or offline).

Authorisation to photocopy items for internal or personal use of specific clients is granted by Elsevier GmbH for libraries and other users registered with the Copyright Clearance Center (CCC) Transaction Reporting Service, provided that the base fee of USD 30.00 per copy is paid directly to CCC, 222 Rosewood Drive, Danvers MA 01923, USA; 0344-0338/04/200 \$ 30.00/0. This consent does not extend to copying for general distribution, for advertising or promotional purposes, for creating new collective works or for resale and other enquiries. In such cases, specific written permission must be obtained from the publisher.

Typesetting: Macmillan India Ltd., Bangalore - 25.

Printing and binding: Giethoorn.

For detailed journal information see our home page: <http://www.elsevier.de/prp>

**Front Cover:** Triple immunohistochemical detection of Ki-67 (black), ESA (dark grey), SMA (light grey) in breast carcinoma ( $\times 200$ ). Photograph: Man and Burgar, published in: Pathol. Res. Pract. Vol. 199 (2003), p. 822



VOL. 82, Supplement 1, 2003

---

# Breast Cancer Research and Treatment

Marc E. Lippman, MD, editor-in-chief

*Special Issue*

26th Annual

San Antonio Breast Cancer Symposium

Kluwer Academic Publishers



marker of cellular proliferation) were recorded for invasive cancers.

#### Results:

None of the four genotypes were associated with an increased risk of breast cancer.

	Genotype	Normal(%) n=244	Cancer(%) n=175	
TGFA Tag	TT	81.6	76.6	Chi <sup>2</sup> 4.5 p=0.11
	GT	17.2	23.4	
	GG	1.2	0.0	
TGFA Bam	AA	75.5	77.4	Chi <sup>2</sup> 1.2 p=0.53
	CC	2.0	3.4	
	CA	22.5	19.2	
TGFA Rsa	CC	18.9	26.8	Chi <sup>2</sup> 3.9 p=0.14
	CT	70.6	65.3	
	TT	10.4	8.0	
EGF	GG	18.6	19.1	Chi <sup>2</sup> 4.3 p=0.12
	GA	58.4	50.3	
	AA	23.1	30.6	

There was no association with lymph node status, size, ER or progesterone status, EGFR status, Ki67 levels or survival on any of the polymorphic sites although the numbers studied were small.

**Discussion:** Polymorphisms in the EGFR ligands are not associated with an increased risk of breast cancer.

## 270

### Recombinant human insulin-like growth factor binding protein-3 (rhIGFBP-3) as a potential therapeutic agent for the treatment of herceptin-resistant breast cancer.

Jerome L, Yu Q, Belanger S, Shiry L, Pegram M, Leyland-Jones B. McGill University, Montreal, QC, Canada; Inmed Incorporated, Richmond, VA; UCLA, Los Angeles, CA

Human epidermal growth factor receptor-2 (HER-2/erbB2) belongs to a family of tyrosine kinase receptors involved in signal transduction pathways that regulate epithelial cell growth and differentiation. HER-2 is overexpressed in 20-30% of human breast cancers and is associated with enhanced tumor aggressiveness and a high risk of relapse and death. Herceptin (Trastuzumab) is a humanized monoclonal antibody that targets HER-2 and has demonstrated clinical activity against HER-2-overexpressing breast tumors. However, development of resistance to Herceptin is common and evidence suggests that the insulin-like growth factor receptor (IGF-IR) may be involved. Preliminary data have shown that interference with IGF-IR signaling via co-treatment with recombinant human IGF-binding protein-3 (rhIGFBP-3) restores the growth-suppressive effect of Herceptin in otherwise resistant breast cancer cell lines (Lu et al. 2001 JNCI).

To further explore the ability of rhIGFBP-3 to sensitize breast tumors to Herceptin, we examined its effect in 2 HER-2-overexpressing breast cancer lines (SKBR3 and BT474) and 3 Herceptin-resistant sublines created by transfection with the IGF-IR (SKBR3/IGF-IR) or HER2 (MCF-7/HER2-18), or by prolonged exposure to Herceptin (BT474/HerR). Elevated IGF-IR levels were confirmed in all 3 Herceptin-resistant lines (Table 1). Using the MTT assay, maximal growth inhibition of parental BT474 (40%) and SKBR3 (33%) was seen at 2.5ug/ml Herceptin. In the cell lines with increased IGF-IR, survival was reduced by only 15-18% at the same Herceptin dose. As a single agent, rhIGFBP-3 showed marked dose-dependent growth inhibition of Herceptin-resistant MCF-7/HER2-18 and SKBR3/IGF-IR, but a less pronounced effect on BT474/HerR. When combined with Herceptin, there was a marginal dose-dependent increase in growth inhibition of MCF-7/HER2-18 as compared to rhIGFBP-3 alone. In contrast, rhIGFBP-3 elicited a strong dose-dependent increase in Herceptin sensitivity of SKBR3/IGF-IR and BT474/HerR. The combination did not significantly enhance Herceptin sensitivity in BT474 and had a modest effect in SKBR3. Thus, rhIGFBP-3 displayed potent single-agent (MCF-7/HER2-18) and combinatorial activity with Herceptin (SKBR3/IGF-IR and BT474/HerR) in Herceptin-resistant breast carcinoma cells. Ongoing in vivo experiments are directed at evaluating the anti-tumor activity of rhIGFBP-3 with models incorporating these cell lines.

Table 1. Effect of rhIGFBP-3 and Herceptin on growth of HER-2-overexpressing human breast cancer cells.

Breast Cancer Cell Line	IGF-IR Status (Western)	Growth Inhibition (MTT Assay)		
		rhIGFBP-3 (0.1-100ug/ml)	Herceptin (2.5ug/ml)	Herceptin (2.5ug/ml) + rhIGFBP-3 (0.1-100ug/ml)
BT474	Low	10-20%	40%	35-47%
BT474/HerR	Moderate	10-26%	18%	30-50%
SKBR3	Low	20-40%	33%	44-54%
SKBR3/IGF-IR	High	12-40%	17%	26-60%
MCF-7/HER2-18	High	15-55%	15%	20-60%

## 271

### Endometase in human breast carcinomas, selective activation of progelatinase B and inhibition by tissue inhibitors of metalloproteinases-2 and -4.

Zhao Y-G, Xiao A-Z, Park H, Newcomer RG, Yan M, Man Y-G, Heffelfinger SC, Sang Q-XA. Florida State University, Tallahassee, FL; University of Cincinnati College of Medicine, Cincinnati, OH; The Armed Forces Institute of Pathology, Washington, DC

**Background:** Matrix metalloproteinases (MMPs) are known to be associated with cancer-cell invasion and metastasis. MMP-26 is a novel enzyme that was recently cloned and characterized by our group and others. MMP-26 mRNA is primarily expressed in cancers of epithelial origin, such as endometrial carcinomas, prostate carcinomas, lung carcinomas, and in a small number of normal adult tissues. Our previous study showed that MMP-26-mediated pro-gelatinase B (MMP-9) activation promotes invasion of androgen-repressed human prostate carcinoma cells.

**Material and Methods:** Enzyme kinetic study and in vitro enzyme assay were used to reveal the regulation of the MMP-26-mediated activation of MMP-9 by its endogenous inhibitors, tissue inhibitor of metalloproteinase (TIMP-1, -2 and -4). Microdissection, RT-PCR and in situ hybridization were used to detect MMP-26 mRNA expression in human breast tissues. Immunohistochemistry, double immunofluorescence labeling and confocal laser scanning were used to detect expression of MMP-26, MMP-9, and TIMP-1, -2 and -4 in human breast tissues.

**Results:** Enzyme kinetic studies showed that TIMP-1, -2 and -4 were potent inhibitors of MMP-26, with apparent K<sub>i</sub> values of 4.7 nM, 1.6 nM, and 0.62 nM, respectively. TIMP-2 and -4, but not TIMP-1, completely blocked the activation of pro-MMP-9 by MMP-26 during in vitro enzymatic assays, which resulted in significant diminution of fibronectin cleavage. Higher levels of mRNA and protein for MMP-26 were detected in human breast carcinomas when compared to normal breast epithelia around the carcinomas. The expressions of MMP-26, MMP-9, TIMP-2 and TIMP-4 proteins in human breast ductal carcinomas in situ (DCIS) were significantly higher than those in infiltrating ductal carcinomas (IDC), atypical intraductal hyperplasia and normal breast epithelia around DCIS and IDC by densitometric analysis. Double immunofluorescence labeling and confocal laser scanning revealed that MMP-26 was co-localized with MMP-9, TIMP-2 and -4 in breast DCIS. These results suggest that MMP-26, MMP-9, TIMP-2 and -4 may play a more important role during the early invasion of human breast DCIS cells that initiate IDC than in human breast IDC spreading.

## 272

### Is hepatocyte growth factor/scatter factor (HGF/SF) lymphangiogenic?

Jiang WG, Parr C, Martin TA, Davies G, Watkins G, Mansel RE. University of Wales College of Medicine, Cardiff, Wales, United Kingdom

**Introduction.** Hepatocyte growth factor (HGF), also known as scatter factor (SF) is a known potent angiogenic factor and is highly expressed in human breast tumours, particularly node positive tumours. HGF/SF is linked to a poor clinical outcome of patients with breast cancer. However, it is not known if HGF/SF has lymphangiogenic functions. This study examined, using both in vitro and in vivo models, the effects of HGF on lymphangiogenic function of endothelial cells.

**Methods.** Human endothelial cells that has lymphatic characteristics and human breast cancer cell MDA MB 231 were used. The effects of recombinant human HGF/SF (rhHGF) on the expression of lymphatic markers, podoplanin, Prox-1, vascular endothelial growth factor

the E-cadherin gene (8/8). All of the cases of ALH tested to date (5/5) show inactivation of E-cadherin but harbor no mutations. **Discussion:** Cases lacking both expression of E-cadherin and gene alterations suggest that another mechanism, involved at the stage of hyperplasia, is causing the lack of protein expression. In light of these findings, studies are in progress to evaluate other mechanisms of gene silencing i.e. LOH and promoter methylation, as well as the expression status of proteins associated with E-cadherin. The completion of these analyses will provide insight into the molecular genetic profile for lobular neoplasia.

### 573

**A subset of normal and hyperplastic appearing mammary ductal cells display invasive features.**

Man YG, Mattu R, Zhang R, Yousefi M, Sang QXA, Shen T. *The Armed Forces Institute of Pathology, Washington, DC; Florida State University, Tallahassee, FL; Temple University Hospital, Philadelphia, PA*

**Background:** Our previous studies in patients with ductal carcinoma in situ revealed the persistence of some ER negative cell clusters that displayed invasive features. The current study attempted to assess whether similar ER negative cell clusters might also be present in normal and hyperplastic mammary ducts.

**Materials and Methods:** Paraffin sections harboring normal and hyperplastic breast lesions were double immunostained with the same protocol. Immunostained sections were examined to identify ER negative cell clusters, defined as groups of  $\geq 5$  ER negative cells overlying disrupted myoepithelial (ME) cell layers, in contrast to the adjacent cells within the same duct that showed intense ER staining and overlay a non-disrupted ME cell layer. The molecular and immunohistochemical features in ER negative cell clusters were compared to those in adjacent ER positive cells, and in micro-invasive breast lesions.

**Results:** ER negative cell clusters were seen in both normal and hyperplastic appearing ducts in about 10% of the cases. Compared to the ER positive cells within the same duct, a subset of ER negative cell clusters displayed several unique features: [1] noticeable alterations in cell morphology and density; [2] reduced or lost expression of p27, a growth inhibitor; [3] a significantly higher rate of cell proliferation; [4] an increased frequency of genetic alterations. These features were comparable to those seen in micro-invasive breast lesions.

**Discussion:** A subset of normal and hyperplastic mammary ductal cells displayed biologic features similar to those in micro-invasive mammary tumors, raising a provocative possibility that some of these ER negative cell clusters might represent the direct precursors of invasive tumors.

**Acknowledgment:** Supported by Congressionally Directed Medical Research Programs, DAMD 17-01-1-0129 and DAMD17-01-1-0130, to Yan-gao Man

treated group individual tumour growth/median control group growth)x100.

#### Results

CELL LINE	HER 18	SKOV3	MDAMB231
COX-2 expression	+	±	++
ER expression	++	+	-
Median tumour growth (mm <sup>3</sup> ) [IQR] TREATED	39.3* [3.9-156.1]	29.5 [-2.2-89.8]	29.7*** [0-53.3]
CONTROL	99.9 [34.8-177.9]	62.1 [11.9-206.7]	96.4 [51.3-284.4]
Median tumour growth inhibition (%)	58.7* [-7.3-98.2]	68.95 [-22.7-101.76]	46.3*** [3.7-97.4]
Median Ki67 (%) TREATED	52.3	33.4	57.4
CONTROL	56.3	32.0	56.5
Median TUNEL (%) TREATED	0.74**	0.56	0.56
CONTROL	0.52	0.48	0.51

[IQR= Interquartile range] \*p=0.029 \*\*p=0.002 \*\*\*p=0.0002 (Mann Whitney U test)

Celecoxib significantly inhibited tumour growth in the HER18 (p=0.029) and MDAMB231 (p=0.0002) cell lines. Apoptosis increased significantly in celecoxib treated HER18 (but not MDAMB231) tumours (p=0.0002).

**Discussion** Celecoxib inhibits tumour growth *in vivo* in EGFR/HER2 positive COX-2 expressing cell lines. The mechanism of tumour growth inhibition in HER2 positive tumours is by increased apoptosis. Further research into the mechanisms of action is underway. COX-2 inhibition is a promising therapy for breast cancers expressing EGFR/HER2.

## 668

**Low to moderate protein expression of HER2/neu in breast cancer by immunohistochemistry (IHC) correlates with low level ErbB2 gene amplification by fluorescence in situ hybridization (FISH); updated results.**

Rugo HS, Moore D, Chen Y-Y, Magrane G, Hwang ES, Waldman FM. University of California San Francisco, San Francisco, CA

**Background:** HER2/neu overexpression in breast cancer is important for prognosis, choice of optimal treatment and use of trastuzumab therapy. Recent data suggests that ERBB2 gene amplification measured by FISH is a powerful predictor of response to the antibody trastuzumab (Mass et al, 2001); FISH positivity is commonly used to select patients for treatment. Concordance between protein overexpression and gene amplification is variable; with amplification in 89% of IHC 3+, 31% of IHC 2+, and <10% of 1+ cancers. The relationship of the intensity of protein overexpression to the level of gene amplification and response to trastuzumab is not well understood. At UCSF, we routinely perform FISH on all IHC 2+ cancers, and for variable staining on IHC 1+ and 3+ as well, to confirm the presence or absence of gene amplification. **Methods:** IHC was performed using either the CB11 monoclonal antibody or HercepTest (Dako) and scored according to standard guidelines. FISH was performed using probes to ErbB2 and centromere 17 (C17); amplification is defined as a mean ratio of > 2 of ERBB2 gene copy # to centromere 17. When possible, at least 50 cells were scored per case for both ERBB2 and C17. **Results:** We have now tested paraffin blocks on 323 cases of invasive breast cancer with both IHC and FISH. Amplification was seen in the following: IHC 0 3/29 (10%), 1+ 10/83 (12%), 2+ 53/172 (31%), 3+ 30/39 (77%). Of IHC 0 and 1+ cases that were found to have ErbB2, 8 cases were node negative, and 10/13 (77%) were ER and/or PR positive. Among FISH + cases, we found a significant trend toward lower gene amplification in tumors with moderate to low versus high protein expression, p value for trend between IHC and gene amplification is <0.0001. The mean ErbB2 ratio for IHC 0-2+ ranged from 2.3-3.7; for IHC 3+ the mean ratio was 7.6. On multivariate analysis, IHC was the only significant variable correlating with low level amplification of ErbB2; there was borderline evidence of a difference with ER/PR status. There was no correlation between amplification and tumor grade, node status, or LVI; a trend was seen between lower amplification and ER/PR positivity (p=0.055). **Discussion:** FISH testing should be performed on all IHC 2+ cancers, and perhaps a subset of IHC 0 and 1+ in addition. The level of protein expression correlates with the magnitude of ErbB2 amplification. It is important to determine the clinical significance of low level gene amplification associated with 0-1+ and 2+ protein expression, in regard to outcome and response to trastuzumab. Correlation of degree of amplification with response to adjuvant and late stage therapy is ongoing and will be presented.

## 669

**Inhibition of breast cancer development in vivo by long-term consumption of the low toxic phenylacetate derivative, 4-chlorophenylacetate.**

Sidell N, Tekmal RR. Emory University, Atlanta, GA; UTHSCSA, San Antonio, TX

The aromatic fatty acid phenylacetate (PA) and its analogs have come under intense investigation due to their ability to cause the growth arrest of a variety of neoplasia, including human breast cancer. We have previously determined that PA and its halide derivative 4-chlorophenylacetate (4-CPA) showed marked antitumor activity on estrogen-dependent breast cancer cells *in vitro*. To test the ability of 4-CPA to affect breast cancer carcinogenesis *in vivo*, we have utilized 7,12-dimethylbenzanthracene (DMBA)-induced mammary tumor development in aromatase transgenic mice as a model system. Pharmacologic studies of 4-CPA demonstrated that mouse blood plasma levels reached peak concentrations 4 hr after bolus intragastric administration of the compound and showed slow clearance characteristics with an apparent half-life of 4 to 8 hrs. As opposed to PA, 4-CPA was found to be essentially odorless and readily consumed in drinking water, giving rise to steady-state blood plasma levels of 4-CPA in the near mM range. Continuous consumption of 4-CPA in this manner for up to 5 months demonstrated no apparent adverse effects on the mice. For our experiments, aromatase transgenic females were divided into two groups, with one group receiving 4-CPA (6.0 mg/ml) continuously in their drinking water starting at 6 weeks of age until they were sacrificed. Both groups were treated with DMBA at 7-8 weeks of age via orogastric tube (1.0 mg in 100-200 ml of corn oil once per week for four weeks). One month after the last administration of DMBA, the mice were palpated for tumors and observations continued weekly for an additional 3 months. Results showed that in the group of mice not receiving 4-CPA, approximately 50% of the animals developed palpable mammary tumors while the remaining 50% showed frank microscopic evidence of ductal carcinoma *in-situ*. In the 4-CPA-treated group, no palpable tumors were detected while on a microscopic level, only mild hyperplasia was evident in some animals. These results demonstrate the ability of 4-CPA to act as a potent low toxic, chemopreventative agent against the development of carcinogen-induced mammary cancer. Histological and biochemical changes induced by the 4-CPA in the mouse tissue will be discussed.

## 670

**A subset of mammary epithelial cells overlying focally disrupted myoepithelial cell layers shows an unusual immunostaining pattern for proliferation-related proteins.**

Man YG, Zhang R, Mattu R, Shen T, Sang QXA. Armed Forces Institute of Pathology, Washington, DC; Temple University Hospital, Philadelphia, PA; Florida State University, Tallahassee, FL

**Background:** Our previous observations in estrogen receptor (ER) positive tumors revealed ER negative cell clusters, defined as groups of ≥ 5 ER negative cells overlying disrupted myoepithelial (ME) cell layers, in contrast to adjacent cells within the same duct that showed intense ER immunostaining and overlay a non-disrupted ME cell layer. This study intended to compare the proliferation status between ER negative cell clusters and their adjacent ER positive counterparts.

**Materials and Methods:** Consecutive sections were cut from selected tissue blocks containing ER negative cell clusters. A set of 6 adjacent sections were immunostained for Ki-67, PCNA, cyclin A, p27, MMP-26 and cytokeratins AE1/AE3. The proliferation status between ER negative cell clusters and adjacent ER positive cells within the same duct was statistically compared.

**Results:** All ER negative cell clusters were immunoreactive for cytokeratins AE1/AE3, suggesting that they were epithelial in nature. Cells in a majority of ER negative clusters were morphologically similar to adjacent ER positive cells, while they showed a significantly higher (p>0.01) proliferation rate. On the other hand, cells in a subset of ER negative clusters were morphologically different, and were also devoid of immunostaining for Ki-67, PCNA, cyclin A, and p27, as well as MMP-26, in contrast to their adjacent ER positive counterparts, which were immunoreactive to these markers.

**Discussion:** A subset of ER negative cells were devoid of expression of known proliferation-related markers, and also morphologically different

from adjacent ER positive cells within the same duct, suggesting that these cells are formed and regulated by a yet to be identified mechanism. **Acknowledgment:** Supported by Congressionally Directed Medical Research Programs, DAMD17-01-1-0129 and DAMD17-01-1-0130, to Dr. Yan-gao Mao.

## 671

### Potential importance of PKC- $\alpha$ activity in defining breast tumor luminal/basal phenotype.

Lacroix M, Laes J-F, Hennuy B, Cardoso F, Lallemand F, Gonze I, Leclercq G, Piccart M, Sotiriou C. Jules Bordet Institute, Brussels, Belgium; BioVallée, Gosselies, Belgium

The phorbol ester PMA is a known activator of the PKC- $\alpha$ . PKC- $\alpha$  activity is higher in basal-like breast cancer cell lines (BCC) such as MDA-MB-231 as compared to luminal-like ones. It has been shown that PKC- $\alpha$  overexpression in the luminal-like MCF-7 BCC leads to more aggressive phenotype. In this study we investigated the effects of PMA on global gene expression in both MCF-7 and MDA-MB-231 BCC lines using a 10000-feature cDNA microarrays (Incyte Genomics). Notable changes observed in MCF-7 included: 1/ down-regulation of estrogen receptor- modulated and/or luminal phenotype-associated genes such as ESR1, BCL2, MYB, PGR, SYK, RERG, LIV1; 2/ up-regulation of basal phenotype associated genes such as MMP1, ICAM1, VEGF, ID1, CEBPB; 3/ modulation of genes involved in the TGF- $\beta$  signaling pathway such as LTBP1, SMAD3; 4/ up-regulation of genes associated to cAMP signaling pathway such as ADORA2A and PRKACA. In contrast to MCF-7 BCC, we observed a considerably lower number of genes regulated in the MDA-MB-231 BCC. Moreover, the majority of these genes were also modulated in the MCF-7 BCC. Our results strongly suggest that PKC- $\alpha$  activity might play a major role in determining the basal-like phenotype in breast tumors. In order to address this issue, we analyzed the transcriptional profiles of a series of breast tumors based on the PMA-regulated subset of genes, as defined by our *in vitro* study. Hierarchical cluster analysis partitioned tumor samples in two major classes that remarkably fitted with the luminal and basal-like phenotype, as defined by a larger gene set. In conclusion, PKC- $\alpha$  mediated signaling pathway seems to be of great importance in defining breast cancer phenotype, by promoting the expression of genes characteristic of basal like cells.

## 672

### The effects of fulvestrant and gefitinib on proliferation, progesterone - receptor and pS2 expression in normal human breast epithelium *in vivo*.

Moore HA, Anderson E, Clarke RB, Warmberg F, Barnes NL, Wakeling AE, Bundred NJ. Christie Hospital NHS Trust, Manchester, United Kingdom; AstraZeneca Pharmaceuticals, Manchester, United Kingdom; South Manchester University Hospital, Manchester, United Kingdom

Fulvestrant ('Faslodex', FAS), an estrogen-receptor antagonist with no known agonist activity, and gefitinib ('Iressa', ZD1839), an epidermal growth factor receptor (EGFR) tyrosine kinase inhibitor, inhibit estrogen-induced proliferation in human breast epithelium. The present study determines the effects of combining the two agents on proliferation and estrogen-regulated proteins in human breast epithelium implanted subcutaneously (sc) into nu/nu mice. After 2 weeks, a 2 mg estradiol (E2) pellet was inserted sc and treatment with FAS (5 mg/mouse/week sc) and/or gefitinib (10 mg/kg daily by gavage) commenced. Controls received vehicle. Tissue was removed at day 0 and 14 days after the start of treatment for immunohistochemical detection of the Ki67 proliferation-associated antigen, progesterone receptor (PR) and pS2. FAS and gefitinib alone or in combination significantly reduced E2-stimulated Ki67 expression compared with control (see table). The effect of combining FAS and gefitinib was greater than that of gefitinib ( $p=0.016$ ) but not FAS ( $p=0.186$ ) alone. Both FAS and gefitinib reduced E2-stimulated PR expression and the effect of the combination was greater than either alone ( $p=0.08$  and  $p=0.017$ , respectively). Expression of pS2 was inhibited by FAS alone and in combination with gefitinib, but not by gefitinib alone. The effects of FAS and gefitinib suggest that both EGFR and estrogen-receptor signaling pathways are involved in controlling proliferation and PR expression in normal human breast epithelium.

Treatment	$\Delta$ Ki67	p	$\Delta$ PR	p	$\Delta$ pS2	p
Control	4.7 $\pm$ 0.6	-	29.3 $\pm$ 2.1	-	9.2 $\pm$ 1.5	-
Gefitinib	2.4 $\pm$ 0.5	0.019	19.2 $\pm$ 1.8	0.003	7.8 $\pm$ 1.6	nsd
FAS	1.7 $\pm$ 0.5	0.0014	16.5 $\pm$ 1.4	0.0001	4.2 $\pm$ 1.0	0.002
Gefitinib+FAS	1.0 $\pm$ 0.6	0.0001	14.1 $\pm$ 1.8	0.0001	2.3 $\pm$ 0.5	0.0001

$\Delta$ , change between day 0 and day 14 (mean  $\pm$  se); p, difference from control by Mann-Whitney U test; FAS, Faslodex; PR, progesterone receptor

'Faslodex' and 'Iressa' are trademarks of the AstraZeneca group of companies.

## 673

### Quantification of receptor tyrosine kinase (RTK) signal transduction expression in human carcinomas and cell culture model systems by automated digital microscopy (ADM) correlates well with western blot analysis.

Webster S, Gottlieb K, Yamamoto K, Torre-Bueno J, Bauer K. ChromaVision Medical Systems, San Juan Capistrano, CA; University of Southern California, Los Angeles, CA

**Background:** RTK signaling mediates key cellular processes such as the regulation of differentiation, proliferation and apoptosis. Protein analysis by immunohistochemistry (IHC) has been limited historically to subjective manual microscopic estimates of IHC stain intensity (e.g. 0-3+), cellular localization (e.g. nuclear vs cytoplasmic), and the proportion of positive cells. In contrast, quantitative estimates of protein content require bulk methods such as western blot (WB) and ELISA that are not appropriate for studying complex human solid tumors *in situ*. A method that provides protein quantification with retention of histological information would be of substantial benefit. These studies investigate feasibility for semiquantitative assessment of RTK signaling by IHC combined with a novel ADM scoring application. **Methods:** PhosphoEGFR (pEGFR) was evaluated in EGF-stimulated A431 cells; phosphoMAPK (pMAPK) and phosphoAkt (pAkt) were assessed in Jurkat cells treated with PMA or LY294002, respectively. Cultures were subjected to WB and formalin fixation/paraffin embedding for IHC. Both methods used the same pEGFR, pMAPK and pAkt antibodies (Cell Signaling Technology). Cell pellet/tumor IHC was visualized with DAB and quantified using ADM (ACIS, ChromaVision). WB was performed using normalized cellular lysates and quantitative image analysis.

**Results:** Concordance between ADM and WB was observed in each system. Within 10 minutes of EGF stimulation, A431 cells exhibited an approximately 20-fold induction of pEGFR, with a significant correlation between ADM and WB ( $r = 0.97$ ;  $p < 0.025$ ). pMAPK in Jurkat cells was increased approximately 5-fold by PMA but was unaffected by LY294002, with ADM and WB showing a significant correlation ( $r = 0.99$ ;  $p < 0.05$ ). Early indications showed a several-fold decrease in Jurkat pAkt levels by LY294002 (but not by PMA) as assessed by both ADM and WB. In preliminary evaluation of human tumors by IHC/ADM, phosphoepitope expression levels varied over a greater than 100-fold range. This was observed both as overall differences between biopsies as well as regional differences within tumors, and provided a context for relating expression levels to histological locations, evaluating the fraction of cells positive for given markers and providing information regarding subcellular localization.

**Discussion:** These studies suggest that ADM analysis of IHC stained specimens can accurately quantify tumor marker expression and provide key morphological data not obtainable by molecular techniques. Since a number of EGFR-based therapies have been (and continue to be) developed, analysis of RTK signaling should be a beneficial and crucial part of clinical evaluations designed to individualize patient treatment. ADM eliminates many of the drawbacks of histopathological analysis by combining a consistent and less subjective scoring system with the ease of automation.

## 674

### Partial intron expression ELF3 mRNA in peripheral blood mononuclear cells (PBMC's) in patients (pts) with breast cancer (Br ca).

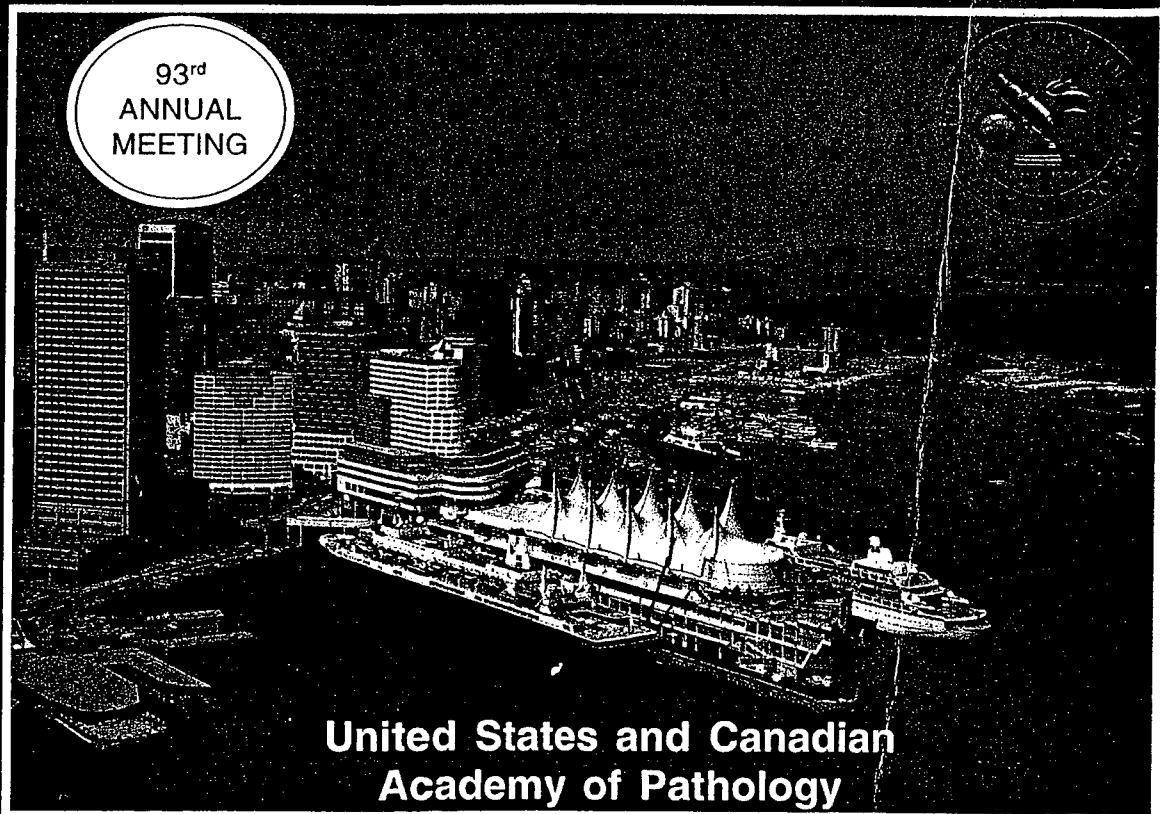
Dosik M, Kaplan MH, Wang X-P. North Shore University Hospital, Manhasset, NY; North Shore Hematology/Oncology Associates, Setauket, NY

**Background:** The ELF-3 gene (also called ESX, ESE-1, ERT, jen) is a member of the ETS family of transcription regulators that is thought to be expressed only in epithelial cells. Previously, retention of intron

# MODERN PATHOLOGY

**Volume 17  
Supplement 1  
January 2004**

93<sup>rd</sup>  
ANNUAL  
MEETING



**United States and Canadian  
Academy of Pathology**

- **March 6-12, 2004, Vancouver, BC, Canada**
- **Vancouver Convention and Exhibition Centre**
- **The largest gathering of physician-pathologists  
in the world**

nature publishing group **npg**



An official journal of the  
United States and Canadian  
Academy of Pathology, Inc.



remaining sections were used for microdissection of ER (-) and adjacent ER (+) cells within the same duct. RNA was extracted from ER (-) and ER (+) cells and amplified using the kits from Arcturus (Mountain View, CA). The amplified anti-sense RNA (RNA) was converted to biotin-labeled cDNA using the Ampo-Labeling Kit from SuperArray (Frederick, MD). The labeled cDNAs were interrogated with the "Cancer Pathway Finder" arrays, nylon membrane based cDNA arrays manufactured by SuperArray Bioscience Corporation (Frederick, MD).

**Results:** Preliminary studies from 4 selected cases showed that several genes involved in cell cycle control (p16Ink4), apoptosis (Survivin and CFLAR), angiogenesis (bFGF and thrombospondin-2), and metastasis (SERPINE1) are upregulated in ER (-) cells that are clustered adjacent to the disrupted myoepithelial layer.

**Conclusions:** Gene expression profiling of ER (+) and ER (-) cells within the same duct has identified several cancer related genes that may underlie the mechanisms of progression from mammary DCIS to invasive carcinoma. **Acknowledgment:** Supported in part by grants DAMD17-01-1-0129 and DAMD17-01-1-0130 from Congressionally Directed Medical Research Programs to Yan-gao Man, MD., PhD.

#### 56 Separate Sample Margins around Breast Lumpectomies for Predicting Residual Carcinoma

*Mascia, K Chu, S Tabbara.* University of Virginia Health System, Charlottesville, VA; The George Washington University, Washington, DC.

**Background:** Currently, the evaluation of breast specimens includes reporting the distance of the tumor from the margins of excision. Controversy exists among different specialties as to what represents a negative margin. The purpose of this study is to determine the significance of such measurements in planning further re-excisions.

**Design:** Patients with documented breast carcinoma who underwent additional sampling of the biopsy cavity at the time of initial lumpectomy were included. Each main lumpectomy specimen was submitted with six separate sample margins representing anterior, posterior, lateral, medial, superior and inferior aspect of the lumpectomy cavity. The separate sample margins consisted of approximately 1.0 centimeter of breast tissue. The main lumpectomy specimen was reviewed for the presence of invasive/in-situ carcinoma. The distance of the carcinoma from each of the anterior, posterior, lateral, medial, superior and inferior margins in the main specimen was measured. The separate sample margins were evaluated for the presence of carcinoma. Subsequent excisions were evaluated for residual carcinoma.

**Results:** Sixty seven cases fulfilled the study criteria. Six patients had DCIS and 59 had invasive carcinoma. A total of 402 lumpectomy margins were measured and 402 separate sample margins were evaluated. The evaluated lumpectomy margin measurements ranged from <0.5mm to >1.0 cm. Nine of 402 lumpectomy margins were involved by carcinoma (2 DCIS, 7 invasive carcinoma). The subsequent separate sample margins were involved in 2 instances (1 DCIS, 1 invasive carcinoma). Additionally, 24 separate sample margins that corresponded to 24 uninvolved lumpectomy margins (<0.5mm-14mm) contained tumor. Six separate sample margins had invasive carcinoma and 18 had DCIS. Re-excision was available in 21 patients with involved margins and demonstrated residual disease in seven patients with previous separate sample margins involved by carcinoma (2 DCIS, 5 invasive carcinoma).

**Conclusions:** Uninvolved lumpectomy margins seem to predict the absence of carcinoma in additional separate sample margins (94% in our study). When a positive separate sample margin was identified in this study, the measurement of tumor to lumpectomy margin was not predictive (<0.5mm-14mm). A positive separate sample margin corresponded to residual disease in further excisions in 30% of cases with follow-up. The numbers in this study are too small for a definitive conclusion, however the evaluation of separate sample margins from the lumpectomy cavity seems to predict residual disease in a significant proportion of patients.

#### 157 Characterization of a Molecular Genetic Profile for Lobular Neoplasia

*TL Mastracci, S Tjan, FP O'Malley, IL Andrusis.* Fred A. Litwin Centre for Cancer Genetics, Samuel Lunenfeld Research Institute, Toronto, ON, Canada; Mount Sinai Hospital, Toronto, ON, Canada; University of Toronto, Toronto, ON, Canada.

**Background:** Lobular neoplasia (LN) is a classification that includes atypical lobular hyperplasia (ALH) and lobular carcinoma *in situ* (LCIS). Both ALH and LCIS are premalignant lesions that are palpable and mammographically silent. Though these lesions are only found incidentally during breast tissue biopsy, LN lesions are significant in terms of implication of risk to the patient in the development of invasive carcinoma. A strong correlation between the lobular histological type and inactivation of E-cadherin, a protein involved in cell adhesion, has been reported. As well, mutations in the E-cadherin gene have been reported in invasive lobular carcinoma (ILC) and LCIS with adjacent ILC. We have been investigating LN lesions, lacking any adjacent invasive carcinoma, for alterations in and expression of known and novel genes/proteins with the goal of characterizing a molecular genetic profile for lobular neoplasia.

**Design:** We have obtained 22 formalin-fixed, paraffin-embedded cases of which there are 14 ALH lesions and 14 LCIS lesions (five cases contain both types of lesion). E-cadherin and beta-catenin protein expression were assessed by immunohistochemistry (IHC) and alterations in the E-cadherin gene (CDH1) were identified using single

strand conformation polymorphism (SSCP) and manual sequencing. Another method of E-cadherin gene inactivation being evaluated is loss of heterozygosity (LOH) at the 16q locus.

**Results:** ALH and LCIS cases able to be tested by IHC have been found to be negative for E-cadherin (26/28) and beta-catenin (24/28) protein expression. All cases have been screened for mutations and alterations in CDH1 have been found in the LCIS lesions (14/14). Moreover, with only one exception, the ALH lesions were found to harbor no CDH1 alterations (13/14). LOH at the 16q locus was found to be an infrequent event in both the ALH (1/14) and LCIS (2/14) cases. Although also uncommon, microsatellite instability was detected in LCIS (2/14).

**Conclusions:** Loss of E-cadherin expression is an early event in lobular neoplasia affecting ALH as well as LCIS. However, loss of expression is accompanied by DNA alterations in LCIS but not in ALH. Cases lacking both protein expression and gene alterations suggest that another mechanism is causing the lack of protein expression. In light of these findings, studies are in progress to evaluate other mechanisms of gene silencing, as well as the expression status of E-cadherin associated proteins. The completion of these analyses will provide insight into the molecular genetic profile for lobular neoplasia.

#### 158 C-Kit Protein Expression in Adenoid Cystic Carcinoma of the Breast

*C Matte, DW Visscher, C Reynolds.* Charles Lemoyne Hospital, Montreal, QC, Canada; Mayo Clinic, Rochester, MN.

**Background:** C-kit protein is a membrane-bound tyrosine kinase receptor and protein overexpression has been noted in several neoplasms. Recent reports have suggested that c-kit protein overexpression is involved in the pathogenesis of adenoid cystic carcinoma (ACC) of the salivary gland. However, c-kit expression has not previously been studied in ACC of the breast.

**Design:** Twenty-four cases of ACC of the breast were identified in our surgical pathology consultation files from 1994 to 2003. Formalin-fixed, paraffin-embedded archival tissue from all cases was immunostained with a polyclonal antibody against c-kit protein (DAKO, 1/600 dilution). Antibodies against keratin (AE1/3), smooth muscle actin, vimentin and S100 protein were also applied to characterize these tumors. The avidin-biotin-peroxidase complex detection method was utilized. Cases were scored as 1+ (1-25% positive), 2+ (26-50% positive), and 3+ (>50% positive). As controls, tissue microarrays were constructed with representative cores from 97 breast cancers and immunostained with anti-c-kit antibody.

**Results:** All 24 cases of ACC of the breast showed c-kit expression (3+, 6 cases; 2+, 13 cases; 1+, 5 cases). C-kit expression was associated with the epithelial component of the ACCs (keratin positive cells), but not with the myoepithelial component (smooth muscle actin, vimentin, S100 positive cells). Overall, the c-kit staining pattern was identical to the keratin staining pattern in these tumors. C-kit expression was rare (1/97 breast cancers) in the control tissues.

**Conclusions:** C-kit protein is expressed in ACC of the breast. The staining pattern of c-kit is distinctive and correlates with the presence of an epithelial phenotype. A potential role for c-kit as a new therapeutic target in the treatment of patients with metastatic ACC should be further investigated.

#### 159 Breast Cancer Isolated Tumor Cell in Axillary Sentinel Node and Prevalence of Additional Non Sentinel Node Metastases

*G Mazzarol, MG Mastropasqua, S Valentini, G Pruneri, S Andrichetto, G Viale.* European Institute of Oncology, Milan, Italy; School of Medicine, Milan, Italy.

**Background:** SLN biopsy is widely accepted procedure to stage breast cancer patients due to the high negative predictive value of the procedure.

Isolated Tumor Cell (ITC) category has been introduced in the new TNM classification in the attempt not to overstage and overtreat patients with single tumor cells or small clusters of cells not larger than 0.2 mm detected in the lymph node. Accordingly, breast carcinoma patients are currently classified as pN0 if the lymph nodes harbor ITCs.

The risk of additional metastases in non sentinel node has not been elucidated in patients with ITCs in the SLN, while SLNs with micrometastasis could have additional positive axillary nodes in approximately 25% of patients.

**Design:** In the attempt to evaluate the predictive value of ITCs in SLN to accurately stage small operable breast cancer patients, we collected 445 positive axillary SLNs (114 with ITCs and 331 with micrometastases), histologically entirely examined by multiple leveling, with known axillary nodal status.

**Results:** Overall, 115/445 (25.8%) of SLNs had metastases in the remaining axillary nodes.

Additional metastases were found in 20/114 (17.5%) and 95/331 (28.7%) patients with ITCs positive and micrometastatic SLNs, respectively (p=0.0026).

Metastases larger than 2 mm in the remaining axilla were present in 58/115 (50%) of the patients. In particular 11/20 (55%) of SLNs harboring ITCs and 47/95 (49%) of SLNs with micrometastatic disease.

**Conclusions:** The detection of breast cancer ITCs in axillary SLNs is predictive of a reduced risk of additional node metastases.

Nevertheless SLNs harboring ITCs may be associated with additional metastases larger than 2 mm in the remaining axilla.

# 871 Allelic Imbalances in Endometrial Stromal Neoplasms: A Model for Genetic Alterations in Tumor and Microenvironmental Tissues

F Moirfar, ML Kremser, YG Mar, S Lax, K Zatloukal, FA Tavassoli, H Denk. Institute of Pathology, Graz, Styria, Austria; University of Yale, New Haven, CT.

**Background:** Loss of heterozygosity (LOH) and microsatellite instability (MSI) have not been previously reported on a larger number of cases with ESS.

**Design:** Using PCR, we examined DNA extracts from microdissected tissues of 27 uterus samples containing malignant stromal cells of ESS (20 low grade and 3 high grade sarcomas), benign tumor cells of endometrial stromal nodules (ESN, 4 cases) as well as tumor-free myometrial and endometrial tissues close to and at a distance to the tumor. Epithelial cells from normal ectocervix (squamous cells) and normal stromal cervical tissue were also microdissected. Fifteen polymorphic DNA markers were tested to identify possible genetic alterations in different tissue components of uteri with endometrial stromal neoplasms on chromosomes 2p, 3p, 5q, 10q, 11q, 13q, and 17p. Samples from 10 women with prolapsed uteri (elongatio coli) without any histopathologic endometrial and myometrial abnormalities were also selected as external controls.

**Results:** While no genetic alterations (LOH, MSI) could be identified in 12 cases (44.5%), 15 (55.5%) revealed LOH with at least one polymorphic DNA marker. LOH were found in 3 (100%), 10 (50%), and 2 (50%) cases of high grade ESS, low grade ESS, and benign ESN, respectively. Although LOH was found more often in the neoplastic stromal cells, several cases showed concurrent and independent LOH in the tumor-free myometrial or endometrial tissues either close to or at a distance from the tumor. While the genetic alterations varied among different tumor suppressor genes including PTEN, FHIT, WT1, and p53, the most common genetic abnormality (LOH) was observed at the PTEN, a tumor suppressor gene located on chromosome 10q. No endometrial stromal neoplasm (ESN, ESS) was associated with MSI. The control group without any abnormalities in endometrial and myometrial tissues did not show LOH or MSI.

**Conclusions:** The frequent occurrence of LOH and the lack of MSI indicate that loss of function(s) of tumor suppressor genes and not mismatch repair deficiency play a key role in the pathogenesis of endometrial stromal neoplasms. The concurrent and independent occurrence of LOH in the stromal tumor cells and the tumor-free and normal appearing myometrial and endometrial tissues strongly support the concept of genetic alterations in microenvironmental tissues and the interaction(s) between different tissue components in the development and progression of endometrial stromal neoplasms.

# 872 Chromosome 10 Rearrangements in Uterine Leiomyomata Involve the Histone Acetyltransferase *MORF*

SDP Moore, SR Herrick, T Ince, P Dal Cin, M Kleinman, CC Morton, BJ Quade. Brigham and Women's Hospital, Boston, MA; Harvard Medical School, Boston, MA; Massachusetts Institute of Technology, Cambridge, MA.

**Background:** Benign uterine leiomyomata (UL) are the most common tumor in women of reproductive age and the leading cause for hysterectomy in the U.S. Clonal cytogenetic aberrations contribute to the pathobiology of 40% of UL. One recurrent aberration in UL is rearrangement of chromosome 10 band q22. Interestingly, rearrangements of 10q22 also have been observed in leiomyosarcoma. Such rearrangements may alter gene expression or create new fusion genes.

**Design:** We mapped chromosomal breakpoints in four UL with rearrangements of 10q22 by fluorescence *in situ* hybridization (FISH) using either metaphase chromosomes or interphase nuclei and human genomic clones (BACs). Mapping results were correlated with human DNA sequence and histologic type.

**Results:** The chromosome 10 breakpoint in a cellular UL with t(10;17)(q22;q21) localized to the third intron of the histone acetyltransferase *MORF* (monocytic leukemia zinc finger protein-related factor) by FISH. Based on experiments with overlapping BACs, the breakpoint was mapped to 15 kb within this large gene. Interphase FISH analysis of three additional UL revealed disruptions in *MORF* in all three cases. Two of these tumors had rearrangements between 10q22 and 17q21-22, one as a simple translocation and the other as a four-way translocation additionally involving chromosomes 6 and 15. The other tumor had two simple translocations involving 10q22 and 4q21 and 6p21 respectively. On-going experiments have mapped the 17q21 breakpoint to a 185 kb interval in at least two of the four tumors. Of note, both tumors available for review were of a particular histological subtype, namely the cellular variant.

**Conclusions:** *MORF* is a member of the histone acetyltransferase (HAT) MYST family, named for its founding members MOZ, Ybf2/Sas3, Sas2, and Tip60. Histone acetylation is one factor controlling gene expression. *MORF* and the closely related MOZ gene (monocytic leukemia zinc finger protein) previously have been found rearranged in some types of acute myeloid leukemia (AML). This is the first instance in which disruption of a HAT has been reported in another tumor type. t(10;17) disrupts *MORF* in the N-terminal portion of the protein between a conserved domain found in histone families 1 and 5 and PHD zinc finger domains. 17q21 breakpoint mapping has identified several candidates including *GCN5L2*, a gene similar to those fused to MOZ and *MORF* in AML. Involvement of *MORF* in four UL with 10q22 rearrangements suggests a role for this HAT in uterine mesenchymal neoplasia.

# 873 Mucinous Adenocarcinoma Arising in Rectovaginal Fistulas Associated with Crohn's Disease

CA Moore-Maxwell, SJ Robboy. Duke University Medical Center, Durham, NC.

**Background:** Crohn's disease is a chronic inflammatory disorder characterized by focal, transmural inflammation. Gynecologic involvement, including rectovaginal fistula formation, is frequent. The chronic, destructive, inflammatory pathology of Crohn's disease predisposes to malignant transformation and progression.

**Design:** We examined the development of mucinous adenocarcinomas in rectovaginal fistulas of 2 women who had long-standing histories of Crohn's disease. Additionally, a literature analysis of this rarely reported phenomenon revealed risk factors associated with the malignant transformation of chronic fistulas in the setting of Crohn's disease.

**Results:** *Case 1:* A 53-year old had a 30 year history of Crohn's disease. She reported sporadic compliance with numerous medical therapies and had an extensive history of perianal fissures, cutaneous fistulas, perianal and rectovaginal fistulas which had required numerous surgeries. Immediately prior to her malignant diagnosis, she began to have increasing complaints of menopausal bleeding and chronic pelvic pain. She developed a foul smelling, purulent drainage from her rectum and a mucopurulent, bloody discharge from her vagina. Physical exam showed a peri-anal sinus tract in the midline of the posterior perineum. A biopsy of lesions identified in the lower and mid vagina revealed a low-grade mucinous adenocarcinoma.

*Case 2:* A 42-year old had a 15 year history of Crohn's disease complicated by numerous abscesses and fistulas. She experienced increasing right lower quadrant pain, nausea, and anorexia that was unresponsive to steroid therapy. Immediately prior to her malignant diagnosis she developed drainage from her vagina. Physical examination revealed an enlarging mass involving the posterior wall of the vaginal vault that connected to the anus by a fistula tract. A biopsy revealed a mucinous adenocarcinoma.

**Conclusions:** The cases reported here, along with literature analysis, support the fact that malignant transformation of persistent rectovaginal fistulas is a potential complication of Crohn's disease. Risk factors for malignant transformation include early onset of disease, duration of disease for more than 10 years, chronic (pan)colitis with high inflammatory activity and the persistence of chronic fistulas and stenosis. Although rare, malignant degeneration should be considered in the differential diagnosis of chronic, nonhealing fistulas.

# 874 Gene Expression Assessed by cDNA Microarray Identifies New Molecular Changes in Endometrioid Endometrial Carcinoma

G Moreno-Bueno, R Cassia, C Sanchez-Esteviz, D Hardisson, M Andujar, A Dopazo, L Lombardia, E Bussaglia, J Prat, X Matias-Guiu, J Palacios. Centro Nacional Investigaciones Oncologicas, Madrid, Spain; Hospital Universitario La Paz, Madrid, Spain; Hospital Marteno Infantil de Las Palmas, Las Palmas de Gran Canaria, Spain; Hospital de la Santa Creu i Sant Pau, Barcelona, Spain; Hospital Arnau de Vilanova, Llerida, Spain.

**Background:** The identification of differentially expressed genes using a cDNA arrays in endometrioid carcinogenesis could help us to characterize new molecular pathways and their specific biological and clinical features in endometrioid endometrial carcinomas (EECs).

**Design:** We analyze different expression pattern of 24 EECs and 8 normal endometrial samples (Nes), using cDNA microarrays containing 6,386 different genes. To validate the array data obtained we analyzed the expression pattern of selected genes by RT-PCR in an independent series of endometrial carcinomas (ECs). In addition, 37 genes were evaluated using immunohistochemistry in TMA containing endometrioid endometrial carcinomas.

**Results:** After supervised analysis of the microarray data, we found 86 genes differentially expressed with at least a two-fold between NE and EECs. The discriminating genes are related to a variety of different functions such as cell adhesion, hormone response, extracellular matrix, and signal transduction. 37 genes were regulated in EECs in comparison with NE, and these included genes known to be involved in the inflammatory and immune response (*HLA class II*, *CD74*, *IL2*, *IL6*). Among the 49 genes over-expressed in NE when compared with EECs, are included genes known to be hormonally regulated during the menstrual cycle and to be important in endometrial homeostasis (*IGF1*, *IGF2*, *WT1*).

**Conclusions:** This study demonstrated the usefulness of cDNA microarray technology for identifying differences in gene expression patterns between normal and tumor endometrial samples.

# 875 Identification of New Markers in Ovarian Cancer with Potential Use in Diagnosis and Treatment

J-M Mosquera, C Torres-Cabala, C Chian-Garcia, C Otis, D Roberts, MJ Marmè. National Cancer Institute - NIH, Bethesda, MD.

**Background:** Ovarian cancer is the fifth most common cancer in women and a leading cause of death from genital cancer. Since no proven screening markers for malignancy exist, new markers for diagnosis as well as for therapy are needed. Recent new proteins have been identified in ovarian carcinomas through proteomics, and microdissected tissue and 2D-PAGE analysis. We describe the immunohistochemical

protein and their correlation with other histopathological markers of cell proliferation, differentiation and apoptosis in breast carcinoma.

**Design:** Formalin-fixed paraffin-embedded histopathological tissue from 146 patients with breast cancer was analyzed by immunohistochemistry (IHC) with a monoclonal antibodies against gamma-synuclein protein (Abcam 169, 1:800 dilution, Cambridge, UK). Positivity was scored qualitatively based on intensity and percentage of cells stained within the neoplastic and non-neoplastic breast tissue. **Results:** Gamma synuclein expression was observed in 18% (27 of 146) cases. Positive staining is present exclusively in neoplastic epithelium. No positive staining was present in epithelial or ductal cells within the adjoining benign breast tissue. However, variably intense positive staining was always present in myoepithelial cells in benign breast tissue. High gamma synuclein expression was observed in 33%, 24%, 14% and 5% of the metastatic, grade III, grade II and grade I carcinomas respectively. High gamma synuclein expression was also observed in 33%, 27%, 18% and 11% of Stage IV, Stage III, Stage II and Stage I carcinomas respectively. Significant correlation was observed between gamma synuclein expression and tumor grade, tumor stage, ER, PR, Her2/neu, Ki67, DNA index, and p53.

**Conclusions:** Gamma synuclein is expressed exclusively in neoplastic breast epithelium; its expression being restricted to only myoepithelial cells in benign breast. Expression is more frequent in high grade lesions and advanced stage breast cancers. Expression also correlates with poor prognostic breast histopathologic prognostic/predictor markers. Thus, gamma synuclein is an ideal marker for follow up of advanced stage and grade tumors. Since gamma synuclein occurs only in myoepithelial cells in benign breast, its expression in neoplastic breast may indicate a basal high grade phenotype.

#### 152 Unsupervised Hierarchical Clustering Analysis of Immunostaining Data Identifies Prognostically Relevant Subgroups of Breast Cancer Patients

N Makretsov, C Bajdik, DG Huntsman, E Yorlida, M Peacock, M Cheang, K Gelmon, T Nielsen, M Hayes, CB Gilks. Genetic Pathology Evaluation Centre, Vancouver General Hospital and University of BC, Vancouver, Canada; Cancer Control Research Program, BC Cancer Agency, Vancouver, Canada; BC Cancer Agency, Vancouver, Canada.

**Background:** Numerous prognostic markers have been identified for breast cancer but the optimal analytical approach to using these data is uncertain. We applied unsupervised hierarchical clustering analysis to immunohistochemical data in an attempt to group breast cancers according to patterns of expression of multiple biomarkers, independent of conventional histopathological and clinical parameters. **Design:** Tissue microarrays from 438 breast cancer specimens seen at Vancouver General Hospital between 1974 and 1991 were used. 34 biomarkers were assessed by immunohistochemistry: ER, PR, Her2, p53, E2F1, NTRK3, Clusterin, Survivin, Relaxin, Chromogranin A, Synaptophysin, NSE, CD3, CD10, CD20, CD43, CD 68, CD117, AKT3, CA9, IGF1R, IGF1, Ki67, Cyclin E, E-cadherin, GFI-1, HSP27, HD3, EphA2, Osteoprotegerin, Podocalyxin, YB1, ILK and PTEN. Patient survival was determined and univariate analyses were used to identify markers predictive of disease specific survival (DSS). Unsupervised hierarchical clustering analysis was used to group tumors and immunostains, and log-rank test was used to assess differences in DSS between these cluster groups.

**Results:** Of 34 biomarkers tested, 15 showed prognostic significance in univariate analyses ( $p < 0.05$ ) and 6 others approached significance ( $p < 0.2$ ). Unsupervised hierarchical clustering analysis with these 21 markers distinguished 2 principal groups (cluster groups), with significantly different DSS ( $p = 0.0001$ ). Sequential removal of least significant biomarkers from the clustering analysis showed that it was possible to group patients based on only ER, PR, Her2, p53, Clusterin, CD10, CD117, CA9, Ki67 and Podocalyxin. The 2 cluster groups identified using this reduced panel of immunomarkers had significantly different DSS ( $p = 0.0001$ ). The first cluster group was associated with a high proportion of ER, PR and stromal CD117 positive tumors. The second cluster group showed lower expression of these markers and a higher proportion of p53, Her2, CA9, Ki67 and Podocalyxin positive cancers.

**Conclusions:** Unsupervised hierarchical clustering analysis of immunostaining data identified prognostically relevant cluster groups of breast cancer cases. This approach allows consideration of multiple markers simultaneously, rather than independently, as is currently done. We developed a novel approach for defining the minimal number of markers necessary to optimally define prognostically significant cluster groups.

#### 153 A Fluorescence In Situ Hybridization Study of ETV6-NTRK3 Fusion Gene in Secretory Breast Carcinoma

N Makretsov, M He, PHB Sorensen, M Hayes, S Chia, DG Huntsman. Genetic Pathology Evaluation Centre of the University of BC, Vancouver, BC, Canada; British Columbia Research Institute for Children and Women Health, Vancouver, BC, Canada; BC Cancer Agency, Vancouver, BC, Canada.

**Background:** Recurrent chromosomal abnormalities are not common events in breast cancer. The translocation t(12;15)(p13;q25) fuses the ETV6 and NTRK3 genes. The biological consequence of this translocation is the expression of a chimeric protein tyrosine kinase with potent transforming activity. This fusion gene was initially described in spindle cell pediatric malignancies (congenital fibrosarcoma and

mesoblastic nephroma) and has been recently detected in secretory breast carcinoma (SBC). Both the rarity of, and lack of stringent diagnostic criteria for SBC's have impeded the determination of the clinical relevance of this subtype of breast carcinoma; this is a particular issue for non juvenile cases.

**Design:** We developed multiple complementary probe sets (both split apart and fusion probes) for the detection of the t(12;15)(p13;q25) by fluorescent in situ hybridization (FISH) in paraffin embedded formalin fixed tissue sections. We then used FISH on tissue microarrays (TMAs) to screen 481 cases of formalin fixed, paraffin embedded tissues of female invasive breast carcinoma of various histological subtypes and tested four additional histologically confirmed cases of SBC for the presence of the ETV6-NTRK3 gene fusion.

**Results:** 202 of 481 cases in the TMAs gave signals of sufficient quality for screening by FISH. Of these only one case showed fusion signals in the majority of tumor cells. Upon whole section H&E slide review, SBC histology was confirmed in this case. On the other hand, none of the fusion-negative breast cancers showed classical SBC histology. Three of the four additional cases of classical SBC revealed fusion signals. In all cases the results from fusion and split apart FISH assay for the ETV6-NTRK3 fusion gene were concordant. The fusion negative case had a high mitotic index, an unusual feature for SBC's.

**Conclusions:** Our data confirm that presence of the ETV6-NTRK3 fusion gene is a consistent and specific finding in secretory breast cancer. This multi-probe FISH approach described could be used both for clinical cases and for retrospective studies designed to determine the clinical behavior of SBC.

#### 154 Differential Expression of Non-Structure Restricted Proteins in Mammary Myoepithelial Cells: A Programmed or Induced Phenomenon?

YG Man, R Barner, R Vang, DT Wheeler, CY Liang, TN Vinh, GL Brattbauer, BL Strauss. Armed Forces Institute of Pathology and American Registry of Pathology, Washington, DC.

**Background:** Recent studies have shown that mammary myoepithelial (ME) cells exclusively or preferentially express 5 non-structure restricted proteins (p-cadherin, Maspin, WT-1, CD10, and p63), in addition to 5 structure restricted proteins. This study attempts to assess if these non-structure restricted proteins are uniformly or differentially expressed among ME cells, and if the expression of these proteins impact the expression of estrogen receptor (ER) and p27 in adjacent epithelial (EP) cells. **Design:** Consecutive sections at 3-4 um thickness were made from 25 breast tumors with co-existing normal, hyperplastic, and *in situ* neoplastic cells. A set of 3 sections from each case were double immunostained with a combination of a nuclear (p63 and WT-1) and a cytoplasmic protein (maspin, CD10, and p-cadherin) and the same ME cells that are clearly identifiable at all 3 sections was assessed for expression of these proteins. To study the impact of the expression of these proteins on adjacent EP cells, sections were double immunostained for each of these proteins plus ER or p27.

**Results:** These non-structure restricted proteins were differentially expressed among ME cells. ME cells associated with normal ducts showed the highest expression of these proteins, and most cells contained 3-4 or all these proteins. The expression of these proteins decreased with the increase of tumor histologic grades. However, a loss of the expression of these proteins was also seen in a subset of the entire ME cell layer of normal and hyperplastic ducts. A focal loss of these proteins in a given duct was generally accompanied by the loss of p27 and ER expression in adjacent EP cells, whereas EP cells within the same duct but away from the altered ME layers showed distinct p27 and ER expression.

**Conclusions:** These findings suggest that the expression of non-structure restricted proteins in ME cells is induced or regulated by reciprocal interactions between ME and adjacent EP cells.

**Acknowledgment:** Supported in part by grants DAMD17-01-1-0129 and DAMD17-01-1-0130 from Congressionally Directed Medical Research Programs to Yan-gao Man, MD., PhD.

#### 155 Cell Clusters Overlying Focally Disrupted Myoepithelial Cell Layers and Their Adjacent Counterparts within the Same Duct Display a Different Pattern of mRNA Expression

YG Man, X Zeng, T Shen, R Vang, R Barner, DT Wheeler, TN Vinh, CY Liang, BL Strauss. Armed Forces Institute of Pathology and American Registry of Pathology, Washington, DC; SuperArray Bioscience Corporation, Frederick, MD; Temple University, Philadelphia, PA.

**Background:** Our previous studies found that a subset of mammary ductal carcinoma *in situ* (DCIS) contained focally disrupted myoepithelial (ME) cell layers that were exclusively overlain by clusters of cells with a total loss of estrogen receptor (ER) expression. These ER (-) clusters displayed a substantially higher rate of loss of heterozygosity and proliferation than their adjacent ER (+) counterparts within the same duct (Man et al. Breast Cancer Res, in press). This study attempted to assess whether these cells also have a unique pattern of mRNA expression.

**Design:** Frozen breast tissues of 7 DCIS with focally disrupted ME cell layers were retrieved from our tissue bank, and 20 consecutive sections were prepared from each case. Sections 1, 10, and 20 were double immunostained for smooth muscle actin and ER, to identify ME cell layer disruptions and overlying ER (-) clusters, while the



**2004 Symposium Volume**

# ***Cancer Detection and Prevention***

**7th International Symposium on Predictive Oncology & Intervention Strategies**

**Hotel Westminster, Nice  
February 7 to 10, 2004**

**Program and Abstracts**

**Official publication of the  
International Society for  
Preventive Oncology**

and Bcl-2 (antiapoptotic factors) significantly ( $p < 0.05$ ) suppressed cell growth. Conclusions: PDTC is a potent inducer of apoptosis in human prostate cancer cells and an inhibitor of androgen action by reducing survivin protein and reversing the stimulatory effects of androgen on inhibitors of apoptosis. These antiandrogen-like effects of PDTC may contribute to the paradoxical augmentation of apoptosis induced in human prostate cancer cells treated with both T and PDTC. These results support the use of antioxidants for chemoprevention and chemotherapy of prostate cancer. We have no conflicts of interest with companies or products.

### 13 (oral session 898)

#### Bone marrow derived osteoprogenitor cells can afford osteogenic ability to radiated bone

T Morishita MD\*, Y Touma MD\*, H Ohgushi MD\*, K Honoki MD\*, Y Miyauchi MD\*, S Miura MD\*, A Kido MD\*, K Yoshitani MD\*, Y Takakura MD\*

Nara Medical University Department Orthopedic Surgery Shijo-cho 840, Kahihara, Nara, Japan, <sup>\*</sup> morito@naramed-u.ac.jp

**AIM:** We attempted to confirm whether bone marrow derived osteoprogenitor cells can afford osteogenic ability to radiated bones which lost their osteogenic potential by irradiation. **METHODS:** Fischer 344 male rats were used. Bone marrow cells were collected from seven-week-old Fischer 344 rats and expanded ex vivo. After one week primary culture, the osteogenic progenitor cells were collected by trypsin treatment and then, cell suspension were made for bone and cell composites. Bones were collected from iliac bones and prepared by 60Gy irradiation. Then, radiated bones were soaked in the marrow-cell suspension for thirty minutes, approximately. Thereafter radiated bones with/without osteoprogenitor cells and bones without any treatments were transplanted into subcutaneous spaces. After four and eight weeks samples were collected and prepared for histological findings. **RESULTS:** We found osteoblasts in some lacunae in radiated bones with cells four weeks after implantation. Newly formed bones surrounded by osteoblast and chondrogenic area were found in radiated bones with cells eight weeks after implantation. However, empty lacunae only were found in bones without cells. **CONCLUSION:** We confirmed the bone marrow derived cells can afford osteogenic ability to the radiated bones by histological assessment. There are no conflict of interest.

### 14 (oral session 898)

#### Phospholipids reduce adhesions of rodent colonic and human gastric cancer cells to extracellular matrix components in vitro

M Jansen MD\*, KH Treutner MD\*, P Lynen-Jansen MD\*, B Schmitz\*, L Tietze MD\*, V Schumpelick Prof\*

Department of Surgery, University Clinic, Pauwelsstr. 30, Aachen, Germany, <sup>\*</sup>Interdisciplinary Center of Clinical Research, Biomat, Aachen, Germany, <sup>\*</sup>Institute of Pathology, University Clinic, Pauwelsstr. 30, Aachen, Germany, m.jansen@ukaachen.de

**AIM:** Nidation of floating tumor cells initiates peritoneal carcinosis and thus prognosis of gastrointestinal tumors. Adhesion of tumour cells to extracellular matrix components is a pivotal step in developing peritoneal dissemination of intraabdominal malignancies. Since phospholipids efficaciously prevented peritoneal adhesion formation in numerous animal studies we investigated their capacity to reduce adhesions of colonic and gastric cancer cells to extracellular matrix components. **Methods:** Cells from colonic adenocarcinoma induced in syngenic BD-IX rats (DHD/K12/TRb, European Collection of Animal Cell Cultures, ecacc, Salisbury, UK) and human gastric cancer cells (NUGC-4, Japanese Cancer Research Resources Bank, Tokyo, Japan) were used in this study. Microtiter plates were coated with collagen IV (coll), laminin (ln) and fibronectin (fn). Nonspecific protein binding of the coated wells was blocked by adding 1% (w/v) BSA (4°C, 12h) and rinsing the wells with Hepes buffer. According

to dilution series, 30,000 - 70,000 tumor cells in 100 µl medium were seeded into each well. Beside the controls, phospholipids were added in concentrations of 0.05, 0.1, 0.5, 0.75, 1.0, and 1.5 mg / 100 µl medium. After the incubation time of 30 min, attached cells were fixed and stained with 0.1% (w/v) crystal violet. The dye was resuspended with 50 µl of 0.2% (v/v) Triton X-100 per well and colour yields were then measured in an ELISA reader at 590 nm. Optical density (OD) showed a linear relationship to the amount of cells and was corrected for dying of BSA/polystyrene without cells. **Results:** The controls revealed a significant increase of adhesions of both cell lines to the extracellular matrix components. The attachment of colonic and gastric cancer cells to collagen IV, laminin, and fibronectin could be significantly reduced up to 53% by phospholipid concentrations of 0.5 mg/µl and higher (ANOVA, p-level adjusted to Bonferroni). **Conclusion:** These results within the scope of additional experimental studies on mice and rats which showed a significant reduction of peritoneal carcinosis demonstrated the capacity of phospholipids in controlling abdominal nidation of tumor cells. Lipid emulsions may be a beneficial adjunct in surgery of gastrointestinal malignancies. The work was supported by Fresenius Kabi, Bad Homburg, Germany.

### 15 (poster session 898)

#### Focal prostate basal cell layer disruptions and leukocyte infiltration are correlated events: Implications for basal cell layer degradation and tumor invasion

YG Man MD PhD\*, T Shen MD PhD\*, YG Zhao MD PhD\*, QX Sang PhD\*

<sup>\*</sup>Department of Gynecologic and Breast Pathology, Armed Forces Institute of Pathology, Washington, DC, United States, <sup>\*</sup>Department of Pathology, Temple University Medical School, Philadelphia, PA, United States, <sup>\*</sup>Department of Chemistry and Biochemistry, Florida University, Tallahassee, FL, United States, man@afip.osd.mil

**AIM:** The normal human prostate epithelium is physically separated from the stroma by both the basal cell layer and basement membrane. Due to this structural feature, the disruption of both basal cell layer and basement membrane is an absolute pre-requisite for tumor invasion and metastasis. The disruption of the basement membrane is believed to result from an elevated production of proteolytic enzymes by the tumor and/or stromal cells, while the mechanism for basal cell layer disruptions is elusive. In a previous study, we identified a subset of mammary ductal carcinoma in situ that contained focal myoepithelial (ME) cell layer disruptions, and that over 97% of these focal disruptions were immediately subjacent to leukocytes (Yousefi et al. AIMM, In press), suggesting that focal leukocyte infiltration may play direct or indirect roles in ME disruptions. As the basal cells are believed to be equivalent to the ME cells, this study attempts to assess whether a similar event occurs in prostate tumors. **METHODS:** Consecutive sections were prepared from 16 patients with prostate tumors containing simultaneous normal, prostatic intraepithelial neoplasia, and organ-confined carcinoma. Two immediate adjacent sections from each case were double immunostained, one for cytokeratin (CK) 34 betaE12 plus leukocyte common antigen, the other for CK 34 betaE12 plus Ki-67. Acini and ducts lined by over 40 epithelial cells were examined for a focal basal layer disruption, defined as the absence of basal cells resulting in a gap equal to or greater than the combined size of 3 basal or epithelial cells. **RESULTS:** Focal basal cell layer disruption was found in all cases, while the frequency among cases varied from less than 5% to over 15% of the acini and ducts examined. Focal leukocyte infiltration was seen in over 90% of the acini and ducts with focally disrupted basal cell layers, while in only about 30% of the acini and ducts without basal cell layer disruptions ( $p < 0.01$ ). A vast majority of the proliferating (Ki-67 positive) cells were located at or near the basal cell layer disruptions. Also, clusters of multiple proliferating cells were frequently seen in acini and ducts with leukocyte infiltration, while were barely detectable in acini and ducts without focal leukocyte infiltration. **CONCLUSIONS:** These findings suggest that leukocytes may play direct roles in basal cell layer disruptions and tumor invasion. Supported in part by DOD grants DAMD17-01-1-0129

and DAMD17-01-1-0130 to YGM and DOD grant DAMA17-02-1-0238, NIH grant CA78646, American Cancer Society grant F01FSU-1 to QXS and YGZ

## 16 (poster session 898)

### Factors affecting ALCAM/ CD166 expression in breast cancer

A Jezierska<sup>a</sup>, WP Olszewski MD<sup>b</sup>, J Pietruszkiewicz MD<sup>b</sup>, WT Olszewski MD<sup>b</sup>, T Motyl Dr<sup>a</sup>

<sup>a</sup>Department of Physiological Sciences, Faculty of Veterinary Medicine, Warsaw Agricultural University, Warsaw, Poland, <sup>b</sup>The Maria Skłodowska-Curie Memorial Cancer Center and Institute of Oncology, Warsaw, Poland, agnieszka.jezierska@poczta.onet.pl

Activated Leukocyte Cell Adhesion Molecule (ALCAM/CD166) is expressed in different kinds of normal and neoplastic tissues. The data on tissue distribution of ALCAM suggest that this protein is involved in a tumour progression and metastasis (e.g. malignant melanoma or prostate cancer). The lack of any data on expression of ALCAM in breast cancer prompted us to undertake the study on involvement of this adhesion molecule in tumour progression and metastases. The relationship between expression ALCAM and expression of estrogen (ER), progesterone (PgR) and cerb-B2 receptors, alpha-catenin, E-cadherin and MMP2 in breast tissue was investigated. The influence of factors affecting breast cancer cell proliferation and survival (17-beta-estradiol, tamoxifen, BCL-2 overexpression and camptothecin) on ALCAM expression and subcellular localization was also examined. Observations were performed on 50 breast cancer cases and breast cancer cell lines: MCF-7 and MDA-MB-231. As a reference cell line HBL-100 was used. Laser scanning cytometry was applied for evaluation of ALCAM and other examined proteins expression. Confocal microscopy was used for the study of coalescence of ALCAM and alpha-catenin, E-cadherin and MMP2. Results of the study revealed that expression of ALCAM/CD166 is higher in ER and PgR positive tumours. Stimulatory effect of 17-beta estradiol on expression of ALCAM was shown in estrogen-dependent MCF-7 cells. On the other hand antiestrogen - tamoxifen diminished ALCAM expression. There was no relationship between expression of cerb-B2 receptors and ALCAM in examined breast cancer tissue sections. A high expression of ALCAM in breast cancer tissue was accompanied by a high expression of alpha-catenin. In breast cancers without metastasis (N0) the ratio of ALCAM to MMP2 expression was usually higher than in metastatic tumours (N1-N4). Apoptosis of breast cancer MCF-7 and MDA-MB-231 cells induced by camptothecin or tamoxifen was associated with formation of large clusters and degradation of ALCAM. Surviving subpopulations of breast cancer cells expressed more ALCAM/CD166, which may indicate its protective effect against apoptotic stimuli. Overexpression of antiapoptotic protein BCL-2 in MCF-7 breast cancer cell lines was accompanied by an increase of ALCAM and decrease of MMP2 expression. In contrast to MCF-7 and MDA-MB-231 breast cancer cells the expression of ALCAM/ in normal breast HBL-100 cells was very low. The following conclusions have been drawn: 1) expression of ALCAM/CD166 is dependent on steroid sex hormones; 2) high expression of ALCAM/CD166 promotes breast cancer cells survival; 3) ALCAM/CD166:MMP2 ratio could be an index of tumour metastatic potential.

## 17 (poster session 898)

### Bombesin increases the expression of c-Met in epithelium and of hepatocyte growth factor in fibroblasts

Y-S Guo MD, J Chang MD, CM Townsend MD, MR Hellmich PhD  
Department of Surgery, The University of Texas Medical Branch, Galveston, TX, United States, yguo@utmb.edu

Gastrin-releasing peptide (GRP) and its cognate receptor (GRP-R) are aberrantly overexpressed in several cancers, such as colorectal, prostate and lung cancers. Bombesin (BBS), a homolog of GRP, has been shown to be a mitogen in several cell types. We have reported that BBS is a potent stimulator of COX-2 gene expression in intestinal epithelial cells

(J Biol Chem 276:22941, 2001). In addition, we recently found that functional GRP-R receptor exists in primary cultures of epithelium and fibroblasts from collagenase-dissociated human colon tumors, suggesting the possibility that BBS may induce stroma-epithelium interaction through stimulating some gene expression in both cell types. Hepatocyte growth factor (HGF) is a potent mitogenic and motogenic stimulator in normal and neoplastic cells and is produced mainly by fibroblasts; whereas its cognate receptor, c-Met, is expressed in epithelium. To date, whether BBS affects the expression of HGF and c-Met has not been reported. AIM. The purpose of this study is to determine the effect of BBS on the expression of HGF gene in 3T3-L1 fibroblasts and the c-Met gene in MC-26 mouse colon cancer cells. METHODS. 3T3-L1 and MC-26 cells were treated with or without BBS (10 nM) in serum-free conditions. Protein levels of HGF and c-Met were determined by Western blotting. The HGF mRNA was examined by cDNA microarray. The c-Met promoter activity was evaluated by transfection with c-Met promoter coupled to a luciferase reported gene and then examined by luciferase assay. RESULTS. BBS increased [Ca<sup>2+</sup>]<sub>i</sub> mobilization in both cell lines, indicating the presence of functional GRP-R. BBS treatment significantly increased the level of HGF mRNA and induced a time-dependent increase of HGF protein in 3T3-L1 cells. In MC-26 cells, BBS increased tyrosine phosphorylation and protein levels of c-Met as well as c-Met promoter activity. CONCLUSIONS. BBS stimulated the expression of HGF mRNA and protein in 3T3-L1 fibroblasts and transactivated c-Met, as well as increased c-Met protein levels and promoter activity in MC-26 cells. These data suggest that in colon cancer, GRP-R may play a role in tumor progression through the establishment of a paracrine growth loop between epithelial and stromal cells.

## 18 (poster session 898)

### DNA repair efficacy of photolyase (Photosome®) in human keratinocytes after UVB irradiation using the comet assay

L Decome PhD<sup>a</sup>, MP De Méo PhD<sup>a</sup>, C Robert PhD<sup>b</sup>, O Doucet PhD<sup>b</sup>, A Botta Pr<sup>a</sup>

<sup>a</sup>Laboratoire de Biogénotoxicologie et Mutagenèse Environnementale, Faculté de Médecine, Marseille, France, <sup>b</sup>Cell Pharmacology department, Coty Beauty Research and development Center, Monaco, michel.demeo@pharmacie.univ-mrs.fr

Aim. The aim of the present study was to evaluate the DNA repair efficacy of photolyase on human keratinocytes after a single dose of UVB irradiation using the comet assay. Methods. Keratinocytes primary cultures were incubated with photolyase (Photosome®, 0.5%) and L-ergothioneine (4 mM) then cells were harvested and comet slides were prepared. Then, the slides were irradiated with 0.06 J/cm<sup>2</sup> UVB. A second UVA irradiation (1.2 J/cm<sup>2</sup>) was performed to activate the photolyase enzyme and the slides were incubated for 60 min at 37 °C in humidified chamber. Finally, the slides were immersed in cold lysing solution. After lysis, slides were incubated with SDS-Proteinase K (0.5%:0.1 mg/ml) for 60 min at 37 °C then were washed with enzymatic buffer before treatment with T4 endonuclease V (T4NV, 75 ng) for 30 min at 37 °C in humidified chamber. Slides were allowed to unwind for 20 min and electrophoresis was performed with an additional period of 20 min. DNA single strand breaks were quantified using an image analysis system. The Tail moment  $\chi^2$  values were compared with Dunnet's test. Results. In order to photoactive photolyase (Photosome®) cells were irradiated with 1.2 J/cm<sup>2</sup> UVA after UVB irradiation. However UVA induced DNA single strand breaks immediately after irradiation via the production of reactive oxygen species. Preliminary experiments showed that L-ergothioneine decreased UVA-induced single strand breaks in dose-dependent manner. For an optimal antioxidant protection against UVA irradiation, L-ergothioneine was used at a concentration of 4 mM in culture medium for 30 min of incubation at 37 °C prior UVB irradiation. If pyrimidine dimers were not repaired by photolyase, damaged sites were blocked and T4 endonuclease V could not repair the pyrimidine dimers sites. A SDS-Proteinase K treatment step was included to release T4NV action by the release of unrepaired pyrimidine dimers sites. With this additional treatment, the number of DNA single strand breaks

each data set (pancreatic adenocarcinoma, PanINIII-Family X and normal adjacent) using a web based tool developed by Jim Lyons-Weiler, Ph.D. at the University of Pittsburgh. The most similarity was found between the normal adjacent tissue and the pancreatic cancers. At least 50% of the genes that show the greatest differential expression are identical in both the cancer and the normal adjacent lists although the rank ordering of significance varies somewhat between the two lists. Genes under expressed on both the cancer and normal adjacent list include regenerating islet-derived 1 alpha, period (*Drosophila*) homolog 1, RNA binding motif, single stranded interacting protein, an EST similar to pancreatitis associated protein and eukaryotic translation elongation factor 2. When we expanded our comparisons to the PanIN III tissue from Family X, we found a subset of genes that were significantly over expressed in all 3 data sets, including ribosomal protein S27a, nucleolin, villin 1 and KIAA 1705. Conclusions: Normal adjacent tissue appears to contain many gene expression changes indicative of the neighboring cancer, indicating that normal adjacent cancer is NOT normal. Some of these same changes occur early in preneoplastic tissues. Genes with the same significant pattern of differential expression in cancer, and in preneoplastic tissues such as normal adjacent and in PanINIII tissues represent possible biomarkers for pancreatic cancer.

## 149 (poster session 892)

### Increasing BP1 expression correlates with progression and invasion of male breast and prostate tumors

YG Man MD PhD, BL Strauss MD PhD, PE Berg PhD

Department of Gynecologic and Breast Pathology, Armed Forces Institute of Pathology and George Washington University Medical Center, Washington, DC, United States, man@afip.osd.mil

AIM: BP1 is a member of the homeobox gene superfamily of transcription factors that are essential for early development. Our recent studies, however, had revealed that the BP1 gene was activated in 80% of female breast infiltrating ductal carcinoma (IDC), while was silent in the adjacent normal cells and in a vast majority of normal controls (Fu et al. Breast Cancer Research 5:82-87, 2003). BP1 expression was significantly higher in estrogen receptor (ER) negative than in ER positive tumors, 100% versus 73%, ( $p = 0.03$ ), and in African American than in Caucasian women, 89% versus 57%, ( $p = 0.04$ ), suggesting that BP1 expression is subject to the influences of the race and ER status. This study attempts to elucidate the expression profile of BP1 in male breast and prostate tumor cells, which are regulated mainly by androgen, to assess whether the expression of BP1 is also subject to influences of hormone types and sex. METHODS: Sections of male breast ( $n=20$ ) and prostate ( $n=16$ ) tumors with simultaneous normal, non-invasive, and invasive components, along with reduction mammoplasties ( $n=34$ ) were immunostained with a polyclonal antibody to BP1 utilizing the ABC method. The frequency and pattern of BP1 immunostaining among cases and among cell types were semi-quantitatively compared. RESULTS: Almost all (>95%) the cells in reduction mammoplasties were devoid of distinct BP1 immunostaining. Distinct BP1 immunostaining was seen in a subset of epithelial cells in both male breast and prostate tissues. The frequency of BP1 expression and the number of BP1 positive cells in both breast and prostate tumors appeared to be linearly increased with the advance of the tumor stages. In tissues contained simultaneous normal, non-invasive, and invasive components, the invasive cells generally displayed the highest intensity of BP1 staining, followed by the non-invasive tumor cells. These findings are comparable to those seen in female breast tumors (Berg et al. Unpublished data). CONCLUSIONS: These findings suggest that BP1 might be an important bio-molecule that is required by multiple types of tumor cells for activation and/or sustenance of invasion. Supported by NIH grant CA91149 (PEB) and DOD grants DAMD17-01-1-0129 and DAMD17-01-1-0130 (YGM). Corresponding author: PE Berg, PhD.

## 150 (poster session 892)

### HDAC6 mRNA expression is correlated with better prognosis in breast cancer

H Iwase MD PhD<sup>a</sup>, H Yamashita MD PhD<sup>a</sup>, T Toyama MD PhD<sup>a</sup>, H Sugiura MD<sup>a</sup>, Z Zhang MD<sup>a</sup>, S Hayashi PhD<sup>b</sup>

<sup>a</sup>Nagoya City University Graduate School of Medical Sciences, Nagoya, Japan, <sup>b</sup>Division of Endocrinology, Saitama Cancer Center Research Institute, Saitama, Japan, h.iwase@med.nagoya-cu.ac.jp

AIM: Gene expression patterns using microarray in MCF-7 cells showed that histone acetylase 6 (HDAC6) gene was one of the early-responsive estrogen-induced genes (J Molecular Endocrinology, 29, 2002). This led us to hypothesize that there was a link between levels of HDAC6 expression and the hormone dependent potential of breast cancer. METHOD: In the present study, the level of HDAC6 mRNA expression was analyzed using quantitative real-time RT-PCR in 158 patients with invasive breast cancer and the protein expressions were also determined by immunohistochemistry. RESULTS: HDAC6 mRNA was expressed at significantly higher levels in breast cancer patients with small tumors measuring less than 2 cm, with non-high histological grade of the tumor, and in estrogen receptor (ER) a and progesterone receptor (PgR) positive tumors. Patients expressing high levels of HDAC6 mRNA have a statistically better prognosis than those expressing low levels. Furthermore, the patients with high levels of HDAC6 mRNA tended to be more responsible to endocrine treatment than those with low levels. Specific staining was found in the nucleus of some normal epithelial cells and in the cytoplasm of the majority of cancer cells. However, no relationship was found between HDAC6 cytoplasmic expression and any clinicopathologic factors or survival. CONCLUSION: We conclude that the expression levels of HDAC6 mRNA could have potential both as a prognostic marker and as a predictive marker for endocrine treatment in breast cancer.

## 151 (poster session 892)

### Identification of risk markers in Acute Lymphoblastic Leukemia.

D Khurana BS<sup>a</sup>, J Qiu MS MD<sup>b</sup>, P Gunaratne PhD<sup>a</sup>, JF Margolin MD<sup>b</sup>, MC Gingras PhD<sup>b</sup>

<sup>a</sup>Department of Molecular and Human Genetics, Baylor College of Medicine, Human Genome Sequencing Center, Houston, Texas, United States, <sup>b</sup>Department of Pediatrics, Baylor College of Medicine, Texas Children's Cancer Center, Houston, Texas, United States, mcgingra@texaschildrenshospital.org

BACKGROUND: There are large differences in outcomes between adult and pediatric patients with Acute Lymphoblastic Leukemia (ALL), as well as between pediatric ALL patients with different chromosomal translocation. These differences are obvious among clinical risk groups. In the lowest risk groups, pediatric patients are cured at a rate of 80-90% but only 50% of adult patients are cured. In higher risk categories, approximately 60% of children but only 10% of adults are cured. We hypothesize that the genes differentially expressed in adult versus pediatric and in lower- versus higher-risk pediatric ALL are involved in mechanisms of drug resistance or drug responsiveness. AIM: Identify risk-associated genes that might control response to treatment. METHODS: We used an integrated approach to facilitate gene expression profiling that combines suppression subtractive hybridization (SSH), concatenated cDNA sequencing (CCS), and quantitative real-time RT-PCR (QR-RT-PCR). We have generated specific high-risk and low-risk ALL gene expression profiles by subtracting pools of cDNA from adult and pediatric t(9;22) ALL against each other. To investigate the risk associated value of these genes, we have measured the expression level of these genes the diagnostic samples for a cohort of 51 ALL patients. The patient distribution included 18 low-risk ALL patients [hyperdiploid and t(12;21)] and 33 high-risk ALL [adult and pediatric t(9;22), pediatric t(1;19) and t(4;11), and adult and pediatric patients with elevated white blood cell count but none of

nuclear hTERT immunoreactivity seems to be an early event in serous ovarian neoplasia; nuclear and cytoplasmic staining may indicate poor outcome. In contrast, c-kit immunoreactivity is restricted to SCA, related with high tumor grade and stage, but not related with outcome in this study.

## 282 (oral session 797)

### Morphologically similar normal and hyperplastic mammary ductal cells associated with and without malignant lesions have a different immunohistochemical profile

**YG Man** MD PhD, **PE Berg** PhD, **R Barner** MD, **TN Vinh** MD, **DT Wheeler** MD, **CY Liang** MD, **BL Strauss** MD  
Department of Gynecologic and Breast Pathology, Armed Forces Institute of Pathology and George Washington University Medical Center, Washington, DC, United States, [man@afip.osd.mil](mailto:man@afip.osd.mil)

**AIM:** Our previous studies revealed that a subset of morphologically normal and hyperplastic mammary ductal cells in tissues of ductal carcinoma in situ (DCIS) shared several malignant features with their malignant counterparts (Man et al. Breast Cancer Res 5: R231-241, 2003). This study attempts to assess whether these cells are immunohistochemically different from normal and hyperplastic cells that are not associated with malignant lesions. **METHODS:** Consecutive sections at 4-5 µm thickness were prepared from reduction mammoplasties with no cancer history, no mammographic and histological abnormalities, from regular ductal hyperplasia, and from DCIS (n=30 for each category) with simultaneous normal, hyperplastic, and neoplastic components. Sections were double immunostained for smooth muscle actin and Ki-67, plus a panel of markers that are reported to be exclusively or preferentially present in malignant cells. The structural integrity of the myoepithelial (ME) cell layers, the cell proliferation rate, and the expression status of those markers among cases were compared. **RESULTS:** Compared to their morphologically similar counterparts in reduction mammoplasties and regular ductal hyperplasia, clusters of non-malignant cells in nearly half of the DCIS cases displayed several unique features, which were shared by the malignant lesions: [1] A significantly higher frequency of focal ME cell layer disruptions; [2] A significantly higher rate of cell proliferation; [3] A significantly higher level of BP1 expression; [4] Over-expression of p53 and/or c-erb B2. These cell clusters were generally adjacent, while some were at a distance, to the malignant lesions. These cell clusters were architecturally and morphologically distinct from the malignant cells, whereas they were indistinguishable from the adjacent non-malignant cells in H & E stained sections. **CONCLUSIONS:** A subset of normal and hyperplastic ductal cells associated with malignant lesions might belong to a not yet defined malignant cell population. Supported by DOD grants DAMD17-01-1-0129 and DAMD17-01-1-0130 (YGM) and NIH grant CA91149 (PEB).

## 283 (oral session 797)

### Cytotoxic effects of fumonisin B<sub>1</sub> on the ultrastructure of a human oesophageal carcinoma cell line - an in vitro study

**RB Myburg** MMS, **N Singh** MMS, **AA Chuturgoon** PhD  
Mycotoxin Research Unit, Nelson R Mandela School of Medicine, Faculty of Health Sciences, University of Natal, Congella, Durban, South Africa, [chutur@nu.ac.za](mailto:chutur@nu.ac.za)

**AIM:** To determine the ultrastructural pathological effects of fumonisin B<sub>1</sub> (FB<sub>1</sub>) on a squamous cell carcinoma cell line using transmission electron microscopy (TEM) and scanning electron microscopy (SEM). In addition, metabolised FB<sub>1</sub> was immunochemically probed using a monoclonal antibody. **METHODS:** The SNO epithelial cells were grown to confluency in culture medium supplemented with 5% foetal calf serum, 1% L-glutamine and 1% penstrep fungizone. The cells were then treated with FB<sub>1</sub> at concentrations of 1 µM, 2 µM, 4 µM, 8 µM and 16 µM for 24 hrs. Control cells received no toxin treatment. After 24 hrs, the flasks were

washed with Hank's balanced salt solution and the cells were fixed in 1% glutaraldehyde for TEM and immunocytochemistry (ICC). Sections were cut and viewed (ultrastructure and immunolocalisation) using a JEOL-JEM 100S electron microscope. A monoclonal FB<sub>1</sub> antibody was used to probe for metabolised toxin. SEM was accomplished using a Hitachi S520 scanning electron microscope. **RESULTS:** The toxin treated SNO cells displayed marked pathological changes which included plasma membrane damage, swelling or microsegregation of the nucleus, microsegregation of the nucleolus and swelling and elongation of mitochondria. These cytotoxic effects were attributed to FB<sub>1</sub>, since FB<sub>1</sub> was actively metabolised as evidenced by immunolocalised FB<sub>1</sub> in the SNO cells. The results also indicate the FB<sub>1</sub> preferentially targets membranes, the nucleus and mitochondria of cells. **CONCLUSIONS:** The cellular pathology observed suggests that the mitochondria, the nucleus and nucleolus are important in oesophageal carcinogenesis. The high levels of FB<sub>1</sub> label found in these organelles show that ultrastructural alterations are due to this toxin and that FB<sub>1</sub> may exert its carcinogenic effect through covalent binding directly to these organelles.

## 284 (oral session 797)

### Mitochondrial DNA damage in non-melanoma skin cancer

**MA Birch-Machin**<sup>a</sup>, **SE Durham**<sup>a</sup>, **K Krishnan**<sup>a</sup>, **J Maki**<sup>b</sup>, **R Parr**<sup>b</sup>, **RE Thayer**<sup>b</sup>

<sup>a</sup>Dermatology, University of Newcastle, Newcastle upon Tyne, United Kingdom, <sup>b</sup>Genesis Genomics Inc, Thunder Bay, ON, Canada, [caroline.karwinski@genesisgenomics.com](mailto:caroline.karwinski@genesisgenomics.com)

**AIM:** Mitochondrial DNA (mtDNA) damage, predominantly encompassing point mutations, has been reported in a variety of cancers (reviewed in Penta et al., (2001). Mutat Res 488: 119-133). Our aim was perform in human skin, the first detailed study of the distribution of multiple forms of mtDNA damage in non-melanoma skin cancer compared to histologically normal perilesional dermis and epidermis. **METHODS:** included long range PCR, 3-primer PCR, back to back primer PCR and automated sequencing. **RESULTS:** We present the first entire spectrum of deletions found between different types of skin tumours and perilesional skin (n=30). Twenty different deletion species were observed in the major deletion arc and four species were observed in the minor deletion arc. Our data clearly shows that more deletions occur in the skin from BCC rather than SCC patients. In addition, we provide the first quantitative data for the incidence of the common deletion as well as the first report of specific tandem duplications in tumours from any tissue. Importantly, this work shows that there are clear differences in the distribution of deletions between the tumour and the histologically normal perilesional skin. Furthermore, DNA sequencing of four mutation "hotspot" regions of the mitochondrial genome identified heteroplasmic changes, which were present in the tumour alone (i.e. somatic) or at least with a greater incidence compared to the surrounding perilesional skin. For example, we identified a previously unreported somatic C to T heteroplasmic mutation at np438 in the non-coding D-loop. There were two further heteroplasmic changes, a T to C transition at np16093 in the non-coding D-loop and an A to G transition at np215 in the coding region, in the tumour of an 88-year-old BCC patient which were absent in the perilesional dermis and barely detectable in the associated epidermis. In addition, 81 unreported and reported homoplasmic single base changes were identified in the other NMSC patients. Unlike the distribution of deletions and the heteroplasmic mutations, these homoplasmic mutations were present in both tumour and perilesional skin. **CONCLUSION:** This suggests that for some genetic studies, the traditional use of histologically normal perilesional skin from NMSC patients may be limited. Currently from this data, it is unclear whether mtDNA damage has a direct causal link to skin cancer or it may simply reflect an underlying nuclear DNA instability. It is clear however from our data and from cancer studies of other tissues, that mtDNA damage is likely to provide a potentially powerful tool in cancer diagnosis.

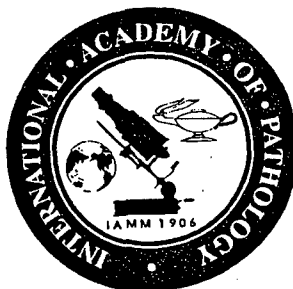
# **UNITED STATES AND CANADIAN ACADEMY OF PATHOLOGY**

(UNITED STATES-CANADIAN DIVISION OF THE  
INTERNATIONAL ACADEMY OF PATHOLOGY)

**ANNUAL MEETING**

**MARRIOTT WARDMAN PARK HOTEL  
WASHINGTON, D.C.  
MARCH 22 – MARCH 28, 2003**

**ABSTRACTS**





from each patient and a tissue array was made with the most representative area of each tumor. The IHC study included p16 (Santa Cruz Biotechnology, 1/20), p27 (DAKO, 1/50), PTEN (Cascade Biosciences, 1/300), BAX (Santa Cruz Biotechnology, 1/200), and pRb (DAKO, 1/5).

**Results:** Histologic grade correlated with mutations: tumors with BRCA1 mutations were grade I in 0 cases; grade II, 15.8%; and grade III, 84.2%. Tumors with BRCA2 mutations were grade I in 7.1%; II, 35.7%; and III, 57.1%. Familial BC without mutations were grade I, 50%; II, 28%; and III, 21.4%. The results of the immunohistochemical study were:

Gen Products	BRCA1 (%)	BRCA2 (%)	No BRCA (%)	p value
p16	89.5	100	80.8	n.s.
p27	57.9	91.7	92.3	0.015
PTEN	50.0	63.6	61.5	n.s.
BAX	72.2	45.5	61.5	n.s.
pRB	66.7	66.7	76.9	n.s.

n.s.: no significance

**Conclusions:** Most tumors from patients with BRCA1 mutation were grade III. Familial BC without mutations were more frequently grade I and II (p 0.005). The only significant difference in the IHC study was the higher loss of p27 expression in tumors with BRCA1 mutations.

### 162 Pathological and Clinical Predictors for Response to Neoadjuvant Chemotherapy in Breast Cancer

G MacGrogan, C Pallud, J Simonie-Lafontaine, C Sagan, V Verrielle, M Antoine, F Ettore, J Treilleux, P Tas, JP Bellocq, A Ulusakarya. Institut Bergonie; Centre Huguénin; Centre Val D'Aurelle; CHU Nantes; Centre Papin; CHU Paris Tenon; Centre Lacassagne; Centre Berard; Laboratoire Les Longs Champs; CHU Strasbourg; Bristol-Myers Squibb, France.

**Background:** Neoadjuvant chemotherapy improves relapse-free survival and increases the frequency of breast conservation surgery for women with invasive breast cancer who would otherwise be candidates for mastectomy. Sparse data is available on which simple pathological and clinical factors may help select patients who would benefit from such therapy.

**Design:** 232 patients presenting with T2, T3, N0, N1, M0 invasive breast cancer and non candidates for breast conservation surgery were enrolled in a prospective randomized parallel multicenter phase II study comparing the efficacy of 4 vs 6 cycles of neoadjuvant adriamycin/Taxol® followed by surgery. Initial microbiopsies and subsequent surgical specimens of 201 patients were available for central review. Predictive factors of tumor response included clinical tumor size, age, histological type, SBR grade, mitotic count, presence of emboli or DCIS and hormonal receptor status on the initial microbiopsy. Pathological response (PR) was graded as: Excellent (EPR) [total or near total therapeutic effect (TE) in tumor and negative nodes (N-)]; Good (GPR) [total or near total TE in tumor and positive nodes (N+)] or [more than 50% TE in tumor and N- or N+ with TE]; Bad (BPR) [less than 50% TE in tumor whatever node status].

**Results:** In the whole group of patients, factors significantly associated with EPR+GPR were T2 vs T3 status (p=0.03), invasive ductal carcinoma type (IDC, p=0.002), presence of DCIS (p=0.03), mitotic count >3 (p=0.002) and negative ER and PR status (p=0.01 and p=0.004), by univariate analysis (UV, Chi square test). Conversely, invasive lobular carcinoma type (ILC) was associated with BPR (p<10<sup>-3</sup>). Only ILC and PR status were independent factors predicting PR, by multivariate analysis (MV, Backward regression). Factors associated with mastectomy were T3 vs T2 status (p<10<sup>-3</sup>), non-IDC type (p=0.001), ILC (p=0.001) and clinical tumor size >50mm (p<10<sup>-3</sup>), by UV. ILC and T3 status were independent factors predicting mastectomy, by MV analysis.

**Conclusions:** T status, Clinical tumor size, histological type (IDC vs ILC), mitotic count and hormonal receptor status are important factors to consider when selecting patients for neoadjuvant breast cancer chemotherapy

### 163 Neuroendocrine Marker Expression in Breast Carcinoma: A Tissue Microarray Study

N Makretsov, A Coldman, M Cheang, D Huntsman, B Gilks. University of British Columbia and Vancouver General Hospital, Vancouver, BC, Canada; British Columbia Cancer Agency, Vancouver, BC, Canada.

**Background:** Neuroendocrine (NE) carcinomas of the breast are defined by their carcinoid-like morphology and expression of NE markers. There are few data on the prognostic significance of this phenotype and its association with other prognostic markers. The aim of this project was to detect NE differentiation by immunohistochemistry and to study its prognostic significance in a series of breast cancers.

**Design:** NE differentiation was studied by immunohistochemistry for synaptophysin (SYN), chromogranin A (ChrA) and neuron-specific enolase (NSE) in paraffin embedded tissues from 334 cases of breast carcinoma (Vancouver General Hospital, 1974-1995). Tissue microarray (TMA) blocks (using 0.6 mm duplicate tissue cores) were made and sections were processed using standard immunocytochemical techniques. Results were scored according to the intensity of cytoplasmic reaction and proportion of positive tumor cells as follows: 0-negative, 1-weak diffuse focal

immunoreactivity or strong staining in <10% of cells, 2-moderate diffuse immunoreactivity or strong staining in 10 to 50% of cells, 3-strong and diffuse immunoreactivity. Data processing and hierarchical clustering analysis were performed using Deconvolter, Cluster and Treeview software (Stanford University).

**Results:** Positivity of breast cancers for SYN was detected in 17% of cases (score 1-12%; 2-2.3%; 3-2.7%), ChrA in 1.8% (1-0.9%; 2-0.9%, 3-0%), NSE in 4.8% (1-3%; 2-1.5%, 3-0.3%). Expression of any NE marker was seen in 18.8% of tumors. Co-expression of two markers was detected in 2.4%, and three markers in 0.9% of cases. No association of NE markers with either grade, nodal status, ER or PR status was found, while the expression of SYN positively correlated only with C-erbB2 status (p<0.001). Kaplan-Meier analysis of disease specific and overall survival showed no prognostic significance of either single or multiple NE marker expression. **Conclusions:** NE expression was detected in 18.8% of breast carcinomas; of these, 3.3% of cases in our series co-expressed 2 or 3 NE markers. NE marker expression in breast carcinoma is not of prognostic significance.

### 164 Expression of NTRK3 (TRKC) in Human Breast Cancers: A Tissue Microarray Study

N Makretsov, PHB Sorensen, E Yorlida, A Coldman, B Gilks, D Huntsman. Academic Pathology Department of University of British Columbia and Vancouver General Hospital, Vancouver, BC, Canada; Children's and Women Health Centre of British Columbia, Vancouver, BC, Canada; British Columbia Cancer Agency, Vancouver, BC, Canada.

**Background:** The t(12;15)(p13;q25) translocation was initially described in pediatric congenital fibrosarcomas and later in cellular mesoblastic nephroma. This translocation fuses ETV6 and NTRK3 genes, forming a chimeric protein tyrosine kinase with potent transforming activity in NIH3T3 cells. The fusion transcript is expressed at low levels in affected cancers. We recently identified this translocation in human secretory breast carcinomas (SBC), a rare subtype of ductal carcinoma. The identification of the ETV6-NTRK3 translocation in SBC raises the possibility NTRK3 signaling may have relevance to other breast cancers.

**Design:** In this study we wished to determine whether the NTRK3 gene is expressed in a wider range breast cancer subtypes, and whether expression levels correlate with cancer grade, nodal status and patient outcomes. The tissue microarray was constructed using paraffin embedded tissue blocks from a clinically annotated series of 122 breast cancer cases. A rabbit polyclonal a-Trk-C antibody (Santa Cruz) with specificity for NTRK3 was applied to the arrays using a standard IHC protocol. The reaction in tumor cells was scored as 0-negative, 1-diffuse weak immunoreactivity or <10% strongly positive cells, 2-intermediate diffuse immunoreactivity or 10-50% strongly positive cells, and 3-diffuse strong immunoreactivity (>50% of cells positively stained). **Results:** NTRK3 nuclear staining was evident in a large proportion of tumors. 11% of tumors were scored as 0, 24% as 1, 42% as 2, and 23% as 3. Kaplan-Meier analysis showed a significantly better disease specific survival in patients with negative TrkC expression versus weak/intermediate/strong positivity (p<0.05). Higher levels NTRK3 expression were significantly associated with lymph node metastasis (p<0.01). No association was found with tumor grade.

**Conclusions:** NTRK3 is expressed in 89% of breast cancers. In this series the subset of breast cancers without detectable NTRK3 expression have a favourable prognosis when compared to NTRK3 expressing tumors. NTRK3 signaling may be a critical process in breast cancer pathogenesis. ETV6-NTRK3 translocations and high level expression of wild-type NTRK3 could be alternative mechanisms for inducing this pathway in breast cancer and are a focus for further studies.

### 165 Development and Progression of Mammary Ductal Tumors Appear To Be Mediated by Surrounding Myoepithelial Cells

YG Man, RS Vang, JS Saenger, BL Strauss, R Barner, DT Wheeler, CY Liang, GL Brattbauer, C Mannion. Armed Forces Institute of Pathology and American Registry of Pathology, Washington, DC; Hackensack University Medical Center, Hackensack, NJ.

**Background:** Our previous studies revealed the co-localization of tumor suppressor proteins, maspin and Wilms' tumor 1, in most morphologically identifiable myoepithelial (ME) cells; ducts without these proteins or without intact ME cell layers showed a significantly higher proliferation rate than their counterparts, suggesting that ME cells may impact the biologic behavior of subjacent epithelial cells. The focus of the current study was to assess the possible roles of ME cells in development and progression of mammary ductal tumors.

**Design:** Sections from normal and non-invasive breast lesions were immunostained with antibodies to ME cells, tumor suppressors and growth related proteins. Cells of interest were microdissected and assessed for micro-satellite instability (MI) or loss of heterozygosity (LOH) with a panel of markers altered in invasive tumors.

**Results:** ME cell layer disruptions were seen in a subset of normal, hyperplastic, and in situ neoplastic ducts. Compared to cells near an intact ME cell layer, cells subjacent to a disrupted ME cell layer often displayed several unique features: [1] alterations in the duct architecture and cell polarity or density; [2] reduced or lost expression of estrogen receptor; [3] reduced or lost expression of growth inhibitors; [4] elevated

rate of cell proliferation; [5] increased frequency of MI or LOH. All these features were increasingly identified in higher grade lesions.

**Conclusions:** The biologic presentations of cells subjacent to disrupted and intact ME cell layers are substantially different, suggesting that the development and progression of human mammary ductal tumors may be mediated by ME cells.

**Acknowledgement:** Supported by grants DAMD17-01-1-0129 & DAMD17-01-1-0130 from Congressionally Directed Medical Research Programs to Yan-gao Man.

### 166 Radial Scar and Carcinoma of the Breast

E Manfrin, D Reghellin, A Remo, F Canal, F Bonetti. Verona University, Verona, Italy.

**Background:** Radial scar (RS) is a benign lesion of the breast. RS measuring less than 1 cm are often an occasional finding, while larger lesions can present clinically, mimicking infiltrating carcinoma. A possible association of RS with carcinoma has been reported.

**Design:** To evaluate the association of RS with carcinoma, we reviewed 86 RS, larger than 1 cm in diameter, detected radiologically as single lesions. Clinical, radiological and histological data were reviewed.

**Results:** Mean age was 52 yr. (range 25-84). All 86 cases were considered radiologically suspect for carcinoma. Histologically, beside the characteristic features of RS, we observed microscopic foci of: atypical hyperplasia in 14 (16.2%), in situ lobular carcinoma in 6 (6.9%), intraductal carcinoma in 10 (11.6%) and infiltrating carcinoma in 15 (17.4%). Multiple sectioning and immunohistochemical analysis was necessary in most cases to reach a correct diagnosis.

**Conclusions:** RS larger than 1 cm is consistently associated with premalignant or overtly malignant lesions (52.1%). RS should be always biopsied. Simple excision seems adequate, for the minimal size of the atypical or neoplastic component.

### 167 P53 and HER2 neu Expression in Breast Carcinoma Occurring in Young Women

D Maru, LP Middleton, S Wang, V Valero, A Sahin. U.T.M.D. Anderson Cancer Center, Houston, TX.

**Background:** Breast carcinoma occurring in young women is uncommon and the tumors tend to be aggressive with a poor prognosis. The biologic characteristics of these tumors have not been well characterized. Previous studies have demonstrated that most carcinomas in young women are high grade invasive ductal carcinomas with low estrogen (ER) and progesterone receptor expression. P53 and Her2 neu overexpression is found in approximately 30% of breast carcinomas in women of all ages and is associated with high rates of lymph node metastases. These observations have not been studied in women younger than 30 years of age.

**Design:** 46 carcinomas in young women (age range 23-30 yrs.) were retrieved from the pathology database at our institution and were studied for p53 and Her2 neu expression by immunohistochemistry (Dako, D07, and Neomarkers respectively). P53 nuclear staining was graded as 0 (negative), 1 (< 25% cells), 2 (25-50% cells) and 3 (> 50% cells). Her2 neu membranous staining was graded as 0 (negative), 1 (incomplete weak staining < 25% cells), 2 (complete staining of 25-50% cells) and 3 (complete strong staining of > 50% cells). Grade 2 and 3 were considered positive. The marker expression was correlated with clinicopathologic features including tumor size, ER expression and axillary lymph node status.

**Results:** The 46 carcinomas consisted of 44 invasive ductal carcinomas, 1 medullary carcinoma and 1 unclassified carcinoma. The clinical stage was T1 (4), T2 (23), T3 (11) and T4 (5) cases. P53 was positive in 24 of 46 (52%) cases and Her2 neu was positive in 21 of 43 (49%) cases. 13 tumors were ER positive and 19 tumors were ER negative. The marker expression and lymph node status results are below.

	p53+	p53-	Her2 neu+	Her2 neu-
N0	5	7	3	8
N1/N2	19	15	18	14
p value	0.39		0.023	

**Conclusions:** P53 overexpression and Her2 neu expression are frequently identified in breast carcinomas in young patients. The incidence of Her2 neu expression in young women is higher than that reported for the general population. Moreover, Her2 neu overexpression in young women significantly correlates with lymph node involvement and may, therefore, be a marker for aggressive clinical behavior in this cohort.

### 168 Atypia in Ductal Lavage: A Follow Up Experience with Ductography, Ductoscopy and Tissue Biopsy

S Masood, S Khan, R Nayar. University of Florida Health Science Center, Jacksonville, FL; Northwestern Memorial Hospital, Feinberg, Chicago, IL.

**Background:** Ductal Lavage (DL) has been successfully used to sample epithelial cells from the breast. However, the sensitivity and specificity of DL has not yet been determined. Follow-up of atypia found in these samples is essential in establishing the potential role of DL in early breast cancer detection and individualized risk assessment. In the current study, we report the histological findings in a subset of women who have undergone surgical resection for atypical findings in DL cytology.

**Design:** Atypical DL cases with follow up ductography and/or ductoscopy and tissue biopsy seen at the University of Florida and Northwestern University were

selected for this study. Specimens were processed using Thin Prep or cytospin protocols and the slides were analyzed following previously established morphologic criteria.

**Results:** Nine cases of atypical DL with follow up tissue biopsy were identified. Five patients have undergone ductography, which showed evidence of space occupying lesions within the central ductal system close to the nipple. Ductoscopy in four cases revealed recognizable abnormalities. Tissue biopsy obtained from duct excisions showed three ductal carcinoma in situ and one papilloma in four cases with the diagnosis of marked atypia on DL. Five cases interpreted as mild atypia in DL preparations, were found to have papilloma in 2 cases, proliferative breast disease with atypia in one case and proliferative breast disease without atypia in two cases in their corresponding histologic follow up.

**Conclusions:** This study demonstrated that atypia seen in DL can be associated with recognizable anatomic abnormalities, among which papilloma seems to be a commonly observed lesion. Further studies are necessary to assess the prognostic significance of centrally located papillomas and to redefine the term atypia.

### 169 Isolated Tumor Cells in the Sentinel Node and Risk of Axillary Non-Sentinel Node Involvement in Patients with Invasive Breast Carcinomas

MC Mathieu, V Suci, JR Garbay, R Rouzier, J Lumbroso, JP Travagli. Institut Gustave-Roussy, Villejuif, France.

**Background:** In the classification of micrometastasis proposed by the UICC(1), isolated tumor cells (ITC) are defined in a separate category pN0(i+) from nodal tumor deposits. The objective of this work was to determine the risk of axillary non-sentinel node (non-SN) involvement when this type of metastasis is found in the sentinel node (SN).

**Design:** Since 1999, the SN protocol has been proposed for patients with a T0-T1 N0 breast carcinoma. Complementary axillary dissection has been performed in 87 cases with a positive SN. The entire SN was included in 1.5-2 mm-thick slices and examined after staining with hematoxylin-eosin-safran (HES). In negative SN, 3 additional levels at 250-µm intervals were stained with HES and studied immunohistochemically (IHC) with cytokeratin (CK22, Dako).

**Results:** Non-SN involvement was present in 35% of cases with a positive SN (30/87 cases). The frequency of non-SN metastases was not significantly different among patients with pN0(i+) isolated cells (30%, 3/10 cases) or with pN1a micrometastases (12%, 4/33 cases). However, the risk was higher for macrometastases (52%, 23/44 cases) (p<0.001). ITC were detected by IHC in 4 cases. Including non-SN, the final pN status was: pN1(i+) in 1 case, pN1a in 1 case and pN1b in one case.

**Conclusions:** In our study, ITC in SN have a capacity to implant in non-SN which is not different from micrometastatic nodal tumor deposits.

(1)HERMANEK, Cancer, 1999, 86:2589.

### 170 c-erbB-2 (HER2/neu) in Infiltrative Lobular Carcinoma: Dissociation between Immunohistochemistry and Fluorescence In Situ Hybridization

W McDonald, Y Chen, C Zaloudek, G Magrane, F Waldman. UCSF, San Francisco, CA.

**Background:** Overexpression of erbB-2 (HER-2/neu) protein or amplification of the ERBB2 gene is required to qualify patients with advanced invasive breast cancer for treatment with trastuzumab. Most studies have shown that ERBB2 gene amplification is almost always associated with overexpression of its protein product. The College of American Pathologists recently asserted that immunohistochemistry (IHC) and fluorescence *in situ* hybridization (FISH) are confirmatory of one another in determining erbB-2 status. Previous studies have not defined the relationship between erbB-2 overexpression and gene amplification in infiltrative lobular carcinoma (ILC).

**Design:** 39 infiltrative lobular carcinomas submitted to UCSF pathology for erbB-2 oncoprotein analysis between February 2000 and August 2001 were analyzed. All cases were IHC-positive for estrogen receptors, progesterone receptors, or both. Herceptest™ (Dako) was performed according to the manufacturer's instructions on all cases and scored according to standard guidelines. FISH was performed on all cases using probes to ERBB2 and centromere 17 (C17). When possible, at least 50 cells were scored per case for both ERBB2 and C17. Cases were considered amplified if the ERBB2:C17 ratio was greater than or equal to 2.0.

**Results:** Of 39 cases examined, 7 (18%) demonstrated overexpression of erbB-2 by Herceptest™ staining (3+), while 9 (23%) showed borderline staining (2+). Only 1 case (3%) displayed ERBB2 amplification by FISH. Herceptest™ was positive (3+ staining) in that case. All 23 cases that were negative by IHC (0 or 1+) lacked gene amplification.

**Conclusions:** There was a clear dissociation between protein overexpression as determined by IHC and amplification of ERBB2, suggesting that other mechanisms of overexpression may play a role in this type of infiltrative breast cancer. This dissociation should be considered when evaluating the ERBB2 status of infiltrative lobular cancers. A negative Herceptest™ accurately predicted absence of gene amplification, suggesting that ILC with scores of 0 or 1+ (negative) may not need to undergo further testing.



was evaluated by 3 of the above authors without knowledge of response data and results were correlated with response to therapy. Membranous staining of EGFR and nuclear staining of p27, Cyclin D1 and PPAR $\gamma$  were defined as positive. Chi-square test is used for statistical analysis.

**Results:** Positive staining in >25% of tumor cells for p27 and in >20% of tumor cells for Cyclin D1 was significantly associated with response to trastuzumab based therapy. EGFR and PPAR $\gamma$  staining did not show a significant correlation with response.

Marker (positive staining)	Response (% Patients)	No Response (% Patients)	p value
EGFR	80	55	Not Significant
p27	75	40	<0.05
Cyclin D1	55	0	<0.05
PPAR $\gamma$	25	14	Not Significant

**Conclusions:** Cyclin D1 and p27 may be important markers for predicting response to trastuzumab based therapy in patients with metastatic breast cancer and the usage of these markers for selection of therapy in this clinical setting merits further study.

## 223 A Subset of Morphologically Identifiable Mammary Myoepithelial Cells Lacks Expression of Corresponding Phenotypic Markers

RR Zhang, Y-G Man, BL Strauss, RL Yang, JS Saenger, R Barner, DT Wheeler, CY Liang. Armed Forces Institute of Pathology, Washington, DC.

**Background:** Immunohistochemical staining for smooth muscle actin (SMA) is commonly used for identifying mammary myoepithelial (ME) cells, whose presence or absence is a reliable criterion for differentiation between in situ and invasive carcinomas. However, some ME cells that are morphologically identifiable on H&E sections fail to stain for SMA. This study attempt to assess whether these SMA(-) cells also lack expression of other ME cell phenotypic markers.

**Design:** Non-invasive lesions harboring ME cells that are focally or entirely SMA (-) in ducts lined by more than 50 epithelial cells were selected, and 8 consecutive sections from each selected case were stained for SMA. Ducts with SMA(-) ME cells were photographed; then, each section was re-stained for one of 8 additional ME markers (below). The same SMA (-) ducts were examined for expression of other markers. **Results:** Some SMA(-) ME cells also failed to display distinct immunoreactivity for other ME cell markers, including calponin, maspin, Wilms' tumor-1, CD-10, smooth muscle myosin-heavy chain, or cytokeratins 5, 14, and 17 (CK-5, -14, and -17). Some SMA(-) ME cells, however, displayed strong immunoreactivities for CK-5, -14, and -17. The distribution of these ME cells appeared to be independent of the ductal size, length, and architecture.

**Conclusions:** A subset of ME cells fail to express corresponding phenotypic markers, suggesting that these SMA (-) cells may have genetic and biochemical properties that are different from their SMA (+) counterparts.

Supported by grants DAMD17-01-1-0129 and DAMD17-01-1-0130 from The Congressionally Directed Medical Research Programs to Yan-gao Man, MD., Ph.D.

## Cardiovascular

### 224 Surgical Pathology of Subaortic Septal Myectomy Not Associated with Hypertrophic Cardiomyopathy: A Study of 98 Cases (1996-2000)

RD Allen, WD Edwards, HD Tazelaar, GK Danielson. Mayo Clinic, Rochester, MN.

**Background:** No series have described the surgical pathology of subaortic septal myectomy in patients with conditions other than hypertrophic cardiomyopathy (HCM).

**Design:** Medical records and microscopic slides were reviewed from 98 non-HCM patients undergoing septal myectomy at Mayo Clinic Rochester from 1996-2000. Concurrently, 229 other patients had myectomy for HCM.

**Results:** The study group (65 women, 33 men) ranged in age from 1.5-92 years (mean, 61). Seventy underwent surgery for aortic stenosis (group 1), 25 for congenital subaortic stenosis (group 2), and 3 for other conditions (group 3). Group 1 patients were older than group 2 (72 vs 26 years;  $p < 0.0001$ ). Microscopic evaluation showed myocyte hypertrophy (97%), vacuolization (35%), left bundle branch tissue (26%) (33% in group 1 vs 8% in group 2;  $p = 0.02$ ), and disarray (19%); interstitial fibrosis (92%), inflammation (10%), and amyloidosis (7%, all prealbumin type, all group 1, >80 years old); vascular thickening (18%), dysplasia (12%), and dilated venules (6%); and endocardial fibrosis (74%) (64% in group 1 vs 100% in group 2;  $p = 0.0001$ ) and chronic inflammation (17%).

**Conclusions:** Of 327 patients undergoing subaortic septal myectomy, 30% had conditions other than HCM. Myocyte disarray was present in 19% of patients without HCM (and was absent in 20% of HCM patients in a companion study). Thus, disarray alone cannot be used reliably to include or exclude a diagnosis of HCM in small surgical specimens. Because amyloid was found unexpectedly in 7 octogenarians, we recommend routine amyloid staining on surgical myectomy tissue from patients over 65 years of age.

### 225 Arrhythmogenic Right Ventricular Cardiomyopathy Causing Sudden Cardiac Death in Boxer Dogs a New Animal Model of Human Disease

C Basso, P Fox, K Meurs, J Towbin, A Spier, F Calabrese, B Maron, G Thiene. University of Padua Medical school, Padova, Italy; Animal Medical Center, New York, NY; Ohio State University College, Columbus, OH; Baylor College of Medicine, Houston, TX; Minneapolis Heart Institute Foundation, Minneapolis, MN.

**Background:** Arrhythmogenic right ventricular cardiomyopathy (ARVC) is a primary and familial heart muscle disease associated with substantial cardiovascular morbidity and high risk of sudden death in the young. Efforts to discern the relevant mechanisms have been impaired by the absence of a suitable animal model.

**Design:** ARVC was clinically suspected in 23 boxer dogs (12 male; 4.5 to 13.7 years old, mean, 9.1 $\pm$ 2.3 years) based upon a phenotype including ventricular arrhythmias of RV origin ( $n = 18$ , 78%), sudden death ( $n = 9$ , 39%), syncope ( $n = 12$ , 52%), or right heart failure ( $n = 3$ , 13%). Six dogs shared similar pedigrees. In vitro magnetic resonance imaging (MRI) and detailed gross, histology and immunohistochemistry investigation was performed in formalin-fixed hearts removed at autopsy. Quantitative computerized morphometry was used to assess myocardial atrophy and fatty tissue replacement.

**Results:** Moderate RV chamber dilatation was present in 8 (35%) and RV aneurysms in 3 (13%). In vitro MRI showed bright RV antero-lateral and/or infundibular wall signals (diffuse in 12, 52% and focal in 6, 26%). Histomorphometry revealed increased RV fatty tissue (mean percent area  $45 \pm 16$ %) versus controls ( $15 \pm 3$ %) ( $P < 0.001$ ) and a decreased residual myocardial area ( $51 \pm 16$ % versus  $83 \pm 3.1$ %, respectively ( $P < 0.001$ )). Fatty infiltration was greatest in the infundibular region. Substantial replacement fibrosis occurred in seven ARVC hearts (30%), mild inflammatory infiltrates in 14 (61%), and apoptotic myocytes in nine (39%).

**Conclusions:** We report a new, spontaneous animal model of ARVC and sudden unexpected death in the boxer dog that closely resembles the human disease. It is characterized by ventricular arrhythmias, sudden death, fatty or fibrofatty myocardial replacement, apoptosis, and myocarditis. Accordingly, this canine model will facilitate investigation of complex clinical and pathophysiologic mechanisms of ARVC and sudden death in humans.

### 226 Surgical Pathology of Pulmonary Thromboendarterectomy: A Study of 54 Cases (1990-2001)

LA Blauwet, WD Edwards, HD Tazelaar, CGA McGregor. Mayo Clinic, Rochester, MN.

**Background:** Thromboendarterectomy may be performed for chronic thromboembolic pulmonary hypertension with obstruction of main, lobar, or segmental pulmonary arteries. The aims of the current study were to document (1) patient age and sex distribution, (2) frequencies of thrombotic or embolic events, (3) presence of coagulopathy or autoimmune disorder, (4) sites of pulmonary artery obstruction, and (5) gross and microscopic features of surgically resected specimens.

**Design:** Medical histories and microscopic slides were reviewed in each case. Slides were stained with hematoxylin-eosin and Verhoeff-van Gieson and were evaluated for the presence of thrombus; intimal collagen, elastin, atherosclerosis, hemosiderin, calcification, and inflammation; medial tissue and inflammation; and adventitial tissue.

**Results:** The study group included 54 patients (30 women, 24 men), ranging from 33-77 years old (mean, 58). Clinically, 28 (52%) had a history of deep leg vein thrombosis and 42 (78%) had a history of pulmonary embolism; 24 (44%) patients had histories of both events. Coagulation abnormalities were documented in 15 (28%), and 8 (15%) had an autoimmune or hematologic disorder. Pulmonary thromboendarterectomy was bilateral in 52 patients (96%) and unilateral in 2. Six patients had obstructions resected from their main pulmonary arteries. Obstruction limited to the segmental arteries occurred only in women. Grossly, right-sided specimens were larger than left-sided ( $p = 0.003$ ). Microscopically, thrombi were of uniform age in 72% and of variable age in 28%. Intima was thickened in all and consisted of collagen (100%), elastin (67%), hemosiderin (56%), inflammation (53%), atherosclerosis (32%), and calcification (15%). Three additional patients, not included among the 54, underwent resection of intraluminal pulmonary artery sarcomas.

**Conclusions:** Pulmonary thromboendarterectomy was most often performed in middle-aged and elderly patients with a history of deep leg vein thrombosis or pulmonary embolism. Most patients did not have an identifiable coagulation, autoimmune, or hematological abnormality. Although most had bilateral procedures, right-sided specimens were generally larger than left-sided. Resected tissues commonly showed organized thrombus. In 5% (3/57), sarcomas mimicked pulmonary thromboembolism.

### 227 Overexpression of Tumor Necrosis Factor (TNF $\alpha$ ) and TNF $\alpha$ Receptors in Human Viral Myocarditis: Clinico-Pathologic Correlations

F Calabrese, E Carturan, C Agostini, A Angelini, M Valente, GM Boffa, A Frustaci, G Thiene. University of Padua, Padua, Italy; Catholic University of Rome, Rome, Italy. **Background:** Proinflammatory cytokines, including TNF $\alpha$ , have been recognized as important pathophysiologic and pathogenic factors in the initiation and continuation of inflammatory cardiomyopathy. Experimental and preliminary human studies have demonstrated that TNF $\alpha$  plays a potentially critical role in enteroviral-induced myocarditis.

**ACR** *American Association  
for Cancer Research*  
Redefining the Frontiers of Science

# 94th Annual Meeting

July 11-14, 2003  
Washington Convention Center  
Washington, D.C.

Volume 44  
2nd Edition  
July 2003



*Proceedings*

E-CD loss and p120ctn mislocalization were observed in all cases, implying that these alterations occur early in the oncogenesis of ILC. By contrast, none of the 119 invasive or in situ ductal carcinomas analyzed in a Tissue Microarray showed p120ctn cytoplasmic accumulation, whereas reduced E-CD and p120ctn in membrane was very common. Moreover, we observed that in breast cancer cell lines completely lacking E-CD expression, including 5 primary lobular cancer cell lines generated by us, p120ctn accumulated in the cytoplasm, and occasionally in the nucleus. To demonstrate the mechanistic link between E-CD loss and p120ctn mislocalization, a breast cancer cell line showing complete silencing of E-CD gene by promoter hypermethylation was treated with the demethylating agent 5-Azacytidine for 72h. After treatment, an epithelial phenotype was restored, and p120ctn was recruited from the cytoplasm to the membrane, where it colocalized with the endogenous re-expressed E-CD. In conclusion, abnormal cytoplasmic accumulation and nuclear localization of p120ctn are novel and characteristic alterations of lobular breast carcinomas. This altered p120ctn expression is mediated by the absence of E-CD, occurs in the earlier stages of the disease, and is maintained during lobular tumor progression to metastasis. Consequently, p120ctn may be an important mediator of the oncogenic effects derived from E-CD inactivation, including enhanced motility and invasion.

**#357 Identification of invasive precursor cells in normal appearing and hyperplastic breast tissue.** Yang Gao Man, J.S. Saenger, R.S. Vang, R. Barner, D. Wheeler, Alfredo Martinez, and James L. Mulshine. *Department of Gynecologic & Breast Pathology, Washington, DC and National Cancer Institute, Bethesda, MD.*

We previously reported discrete genetic changes in pre malignant and adjacent normal appearing bronchial epithelium that were shared with overt cancerous tissue. We recently defined a similar clonal phenotype in ductal carcinoma in situ breast cells. The current investigation evaluates if a similar situation exists with other normal appearing and hyperplastic breast cells. To define the cell populations, sections from patients with cancer or suspected cancer including both normal and hyperplastic appearing breast tissue were double immunostained using antibodies to estrogen receptor (ER) and smooth muscle actin (SMA) to demonstrate epithelial (EP) or myoepithelial (ME) cells. Immunostained sections were examined to identify ER (-) cell clusters, defined as a group of  $\geq 5$  ER (-) cells. These foci were found adjacent to disrupted ME cell layer. In contrast, for areas with an intact ME cell layer, the adjacent epithelial cells showed intense ER (+) immunostaining. ER (-) cell clusters were seen in both the normal and hyperplastic appearing ducts in a small portion ( $\approx 10\%$ ) of the cases. The immunohistochemical and genetic features in ER (-) clusters were compared to those in the ER (+) clusters. Compared to their ER (+) counterpart within the same duct, the ER (-) cell clusters generally displayed the following unique features: [1] more abundant surrounding stromal and vascular structures; [2] a lower frequency of p27 expression; [3] a higher cell proliferation rate; [4] a higher frequency of loss of heterozygosity (LOH) and micro-satellite instability (MI). These features were comparable to those seen in invasive mammary tumors. Conclusions: ER (-) cell clusters in both normal appearing and hyperplastic ducts generally displayed biological and molecular features similar to those of invasive mammary tumors, suggesting that these ER (-) cell clusters adjacent to disrupted ME cell layer represent invasive clonal cell populations. Supported by grants, DAMD17-01-1-0129 and DAMD17-01-1-0130, Congressionally Directed Medical Research Programs to Yan-gao Man, MD., Ph.D.

**#358 Expression of HIF-1 $\alpha$  in squamous cell carcinoma of the tongue: A new parameter for predicting cancer cell metastasis.** Takao Ueno, Ken-ichi Notani, Fumihiko Higashino, Takao Kohgo, and Masanobu Shindoh. *Hokkaido University Graduate School of Dental Medicine, Sapporo, Japan.*

Hypoxia-inducible factor 1 (HIF-1) is an oxygen-regulated transcriptional activator that plays an essential role in maintaining oxygen homeostasis. HIF-1 adapted cells to hypoxic conditions for regulating transcriptional activation of several genes that respond to the lack of oxygen, including vascular endothelial growth factor (VEGF). HIF-1 consists of dimerization of  $\alpha$  and  $\beta$  subunits. HIF-1 $\beta$  is a constitutive nuclear protein, whereas HIF-1 $\alpha$  subunit could generally not be detected in normal tissue by rapid degradation. HIF-1 $\alpha$  protein is stabi-

lized and accumulated when cells were exposed to hypoxic condition. Recently, it has been reported that HIF-1 $\alpha$  plays an important role promoting tumor progression. We investigated the expression of HIF-1 $\alpha$  in squamous cell carcinoma (SCC) of the tongue by immunohistochemical methods and compares the relation to the clinico-pathological findings. HIF-1 $\alpha$  was identified in 12 of 39 cases (31%) examined. HIF-1 $\alpha$  positive signal was observed in both nuclei and cytoplasm of cancer cells. HIF-1 $\alpha$  expression was not significantly associated with clinical parameters such as age, gender and clinical staging of patients, nor with pathological findings as grading of tumor malignancies and mode of invasion of cancer cells. There was a statistically significant correlation between HIF-1 $\alpha$  expression and cancer cell metastasis to cervical lymph nodes or distant organs. Kaplan-Meier analysis showed a significant influence of HIF-1 $\alpha$  expression on the cumulative overall survival rate ( $p=0.0030$ , log-rank test). VEGF was shown to be the downstream gene of HIF-1 $\alpha$ , and neo-vascularization. VEGF has been thought to correlate highly with metastasis of cancer cells. The number and diameter of blood vessels around the tumor tissue was investigated by immunostaining of endothelial cells with antibody against CD34. There was a high ratio of neo-vascularization in HIF-1 $\alpha$  positive tumors, with a large number and smaller diameter of blood vessels, which was more obviously seen in the stromal tissue than in HIF-1 $\alpha$  negative tumors. It has been reported that p53 interacts with HIF-1 $\alpha$  to reduce the activity of neo-vascularization by downregulating VEGF. In this study, mutant-p53 (mt-p53) expression was significantly associated with HIF-1 $\alpha$  expression; however, cases with both mt-p53 and HIF-1 $\alpha$  expression highly correlate with metastasis and showed significant shorter cumulative overall survival. Our results suggest that HIF-1 $\alpha$  expression in combination with p53 status would be an indicator of neo-vascularization, which could be used as a predictive and prognostic parameter for metastasis in tongue SCC.

**#360 Translational upregulation of Src by erbB2-mediated activation of mammalian target of rapamycin contributes to human breast cancer progression and metastasis.** Ming Tan, Ping Li, Kaitane Kios, Yoichi Nagata, and Dihua Yu. *The University of Texas M.D. Anderson Cancer Center, Houston, TX.*

ErbB2, a member of the EGFR receptor tyrosine kinase family, has been demonstrated to play an important role in breast cancer progression and metastasis. However, the molecular mechanism of ErbB2-mediated breast cancer metastasis is poorly understood. To elucidate the mechanism underlying ErbB2-mediated breast cancer metastasis, we investigated the signaling pathways downstream of ErbB2 that contribute to ErbB2-mediated metastasis. We transfected wild-type and mutant ErbB2 expression constructs into an ErbB2-low-expressing human breast cancer cell line MDA-MB-435. We found that ErbB2 overexpressing cells, which had higher metastatic potential in vitro in vivo, had significantly increased Src protein level and kinase activity comparing to ErbB2 low-expressing control cells. However, Src levels among ErbB2 high- and low-expressing cells were similar. Preliminary study suggested that the increased Src protein level in ErbB2 high-expressing cells was due to the upregulation of Src translation, which resulted from the activation of mTOR pathway by ErbB2. To assess the significance of Src upregulation in breast cancer metastasis, we injected ErbB2 low-expressing MDA-MB-435 and ErbB2 high-expressing 435.eB cells into ICR-SCID mice. Mice were treated with the Src specific inhibitor PP2. We found that PP2 dramatically inhibited ErbB2-mediated cancer cell metastasis. These results indicate that overexpression of ErbB2 translationally upregulates Src through the activation of the mTOR pathway and this mechanism plays an important role in ErbB2-mediated breast cancer progression and metastasis.

**#361 IGFBP-3 effect in prostate cancer cells and osteoblasts.** Jun Yang, Erica L. Kreimann, Charles R. Sikes, Clifton L. Steppe, Sue-Hwa Lin, Sara Peleg, Matilde Olive, Christopher J. Logothetis, Gerard Karsenty, and Nora M. Navone. *University of Texas M.D. Anderson Cancer Center, Houston, TX and Baylor College of Medicine, Houston, TX.*

Advanced prostate cancer (PCa) is dominated by complications arising from bone metastases (BM). Bone metastases of PCa are characteristically blastic, i.e., they involve excessive bone formation, and is frequently the only site of progression. These observations suggest

# THE FASEB JOURNAL

A MULTIDISCIPLINARY RESOURCE FOR THE LIFE SCIENCES

**Experimental Biology 2004®**

Washington, DC

April 17–21, 2004

**ABSTRACTS**

**PART II**

Abstracts 480.1–860.14

Official Publication of the Federation of American Societies for Experimental Biology  
Volume 18, Number 5, March 24, 2004



polyphenols (flavonoids) from lowbush blueberries (*Vaccinium angustifolium*) would affect MMP expression. A crude fraction, an anthocyanin-enriched (AN) and a proanthocyanidin-enriched (PAC) fraction were evaluated. MMP activity was measured (using zymography) in DU145 cells following 24 hour exposure to 0.1, 0.5, and 1.0 mg/ml of each fraction. Crude fraction inhibited MMP-9, MMP-2, and MMP-7 in a dose-dependent manner, while MMP-3/10 activity remained unchanged. The AN fraction inhibited MMP-2 and MMP-7 in a dose-dependent manner, while MMP-9 activity was inhibited only by 1.0 mg/ml AN. MMP-3/10 activity remained apparently unaffected by the AN fraction. PAC's also inhibited MMP activity in a dose-dependent manner. Decreased MMPs' activity was not due to either apoptotic or necrotic cell death indicating that these fractions' effects are specific/target-directed. "Bioactive" fractions from blueberries may possess the ability to decrease ECM degradation in prostate cancer cells, in part, by decreasing MMP activity levels. [PEI Cancer Research Council funded]

#### 786.10

**NVPAAL993, a VEGF-R2, R3 antagonist prevents VEGF-C mediated proliferation of lymphatic endothelial cells in vitro.**

April Carpenter<sup>1</sup>, Amer Rassam<sup>2</sup>, Jonathan Glass<sup>2</sup>, Christopher G Kevil<sup>3</sup>, James Cardelli<sup>2</sup>, Jeffrey Houghton<sup>4</sup>, Paul Manley<sup>5</sup>, John W Elrod<sup>4</sup>, Jonathan Alexander<sup>6</sup>. <sup>1</sup>Physiology, LSU Health Sciences Center, 1501 Kings Highway, Shreveport, LA 71130, <sup>2</sup>Feist Weiler Cancer Center, Louisiana State University Health Sciences Center, Shreveport, LA, <sup>3</sup>Pathology, LSUHSC-S, Shreveport, LA, <sup>4</sup>Molecular and Cellular Physiology, Louisiana State University Health Sciences Center, Shreveport, LA, <sup>5</sup>Feist Weiler Cancer Center, Novartis, Shreveport, LA, <sup>6</sup>Physiology, Louisiana State University Health Sciences Center, Shreveport, LA

In addition to blood vessel formation (angiogenesis), lymphangiogenesis is now also known to influence growth of tumors and tumor metastasis. Therefore, drugs which would limit the proliferation of lymphatic endothelial cells (and lymphangiogenesis) might represent important new treatments for limiting cancer growth. We examined the proliferation of murine lymphatic derived endothelial cells (MJC-1) cells, a lymphatic endothelial cell line expressing VEGF-R3 (measured by RT-PCR and Flt-4 western blotting), in the presence of VEGF-C, (a lymphatic endothelial growth factor) and in the presence of VEGF-C plus the anthranilamide antagonist of VEGF-R2/R3, NVPAAL993, (2-[(4-pyridyl) methyl]amino-N-[3-(trifluoromethyl)phenyl] benzamide). (NVPAAL993 inhibits VEGF-R2 and R3 with IC50s of 23 and 18 nM respectively using purified enzyme). We found that NVPAAL993 dose dependently blocked the proliferation of lymphatic endothelial cells (measured at 48 hours) with an IC50 of approximately 2  $\mu$ M. These data suggest that NVPAAL993 might represent an important therapeutic agent for reducing lymphoproliferation in cancer, and possibly lymphoproliferation in chronic inflammatory diseases.

#### 786.11

**Morphologically comparable prostate acini and ducts with and without a focal basal cell layer disruption have a different cell proliferation rate: Implications for tumor invasion**

Yan-gao Man<sup>1</sup>, Ting Shen<sup>2</sup>, yunge Zhao<sup>3</sup>, Qing-Xiang Amy Sang<sup>3</sup>. <sup>1</sup>Gynecologic & Breast Pathology, Armed Forces Institute of Pathology, 6825 16th Street, NW, Washington, DC 20306-6000, <sup>2</sup>Pathology, Temple University Medical School, Philadelphia, PA, <sup>3</sup>Chemistry and Biochemistry, Florida State University, Tallahassee, FL

Our previous studies revealed that a subset of mammary ductal carcinoma in situ contained focally disrupted myoepithelial (ME) cell layers. As prostate basal cells are believed to be equivalent to breast ME cells, this study attempts to assess whether focal basal cell layer disruptions are detectable in prostate tumors. Two consecutive sections from each of 16 patients with prostatic intraductal neoplasia and organ-confined carcinoma were double immunostained for cytokeratin (CK) 34 beta E12 plus androgen receptor (AR) and CK 34 beta E12 plus Ki-67, respectively. Acini and ducts lined by over 40 epithelial cells were examined for a focal basal cell layer disruption, defined as the absence of basal cells resulting in a gap equal to or greater than the combined size of 3 basal or epithelial cells. Focal basal cell layer disruptions were seen in about 10% of the acini and ducts examined. Over 80% of the disruptions were overlain by or subjacent to AR positive cell clusters. Acini and ducts with focal basal cell layer disruptions showed a

significantly higher ( $p < 0.01$ ) proliferation rate than their morphologically comparable counterparts without disruptions. A vast majority of the proliferating cells were located at or near the basal cell layer disruptions. In some cases, cells in focally disrupted basal cell layers appeared to be directly connected to the invasive component.

#### 786.12

**A model to study sentinel lymph node (LN) metastasis**

CHAO-NAN QIAN<sup>1</sup>, Bree Berghuis<sup>2</sup>, Galia Tsarfaty<sup>3</sup>, MaryBeth Bruch<sup>3</sup>, Eric J. Kort<sup>1</sup>, David Jackson<sup>4</sup>, James H. Resau<sup>2</sup>, Bin Tean Teh<sup>1</sup>. <sup>1</sup>Lab of Cancer Genetics, Van Andel Research Institute, 333 Bostwick Ave NE, Grand Rapids, MI 49503, <sup>2</sup>Lab of Analytical, Cellular and Molecular Microscopy, Van Andel Research Institute, Grand Rapids, MI, <sup>3</sup>Lab of Molecular Oncology, Van Andel Research Institute, Grand Rapids, MI, <sup>4</sup>MRC Human Immunology Unit, Weatherall Institute of Molecular Medicine, John Radcliffe Hospital, Oxford, United Kingdom. Understanding metastases is the key to defeating cancer. A high LN-metastatic cellular clone (C-18) from the parental human nasopharyngeal carcinoma cell line CNE-2 was isolated *in vitro* by using the limited dilution method and the migration/invasion assay, and then confirmed *in vivo* by using the foot-pad model, which included inoculation of the tumor cells into the left hind foot-pad of nude mouse and resulted in metastasis to the popliteal (sentinel) lymph node (PLN) (Fig 1). The PLN metastasis rates were 75% on Day 40 and 100% on Day 50 after implantation of C-18.

Angiogenesis and lymphangiogenesis in the sentinel, contra-lateral, and normal PLNs were evaluated by ultrasonography, dextran-FITC perfusion, histological analyses (Fig 2), and detections of circulating cytokines and endothelial cells. There are two morphologic variants of blood vessels in the normal PLN. Certain vessels can be activated in a unique way in the sentinel PLN as well as in the contra-lateral PLN during tumor-induced angiogenesis. Our studies support the conclusion that the primary tumor can induce angiogenesis in the LN. This model is useful for the studies of the mechanism(s), the prevention and the treatment of LN metastasis.

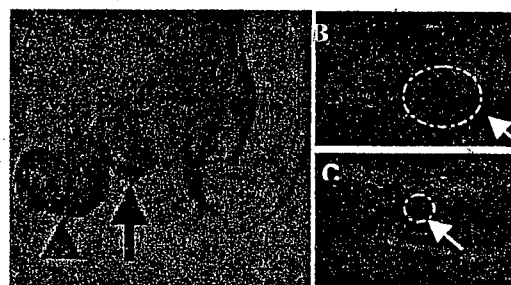


**Figure 1.** The LN metastasis model. The black arrow head (A) indicates primary tumor. The back arrow indicates the spontaneous metastasis of the tumor cells to the PLN. Ultrasonography showed the metastatic PLN (white arrow in B) was enlarged compared to the contralateral PLN (white arrow in C).

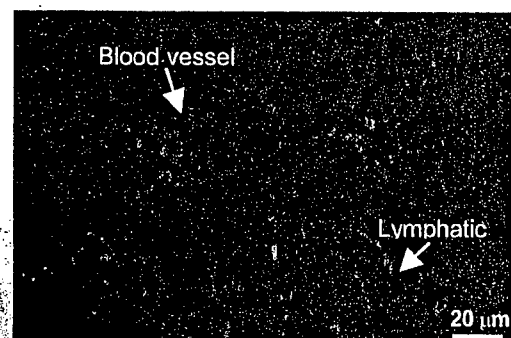


**Figure 2.** Merged image of triple immunofluorescence staining. The lymphatic endothelial cells (stained with LYVE-1, secondarily stained with FITC) and the vascular endothelial cells (stained with CD31, secondarily stained with rhodamine) can be clearly distinguished in LN. DAPI (blue) stained the nuclei.

*Divergent effect of progression of breast cancer from the in situ to the invasive stage on the expression of the retinoic acid biosynthetic enzyme retinaldehyde dehydrogenase 2 (RALDH2): Implications for chemoprevention and treatment of breast cancer.*

Judith Weisz,<sup>\*,1</sup> Debra A. Shearer,<sup>\*</sup> Elizabeth E. Fraumenhoffer,<sup>\*\*</sup> Yan-Gao Man<sup>\*\*\*</sup> Peter McCaffery<sup>\*</sup>

Departments of Obstetrics and Gynecology<sup>\*</sup> and Pathology,<sup>\*\*</sup> Pennsylvania State University College of Medicine, Hershey, Pennsylvania, The Department of Gynecology and Breast Pathology, Armed Forces Institute of Pathology, Washington DC<sup>\*\*\*</sup> and University of Massachusetts E. K. Shriver Center, Waltham, MA<sup>\*</sup>.

Short Title: RALDH2 and breast cancer

Supported by National Institutes of Health grants CA65532 (to JW), HD05515 (to P.M.) Congressionally Directed Medical Programs, Grants DAMD-17-01-0129 and DAMD-17-01-0130 (to Y-g. M.) and CA0145 (to G.C.) that provided the system used for capturing immunocytochemical images and for densitometric image analysis.

Address reprint requests to Judith Weisz, M.B. B.Chir. Pennsylvania State University College of Medicine, Department of Obstetrics and Gynecology, The M.S. Hershey Medical Center, 500 University Drive, Hershey, PA 17033. E-mail: jxw7@psu.edu.

Pages (Text + 1 Table + 1 figure): 18 pages

Colored phomicrographs: 4 pages

Previously, we reported finding a marked difference between in situ and invasive components of breast cancers in the expression of the enzyme UGT2B7 that by glucuronidating retinoic acid (RA) generates the potent retinoid retinoyl- $\beta$ -glucuronide. While UGT2B7's expression in invasive cancers was at most minimal, within in situ lesions it was higher than in normal mammary epithelium. The virtual absence of UGT2B7 in invasive cancer was consistent with retinoids' importance as differentiating agents. However, its *increased* expression in pre-invasive cancers suggested that RA biosynthesis might be paradoxically increased pre- rather than decreased in pre-invasive lesions. To test this notion, here we examined normal and neoplastic human breast tissue for the expression of retinaldehyde dehydrogenase 2 (RALDH2 that catalyzes the oxidation of retinal to RA. In normal breast parenchyma, RALDH2 was identified by isoelectric focusing immunoblot analysis, localized by immunocytochemistry in the mammary epithelium and oxidation of retinal to RA demonstrated by a reporter assay. RALDH2 immunostaining was minimal in invasive cancers but markedly elevated within in situ cancers. Sites of invasion, where the myoepithelial barrier surrounding in situ lesions had been breached, were largely occupied by immunonegative cancer cells. These findings lead us to postulate that these differences in expression of RALDH reflect changes in the microenvironment associated with disease progression. Specifically, we postulate that cancer cells within the microenvironment maintained by an intact myoepithelial barrier are driven towards differentiation, but that with breakdown of this barrier, a lineage of less differentiated cancer cells can become dominant and initiate invasion.



Retinoic acid (RA), the major known mediator of actions of retinoids, is a critical contributor to regulatory mechanisms essential for the normal development of epithelia and their maintenance in a differentiated state<sup>1</sup>. Therefore, from the perspective of cancer biology, RA is an anti-carcinogenic, "tumor suppressor" agent. Attesting to RA importance in tumor suppression are the many observations of aberrant expression in diverse cancers of genes encoding proteins on which RA homeostasis and action depend, and the effectiveness of retinoids in the treatment and chemoprevention of some cancers<sup>1,2</sup>. Studies of mechanisms underlying this phenomenon have largely focused on the effects of carcinogenesis on the RA receptors (RAR and RXR), the transcription factors that mediate RA's actions on the genome, and on proteins that bind RA or its precursor retinol (CRABPs and CRBPs)<sup>3-11</sup>. Recent studies suggest that aberrant expression of enzymes that regulate RA levels within target cells may also contribute to the disruption of RA's tumor suppressor functions in cancers of epithelial origin, including breast cancer<sup>12-17</sup>.

The requirement of epithelia for RA is thought to be met largely by RA generated in situ from micronutrient/prehormone retinol (vitamin A) delivered via the circulation from retinol that is stored in its esterified form in liver<sup>18</sup>. Both excess and deficiency of RA result in pathology<sup>19</sup>. Hence, the importance of enzymes that regulate RA levels in target tissues. These enzymes fall into three functional categories, ones that convert retinol to RA, ones responsible for sequestering excess retinol in its esterified form, and ones that metabolize excess RA<sup>20</sup>. Based on RA's putative function as a tumor suppressor, the expression of enzymes in some or all of these categories could be expected to be reduced or abrogated in the course of carcinogenesis. That this may be the case was first suggested by observations on breast cancer cell lines. Some transformed cell lines were reported to be deficient in the expression of the retinol storage enzymes lecitin:retinol-acyltransferase (LRAT) as well as in RA biosynthesis when compared to immortalized, non-transformed breast cancer cell lines<sup>12,13</sup>. Similar observations were made when the expression of one of the retinaldehyde dehydrogenases (RALDH6) was compared with that by immortalized non-transformed breast cell lines<sup>15</sup>. Very little is known, however, about which of the many enzymes implicated in the RA biosynthesis and metabolism RA are actually expressed in normal human mammary epithelium and about their status in breast cancer.

The notion that altered expression of enzymes that regulate RA biosynthesis and metabolism contribute to the disruption of its control over epithelial differentiation in neoplastic human breast parenchyma is supported by our recent studies of the expression of class I alcohol dehydrogenase (ADH) and the glucuronosyltransferase UGT2B7<sup>17,21</sup>. The link between class I ADH and RA homeostasis is its potential to catalyze the oxidation of retinol to retinal, the first and presumed rate-limiting step in RA biosynthesis. The link between UGT2B7 and RA homeostasis is its potential to glucuronidate RA. We identified both class I ADH and UGT2B7 in normal human mammary epithelium and, based on cytochemical and immunoblot analyses and enzyme assays, concluded that their expression was markedly reduced or abrogated in invasive cancers<sup>17,21</sup>.

The initial goals of the above two studies were unrelated to the potential role of these enzyme in RA biosynthesis. The aim of the study of class I ADH expression in human breast parenchyma was to determine whether and which of the medium chain alcohol dehydrogenases that can contribute to the oxidation of ethanol to acetaldehyde was expressed in the mammary epithelium. Oxidation of ethanol and detoxification of acetaldehyde can contribute to oxidative cellular and DNA damage and drain cellular antioxidant defenses. Hence, actions of enzymes such as class I ADH that can catalyze this reaction can contribute to carcinogenesis. The finding that the expression of class I ADH was virtually abrogated in invasive cancer was, therefore, unexpected<sup>21</sup>. It suggested that besides its role in oxidation of ethanol, class I ADH has some anti-carcinogenic, tumor suppressor function in the mammary epithelium. The one catalytic function of class I ADH that can be considered anti-carcinogenic is its potential to catalyze the oxidation of retinol to retinal.

Our interest in the expression of UGT2B7 in normal and neoplastic human breast parenchyma was in its potential to glucuronidate 4-hydroxyestrone and, thereby, prevent the oxidation of this catecholesterogen to its potentially mutagenic quinone metabolite. While this study was in progress, UGT2B7 was shown to have the potential to catalyze RA as well. This reaction too can be considered anti-carcinogenic since the product of the reaction, retinoid retinoyl- $\beta$ -glucuronide is a potent retinoid that, moreover, is less toxic than the parent compound (see in<sup>17</sup>). The finding that UGT2B7 was expressed in normal human mammary epithelium but not in invasive breast cancers was consistent with the enzyme's putative anti-carcinogenic, tumor suppressor functions, both via its effects on RA and on catecholesterogen homeostasis. This study, however, alerted us to a

seemingly paradoxical phenomenon, the presence in pre-invasive (*in situ*) cancers of UGT2B7 immunostaining that was often markedly higher than that in the normal mammary epithelium. We also noted that at sites of transition from *in situ* to invasive lesions, where the myoepithelial barrier surrounding *in situ* lesions was breached, were occupied predominantly by UGT2B7 immunonegative cancer cells. Together, these findings led us to suggest that the over-expression of UGT2B7 in cancer cells within *in situ* lesions reflects a defensive response<sup>17</sup>.

The present study was designed to test more directly the hypothesis that progression of breast cancer from the *in situ* to invasive stage has a divergent effect on genes encoding enzymes required for RA biosynthesis. To this end, we examined normal and neoplastic human breast parenchyma for the expression of retinaldehyde dehydrogenase 2 (RALDH2), the enzyme that catalyzes the second, final and irreversible step in RA biosynthesis. We chose RALDH2 for this study because of evidence that it has a particularly important gate-keeping function in RA biosynthesis<sup>19,22</sup>. Unlike class I ADH and UGT2B7 that are characterized by broad substrate specificity, RALDH has a high specificity for retinal<sup>23,24</sup>. During embryogenesis, a process in which RA plays a particularly critical role, expression of RALDH2 is under strict temporal and spatial control, and RALDH2 null mice do not survive<sup>22</sup>. The gene encoding the enzyme is also highly conserved across species (>96% homology between human, rat and mouse)<sup>25</sup>. Here we present immunocytochemical evidence that the expression of RALDH2 parallels that of UGT2B7. While RALDH2 immunostaining in cancer cells in invasive components of cancers was dramatically reduced or absent, it was markedly higher within *in situ* components of breast cancers than immunostaining in the normal mammary epithelium.

## **Materials and Methods**

### ***Breast Tissue.***

Normal and neoplastic breast parenchyma was obtained from a tissue bank containing fresh surgical specimens from patients with simple macromastia (normal) and breast cancer. The specimens used were processed by or under the supervision of one of the two investigators (J.W or D.S.). They were freed from excess fat cells by blunt dissection and by trimming with surgical scissors. Some portions were snap-frozen at -80°C and stored at -80°C, while others were fixed in 10% neutral buffered formalin from 12-24 hr and then

embedded in paraffin. Particular care was taken to minimize contamination with fat those specimens that were snap-frozen for future use in molecular biological or biochemical studies. Additional formalin-fixed paraffin embedded breast cancer specimens were obtained from the archives of the Armed Forces Institute of Pathology. All of the cancers were >1.5 cm in size. Authorization for the use of these tissues for research was obtained from the Review Board of the two institutions.

#### *Antibodies.*

The antibody was developed in a rabbit against recombinant mouse RALDH-2, a protein that is >95% homologous with human RLDH2<sup>26</sup>. The antibody was purified and characterized as described previously<sup>26</sup>. Briefly, it was preabsorbed with acetone powder from chicken liver, a tissue rich in aldehyde dehydrogenases except RALDH2. The antibody so purified was then shown to recognize as single band in isoelectric focusing (IEF) gels of protein from tissues from mouse and chicken embryos showing strong immunoreactivity with the antibody by immunocytochemistry. Bands dissected from such immunoblots were shown to have retinaldehyde dehydrogenase activity. The polyclonal antibody against  $\alpha$ -smooth actin was purchased from Dako (Carpenteria, CA)

#### *Immunocytochemistry.*

Immunocytochemistry was carried out on archival tissue from reduction mammoplasty surgical specimens (normal) from 14 patients with simple macromastia, and neoplastic tissue from mastectomy specimens from 26 patients with breast cancer. In two of the breast cancer cases, normal tissue from sites distant from the cancer were included in the study. The age of macromastia patients ranged from 16 to 54 years and that of the breast cancer patients from 25 to 76. Immunocytochemistry was carried out as described previously on 5  $\mu$ m sections cut from tissue that had been fixed in neutral buffered formalin and embedded in paraffin<sup>17</sup>. Briefly, the sections were placed on ProbeOn+ slides (Fisher Biotech, Atlanta, GA), dewaxed and re-hydrated in decreasing concentrations of ethanol and then subjected to low-temperature antigen retrieval. Endogenous alkaline phosphatase was inhibited by incubating the sections in 0.2 N HCl for 5 min. Nonspecific binding was blocked by incubating sections for 20 min at room temperature in 5% normal goat serum and 10% fetal bovine

serum in phosphate-buffered saline (PBS) containing 0.3% Triton X-100. This was followed by incubating the section overnight with the primary antibody in a humid chamber at 4°C and then with biotin conjugated goat-anti-rabbit secondary antibody (Promega, Madison, WI) in PBS for 1 hr at room temperature. The signal was amplified using Vectastain ABC reagent with alkaline phosphatase serving as the reporter and Vector Red™ as the chromogenic substrate (Vector, Burlingame, CA). The reaction was arrested by immersing the slides in distilled water, dehydrated in ethanol, cleared in xylene and mounted with Permount (Fisher Biotech, Atlanta, GA). One of two adjacent sections from each tissue block was counterstained with Meyer's hematoxylin. In order to identify sites where the myoepithelial/basement membrane barrier surrounding in situ lesion was breached, sections from an additional 10 breast cancer specimens were immunostained successively for  $\alpha$ -smooth actin, a marker for myoepithelial cells, and for RALDH2. In these experiments the protocol was modified as follows. In order to block both endogenous peroxidases and alkaline phosphatase, sections were exposed sequentially with fresh H<sub>2</sub>O<sub>2</sub>, and 0.2 N hydrochloric acid. Following completion of RALDH2 immunocytochemistry, the sections were incubated overnight with the  $\alpha$ -smooth actin antibody in a humid chamber at 4°C and then with biotin conjugated goat-anti-rabbit secondary antibody (Promega, Madison, WI) in phosphate buffered saline for 1 hr at room temperature. The signal was amplified using Vectastain ABC reagent with hydrogen peroxide serving as the reporter and Peroxidase Elite kit (Vector, Burlingame, CA) as the chromogenic substrate. Sections from normal and neoplastic breast tissue were included in each assay. Hematoxylin and eosin stained sections from each tissue block were used for histological analysis. Sections were examined and recorded using a Nikon Digital Camera DXM 1200 and Nikon, ACT1 software (version 2).

#### *Immunoblotting of Proteins separated by Agaros Isoelectric Focusing Gel*

RALDH proteins can not be effectively separated by conventional Western analysis because of the close similarity in their size. Therefore, to confirm the immunocytochemical findings, immunoblotting was carried out following IEF that effectively separates RALDHs based on differences in their isoelectric focusing point (pI). The analysis was carried out on protein obtained from 20  $\mu$ m cryosections that were collected in Eppendorf tubes cooled to -80°C on dry-ice (20 cryosections/tube) and then stored at -80°C until assayed. Using

cryosections greatly facilitates disrupting normal breast parenchyma that is highly collagenous and provides a high yield of protein. Cytosolic protein was obtained by probe sonication of sections for 60 seconds on ice in 10 mM phosphate buffer, pH 7.2 containing 1 mM phenylmethyl sulfonyl fluoride, 10 mg/ml aprotinin, 1mM leupeptin and 1 mM pepstatin. The homogenates were then subjected to freeze/thawing three times using liquid nitrogen and a 37°C water bath in order to promote further lysis. Large particles in the homogenates were sedimented by centrifugation at 16,000xg for 10 min at 4°C. Protein concentration in the supernatants was measured using the micro-BCA kit [Pierce, Rockford, IL].

From each specimen, 275 ng of protein was subjected to IEF using the Resolve system Cerebrospinal fluid test kit (E.G. and G. Wallace, FR-8030) with an agarose IEF gel of pH 3-10 range following the manufacturers directions. The IEF standards used were lactic dehydrogenase (pI 8.55), myoglobin (pI 7.16), beta-lactoglobulin (pI 5.13) and methyl red (pI 3.75). Following electrophoresis, the protein were transferred to a nitrocellulose membrane and visualized using Ponceau S. After recording the image, the nitrocellulose was washed in 0.1M phosphate buffer pH 7.2 over 30 minutes with three changes of buffer to remove the stain. The blot was blocked overnight in 0.1M phosphate buffer pH 7.2 with 20% calf serum, immunostained with antibody to RALDH2 and visualized using alkaline phosphatase conjugated second antibody with nitro blue tetrazolium/5-bromo-4-chloro-3-indolyl phosphate (NBT/BCIP) substrate<sup>26</sup>.

#### *Enzyme assay*

The potential of protein from normal and neoplastic breast parenchyma to catalyze the oxidation of retinal to RA was measured using a reporter assay<sup>27</sup>. This assay utilizes an F9-carcinoma cell line (Sil-15) transfected with plasmid containing the  $\beta$ -galactosidase gene under the control of the RA response element from RA receptor  $\beta$ . Protein for the assays was obtained from homogenates of 20  $\mu$ m cryosections as for IEF (see above). Three aliquots of 420 ng protein from each of the samples was incubated at 37°C with Sil-15 reporter cells grown to confluence in a 96 well plate in medium containing 10% fetal calf serum, 1 mM DTT, 1.2 mM NAD and 40 nM retinol. After an overnight incubation, the cells were fixed with 1% glutaraldehyde

and  $\beta$ -galactosidase induced by RA generated from retinol by the cells was quantified as a colorimetric reaction product in an ELISA plate reader. The values provide a relative measure of RALDH activity in samples processed in parallel. Although individual cells vary in their response to RA, the Elisa reading in an average of  $10^5$  cells is highly reproducible.

The values obtained for  $\beta$ -galactosidase activity were corrected for differences in cell density among tissue specimens using values obtained for nuclear cell area measured in representative cryosections by densitometric image analysis (see in<sup>17</sup>). The measurements were carried out on three cryosections stained with Meyers hematoxylin, one section each from the beginning, middle and end of the twenty 20  $\mu$ m sections used to obtain protein for the enzyme assays.

## **Results**

### *Immunocytochemistry of RALDH2: Normal Breast Parenchyma*

Immunoreactive RALDH was localized in the mammary epithelium in basal and luminal epithelial cells (Fig. 1). Intensity of immunostaining varied greatly among individuals. There were no consistent differences in immunostaining intensity between type 1, type 2 and type 3 lobules. In many specimens there was intense immunostaining associated with small blood vessels, sometimes surrounding weakly immunopositive lobules (Fig 1 B, C and D). There was also immunostaining associated with larger blood vessels (Fig. 1B, bv). The identity of occasional large immunopositive cells in the inter- and intralobular stroma in some specimens remains to be determined (1A-2). The size of these cells and their general appearance suggests that they may be macrophages.

### *Immunocytochemistry of RALDH2: Breast Cancer*

The pattern of RALDH2 immunostaining paralleled our previously reported observations on the pattern of UGT2B7 immunostaining. Advanced invasive cancers were essentially RALDH2 immunonegative (Fig. 2). In contrast, within in situ and intraductal cancers, RALDH2 immunostaining was intense (Fig. 3). Blood vessels associated with in situ lesions were also strongly immunopositive. However, we noted a few lesions with in situ



morphological characteristics that were occupied by cells with little or no RALDH2 immunostaining (4-E). Sites of transition from in situ to invasive lesions were largely occupied by essentially immunonegative cancer cells (Fig. 3-C, 3-G and Fig. 4-A and 4-B). Thus, the heterogeneity of immunostaining could be related to the presence in tissue sections of lesions at different stages in the progression of the disease (Fig. 4 B). According to this interpretation, cancer cells that over-express RALDH2 predominate at the in situ stage of the disease when the lesion is still confined within an intact myoepithelial barrier. The breakdown of this barrier allows for the emergence of cancer cells of the invasive immunophenotype that express little or no RALDH2. Experiments in which sections were immunostained for both RALDH2 and  $\alpha$ -smooth actin (Fig. 4-C to 4-F) support the notion that the low RALDH2 expressing invasive phenotype correlates with breaches in the myoepithelial layer. Circumscribed lesions of in situ phenotype that were occupied by immunonegative cancer cells were seen to be surrounded by at most fragments of  $\alpha$ -smooth actin (Fig. 4-E and 4-F).

#### *Immunoblotting of Proteins Separated by Agarose IEF Gel*

The presence of RALDH2 protein identified by immunocytochemistry was confirmed by immunoblotting of proteins separated based on differences in their pI. The pH range of 3-10 used encompasses the pI all RALDHs identified in vertebrates to date (range from pH4-pH9). There is as yet no detailed information on the characteristics of RALDH2(s) in humans. Hence, for interpreting results from these experiments we have to rely on information available on RALDH2s in experimental animals.

Immunoreactive bands from human breast parenchyma clustered between pH 5-6 that is characteristic of RALDH2. The multiplicity of bands suggests the presence of RALDH2 isoforms of the enzyme. There was no immunostaining of protein(s) in pH 8 range that is characteristic of RALDH3 (also referred to as RALDH6). The intensity of immunostaining ranged from strong to minimal. The large differences among tissue samples in the percent of the tissue occupied by immunoreactive cells and in cell density and heterogeneity of neoplastic lesions (see in<sup>17</sup> and Table 1) preclude any meaningful quantitative comparisons among samples. A band corresponding to pI of 5.13 was present in all samples, whether normal or neoplastic. A second band, corresponding to a pI of 5.0 was clearly seen in 11 of the 18 samples analyzed. Its intensity was highest in the

samples from a patients with cancer found by immunocytochemistry to be occupied by many intensely immunopositive in situ lesions. This intense band, corresponding to a pl of 5.0, was also seen in a sample of histologically normal tissue taken distant from the cancer from one of the patients and in one of the normal tissues from a patient with macromastia.

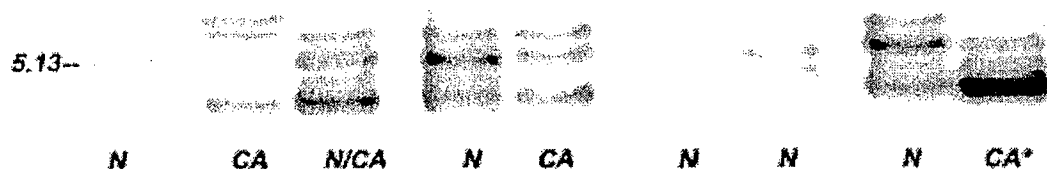


**Figure 5. RALDH2 immunoblots of homogenates of normal (N) and neoplastic (CA) human breast parenchyma following separation of the proteins by isoelectric focusing.** Tissue homogenates were prepared and isoelectric focusing carried out as described in "Methods". 5.13 corresponds to the localization of  $\alpha$ -lactalbumin marker (pl of 5.13). N= normal tissue from reduction mammoplasty: N/CA=histologically normal tissue from a patient with breast cancer taken from a site distant from the cancer: CA\*=tissue neoplastic tissue from a patient with multiple in situ lesions of the comedo that stained intensely for RALDH2.

#### *Retinol Dehydrogenase Activity*

The assays were carried out on disrupted cryosections. This facilitates disrupting the collagenous normal breast parenchyma and provides a means to estimating cell density in the tissue samples by measuring nuclear area in representative section by densitometric image analysis. In tissue from four normal (reduction mammoplasty) surgical specimens, the percent of the specimen assayed that was occupied by nuclei ranged from 1.4 to 7.5% and that from the cancers from 7.18 to 45%. Corrected for cellularity, enzyme activity in the four non-neoplastic samples ranged from 0.59 to 12.2. This large difference is consistent with the inter-individual differences in the intensity of RALDH2 immunostaining identified by immunocytochemistry. Retinal dehydrogenase activity of neoplastic specimens, corrected for nuclear area, ranged from .07-7.2. The highest

activity (7.18) was associated with tissue from a patient with extensive, intensely RALDH2 immunopositive in situ lesions, while the lowest activities (0.07 and 0.20) with tissue from two advanced, highly invasive cancers that were essentially immunonegative.

Normal			Cancer			
Subject	RALDH Activity*	Nuclear Area (%)	Subject	RALDH Activity	*Nuclear Area (%)	Pathology
1	0.69	7.50	1	0.07	12.80	Advanced Invasive
2	2.21	1.65	2	0.20	45.00	Advanced Invasive
3	2.51	1.40	3	2.89	19.20	Invasive + Normal (Approx. 1:1)
4	12.20	7.10	4	7.20	7.18	<u>In situ</u> (comedo) prominent

**Table 1. Retinol dehydrogenase activity of normal and neoplastic breast parenchyma.** Enzyme activity was measured in triplicates samples by a reporter assay in cytosolic fraction prepared from homogenates of cryosections as described under "Methods". Percent area occupied by hematoxylin stained cell nuclei in three representative sections from each specimen was measured by densitometric image analysis. The values obtained for nuclear area were then used to correct for differences in cellularity among specimens. \*  $\beta$  galactosidase activity expressed as colorimetric reading in an ELISA plate reader and corrected for percent nuclear area.

### Discussion

That tumor suppressor functions of RA may be compromised in breast cancer, in part, because a lack of or low level of expression of some of the enzymes required for RA biosynthesis was first suggested by findings from studies of breast cancer cells lines in vitro<sup>12,15</sup>. These include the observation by Rexer et al., that MTSV-1.7, an immortalized non-transformed cell line, but not the MCF-7 transformed cells express RALDH6 and convert retinal to RA<sup>15</sup>. Findings from studies of the expression of RALDH2 in normal and neoplastic human breast parenchyma reported here, together with our previously reported findings on the expression of UGT2B7 in the

two types of lesions<sup>17</sup>, reveal a more complex story. They show that while a lack of or low level of expression of enzymes tissue levels of RA is a characteristic of invasive components of breast cancers, the expression of these same enzymes within in situ lesions is typically greatly increased. A similar divergent effect of cancer progression on some other gene products important for RA homeostasis is suggested by studies by others. Using in situ hybridization, Lawrence et al, identified an increase in RXR mRNA in ductal carcinomas in situ (DCIS) as compared to normal mammary epithelium<sup>8</sup>. Also, when protein expression profiles of normal terminal lobular ductal units and in situ breast cancers were compared, CRABP2 was among the proteins found to be increased in DCIS<sup>28</sup>. Interestingly, this finding parallels an observation made over two decades ago by Kunge et al<sup>29</sup>. These investigators, using a multiphasic polyacrylamide disc gel electrophoresis, reported finding elevated cellular RA binding activity in dysplastic and preneoplastic breast lesions.

A decrease or lack of expression of genes required for RA biosynthesis and action in invasive components of breast cancers is consistent with retinoids many tumor suppressor functions. However, the marked *increase* in their expression within in situ lesions can not be readily reconciled with retinoids' role in tumor suppression. It is noteworthy that some of the most intense immunostaining for RALDH2, as for UGT2B7<sup>17</sup>, was seen in comedo carcinomas, lesions associated with particularly poor prognosis (see in<sup>30</sup>. Similarly, Lawrence e. al., noted the greatest increases in RXR mRNA in comedo carcinomas<sup>8</sup>. Hence, the difference in RALDH2 protein between in situ and invasive breast cancer can not be attributed simply to a progressive loss of expression of RALDH2 with acquisition of a more aggressive phenotype. Rather, it suggests some fundamental phenotypic differences between cancer cells within in situ and invasive lesions that may depend on the differences in the microenvironment in the two types of lesions.

The importance of the microenvironment as a determinant of differentiation of both normal and neoplastic epithelial cells has been demonstrated in a number of experimental settings. In situ lesions are defined by an intact myoepithelial/basement membrane layer, and a loss of integrity of this layer is the sine qua non of invasiveness. There is growing evidence that the myoepithelial/basement membrane layer provides not only a physical but also a biochemical barrier that limits the access of endo- and xenobiotics to the mammary epithelium. Hence, its integrity is likely to be critical for maintaining differences between the microenvironment

of the mammary epithelium and surrounding stroma. In our studies, the relationship between an intact myoepithelial layer and immunophenotype of cancer cells was evident in tissue sections immunoreacted for both RALDH2 and  $\alpha$ -smooth actin. Together, these considerations lead us to postulate that within microenvironment maintained by the myoepithelial/basement membrane barrier, cancer cells are driven towards differentiation, and that breakdown of this barrier allows cancer cells of a less differentiated phenotype to proliferate and invade the surrounding stroma. The increased expression of genes that serve to maintain local levels of RA could then be one of the driving forces toward differentiation in the in situ cancers.

The notion that the differences in immunophenotype of cancer cells within in situ and invasive lesions reflects a difference in their state of differentiation, and that this is related to the integrity of the myoepithelial barrier, is supported by observations of the expression of certain other presumptive markers of differentiation. Man et al. have presented compelling immunocytochemical evidence that cancer cells within in situ lesions are overwhelmingly ER  $\alpha$  positive, while those at sites of invasion are overwhelmingly ER $\alpha$  negative<sup>31</sup>. These findings parallel our immunocytochemical findings on the expression in breast cancers of P450 aromatase, the key enzyme in estrogen biosynthesis, as well as P4501B1 and P4503A4 that are estrogen-4- and estrogen-2-hydroxylases, respectively (Weisz et al. unpublished). Evidence, as yet more limited, indicates that the two populations of cancer cells differ also in their genotype. ER $\alpha$  positive and ER $\alpha$  negative breast cancer cells isolated from the same duct were shown to differ in the frequency and pattern of loss of heterozygosity and microosomal instability at 10 of 15 DNA markers examined<sup>31</sup>.

In as much as differentiation limits the number of replications that cells may undergo before senescence, the drive for differentiation on cancer cells within in situ lesions can be interpreted as a *defensive* response. Conversely, the less differentiated cancer cells that can evolve once the myoepithelial/basement membrane barrier is compromised would be expected to have a greater replicative potential. This prediction is borne out by finding of Man et al. of an inverse relationship between expression of ER $\alpha$  and Ki67 within in situ and microinvasive lesions<sup>31</sup>.

According to the above hypothesis, expression of RA receptor(s) would be expected to be associated with the differentiated in situ phenotype, and a lack of RA receptor(s) expression with the undifferentiated, invasive phenotype. Whether this is the case can not be deduced from reported cytochemical studies of RA receptors in breast cancer since the findings were presented as % of cells immunopositive for a particular receptor and % of tissue samples with significant numbers of such cells. Hence, the need to re-examine breast cancers for RA receptors from the perspective of how their expression correlates with markers of invasive and in situ phenotype. The contrast between the in situ and the invasive phenotype in our study was most striking in tissue sections from cancers that encompassed both types of lesions. With the large and growing number of breast cancer patients in whom the diagnosis is made at a relatively early stage of the disease, such heterogeneous sections are becoming the norm. They offer a unique opportunity to characterize changes in pheno- and genotype of cancer cells in lesions that represent stages in the progression of the disease from its in situ to invasive stage.

A critical question is whether over-expression of RALDH2 and UGT2B7 in pre-invasive lesions does, in fact, results in elevated levels of RA and its potent metabolite, retinoyl- $\beta$ -glucuronide. The effect of an increase in rate of RA biosynthesis could be negated if it results in induction, for example, of CYP26 that catalyzes the oxidation of RA. There are no assays currently available sensitive enough to determine concentration of RA or its glucuronidated metabolite in discrete, cytochemically characterized cell populations isolated from breast cancers. The question could, however, be addressed indirectly by assessing the level of expression of RA inducible genes in the two types of lesions. This is of importance because of the potential detrimental effects of excess RA and because of an interest in using retinoids in chemoprevention. Although toxicity of excess RA has long been recognized, very little is known about mechanisms underlying this phenomenon. Some of the consequences of excess RA identified could be pro-carcinogenic. For example, inappropriate induction of n-glycine-methyltransferase by RA<sup>32</sup> could lead to aberrant gene expression by creating or contributing to a state of hypomethylation DNA<sup>33</sup>. The potential of RA at high concentrations to promote the breakdown of RA receptors  $\alpha$  and  $\gamma$ , at least in vitro, in MCF-7 human breast cancer cells<sup>34</sup>, suggests a further mechanism by which overproduction of

RA could contribute to carcinogenesis, Together, these observations point to the importance of a need to understand mechanisms associated not only with RA deficiency but also RA excess.

The finding of elevated RA in pre-invasive lesions could explain some of the disappointing and even adverse results from clinical trials using RA agonists as chemopreventive agents in subjects at high risk for some solid tumors, including breast cancer<sup>2</sup>. If, as our data suggests, RA may already be produced in excess in pre-invasive lesions, exogenous RA or its agonists would not be expected to have a beneficial effect on cancer cells within in situ lesions. On the other hand, cancer cells of the undifferentiated, invasive phenotype would not be expected to respond to retinoids if they do not express the relevant RA receptors. There is a clear need to characterize the phenotypically and genotypically diverse populations of neoplastic cells present in cancers and at different stages in the progression of the disease, in order to identify appropriate molecular, stage-specific targets for intervention. Techniques already exist, and additional ones are being developed, for characterizing discrete cell populations within a cancer, for establishing their topography and their relationship to each other. These techniques can also help identify factors in the microenvironment that may be important for driving or sustaining the diversity. Mathematical models have been developed to characterize population diversity in other system and to predict the consequences of interventions. Intriguing results have been obtained when one such analytical tool, metapopulation analysis, was applied to examine genotypic diversity in advanced colon cancer specimens and phenotypic diversity during stages in the development of estrogen-induced renal cancers in hamsters<sup>35,36</sup>. The findings from these studies suggest that diversity in cancers is not random and that interactions between cell populations may determine, drive and sustain the diversity. The success of early detection of breast cancer has led to an exponential increase in the proportion of patients in whom the disease is identified at the pre-invasive and early invasive stages of the disease<sup>37</sup>. Those diagnosed with in situ disease are estimated to account now for one in five breast cancer cases. There is an urgent need to apply such methodologies to characterize the genotypic and phenotypic diversity present in pre-invasive and early invasive cancers in order to identify appropriate molecular targets for intervention in such cases.

#### REFERENCES



1. Hansen LA, Sigman CC, Andreola F, Ross SA, Kelloff GJ, De Luca LM: Retinoids in chemoprevention and differentiation therapy. *Carcinogenesis* 2000, 21:1271-1279
2. Freemantle SJ, Spinella MJ, Dmitrovsky E: Retinoids in cancer therapy and chemoprevention: promise meets resistance. *Oncogene* 2003, 22:7305-7315
3. Roman SD, Clarke CL, Hall RE, Alexander IE, Sutherland RL: Expression and regulation of retinoic acid receptors in human breast cancer cells. *Cancer Res* 1992, 52:2236-2242
4. van der Burg B, van der Leede BM, Kwakkenbos-Isbrucker L, Salverda S, de Laat SW, van der Saag PT: Retinoic acid resistance of estradiol-independent breast cancer cells coincides with diminished retinoic acid receptor function. *Mol Cell Endocrinol* 1993, 91:149-157
5. Jing Y, Zhang J, Bleiweiss IJ, Waxman S, Zelent A, Mira YLR: Defective expression of cellular retinol binding protein type I and retinoic acid receptors alpha2, beta2, and gamma2 in human breast cancer cells. *Faseb J* 1996, 10:1064-1070
6. van der Leede BM, Geertzema J, Vroom TM, Decimo D, Lutz Y, van der Saag PT, van der Burg B: Immunohistochemical analysis of retinoic acid receptor-alpha in human breast tumors: retinoic acid receptor-alpha expression correlates with proliferative activity. *Am J Pathol* 1996, 148:1905-1914
7. Xu XC, Sneige N, Liu X, Nandagiri R, Lee JJ, Lukmanji F, Hortobagyi G, Lippman SM, Dhingra K, Lotan R: Progressive decrease in nuclear retinoic acid receptor beta messenger RNA level during breast carcinogenesis. *Cancer Res* 1997, 57:4992-4996
8. Lawrence JA, Merino MJ, Simpson JF, Manrow RE, Page DL, Steeg PS: A high-risk lesion for invasive breast cancer, ductal carcinoma in situ, exhibits frequent overexpression of retinoid X receptor. *Cancer Epidemiol Biomarkers Prev* 1998, 7:29-35
9. Sommer KM, Chen LI, Treuting PM, Smith LT, Swisshelm K: Elevated retinoic acid receptor beta(4) protein in human breast tumor cells with nuclear and cytoplasmic localization. *Proc Natl Acad Sci U S A* 1999, 96:8651-8656
10. Yang Q, Sakurai T, Kakudo K: Retinoid, retinoic acid receptor beta and breast cancer. *Breast Cancer Res Treat* 2002, 76:167-173
11. Paik J, Blaner WS, Sommer KM, Moe R, Swisshelm K: Retinoids, retinoic acid receptors, and breast cancer. *Cancer Invest* 2003, 21:304-312
12. Chen AC, Guo X, Derguini F, Gudas LJ: Human breast cancer cells and normal mammary epithelial cells: retinol metabolism and growth inhibition by the retinol metabolite 4-oxoretinol. *Cancer Res* 1997, 57:4642-4651
13. Guo X, Ruiz A, Rando RR, Bok D, Gudas LJ: Esterification of all-trans-retinol in normal human epithelial cell strains and carcinoma lines from oral cavity, skin and breast: reduced expression of lecithin:retinol acyltransferase in carcinoma lines. *Carcinogenesis* 2000, 21:1925-1933.
14. Mira YLR, Zheng WL, Kuppumbatti YS, Rexer B, Jing Y, Ong DE: Retinol conversion to retinoic acid is impaired in breast cancer cell lines relative to normal cells. *J Cell Physiol* 2000, 185:302-309
15. Rexer BN, Zheng WL, Ong DE: Retinoic acid biosynthesis by normal human breast epithelium is via aldehyde dehydrogenase 6, absent in MCF-7 cells. *Cancer Res* 2001, 61:7065-7070
16. Guo X, Knudsen BS, Peehl DM, Ruiz A, Bok D, Rando RR, Rhim JS, Nanus DM, Gudas LJ: Retinol metabolism and lecithin:retinol acyltransferase levels are reduced in cultured human prostate cancer cells and tissue specimens. *Cancer Res* 2002, 62:1654-1661
17. Gestl SA, Green MD, Shearer DA, Frauenhoffer E, Tephly TR, Weisz J: Expression of UGT2B7, a UDP-glucuronosyltransferase implicated in the metabolism of 4-hydroxyestrone and all-trans retinoic acid, in normal human breast parenchyma and in invasive and in situ breast cancers. *Am J Pathol* 2002, 160:1467-1479
18. Kurlandsky SB, Gamble MV, Ramakrishnan R, Blaner WS: Plasma delivery of retinoic acid to tissues in the rat. *J Biol Chem* 1995, 270:17850-17857
19. McCaffery PJ, Adams J, Maden M, Rosa-Molinari E: Too much of a good thing: retinoic acid as an endogenous regulator of neural differentiation and exogenous teratogen. *Eur J Neurosci* 2003, 18:457-472

20. Ross AC, Zolfaghari R, Weisz J: Vitamin A: recent advances in the biotransformation, transport, and metabolism of retinoids. *Curr Opin Gastroenterol* 2001, 17:184-192.
21. Triano EA, Slusher LB, Atkins TA, Beneski JT, Gestl SA, Zolfaghari R, Polavarapu R, Fraumenhoffer E, Weisz J: Class I alcohol dehydrogenase is highly expressed in normal human mammary epithelium but not in invasive breast cancer: implications for breast carcinogenesis. *Cancer Res* 2003, 63:3092-3100
22. Duester G: Genetic dissection of retinoid dehydrogenases. *Chem Biol Interact* 2001, 130-132:469-480
23. Zhao D, McCaffery P, Ivins KJ, Neve RL, Hogan P, Chin WW, Drager UC: Molecular identification of a major retinoic-acid-synthesizing enzyme, a retinaldehyde-specific dehydrogenase. *Eur J Biochem* 1996, 240:15-22
24. Gagnon I, Duester G, Bhat PV: Kinetic analysis of mouse retinal dehydrogenase type-2 (RALDH2) for retinal substrates. *Biochim Biophys Acta* 2002, 1596:156-162
25. Duester G: Families of retinoid dehydrogenases regulating vitamin A function: production of visual pigment and retinoic acid. *Eur J Biochem* 2000, 267:4315-4324
26. Berggren K, McCaffery P, Drager U, Forehand CJ: Differential distribution of retinoic acid synthesis in the chicken embryo as determined by immunolocalization of the retinoic acid synthetic enzyme, RALDH-2. *Dev Biol* 1999, 210:288-304
27. McCaffery P, Drager UC: A sensitive bioassay for enzymes that synthesize retinoic acid. *Brain Res Brain Res Protoc* 1997, 1:232-236
28. Wulfschuhle JD, Sgroi DC, Krutzsch H, McLean K, McGarvey K, Knowlton M, Chen S, Shu H, Sahin A, Kurek R, Wallwiener D, Merino MJ, Petricoin EF, 3rd, Zhao Y, Steeg PS: Proteomics of human breast ductal carcinoma in situ. *Cancer Res* 2002, 62:6740-6749
29. Kung WM, Geyer E, Eppenberger U, Huber PR: Quantitative estimation of cellular retinoic acid-binding protein activity in normal, dysplastic, and neoplastic human breast tissue. *Cancer Res* 1980, 40:4265-4269
30. Ottesen GL, Graversen HP, Blichert-Toft M, Christensen IJ, Andersen JA: Carcinoma in situ of the female breast. 10 year follow-up results of a prospective nationwide study. *Breast Cancer Res Treat* 2000, 62:197-210.
31. Man YG, Tai L, Barner R, Vang R, Saenger JS, Shekitka KM, Bratthauer GL, Wheeler DT, Liang CY, Vinh TN, Strauss BL: Cell clusters overlying focally disrupted mammary myoepithelial cell layers and adjacent cells within the same duct display different immunohistochemical and genetic features: implications for tumor progression and invasion. *Breast Cancer Res* 2003, 5:R231-241
32. Rowling MJ, McMullen MH, Schalinske KL: Vitamin A and its derivatives induce hepatic glycine N-methyltransferase and hypomethylation of DNA in rats. *J Nutr* 2002, 132:365-369
33. Dunn BK: Hypomethylation: one side of a larger picture. *Ann N Y Acad Sci* 2003, 983:28-42
34. Tanaka T, Rodriguez de la Concepcion ML, De Luca LM: Involvement of all-trans-retinoic acid in the breakdown of retinoic acid receptors alpha and gamma through proteasomes in MCF-7 human breast cancer cells. *Biochem Pharmacol* 2001, 61:1347-1355
35. Gonzalez-Garcia I, Sole RV, Costa J: Metapopulation dynamics and spatial heterogeneity in cancer. *Proc Natl Acad Sci U S A* 2002, 99:13085-13089
36. Toubreau G, Nonclercq D, Laurent G, Brohee R, Zanen J, Van Cauwenberge A, Alexandre H, Falmagne P, Heuson-Stiennon JA: Immunohistochemical analysis of diethylstilbestrol-induced renal tumors in adult male Syrian hamsters: evidence for relationship to peripheral nerve sheath tumors. *Histochem Cell Biol* 2001, 115:429-438
37. Skinner KA, Silverstein MJ: The management of ductal carcinoma in situ of the breast. *Endocr Relat Cancer* 2001, 8:33-45

## **cDNA expression profiling identifies elevated expressions of tumor progression and invasion related genes in cell clusters of in situ breast tumors**

Yan-gao Man, Yi Zhang<sup>1</sup>, Ting Shen<sup>2</sup>, Tuyethoa N.Vinh, Xiao Zeng<sup>1</sup>, Jordi Tauler<sup>3</sup>, James L. Mulshine<sup>3</sup>, Brian L. Strauss.

Department of Gynecologic and Breast Pathology, Armed Forces Institute of Pathology and American Registry of Pathology, Washington DC; <sup>1</sup>SuperArray Bioscience Corporation, Frederick, MD, <sup>2</sup>Quest Diagnostics, Inc, Teterboro, NJ, <sup>3</sup>Intervention Section, Cell and Cancer Biology Branch, NCI, NIH, Bethesda, MD

### E-mail address of the authors:

Dr. Man: [man@afip.osd.mil](mailto:man@afip.osd.mil)

Yi Zhang: [yzhang@superarray.net](mailto:yzhang@superarray.net)

Dr. Shen: [Ting.X.Shen@questdiagnostics.com](mailto:Ting.X.Shen@questdiagnostics.com)

Dr. Vinh: [Vinh@afip.osd.mil](mailto:Vinh@afip.osd.mil)

Dr. Zeng: [xzeng@superarray.net](mailto:xzeng@superarray.net)

Dr. Tauler: [taulerj@mail.nih.gov](mailto:taulerj@mail.nih.gov)

Dr. Mulshine: [mulshinej@bprb.nci.nih.gov](mailto:mulshinej@bprb.nci.nih.gov)

Dr. Strauss: [Strauss@afip.osd.mil](mailto:Strauss@afip.osd.mil)

### Address of corresponding author:

Yan-gao Man, MD., PhD

Department of Gynecologic & Breast Pathology

The Armed Forces Institute of Pathology and American Registry of Pathology

6825 16<sup>th</sup> Street, NW

Washington, DC 20306-6000

Phone: 202-782-1612

Fax: 202-782-3939

E-mail: [man@afip.osd.mil](mailto:man@afip.osd.mil)

The opinions and assertions contained herein are the private viewpoints of the authors and do not reflect the official views of the Department of Defense or Department of the Army

## Abstract

**Background:** Our previous studies revealed that a subset of estrogen receptor (ER) positive mammary ductal carcinoma in situ (DCIS) contained focally disrupted myoepithelial (ME) cell layers that were preferentially overlain by ER negative cell clusters, which showed a substantially higher rate of loss of heterozygosity and cell proliferation than their adjacent ER positive counterparts within the same duct. This study attempted to assess whether these cells also had a different profile of mRNA expression in tumor progression and invasion related genes.

**Design:** Consecutive sections were prepared from frozen tissues of 30 DCIS with focally disrupted ME cell layers. Sections 1, 10, and 20 from each case were double immunostained to elucidate ME layer disruptions and overlying ER negative cells, while remaining sections were used for microdissection of ER negative and positive cells within the same duct. Microdissected cells were subjected to RNA extraction and amplification. Amplified RNA was converted to biotin-labeled cDNAs, which were interrogated with "Cancer PathwayFinder" arrays.

**Results:** A total of 15 genes were found differentially expressed, and of which, 11 (73.3%) were seen predominantly in ER negative cells, 2 (13.3%) were mainly in ER positive cells, and 2 (13.3%) were equally expressed in ER negative and positive cells. The difference in mRNA expression frequencies between negative and positive cells was statistically significant ( $p < 0.01$ ). Of the 11 up-regulated genes in ER negative cells, 6 are involved in apoptosis and cell cycle control, 2 in cell adhesion, one in signal transduction, one in angiogenesis, and one in invasion and metastasis.

**Conclusion:** ER negative cells showed a substantially higher frequency and level of mRNA expression for multiple tumor progression and invasion related genes than their adjacent ER positive counterparts, suggesting that they are biologically more aggressive and some of which might represent the precursor of invasive lesions.

**Key words:** Ductal carcinoma *in situ*; Tumor progression and invasion; Myoepithelial cell layer; cDNA microarray; Marker genes; mRNA expression.

### Introduction

The epithelial component of normal and non-invasive human breast tissues is physically separated from the stroma by both the myoepithelial (ME) cell layer and basement membrane. ME cells are joined by intercellular junctions and adhesion molecules, forming a continuous sheet or belt that encircles the epithelial cells (1-3). The basement membrane is composed of a group of fibrous proteins embedded in a hydrated polysaccharide gel, constituting a continuous lining surrounding and attaching to basal cells via hemidesmosomes and focal adhesion complexes (4-6). Both the ME cell layer and basement membrane are permanent normal structural constituents, which normally only allow the exchange of water, oxygen, and other small molecules between the epithelial and stromal components (1-6). Due to the interposition of the ME cell layer and basement membrane between the stroma and epithelium, tumor cells must first force through the ME cell layer followed by the basement membrane in order to physically reach the stroma. In other words, the disruption of both the ME cell layer and basement membrane is an absolute pre-requisite for tumor invasion and metastasis.

As invasive and metastasized tumors account for a vast majority of breast cancer related-deaths (7), the identification of the mechanism(s) of tumor invasion and the precursor of the invasive lesions are expected to lead to more effective therapeutic approaches to reduce breast cancer mortality. The generally accepted hypothesis for the cause of basement membrane disruptions and tumor invasion has been attributed primarily, if not solely, to an over-production of proteolytic enzymes by the tumor and stromal cells (8-9). This hypothesis alone, however, appears to not reflect the intrinsic mechanism of these events for three main reasons: [1] neither the normal cellular kinetics nor the dynamic alterations

of ME cells during tumor invasion have been elucidated; [2] the ME cell layer is a normal structural constituent, which should not be target of the host's own enzymes, and [3] although results from in vitro tests and animal models have well documented that proteolytic inhibitors could effectively inhibit and prevent tumor invasion, results from all proteolytic inhibitors based human clinical trials have been very disappointing (10-11).

While attempting to identify the early sign of ME layer disruptions and precursor of invasive breast lesions, we have recently carried out a number of studies, focusing on the correlation between the structural integrity in ME cell layers and the immunohistochemical and genetic profiles in adjacent epithelial cells. In 5,698 duct cross sections from 220 patients with estrogen receptor (ER) positive, non-invasive breast tumors, we detected a total of 405 focal ME cell layer disruptions, defined as the absence of ME cells resulting in a gap equal to or greater than the combined size of 3 ME or epithelial cells (12). Of these disruptions, 350 (86.4%) were overlaid by clusters of cells with no or substantially reduced ER expression, in a sharp contrast to their adjacent cells within the same duct, which showed uniform and strong ER immunoreactivity and overlaid a non-disrupted ME cell layer (12). Compared to their adjacent ER positive counterparts within the same duct, microdissected ER negative cells had a substantially higher frequency and different pattern of loss of heterozygosity at multiple chromosomal loci, including those harboring tumor suppressor genes fragile histidine triad (FHIT) and Wilms' tumor 1 (WT-1) (12-13). Cells in ducts with these clusters also showed a significantly higher ( $p < 0.01$ ) proliferation rate, 18.2% versus 3.6% and 19.9% versus 4.4%, compared to cells in morphologically comparable ducts without ME cell layer disruptions, assessed by immunohistochemical staining for Ki-67 in three separate studies (14-16).

As it has been well documented [1] breast tumor progression is paralleled by a progressively hormonal independence (17-18), [2] ER negative tumors have a substantially worse prognosis than ER

positive tumors (19-20), [3] a deregulated cell proliferation is a direct cause of malignancies (21-22), the current study attempted to test a hypothesis that these ER negative cell clusters might represent a biologically more aggressive clone and some of these might be the direct precursor of invasive lesions. Consequently, these ER negative cell clusters might have a substantially different expression profile for tumor progression and invasion related genes, compared to their adjacent ER positive counterparts within the same duct. The specific goal of this study was to identify the potential "signature" gene(s) exclusively or preferentially expressed in these ER negative cell clusters that could be utilized for the development of therapeutic agents for early detection, treatment, and prevention of breast tumors.

## **Materials and Methods**

### **Case selection and immunohistochemical staining**

A set of 5-7 consecutive sections at 5-7 $\mu$ m thickness was prepared from each of 200 frozen breast tissue samples selected from our tissue bank. The first and last sections from each case were stained with hematoxylin and eosin (H & E) for morphologically classification based on our published criteria (23). A total of 130 cases were found to contain multiple (> 3) clusters of DCIS, and were consequently selected for immunohistochemical assessment. The sections were fixed in 100% ethanol for 10 minutes at room temperature, washed in 1X TBS (pH 7.4) three times, each for 10 minutes, and incubated with normal goat serum (diluted 1 in 5 with TBS) for 10 minutes at room temperature. The sections were then incubated with a monoclonal antibody to ER (NCL-ER-6F11, Vector, Burlingame, CA) for 1-2 hours at room temperature. After the incubation, sections were washed in TBS, and the antigen-antibody complex was detected with the ABC method, using a DAB substrate kit with nickel solution (Vector, Burlingame, CA), as previously described (24). After the substrate reaction, sections were washed in tap water, incubated in 80 °C TBS for 5-10 minutes to inactivate the potential enzyme



residues, followed by 3 washes in TBS at room temperature, each for 3-5 minutes. Sections were incubated with a monoclonal antibody to smooth muscle actin (SMA, NCL-SMA, Burlingame, CA) for 60 minutes at room temperature. The antigen-antibody complex was detected with the ABC method, using an AP-red substrate kit (Zymed, San Francisco, CA). Sections were counterstained with hematoxylin, mounted with 3% gelatin, and examined under a microscope to identify the cases that contained focally disrupted ME cell layers and associated ER negative cell clusters, as previously described (12). A total of 30 such cases with large (>15 cells) ER negative cell clusters were selected for further analyses. Of these cases, 11 were collected four years ago, and 19 were recently collected (no more than 12 months). To assess the histological origin of these ER negative cell clusters, a set of 2 adjacent sections from each case were immunostained for both epithelial and stromal phenotypic markers, with monoclonal antibodies to epithelial specific antigen (ESA) and vimentin (Vector, Burlingame, CA), respectively.

### **Microdissection of ER positive and negative cells for RNA extraction**

For each selected tissue block, 20 consecutive sections at 10-12  $\mu\text{m}$  thickness were made, sequentially placed on positively charged microscopic slides, and stored in a  $-80^{\circ}\text{C}$  freezer. To prevent carryover, which may interfere with the molecular biologic assays, a new blade was used for each tissue block. Sections 1, 10, and 20 from each case were double immunostained for ER and SMA, as described above. The ER negative cell clusters overlying focally disrupted ME cell layers were first identified in immunostained sections, which were used as guides to locate the same lesions in adjacent sections. Adjacent sections were washed in TBS in ice three times, each for 3-5 minutes, and briefly stained in an ice-cooled hematoxylin solution, followed by three washes in TBS in ice, each for 2-3 minutes. To prevent RNA degradation and facilitate the collection of microdissected cells,

only 3-4 sections were processed each time, and sections were soaked in ice-cooled TBS solution containing RNase inhibitors and 20% glycerin. Microdissection was carried out under a standard microscope using 30 G needles. The unwanted tissues surrounding the duct of interest were carefully scraped and washed off with the needle and TBS first, leaving the duct untouched. Then, ER positive cells (which usually account for a vast majority of the total cells) were carefully collected, leaving ER negative cells untouched. After the collection of ER positive cells, the slide was carefully examined first under a 4X objective and then under a 20X objective, to completely remove all unwanted cells and debris. Then, ER negative cells were carefully scraped off with a new needle or blade. Microdissected ER positive and negative cells were separately placed into two different micro-centrifuge tubes with the same RNA extraction buffer (Arcturus Bioscience, Inc, Mountain View, CA). The cells collected from different sections were pooled, based on their ER expression status. To ensure the comparison was carried out under the same conditions, the number of microdissected ER positive and ER negative cells in each case was very similar, and dissected cells were treated under the same condition during the entire process. Overall, 30 pools of ER positive and 30 pools of ER negative cells were collected and the samples were paired based on the origin, i.e., the cells from the same duct were in the same pair for subsequent tests.

#### **RNA extraction, amplification, and aRNA labeling**

The PicoPure™ RNA Isolation Kit from Arcturus Bioscience, Inc (Mountain View, CA) was used for the mRNA extraction from microdissected cells, according to the protocol provided by the manufacturer. The extracted mRNA was linearly amplified using RiboAmp® OA 1 Round RNA Amplification Kits (Arcturus Bioscience, Inc, Mountain View, CA). The amplified antisense RNA

(aRNA) products from different samples were converted to biotin-labeled cDNA, using the AmpoLabeling kit from the SuperArray Bioscience Corporation (Frederick, MD).

### **cDNA microarray gene expression profiling and data analysis**

To concentrate our effort on the genes known to be involved in tumor progression and invasion, the Cancer PathwayFinder GEMArray (SuperArray Bioscience Corporation, Frederick, MD), a focused cDNA microarray with the sequences of 96 genes that control cell cycle, apoptosis, adhesion, growth factor signaling, angiogenesis, and metastasis was used. Labeled cDNAs were hybridized to the array and processed according to the instruction by the manufacturer (SuperArray Bioscience Corporation, Frederick, MD). Chemiluminescent array images were captured and digitized using the FluorChem 8800 Imaging System (Alpha Innotech, San Leandro, CA). Each pair (ER positive and ER negative samples from the same duct) of the datasets was exported to GEMArrayAnalyzer, a software developed by SuperArray. For each gene spotted on the array, if the integrated density value (IDV) was equal to or greater than the 1.5x of the median IDV of the array, the expression of the gene was considered "present"; otherwise, this gene was considered "absent" in the sample. While comparing the relative expression level of the same gene between two samples of the same pair the minimum IDV was used for background subtraction, and subsequently the median value was used for normalization. The expression level of a given gene was considered higher in one sample only if 1> this gene is "present" in the sample and 2> the normalized IDV of this gene is equal or greater than 1.2 fold that of its counterpart on the pairing array. A gene is considered equally expressed in both samples only when 1> this gene is "present in both samples, and 2> the normalized IDV of this gene is between (not including) 0.8 to 1.2 fold that of its counterpart on the pairing array.

## **Identification of signification genes for ER negative cells and verification of the results**

After the analysis, the top up-regulated genes identified in ER negative cells were selected for further assessment, to determine whether they, as a set, could be used as signature genes, or biomarkers for ER negative cells. The ratio of the total number of the up-regulated genes over the total number of the down-regulated genes within the gene set in these 20 informative cases was calculated, using the ratio  $\geq 2$  as the standard for ER negative cells. To further assess whether this gene set could be used as biomarkers to differentiate cells overlying focally disrupted ME cell layers (or basal cell layers in prostate) and the adjacent cells within the same duct, additional tissue samples of DCIS and prostatic intraepithelial neoplasia were selected for further assessment with this gene set. The breast samples were processed with the same method described in the "Materials and Methods" section without modification. The prostate tissues were first immunostained for cytokeratin 34 $\beta$ E-12, the most commonly used phenotypic marker for basal cells; then, tumor cells near and away from focally disrupted basal cell layers were separately microdissected and processed for microarrays, using the same method in the "Materials and Methods" section without modification. The expression profiles of this gene set between two cell types of the same pair were assessed, using the same method listed above. The results of cDNA gene expression profiling were verified, using the real time RT PCR method.

## **Results**

### **Morphologic and immunohistochemical features of ER negative cell clusters**

The morphologic and immunohistochemical features of ER negative cell clusters overlying focally disrupted ME cell layers in selected cases are shown in Figure 1. The cells in all these ER negative clusters were negative to stromal phenotypic markers vimentin and SMA, whereas were

positive to the epithelial specific antigen (data not shown), indicating that they are epithelial in nature. The size of these clusters varied substantially, from about 30 (Figures 1a and 1d) to over 300 (Fig 1h) cells in a given section. Morphologically, the cells consisting of each cluster and among clusters were identical or similar, while differed markedly from their adjacent ER positive counterparts within the same duct in size, shape, density, and polarity (Fig 1). The cells in these clusters were generally densely packed and arranged as triangle-shaped edges “protruding” or “puncturing” into the stroma, facilitating the separation from their adjacent ER positive counterparts within the same duct, or from the surrounding stromal tissues (Fig 1). A vast majority of these ER cell clusters occurred in DCIS, while about 10% of them were seen in normal and hyperplastic ducts, consistent with our previous findings in paraffin-embedded tissue sections (12).

#### **The collection of ER negative and ER positive cells**

As described above, ER positive and ER negative cells were relatively easy to be separated, because of their unique morphology and distribution. The ER positive and negative cells were also relatively easy to be collected into the tubes, due to the pre-removal of unwanted tissues and addition of glycerin, which is very viscous, facilitating the formation of a cell mass that can be easily seen and picked up. The collection of a large number of ER negative cells, however, was often difficult or impossible, because the ER negative clusters in a majority of the cases were present at no more than five sections. Due to this reason, the ER negative cells collected for RNA extraction in one third of our selected cases were less than 200 per case. The number of ER negative cells collected in the remaining cases varied substantially, from about 200 to 2000 cells per case, with an average of about 250 cells per case.

### **Gene expression profiles between ER negative and ER positive cells**

We started with 30 pairs of samples, while 10 of which had to be discarded because of the apparent problem of RNA degradation. The samples from the remaining 20 cases were subject to further analysis.

Among the 96 genes spotted on the array, 88 were scored “present” at least once on the arrays (see Material and Method section for the definition of “present”). Among these 88 genes, 15 were scored “present” on more than a half or all of the 20 pairs examined. Of these 15 genes, 11 (73.3%) were predominantly expressed in ER negative cells, 2 (EGFR and TNF; 13.3%) were slightly more in ER positive cells, and 2 (13.3%) were equal in two different cell types (Table 1). The difference in the expressing frequency of these genes between ER negative and ER positive cells was statistically significant ( $p < 0.01$ ; Table 2).

The most noticeable difference was seen in genes for apoptosis and cell cycle control, in which all the 6 genes were predominantly expressed in ER negative cells (Table 1). The second noticeable difference was seen in genes for cell adhesion, in which 2 of the 3 genes were predominantly expressed in ER negative cells, and the difference between ER negative and ER positive cells was more than 3 folds (Table 1). The genes for invasion and metastasis, and signal transduction related molecules were also mainly expressed in ER negative cells. On the other hand, 2 of the 3 genes for angiogenesis were mainly expressed in ER positive cells (Table 1). Collectively, among a total of 247 informative pairs with measurable signals in both ER positive and negative cells of these 20 cases, 134 (54.3%) showed a higher expression in ER negative cells, 69 (27.9%) showed a higher expression level in ER positive cells, and 44 (17.8%) showed an equal expression in two cell types (Table 1). The differences among those were statistically significant ( $p < 0.05$ ; Table 1). The cDNA microarray images in selected cases were presented in Figure 2 (a-c).

### **The value of signature genes in differentiation between ER negative and positive cells**

The expression level of this gene set appeared to be useful in the differentiation between ER negative and ER positive cells. As shown in Table 3, a majority of the genes within this set showed the up-regulation in ER negative cells in 15 (75%) of the 20 cases, using the ratio  $\geq 2$  as the standard for ER negative cells. The relative expression levels of these 6 genes in 3 newly selected sample pairs were shown in Table 4. In the breast samples, 11 of the 12 (91.7%) compared pairs showed a clear distinction between ER negative and ER positive cells, using the same standard for ER negative cells. The same pattern was seen in prostate samples (Table 4). The up-regulations of these genes were confirmed by the results of real-time RT PCR (data not shown).

### **Discussion**

In previous studies, we revealed that a subset of ER positive mammary DCIS contained focally disrupted ME cell layers that were exclusively or preferentially overlain by ER negative cell clusters (12-14, 16). Compared to their adjacent ER positive counterparts within the same duct, these ER negative cells had a significantly higher rate of proliferation and LOH at chromosomal loci harboring tumor suppressor genes FHIT and WT-1 (12-13), suggesting that these cells might have genetic alterations in cell growth (including apoptosis and cell cycle control) related genes. Our current study reveals that all the six genes for apoptosis and cell cycle controls are predominantly expressed in ER negative cell clusters, supporting our previous findings and speculation. Our current study further reveals that these ER negative cell clusters also have a higher expression for genes involved in cell adhesion, invasion and metastasis, and signal transduction, compared to their adjacent ER positive counterparts within the same duct.



Our findings are consistent with those of a recent study, which reveals that microdissected cells from the periphery and the center of the same DCIS or invasive breast cancers have a substantially different frequency and pattern in the expression of 22 genes, assessed with Atlas human Cancer 1.2 Arrays containing 1176 known genes (25). In the DCIS, 9 genes are up-regulated (1.59 – 2.24-fold) in the peripheral rim relative to the center of the same DCIS. Of the 9 up-regulated genes, 6 (66.7%) are associated with apoptosis and cell cycle control (25). In the invasive lesions, several metastasis related genes, including RhoC, EF-1 $\alpha$ , and TSG101, are differentially expressed between cells from the center and infiltrating edge of the same invasive component (25). Our findings are also in an agreement with those of a previous study that compared the mRNA expression profiles between cells microdissected from the invasive edge and tumor core of human glioblastomas, using the differential display method (26). In that study, about 50-60 differentially expressed cDNA bands were detected in cells located at two different locations of the same tumor (26). One of the sequences preferentially overexpressed by the invasive cells showed 99% homology to the P311 gene, a putative invasion associated gene (26). Our findings are also in line with those of a previous study using reverse-phase protein microarrays, which detected a significantly elevated activation of pre-survival pathways at the invasion front during the progression of human prostatic intraepithelial neoplasia to invasive cancer (27).

The differential gene expression between cells at different locations of the same tumor could results from the differences in the distance of tumor cells to the stroma, or the extent of interactions with the stroma. As the epithelial component of the breast is normally devoid of lymphatic ducts and blood vessels, it totally depends on the stroma for its needed materials for normal metabolism, growth, and function. Consequently, the cells near the ME cell layer and basement membrane and the cells at invasive edges are supposedly to be biologically and functionally more active with a higher level of gene expressions than luminal cells within the same duct. Therefore, a deregulated cell proliferation

near a focally disrupted ME cell layer is likely to be more lethal than a similar growth near the duct lumen, as the former has a greater advantage to invade the stromal and vessels. Although not all the up-regulated genes in the periphery of the tumor are obligated to promote tumor progression or invasion, they may trigger reciprocal interactions between the tumor and stromal cells, which may subsequently result in pathologic alterations in both tumor and surrounding stromal cells. Previous studies in our and other laboratories have repeatedly demonstrated that tumor cells of the breast, lung, and cervix share a higher degree of common genetic and biochemical alterations with the surrounding stromal cells (28-32).

Alternatively, the differential gene expression might result from the difference in tumor stages. Previous studies have suggested that the progression and invasion of breast tumors are initiated and driven by a sequential or progressive expression of tumor stage-related "signature" genes (33-34), recapitulating the normal developmental process. As the disruption of the ME cell layer and basement membrane is an absolute pre-requisite for tumor invasion and metastasis, these genes are likely to be exclusively or preferentially expressed at the invasive edge near the focally disrupted ME cell layers and basement membrane at the early stage. Also, as genetic alterations not only determine the scope and extent of, but also precede, morphological and biochemical alterations, these genes are very likely to be expressed at the precursor of invasive lesions at the pending invasive sites. These up-regulated genes, especially those that are responsible for the initiation events, however, might not be detectable, as the cells involved are likely to be limited in number (35), and their genetic presentation could be masked by the luminal cells, which generally account for a vast majority of the total cell population.

In either case, however, the up-regulation of these genes in a given location, especially those at or near focally disrupted ME cell layers, is likely to result in variable consequences, depending on the nature of the involved cells. If they are fully differentiated, no substantial alteration may be detectable.

If they are partially differentiated, a limited or mild increase in cell proliferation might be seen, which may lead to a localized stromal invasion. If they are primitive stem cells, an extensive, localized cell proliferation may be seen, which may lead to the formation of new structures with normal morphology and functions (36-37). If they are mutated stem cells, a series of events that markedly differ from the cell proliferation mediated by either the primitive stem cells or differentiated progenitors might take place. Previous studies have shown that a mutated stem cell is capable of giving rise to multiple cell types and tissue structures, including blood vessels and lymphatic ducts (38-39). Thus, the elucidation and characterization of the "signature" genes exclusively or preferentially expressed in cells overlying or near disrupted ME cell layers could potentially lead to the development of novel therapeutic agents that specifically target on these gene products, providing more effective and less toxic means for the early detection, treatment, and prevention of breast tumors. A previous study has revealed that the progression of malignant melanomas is correlated with an increased expression of integrin subunits by the melanoma cells, while synthetic Arg-Gly Asp (RGD)-containing peptides that disrupt integrin functions, could effectively inhibit melanoma invasion (40-41).

The ER negative cell clusters seen in the current study are likely to be generated by mutated or primitive stem cells, for the following reasons. First, the cells consisting of a given cluster or among clusters are morphologically and immunohistochemically identical or similar, suggesting a common progenitor. Second, these clusters are exclusively located at or near focally disrupted ME cell layers, perfectly matching the expected location of undifferentiated stem cells. Third, these clusters have a significantly higher frequency and level of mRNA expression in all apoptosis and cell cycle control related genes tested in this study. Fourth, our previous study have revealed that a subset of these clusters in a majority of the cases show a detectable expression of c-erb-B2, a well-defined oncoprotein, while all or a vast majority of their adjacent ER positive cells within the same duct are devoid

of the expression of this protein (42). Fifth, our previous studies have revealed that microdissected ER negative cells have a significantly higher rate of proliferation and LOH at the chromosomal loci harboring tumor suppressor genes FHIT and WT-1, compared to the adjacent ER positive cells within the same duct (12-13). These ER negative cell clusters are very likely to be biologically and clinically more aggressive than their adjacent ER positive counterparts within the same duct, or represent the precursor of invasive and metastatic lesions, because of the above features, along with a previously identified nature that about 15% of these clusters directly spread into tube-like structures that appear to be blood vessels or lymphatic ducts (42).

It is not known whether or to what extent our hypothesis reflect the intrinsic nature of these ER negative cell clusters, as our data are obtained from a small sample size, which might not reflect the real status in the general population. However, given the facts that the disruption of both the ME cell layer and basement membrane is an absolute pre-requisite for breast tumor invasion and metastasis, and that ER negative cells are biologically and clinically more aggressive, our study and hypothesis might have important scientific and clinical implications. In the scientific field, our findings and hypothesis may be useful in reconciliation of the conflicting reports regarding immunohistochemical and genetic profiles of the breast lesions, as our findings clearly implicate that those conflicts are likely to result from the presence or absence of ME cell layer disruptions, and the differences in the nature and growth pattern of the cells overlying or adjacent to ME cell layer disruptions. In the clinical field, microdissection of these ER negative cell clusters and their adjacent ER positive counterparts within the same duct for proteomics may lead to the identification of the specific protein(s) associated with the early events of ME cell layer disruptions, tumor invasion and metastasis. The development of antibodies or chemical reagents to target these cells might provide a more effective and less toxic means to block tumor invasion at the very early stage. Also, microdissection of these ER negative

cell clusters for tissue culture may lead to the establishment of useful cell lines that benefit stem cell researches. This is an ongoing project. Our current efforts are on the identification of the potential unique genes that are exclusively expressed in ER negative cells, using more sensitive detection methods.

### Conclusions

ER negative cell clusters overlying focally disrupted ME cell layers displayed substantially different morphological features, along with a significantly higher expressing level and frequency on all 6 tested tumor progression and invasion related genes, compared to their ER positive counterparts within the same duct. These ER negative cell clusters are likely to be formed by a clone proliferation of mutated or primitive stem cells and some of them might represent the direct precursor of invasive lesions.

### Acknowledgment

This study was supported in part by grants DAMD17-01-1-0129 and DAMD17-01-1-0130 to Dr. Yan-gao Man, from Congressionally Directed Medical Research Programs

### References

1. Tsubura A, Shikata N, Inui T, Morii S, Hatano T, Oikawa T: **Immunohistochemical localization of myoepithelial cells and basement membrane in normal, benign and malignant human breast lesions.** *Virchows Arch* 1988, 413:133-139.
2. Jolicoeur F, Seemayer TA, Gabbiani G: **Multifocal, nascent, and invasive myoepithelial carcinoma(malignant myoepithelioma) of the breast: an immunohistochemical and ultrastructural study.** *Int J Surg Pathol* 2002, 10: 281-291.
3. Pasqualini JR: **Breast cancer-Prognosis, treatment, and prevention.** Marcel Dekker, Inc, New York, 2002.

4. Miosge N: **The ultrastructural composition of basement membrane in vivo.** *Histol Histopathol* 2001, 16:1239-1248.
5. Nerlich A: **Morphology of basement membrane and associated matrix proteins in normal and pathological tissues.** *Veroff Pathol* 1995, 145:1-139.
6. Bissell MJ, Bilder D: **Polarity determination in breast tissue: Desmosomal adhesion, myoepithelial cells, and laminin 1.** *Breast Cancer Res* 2003, 5:117-119.
7. Parker SL, Tong T, Bolders S, Wingo PA: **Cancer statistics.** *Cancer J Clin* 1997, 47: 5-27.
8. Goldfarb RH, Liotta LA: **Proteolytic enzymes in cancer invasion and metastasis.** *Semin Thromb Hemost* 1986, 12: 294-307.
9. Duffy MJ, Maguire TM, Hill A, McDermott E, O'Higgins N: **Metalloproteinases: role in breast carcinogenesis, invasion and metastasis.** *Breast Cancer Res* 2000; 2: 252-257.
10. Coussens LM, Fingleton B, Matrisian LM: **Matrix metalloproteinase inhibitors and cancer: trial and tribulations.** *Science* 2002, 295 (5564): 2387-2392.
11. Matrisian LM, Sledge GW Jr, Mohla S: **Exacellular proteolysis and cancer: meeting summary and future directions.** *Cancer Res* 2003, 63: 6105-6109.
12. Man YG, Tai L, Barner R, Vang R, Saenger JS, Shekitka KM, Bratthauer GL, Wheeler DT, Liang CL, Vinh TN, Strauss BL: **Cell clusters overlying focally disrupted mammary myoepithelial cell layers and adjacent cells within the same duct display different immunohistochemical and genetic features: implications for tumor progression and invasion.** *Breast Cancer Res* 2003, 5: R231-241.
13. Man YG, Shekitka KM, Bratthauer GL, Tavassoli FA: **Immunohistochemical and genetic alterations in mammary epithelial cells overlying focally disrupted myoepithelial cell layers.** *Breast Cancer Res Treat* 2002, 76 (sup 1): S143, 569.
14. Man YG, Vang RS, Saenger JS, Strauss B, Bratthauer GL, Chen PY, Tavassoli FA: **Co-expression of maspin and wilms' tumor 1 proteins in mammary myoepithelial cells---implication for tumor progression and invasion.** *Proceedings of Department of Defense Breast Cancer Research Program Meeting.* 2002, 1: P9,16.
15. Man YG, Saenger JS, Strauss B, Vang RS, Bratthauer GL, Chen PY, Tavassoli FA: **Focal alterations of p27 expression and subjacent myoepithelial cell layer disruptions are correlated events in ER (-) ductal intraepithelial neoplasia.** *Proceedings of Department of Defense Breast Cancer Research Program Meeting.* 2002, 1: P9,14.
16. Yousefi M, Mattu R, Gao C, Man YG: **Mammary ducts with and without focal myoepithelial cell layer disruptions show a different frequency of white blood cell infiltration and growth**

**pattern: Implications for tumor progression and invasion.** *AIMM*, In press

17. Schmitt FC: **Multistep progression from an oestrogen-dependent growth towards an autonomous growth in breast carcinogenesis.** *Eur J Cancer* 1995, 31A: 2049-2052.
18. Clarke R, Brunner N, Katzenellenbogen BS: **Progression of human breast cancer cells from hormone-dependent to hormone-independent growth both in vitro and in vivo.** *Proc Natl Acad Sci USA* 1989, 86: 3649-3653.
19. Murphy LC: **Mechanism of hormone independence in human breast cancer.** *In Vivo* 1998, 2: 95-106.
20. Sheikh MS, Garcia M, Pujol P, Fontana JA, Rochefort H: **Why are estrogen receptor negative breast cancers more aggressive than the estrogen receptor positive breast cancers?** *Invasion Metastasis* 1994-95, 14: 329-336.
21. Pan H, Yin C, Van Dyke T: **Apoptosis and cancer mechanism.** *Cancer Surv* 1997, 29:305-327.
22. Pierce GB, Speers WC: **Tumors as caricatures of the process of tissue renewal: prospects for therapy by directing differentiation.** *Cancer Res* 1996, 48:1990-2004.
23. Tavassoli FA, Man YG: **Morphofunctional features of intraductal hyperplasia, atypical hyperplasia, and various grades of intraductal carcinoma.** *Breast J* 1995, 1(3):155-162.
24. Man YG, Ball WD, Culp AJ, Hand AR, Moreira JE: **Persistence of a perinatal cellular phenotype in the ducts of adult glands.** *J Histochem Cytochem* 1995, 43(12):1203-1215.
25. Zhu G, Reynolds L, Crnogorac-Jurceic T, Gillett CE, Dublin EA, Mars Barnes D, D'Arrigo C, Van Trappen PO, Lemoine NR, Hart IR: **Combination of microdissection and microarray analysis to identify gene expression changes between differentially located tumour cells of breast cancer.** *Oncogene* 2003, 22:3742-3748.
26. Mariani L, McDonough WS, Hoelzinger DB, Beaudry C, Kaczmarek E, Coons SW, Giese A, Moghaddam M, Seiler RW, Berens ME: **Identification and validation of P311 as a glioblastoma invasion gene using laser capture microdissection.** *Cancer Res* 2001, 61: 4190-4196.
27. Paweletz CP, Charboneau L, Bichsel VE, Simone NL, Chen T, Gillespie JW, Emmert-Buck MR, Roth MJ, Petricoin III EF, Liotta LA: **Reverse phase protein microarrays which capture disease progression show activation of pro-survival pathways at the cancer invasion front.** *Oncogene* 2001, 20: 1981-1989
28. Moinfar F, Man YG, Arnould L, Bratthauer GL, Ratschek M, Tavassol FA: **Concurrent and independent genetic alterations in the stromal and epithelial cells of mammary carcinoma: Implications for tumorigenesis.** *Cancer Res* 2000, 60: 2562-2566.



29. Man YG, Martinez A, Avis IM, Hong SH, Cuttitta F, Venzon DJ, Mulshine JL: **Phenotypically different respiratory epithelial cells with hnRNP A2/B1 over-expression display similar genetic alterations.** *Am J Respir Cell Mol Biol* 2000, **23**: 636-645.
30. Man YG, Mannion C, Albores-Saavedra J, Bratthauer GL, Kuhls E, Tavassoli FA: **Allelic losses at 3p and 11p are detected in both epithelial and stromal components of cervical small cell neuroendocrine carcinoma.** *AIMM* 2001, **9**: 340-345.
31. Bissell MJ, Radisky DC, Rizki A, Weaver VM, Petersen OW: **The organizing principle: microenvironmental influences in the normal and malignant breast.** *Differentiation* 2002, **70**: 537-546.
32. Muschler J, Levy D, Boudreau R, Henry M, Campbell K, Bissell MJ: **A role for dystroglycan in epithelial polarization: loss of function in breast tumor cells.** *Cancer Res* 2002, **62**: 7102-7109.
33. Beckmann MW, Niederacher D, Schnurch HG, Gusterson BA, Bender HG: **Multistep carcinogenesis of breast cancer and tumour heterogeneity.** *J Mol Med* 1997, **75**: 429-439.
34. Lakhani SR: **The transition from hyperplasia to invasive carcinoma of the breast.** *J Pathol* 1999, **187**: 272-278.
35. Nowell PC: **The clonal evolution of tumor cell populations.** *Science* 1976, **194** (4260): 23-28.
36. Lochter A: **Plasticity of mammary epithelia during normal development and neoplastic progression.** *Biochem Cell Biol* 1998, **76**: 997-1008.
37. Kordon EC, Smith GH: **An entire functional mammary gland may comprise the progeny from a single cell.** *Development* 1998, **125**: 1921-1930.
38. Sell S, Pierce GB: **Maturation arrest of stem cell differentiation is a common pathway for the cellular origin of teratocarcinomas and epithelial cancers.** *Lab Invest* 1994, **70**: 6-22.
39. Trosko JE, Chang CC: **Role of stem cells and gap junctional intercellular communications in human carcinogenesis.** *Radia Res* 2001, **155**: 175-180.
40. Gehlsen KR, Argraves WS, Pierschbacher MD, Ruoslahti E: **Inhibition of in vitro tumor cell invasion by Arg-Gly-Asp-containing synthetic peptides.** *J Cell Biol* 1988, **106**: 925-930.
41. Marshall JF, Hart IR: **The role of alpha v-integrins in tumor progression and metastasis.** *Semin Cancer Biol* 1996, **7**: 129-138.
42. Man YG, Shen T, Sang QXA: **A subset of epithelial cells overlying focally disrupted mammary myoepithelial cell layers shows an unusual growth pattern: A mutated stem cell mediated clonal proliferation?** *Submitted*

**Table 1. Comparison of gene expression frequencies between ER (-) and ER (+) cells**

Gene group	Gene name	Higher in ER(-)	Higher in ER(+)	Equal in both	Case number
Adhesion	CD44	13	4	1	18
	CDH1	13	4	3	20
	MUC18L	5	5	2	12
Angiogenesis	EGFR	5	6	1	12
	IFNA1	10	5	2	17
	TNF	5	9	6	20
Apoptosis	BAX	9	4	0	13
	CASP9	9	5	5	19
	CFLAR	10	5	1	16
Cell cycle control	CDC25A	9	1	7	17
	CDKN2A	10	4	2	16
	RAD53	9	1	2	12
Inv & metastasis	NME4	10	4	6	20
	TIMP1	6	6	3	15
Signal transduct	NFKB1	11	6	3	20
Total:		134 (54.3%)	69 (27.9%)	44 (17.8%)	247
P:		< 0.05			

The frequencies of the higher and lower mRNA expression in all informative pairs (defined as the presence of measurable signals in both ER negative and ER positive cells of the same pair) were statistically compared with the Student-t-Test.

**Table 2. Comparison of the gene expressing level between ER (-) and ER (+) cells**

Total genes	Higher in ER (-)	Higher in ER (+)	Equal in two	P
15	11 (72.2%)	2 (13.3%)	2 (13.3%)	< 0.01

The frequencies of the higher mRNA expression among these 15 genes between ER negative and ER positive cells were statistically compared with the Student-t-Test.

**Table 3. The expression level of 6 selected genes among different cases**

Gene name	Case number																				Total	
	1	2	3	4	5	6	7	8	9	10	11	12	13	14	15	16	17	18	19	20	-	+
BAX	+	+	-	-	+	-	+	-	+	+	NI	NI	NI	+	+	+	NI	NI	NI	NI	4	9
CD44	-	+	+	+	-	+	+	-	+	-	+	+	+	+	+	+	+	NI	NI	-	5	13
CDH1	+	+	+	-	+	+	+	-	+	+	+	+	-	-	-	-	+	+	-	+	7	13
CDKN2A	-	-	+	+	+	+	+	-	NI	-	+	-	+	+	NI	NI	+	+	NI	-	6	10
CFLAR	-	+	+	+	+	+	+	-	+	-	+	-	+	+	NI	NI	-	-	NI	NI	6	10
RAD53	+	+	+	+	NI	+	+	-	+	-	-	+	+	NI	NI	NI	NI	NI	NI	NI	3	9
-/case	3	1	1	2	1	1	0	6	0	4	1	2	1	1	1	1	1	1	1	2	31	
+/case	3	5	5	4	4	5	6	0	5	2	4	3	4	4	2	2	3	2	0	1		64

The ratio of the total number of the up-regulated genes over the total number of the down-regulated genes within the 6-gene set was calculated, using the ratio  $\geq 2$  as the standard for ER negative cells.

+: The ratio  $\geq 2$ . -: The ratio  $< 2$ . NI: Not informative. Note that 15 of the 20 cases show un-regulation of this gene set in ER negative cells.

**Table 4. The expression level of 6 selected genes in newly selected breast and prostate tissues**

Pair#	Sample	Gene Names					
		BAX	CD44	CDH1	CDKN2A	CFLAR	RAD53
1	A (ER+)	1.00	1.00	1.00	1.00	1.00	1.00
	B (ER -)	6.30	5.00	12.60	3.20	4.22	4.26
2	A (ER +)	1.00	1.00	1.00	1.00	1.00	1.00
	B (ER -)	6.15	3.70	4.18	4.18	5.12	1.84
3*	A (Away)	1.00	1.00	1.00	1.00	1.00	1.00
	B (Near)	2.56	2.27	5.00	0.81	2.50	2.32

\*: Prostatic intraepithelial neoplasia.

Cells away and near focally disrupted basal cell layers were microdissected and processed for cDNA microarrays as described in "Materials and Methods". The ratio of the total number of up-regulated genes over the total number of down-regulated genes within the 6-gene set was calculated, using the ratio  $\geq 2$  as the standard for ER negative cells.

### **Figure 1. Morphological and immunohistochemical features of ER negative cell clusters**

Frozen human breast tissue sections were double immunostained for ER (black or brown) and SMA (red). ER negative cell clusters overlying focally disrupted ME cell layers were circled. The same cells and their adjacent ER positive counterparts within the same duct in adjacent sections were microdissected for RNA extraction. Note that the number of ER negative cells among clusters varies substantially, from about 30 (Figs 1a-1d) to over 300 (Fig 1h) in a given section, while the morphology of the ER negative cells within a given cluster or among clusters is very similar.

1a-1g: 300X; 1h: 100X.

### **Figure 2. The cDNA microarray images in selected cases**

Chemiluminescent array images were captured and digitized using the FluorChem 8800 Imaging System (Alpha Innotech, San Leandro, CA). Each pair of the datasets was exported to GEMArrayAnalyzer, a software developed by SuperArray (Frederick, MD). For each gene spotted on the array, if the integrated density value (IDV) was equal or greater than the 1.5x of the median IDV of the array, the expression of the gene was considered "present"; otherwise, this gene was considered "absent" in the sample. The integrated density values in paired samples with distinct signals in both ER negative and ER positive cells were measured and compared. The expression level of a given gene was considered higher in one sample only if 1> this gene is "present" in the sample and 2> the normalized IDV of this gene is equal or greater than 1.2 fold that of its counterpart on the pairing array. A gene is considered equally expressed in both samples only when 1> this gene is "present in both samples, and 2> the normalized IDV of this gene is between (not including) 0.8 to 1.2 fold that of its counterpart on the pairing array.

## **Cell clusters in a subset of *in situ* breast tumors show an unusual growth pattern: Implications for invasion and metastasis**

Yan-gao Man, Ting Shen<sup>1</sup>, Qiang-xiao Amy Sang<sup>2</sup>, Patricia E. Berg<sup>3</sup>, Arnold M. Schwartz<sup>3</sup>

Department of Gynecologic and breast Pathology, Armed Forces Institute of Pathology and American Registry of Pathology, Washington DC

<sup>1</sup>Department of Pathology, Temple University Hospital, Philadelphia, PA

<sup>2</sup>Department of Chemistry and Biochemistry, Florida State University, Tallahassee, FL

<sup>3</sup>Department of Pathology and Department of Biochemistry and Molecular Biology, George Washington University Medical Center, Washington DC.

### E-mail address of the authors:

Dr. Yan-gao Man: [man@afip.osd.mil](mailto:man@afip.osd.mil)

Dr. Ting Shen: [tshen@tuhs.temple.edu](mailto:tshen@tuhs.temple.edu)

Dr. Qiang-xiang Amy Sang: [qsang@chemmail.fsu.edu](mailto:qsang@chemmail.fsu.edu)

### Address of corresponding author:

Yan-gao Man, MD., PhD

Department of Gynecologic and Breast Pathology

Armed Forces Institute of Pathology and American Registry of Pathology

6825 16<sup>th</sup> Street, NW

Washington DC 20306-6000

USA

Tel: 202-782-1612; Fax: 202-782-3939

The opinions and assertions contained herein represent the personal views of the authors and are not to be construed as official or as representing the views of the Department of the Army or the Department of Defense.

## Abstract

**Introduction:** Our previous studies revealed that a vast majority of estrogen receptor (ER) negative cell clusters overlying focally disrupted mammary myoepithelial cell layers showed a significantly elevated proliferation rate, whereas about 10% of these were completely devoid of the expression of Ki-67, a most commonly used proliferation marker. This study attempted to assess whether these cell clusters were also devoid of the expression of other proliferation and differentiation related markers

**Methods:** Fifteen cases of ductal carcinoma *in situ* containing focally disrupted myoepithelial cell layers and ER negative clusters with no Ki-67 immunoreactive cells were selected from our previous studies. Consecutive sections were immunohistochemically stained for proliferation, differentiation, and other related markers.

**Results:** In addition to ER and Ki-67, these clusters also lacked the expression of other markers, including PCNA, cyclin A, cyclin D1, p27, MMP-26, and BP1, in a sharp contrast to their adjacent ER positive counterparts within the same duct, which expressed a high level of each of those markers. A subset of these clusters in 9 (60%) of the 15 cases, however, showed untypical expression of c-erb-B2, while all or a vast majority of their adjacent ER positive counterparts within the same duct were devoid of the expression of this protein. Morphologically, cells consisting of each cluster and among clusters were identical or similar, while differed markedly from their adjacent ER positive counterparts within the same duct in size, shape, density, and polarity. Cells in these clusters were generally arranged as triangle-shaped edges “protruding” or “puncturing” into the stroma, some of them appeared to become invasive lesions, and about 10% of those spread into tube-like structures that resemble blood vessels.

**Conclusions:** These finding suggest that these cell clusters are formed and regulated by a yet to be defined mechanism, and that a subset of these clusters may represent the direct precursor of invasive and metastatic breast lesions.

## Introduction

The epithelium of the normal human breast and *in situ* breast tumors is physically separated from the stroma by both the myoepithelial (ME) cell layer and basement membrane (1-3). ME cells are joined by intercellular junctions and adhesion molecules, forming a sheet or belt that encircles the epithelial cells (1-3). The basement membrane is composed of a group of fibrous proteins embedded in a hydrated polysaccharide gel, constituting a continuous lining surrounding and attaching to the ME cells via hemidesmosomes and focal adhesion complexes (4-5). Both the ME cell layer and basement membrane are structural constituents, which normally only allow the exchange of water, oxygen, and small molecules between the epithelial and stromal component (1-5). Due to the interposition of the ME cell layer and basement membrane between the stroma and the epithelium, tumor cells have to first pass through the ME cell layer, followed by the basement membrane in order to physically contact the stroma. Hence, the disruption of both the basement membrane and the ME cell layer is an absolute pre-requisite for tumor invasion and metastasis.

As invasive and metastasized tumors have a significantly higher mortality rate and account for a vast majority of breast cancer-related deaths, compared to *in situ* tumors (6), the identification of the mechanism(s) of tumor invasion and metastasis is expected to bring vast benefits and advances to early detection, treatment, and prevention of breast tumors. A generally accepted hypothesis for the direct cause of basement membrane disruptions and tumor invasion has been attributed primarily, if not solely, to the over-production of proteolytic enzymes by tumor or stromal cells (7-8). This hypothesis alone, however, might not reflect the intrinsic mechanism of these events for three main reasons: [1] The ME cell layer is a normal structural constituent, which should not be the target of the host's own enzymes; [2] Neither the normal cellular kinetics nor dynamic alterations of ME cells during tumor invasion have been well elucidated; [3] While the results from *in vitro* tests and animal models have

clearly demonstrated that proteolytic inhibitors effectively prevent tumor invasion, the results from all the proteolytic inhibitor-based clinical trials have been very disappointing (9-10).

While attempting to identify the early sign of ME layer disruptions and precursor of invasive breast lesions, we have recently carried out a number of studies, focusing on the correlation between the structural integrity in ME cell layers and the immunohistochemical and genetic profiles in adjacent epithelial cells. In 5,698 duct cross sections from 220 patients with estrogen receptor (ER) positive, non-invasive breast tumors, we detected a total of 405 focal ME cell layer disruptions, defined as the absence of ME cells resulting in a gap equal to or greater than the combined size of 3 ME or epithelial cells (11). Of these disruptions, 350 (86.4%) were overlaid by clusters of cells with no or substantially reduced ER expression, in a sharp contrast to their adjacent cells within the same duct, which showed uniform and strong ER immunoreactivity and overlaid a non-disrupted ME cell layer (11). Compared to their adjacent ER positive counterparts within the same duct, microdissected ER negative cells had a substantially higher frequency and different pattern of loss of heterozygosity at multiple chromosomal loci, including those harboring tumor suppressor genes fragile histidine triad (FHIT) and Wilms' tumor 1 (11-12). Cells in ducts with these ER negative clusters also had a significantly higher ( $p < 0.01$ ) proliferation rate, 18.2% versus 3.6% and 19.9% versus 4.4%, compared to cells in morphologically compared ducts without ME cell layer disruptions, assessed by immunohistochemical staining for Ki-67 in three separate studies (13-15).

It was interesting to note that, however, a subset (about 10%) of these ER negative cell clusters were completely devoid of distinct Ki-67 immunoreactive cells, in a sharp contrast to the adjacent ER positive cells within the same duct, which had a significantly elevated number of Ki-67 positive cells (13-15). As it has been well documented [1] breast tumor progression is paralleled by a progressively hormonal independence (16-17), [2] ER negative tumors have a substantially worse prognosis than ER



positive tumors (18-19), [3] a deregulated cell proliferation seems to be a direct cause of malignancies (20-21), this study attempted to assess the proliferation status of these cell clusters with a panel of cell proliferation and phenotype related markers. The hypothesis to be tested was that these cell clusters were newly formed through a clonal proliferation of a mutated stem cell, which might genetically and biochemically differ from both primitive stem cells and partially committed progenitors. Therefore, these ER negative cell clusters might have a unique immunostaining pattern for all currently available proliferation related markers that are not designed for potentially mutated proteins.

### **Materials and Methods**

A total of 15 cases of ductal carcinoma *in situ* (DCIS) containing focally disrupted ME cell layers and ER negative cell clusters with no distinct Ki-67immunoreactive cells were selected from our previous studies (11-15). Consecutive sections at 4-5  $\mu$ m thickness were prepared from each case and sequentially placed on positively charged microscopic slides, and processed for morphological and immunohistochemical assessments, as previously described (22-23). Briefly, deparaffinized sections were incubated in 10 mM citrate buffer overnight at 80 °C. After incubation, sections were washed with tap water and PBS (pH 7.4), each for 10 to 15 minutes, and incubated in 0.3% H<sub>2</sub>O<sub>2</sub> and normal serum, each for 30 minutes. Then, sections 1, 11, and 21 from each case were double immunostained for ER and SMA, as previously described (11). Immunostained sections were examined to assess the size of the ER negative cell clusters. The clusters were defined as large if they were appreciable in more than 10 sections, or as small if they were present in less than 10 sections.

To assess the proliferation status of these cell clusters, a panel of commonly used markers, including proliferating cell nuclear antigen (PCNA), Ki-67, cyclin A, cyclin D1, as well as p27, a

known tumor suppressor (Vector, Burlingame, CA), were used. To assess the histological origin of these clusters, sections were immunostained for both stromal cell specific markers (vimentin and smooth muscle actin) and epithelial cell phenotypic markers (epithelial specific antigen, cytokeratins 5, 8, and AE1/AE3, Vector, Burlingame, CA; Dako, Carpinteria, CA). To assess the differentiation status and biologic behavior of these clusters, sections were immunostained for c-erb-B2 (Vector, Burlingame, CA), a well defined onco-protein whose over-expression has been reported to correlate with more aggressive clinicopathologic presentation and to enhance the metastatic potential (24-25), MMP-26, a metalloproteinase that is preferentially present at *in situ* breast tumors (26), and BP1, a homeotic protein that is predominantly present in invasive breast tumors (27-28).

In cases with large ER negative cell clusters, sections 2 to 13 from each case were individually incubated with one or a mixture of two corresponding antibodies for 1-2 hours at 37 °C. In cases with small ER negative cell clusters, three sections were utilized for immunostaining each group of the above proteins, which was carried out by a sequential incubation of all the antibodies in a given group, 1-2 hours for each at 37 °C, followed by 3 washes in PBS, 5-7 minutes for each. The antigen-antibody complex was detected with the ABC method, using a biotinylated secondary antibody and Elite ABC detection and the diaminobenzidine (DAB) substrate kit (Vector, Burlingame, CA). After the substrate reaction, sections were washed in tap water for 5 minutes and incubated at 80 °C for 5-10 minutes, to inactivate the potential enzyme residues, followed by 3 washes in PBS, each for 5-7 minutes. Then, the sections were incubated with smooth muscle actin (Vector, Burlingame, CA) and developed with the AP-red substrate kit (Zymed, San Francisco, CA) to elucidate ME cell layers. The expression status of these markers in the same cell cluster at different sections were examined and photographed, as previously described (11, 15).

## Results

Distinct focal myoepithelial cell layer disruptions and associated ER negative cell clusters with no Ki-67 immunoreactive cells were clearly identifiable in all 15 cases. The number of these clusters among cases varied substantially, ranged from one to over 15. The size of these clusters also varied substantially, ranged from less than 15 to over 100 cells in a given section (Fig 1). These cell clusters were also completely devoid of the expression of PCNA, cyclin A, cyclin D, p27, MMP-26, and BP1, in a sharp contrast to their adjacent ER positive counterparts within the same duct, which showed an elevated expression for each of those markers (Figs 2-3). These cell clusters also showed a markedly reduced (but clearly appreciable) expression of epithelial specific antigen, cytokeratins AE1/AE3 and the mixture of cytokeratins 5 and 8, compared to their adjacent ER positive counterparts within the same duct (Fig 3). In contrast, a subset of these clusters in 9 of the 15 cases displayed appreciable expression of c-erb-B2, whereas all or a vast majority of their adjacent ER positive counterparts within the same duct were devoid of the expression of this proteins (Figs 1 and 4). The c-erb-B2 protein, however, was distributed predominantly in the cytoplasm, rather than the typical membrane-associated localization (Figs 1 and 4). All these ER negative cells and their adjacent ER positive counterparts within the same duct were negative for stromal phenotypic markers vimentin and smooth muscle actin (data not shown).

Morphologically, all the cells consisting of each ER negative cell cluster and among different clusters were identical or very similar (Figs 1-4). However, compared to their adjacent ER positive counterparts within the same duct or acinus, a vast majority of these cells were noticeably smaller in size with dark, elongated, or irregular nuclei, and were often densely packed, making the detection of mitotic figures difficult or impossible (Figs 1-4). These clusters were exclusively located at or near focally disrupted ME cell layers, and cells in these clusters were generally arranged as triangle-shaped

edges “protruding” or “puncturing” into the stroma (Figs 1-4), and some of them appeared to directly transfer into micro-invasive lesions (Figs 1g and 1h). Cells in about 10% of these clusters, however, had a non-cohesive or “floating” appearance and appeared to directly spread into tube-like structures that resemble blood vessels (Figs 5a – 5c). Our subsequent immunohistochemical studies in adjacent sections of selected cases showed that cells within the tube-like structures were positive for epithelial specific antigen (Figs 5e – 5f), suggesting that they are epithelial in nature. The lining of the duct-like structures was negative to the ME cell specific marker, p63 (Fig 5e), whereas was positive to the blood vessel specific marker, CD31 (Fig 5f), suggesting that they might be indeed vascular structures. In contrast, the surrounding of the ducts was positive to p63, while was negative to CD31 (Fig 5e – 5f). It was interesting to note that the ME cells appeared to be directly fused with CD 31 positive structures (Figs 5e – 5f).

### **Discussion**

In our previous studies (11-15), we revealed that a subset of DCIS contained focally disrupted ME cell layers that were overlain preferentially or exclusively by ER negative cell clusters. A vast majority of these ER negative cell clusters showed a substantially elevated proliferation rate, compared to their adjacent ER positive counterparts within the same duct. A subset of these clusters, however, were completely devoid of the expression of Ki-67, in a sharp contrast to the adjacent ER positive cells within the same duct that showed a substantially elevated number of Ki-67 positive cells. Our current study has not only confirmed our previous findings, but also further revealed that, compared to their adjacent ER positive counterparts within the same duct, these cell clusters possess additional unique features: [1] they lack the expression of other commonly used proliferation markers, including PCNA,

cyclin A, cyclin D1, and p27, as well as two-tumor progression related proteins, MMP-26 and BP1 (26-28); [2] they showed a substantially weaker expression of epithelial phenotypic markers; [3] a subset of these clusters in 9 (60%) of 15 cases showed untypical expression of c-erb-B2, a well-defined onco-protein; [4] cells within each cluster and among different clusters are morphologically identical or very similar; [5] They are exclusively located at or near focally disrupted ME cell layers; [6] cells in these clusters are generally arranged as triangle-shaped edges “protruding” or “puncturing” into the stroma, and a subset of these clusters directly spread into tube-like structures that appear to be blood vessels or lymphatic ducts. To the best of our knowledge, such or similar cell clusters and cell growth pattern have not been previously reported in the English literatures.

The mechanism(s) for focal ME layer disruptions and formation of ER negative cell clusters is unknown, but is likely to result from a localized ME cell death and leukocyte infiltration and resultant responses, based on the following reasons. First, no morphologically distinct ME cells are detectable at the disruptions in multiple consecutive sections in all cases, indicating the physical absence of ME cells. Second, our previous studies have shown that the frequency of focal ME cell layer disruptions is independent of the size, length, and architecture of ducts and acini, suggesting that the disruption is unlikely induced by mechanic forces, such as an elevated pressure in the lumen and an increased cell number. Third, our previous studies have shown that 97.4% of the ducts with focal ME disruptions showed leukocyte infiltration, compared to 22.2% ( $p < 0.01$ ) in morphologically similar ducts without focal ME cell layer disruptions (15). Fourth, our recent studies further showed that focally disrupted human prostate basal cell layers had a substantially lower cell proliferation rate, compared to their morphologically similar counterparts (29). Also, basal cells surrounded by or adjacent to leukocytes often showed distinct morphological alterations, and that clusters of multiple proliferating cells were almost exclusively located at or near the focal disruptions (29).

Our speculation is further supported by several lines of evidence. Increasing data have shown that a variety of external and internal insults could specifically impact the physical and functional status of the ME cells. The exposure to lambdacarrageenan could specifically result in filament disassembly and loss of ME cells, while the exposure to oxytocin could substantially enhance ME cell proliferation and differentiation (30-31). ME cells exclusively or preferentially express a high level of multiple non-structure-restricted proteins, including CD10, p-cadherin, and p63, as well as tumor suppressors, including Wilms' tumor 1 and maspin (32), and the expression frequency and level of these proteins linearly decreased with the advance of tumor stages (13-14). In addition, a subset of morphologically distinct ME cells is completely devoid of the expression of all corresponding immunophenotypic markers (33), suggesting that ME cells are also subject to pathological alterations. It has been well documented that leukocyte infiltration into tumor tissues is a common event, and that the number of leukocytes within tumor tissues is linearly increased with tumor progression (34-36). The increase of leukocytes is particularly evident during the progression of DCIS to infiltrating ductal carcinoma, in which up to a four-fold increase of lymphoid infiltration has been reported (34-36). The extent of the increased macrophages in tumor tissues has been found to inversely correlate with a worse prognosis and a significantly higher mortality rate (34-36). Also, patients with lymphocyte infiltration at the tumor edge were found to have a noticeable poorer short-term prognosis, compared to those with lymphocyte infiltration in other locations (37). More importantly, it has been well elucidated that leukocytes are capable of freely crossing through both the basement membrane and ME cell layer, and that leukocytes contain a number of digestive enzymes that can effectively degrade both the basement membrane and altered host cells (38-40).

Based on these findings, we propose that a localized ME cell death and resultant immunoreactions are the triggering factor for disruptions in ME cell layers, the formation of ER negative cell clusters, and subsequent stromal and vascular invasion. Our hypothesized main processes are the following:

1. The ME cells belong to a self-renewal population, which normally undergoes proliferation to replace aged or injured ME cells.
2. An external or internal insult, such as a localized trauma or the exposure to lambda-carrageenan (30), directly disrupts the structural integrity of the ME cell layers or impairs the normal replacement process, resulting in a cluster of dying ME cells.
3. The degradation products of dying ME cells attract leukocytes, which migrate to the injured site and interact with altered ME cells.
4. Leukocytes release digestive enzymes, leading to the physical destruction of altered ME cells and basement membrane, resulting in a focal disruption or gap that allows the direct communications between the tumor and stromal cells.
5. The focal disruption or gap results in a focally increased permeability for metabolism- and growth-related molecules to overlying and adjacent cells.
6. The altered micro-environment leads to variable consequences in overlying tumor and adjacent ME cells, depending on the nature of these cells. If the overlying and adjacent cells are fully differentiated, no substantial alteration may be detectable. If the cells are partially differentiated, a limited or mild increase in cell proliferation might be seen, which might lead to a localized stromal invasion. If they are primitive stem cells, an extensive cell proliferation may be seen, which may lead to the formation of new structures with normal morphology and functions (41). If they are mutated stem cells, a series of events that markedly differ from both primitive stem cells mediated and differentiated progenitors mediated proliferation might take place. Previous studies have shown that a mutated stem cell is the common cellular origin of teratocarcinomas, epithelial cancers, and blood vessels and lymphatic ducts (42-43).
7. The newly formed cell clusters undergo differentiation, releasing invasion-associated molecules, which trigger angiogenesis, tissue remodeling, and increasing production of growth factors

in the stroma, providing a favorable environment for tumor cell growth (44-48). 8. The interactions between tumor and stromal cells lead to further degradation of ME layers and basement membrane, and a deeper and wider migration of the newly formed cell clusters (44-48).

A majority of the ER negative cell clusters seen in the current study appear to be generated by a clonal proliferation of mutated stem cells for four main reasons. First, a subset of these clusters in 9 (60%) of the 15 cases showed detectable expression of c-erb-B2, a well-defined onco-protein, while all or a vast majority of their adjacent ER positive cells within the same duct are devoid of the expression of this protein. Second, the cells consisting of a given cluster or among clusters are morphologically and immunohistochemically identical or similar, suggesting a common origin. Third, these clusters are exclusively located at or near focally disrupted ME cell layers, perfectly matching the expected location of undifferentiated stem cells. Fourth, these clusters are devoid of the expression of MMP-26 and BP1 that are preferentially present in advanced stages of breast tumors (26-28), and also show a substantially weaker immunostaining for epithelial phenotypic markers, implicating that they are new formed and have not gained the full capacity to manufacture these proteins. Our previous studies have shown that at the initial stage of normal cellular replacement or regeneration after a partial extirpation, the progenitor cells are intensely labeled with tritiated-thymidine ( $^3\text{H}$ -TDR), while are devoid of the expression of all adult secretory proteins (49-50). The newly formed cells gradually start to express increasing levels of these proteins with time (49-50).

These ER negative cell clusters are likely to be biologically more aggressive and represent the direct precursor of invasive and metastatic lesions for the following reasons. First, a subset of these clusters in 60% of the cases showed an untypical expression of c-erb-B2, whose expression is correlated with tumor aggressiveness and a worse prognosis (51). Second, cells in about 15% of these clusters directly spread into tube-like structures that are likely to be blood vessels or lymphatic ducts.



Third, our previous studies have revealed that microdissected ER negative cells have a significantly higher frequency or different pattern of LOH at multiple chromosomal loci, including those harboring tumor suppressor genes FHIT and WT-1, compared to the adjacent ER positive cells within the same duct (11-12). Fourth, our recent studies further show that these ER negative cell clusters also have a significantly higher frequency and level of mRNA expression for a number of tumor invasion- and metastasis related genes, including CD44, CDH1, and CDKN2A (52).

It is not known, however, whether or to what extent our hypothesis reflect the intrinsic mechanism of ME cell disruptions and the formation of these ER negative tumor cell clusters for three main reasons: [1] our data are limited, extracted from a small sample size, which might not reflect the real status in the general population; [2] the underlined mechanism(s) and detained processes for each of our hypothesized steps has not be elucidated; [3] the complete lack of the expression of all growth-related markers is hard to reconcile with the expected features of a stem cell-mediated proliferation. However, given the facts that the results of human clinical trials disfavor the traditional belief that elevated proteolytic enzymes is the primary, if not the only, cause for basement membrane disruptions and tumor invasion (9-10), our hypothesis might have important scientific and clinical implications. In the scientific field, our hypothesis may open a new window for the exploration of the mechanism of ME cell layer disruptions and tumor invasion. Our hypothesis might also be useful in reconciliation of the conflicting reports regarding the immunohistochemical and genetic profiles of the breast lesions, as our findings clearly implicate that those conflicts are likely to result from the presence or absence of ME cell layer disruptions, and the differences in the nature and growth pattern of the cells overlying or adjacent to the disruptions. In the clinical field, our hypothesis might be beneficial for the early detection and treatment of breast tumors. Microdissection of these ER negative cell clusters and their adjacent ER positive counterparts in frozen tissues for genetic and biochemical comparisons could

potentially lead to the identification of specific molecules associated with the early events of ME cell layer disruptions, tumor invasion and metastasis. The development of antibodies or chemical reagents to target these cells might provide a more effective and less toxic means to block tumor invasion at the very early stage. Also, microdissection of these ER negative cell clusters in frozen tissues for tissue culture may lead to the establishment of useful cell lines that benefit stem cell researches.

### Acknowledgment

This study was supported by grants, DAMD17-01-1-0129 and DAMD17-01-1-0130, from The Congressionally Directed Medical Research Programs to Yan-gao Man, MD., Ph D.

### **References**

1. Tsubura A, Shikata N, Inui T, Morii S, Hatano T, Oikawa T: **Immunohistochemical localization of myoepithelial cells and basement membrane in normal, benign and malignant human breast lesions.** *Virchows Arch* 1988, 413:133-139.
2. Jolicoeur F, Seemayer TA, Gabbiani G: **Multifocal, nascent, and invasive myoepithelial carcinoma(malignant myoepithelioma) of the breast: an immunohistochemical and ultrastructural study.** *Int J Surg Pathol* 2002, 10: 281-291.
3. Slade MJ, Coope RC, Gomm JJ, Coombes RC: **The human mammary gland basement membrane is integral to the polarity of luminal epithelial cells.** *Exp Cell Res* 1999, 247: 267-278.
4. Miosge N: **The ultrastructural composition of basement membrane in vivo.** *Histol Histopathol* 2001, 16:1239-1248.
5. Nerlich A: **Morphology of basement membrane and associated matrix proteins in normal and pathological tissues.** *Veroff Pathol* 1995, 145:1-139.
6. Howe HL, Wingo PA, Thun MJ: **Annual report to the nation on the status of cancer (1973 through 1998), featuring cancer with recent increasing trends.** *J Natl Cancer Inst* 2001, 93: 824-842.
7. Goldfarb RH, Liotta LA: **Proteolytic enzymes in cancer invasion and metastasis.**

*Semin Thromb Hemost* 1986, 12: 294-307.

8. Pasqualini JR: *Breast Cancer---Prognosis, Treatment, and Prevention*. New York: Marcel Dekker; 2002
9. Coussens LM, Fingleton B, Matrisian LM: **Matrix metalloproteinase inhibitors and cancer: trial and tribulations**. *Science* 2002, 295 (5564): 2387-2392.
10. Matrisian LM, Sledge GW Jr, Mohla S: **Exacellular proteolysis and cancer: meeting summary and future directions**. *Cancer Res* 2003, 63: 6105-6109.
11. Man YG, Tai L, Barner R, Vang R, Saenger JS, Shekitka KM, Bratthauer GL, Wheeler DT, Liang CL, Vinh TN, Strauss BL: **Cell clusters overlying focally disrupted mammary myoepithelial cell layers and adjacent cells within the same duct display different immunohistochemical and genetic features: implications for tumor progression and invasion**. *Breast Cancer Res* 2003, 5: R231-241.
12. Man YG, Shekitka KM, Bratthauer GL, Tavassoli FA: **Immunohistochemical and genetic alterations in mammary epithelial cells overlying focally disrupted myoepithelial cell layers**. *Breast Cancer Res Treat* 2002, 76 (sup 1): S143, 569.
13. Man YG, Vang RS, Saenger JS, Strauss B, Bratthauer GL, Chen PY, Tavassoli FA: **Co-expression of maspin and wilms' tumor 1 proteins in mammary myoepithelial cells---implication for tumor progression and invasion**. *Proceedings of Department of Defense Breast Cancer Research Program Meeting*. 2002, 1: P9,16.
14. Man YG, Saenger JS, Strauss B, Vang RS, Bratthauer GL, Chen PY, Tavassoli FA: **Focal alterations of p27 expression and subjacent myoepithelial cell layer disruptions are correlated events in ER (-) ductal intraepithelial neoplasia**. *Proceedings of Department of Defense Breast Cancer Research Program Meeting*. 2002, 1: P9,14.
15. Yousefi M, Mattu R, Gao C, Man YG: **Mammary ducts with and without focal myoepithelial cell layer disruptions show a different frequency of white blood cell infiltration and growth pattern: Implications for tumor progression and invasion**. *AIMM*, In press
16. Schmitt FC: **Multistep progression from an oestrogen-dependent growth towards an autonomous growth in breast carcinogenesis**. *Eur J Cancer* 1995, 31A: 2049-2052.
17. Clarke R, Brunner N, Katzenellenbogen BS: **Progression of human breast cancer cells from hormone-dependent to hormone-independent growth both in vitro and in vivo**. *Proc Natl Acad Sci USA* 1989, 86: 3649-3653
18. Murphy LC: **Mechanism of hormone independence in human breast cancer**. *In Vivo* 1998, 2: 95-106
19. Sheikh MS, Garcia M, Pujol P, Fontana JA, Rochefort H: **Why are estrogen receptor negative**

**breast cancers more aggressive than the estrogen receptor positive breast cancers?** *Invasion Metastasis* 1994-95, 14: 329-336.

20. Pan H, Yin C, Van Dyke T: **Apoptosis and cancer mechanism.** *Cancer Surv* 1997, 29:305-327.
21. Pierce GB, Speers WC: **Tumors as caricatures of the process of tissue renewal: prospects for therapy by directing differentiation.** *Cancer Res* 1996, 48:1990-2004.
22. Man YG, Tavassoli FA: **A simple epitope retrieval method without the use of microwave oven or enzyme digestion.** *Appl Immunohistochem* 1996, 4(2):139-141.
23. Man YG, Bugar A: **An antigen unmasking protocol that satisfies both immunohistochemical and subsequent molecular biological assessments.** *Pathology-Research & Practice* 2003, 199:815-825.
24. Sahin AA: **Biologic and clinical significance of HER-2/neu (cerbB-2) in breast cancer.** *Adv Anat Pathol* 2000, 7: 158-166.
25. Ross JS, Fletcher JA. **The HER-2/neu oncogene in breast cancer: prognostic factor, predictive factor, and target for therapy.** *Stem Cells* 1998, 16: 413-428.
26. Zhao YG, Xiao AZ, Park HI, Newcomer RG, Yan M, Man YG, Heffelfinger SC, Sang QX: **Endometase in human breast carcinoma, selective activation of progelatinase B and inhibition by tissue inhibitors of metalloproteinases-2 and -4.** *Cancer Res* 2004, 64: 590-598.
27. Man YG, Strauss BL, Berg PE: **Increasing BP1 expression correlates with progression and invasion of male breast and prostate tumors.** *Cancer Detect Prev*, 2004 Symposium Issue 2004, S-95: 149.
28. Berg P, Fu SW, Pinzone JJ, Man YG: **The Expression of BP1, a homeotic protein, increases with breast tumor progression.** *Cancer Res*, in press (abstract)
29. Man YG, Shen T, Zhao YG, Sang QX: **Focal prostate basal cell layer disruptions and leukocyte infiltration are correlated events: Implications for basal cell layer degradation and tumor invasion.** *Cancer Detect Prev*, 2004 Symposium Issue 2004, S-51: 15.
30. Tobacman JK: **Filament disassembly and loss of mammary myoepithelial cells after exposure to lambda-carrageenan.** *Cancer Res* 1997, 57: 2823-2826.
31. Sapino A, Macri L, Tonda L, Bussolati G: **Oxytocin enhances myoepithelial cell differentiation and proliferation in the mouse mammary gland.** *Endocrinology* 1993, 133: 838-842
32. Man YG, Barner R, Vang R, Wheeler DT, Liang CY, Vihn T, Bratthauer GL, Strauss BL: **Non-smooth muscle restricted proteins exclusively or preferentially expressed in mammary myoepithelial cells: a programmed or induced phenomenon?** *Mod Pathol* 2004,

17 (supplement 1): 40a.

33. Zhang R, Man YG, Vang RS, Saenger JS, Barner R, Wheeler D, Liang CY, Vinh TN, Bratthauer GL: **A subset of morphologically distinct mammary myoepithelial cells lacks corresponding immunophenotypic markers.** *Breast Cancer Res* 2003, 5: R151-156.
34. Ben-hur H, Mordechay E, Halperin R, Gurevich P, Zandbank J, Herper M, Zusman I: **Apoptosis-related proteins (Fas, Fas ligand, bcl-2 and p53) in different types of human breast tumors.** *Oncol Rep* 2002, 9:977-980.
35. Ben-Hur H, Cohen O, Schneider D, Gurevich P, Halperin R, Bala U, Mozes M, Zusman I: **The role of lymphocytes and macrophages in human breast tumorigenesis: an immunohistochemical and morphometric study.** *Anticancer Research* 2002, 22(2B): 1231-1238.
36. Harmey JH, Dimitriadis E, Kay E, Redmond HP, Bouchier-Hayes D: **Regulation of macrophage production of vascular endothelial growth factor (VEGF) by hypoxia and transforming growth factor beta-1.** *Ann Surg Oncol* 1998, 5: 271-278.
37. Hartveil F: **Breast cancer: poor short-term prognosis in cases with moderate lymphocyte infiltration at the tumor edge: a preliminary report.** *Oncol Rep* 1998, 5: 423-426.
38. Zhang XD, Schiller GD, Gill PG, Coventry BJ: **Lymphoid cell infiltration during cancer growth: a syngeneic rat model.** *Immunol Cell Biol* 1998, 76:550-555.
39. Steadman R, Irwin MH, St John PL, et al: **Laminin cleavage by activated human neutrophils yields proteolytic fragments with selective migratory properties.** *J Leukoc Biol* 1993, 53: 354-365.
40. Heck LW, Blackburn WD, Irwin MH, Abrahamson DR: **Degradation of basement membrane laminin by human neutrophil elastases and cathepsin G.** *Am J Pathol* 1990, 136: 1267-1274.
41. Kordon EC, Smith GH: **An entire functional mammary gland may comprise the progeny from a single cell.** *Development* 1998, 125: 1921-1930.
42. Sell S, Pierce GB: **Maturation arrest of stem cell differentiation is a common pathway for the cellular origin of teratocarcinomas and epithelial cancers.** *Lab Invest* 1994, 70: 6-22.
43. Trosko JE, Chang CC: **Role of stem cells and gap junctional intercellular communications in human carcinogenesis.** *Radia Res* 2001, 155: 175-180.
44. Moynfar F, Man YG, Arnould L, Bratthauer GL, Ratschek M, Tavassol FA: **Concurrent and independent genetic alterations in the stromal and epithelial cells of mammary carcinoma: Implications for tumorigenesis.** *Cancer Res* 2000, 60: 2562-2566.

45. Man YG, Martinez A, Avis IM, Hong SH, Cuttitta F, Venzon DJ, Mulshine JL: **Phenotypically different respiratory epithelial cells with hnRNP A2/B1 over-expression display similar genetic alterations.** *Am J Respir Cell Mol Biol* 2000, 23:636-645.
46. Man YG, Mannion C, Albores-Saavedra J, Bratthauer GL, Kuhls E, Tavassoli FA. **Allelic losses at 3p and 11p are detected in both epithelial and stromal components of cervical small cell neuroendocrine carcinoma.** *AIMM* 2001, 9:340-345.
47. Bissell MJ, Radisky DC, Rizki A, Weaver VM, Petersen OW: **The organizing principle: microenvironment influences in normal and malignant breast.** *Differentiation* 2002, 70: 537-546.
48. Ponder BA: **Cancer genetics.** *Nature* 2001, 411:336-341.
49. Man YG, Ball WD, Culp AJ, Hand AR, Moreira JE: **Persistence of a perinatal cellular phenotype in the ducts of adult glands.** *J Histochem Cytochem* 1995, 43(12):1203-1215.
50. Man YG, Ball WD, Marchetti L, Hand AR: **Contributions of intercalated duct cells to normal parenchyma of submandibular glands of adult rats.** *Anat Rec* 2001, 263:202-214.
51. Bezwoda WR: **C-erb-B2 expression and response to treatment in metastatic breast cancer.** *Mod Onco* 2000, 17:22-28
52. Man YG, Zeng X, Shen T, Vang R, Barner R, Wheeler DT, Vihn T, Liang CY, Strauss BL: **Cell clusters overlying focally disrupted myoepithelial cell layers and their adjacent counterparts within the same duct display a different pattern of mRNA expression.** *Mod Pathol* 2004, 17 (supplement1): 40-41a.

### **Figure Legend**

Figure 1. Morphologic and immunostaining profiles of cell clusters overlying focally disrupted ME cell layers

Paraffin-embedded breast tissue sections were double immunostained for ME cells with an antibody to smooth muscle actin (red) and tumor cells with several proliferation related markers (brown or black).

1a & 1b: ER, PCNA, p27, Ki-67, cyclin A, cyclin D + SMA. 1a: 200X; 1b: 400X

1c – 1f: ER, p27, Ki-67, cyclin A, cyclin D + SMA. 400X.

1g & 1h: ER, PCNA, p27, Ki-67, cyclin A, cyclin D + SMA, 100X.

Arrows identify cell clusters that are devoid of the expression of proliferation related markers.

Figure 2. The lack of proliferation related markers in cell clusters overlying focally disrupted ME cell layers

A set of consecutive paraffin-embedded breast tissue sections were singly or double immunostained for ME cells with an antibody to smooth muscle actin (red) and tumor cells with several proliferation related markers (brown or black).

2a: BP1; 2 b: ER + SMA; 2c: Ki-67 + SMA; 2d: p27 + SMA; 2e: PCNA + SMA; 2f: cyclin A + SMA; 2g: Cyclin D + SMA; 2h: c-erb-B2 (brown) + MMP-26 (red).

Arrows identify cell clusters that are devoid of the expression of proliferation related markers.

Figure 3. The expression status of MMP-26, BP1 and cytokeratins in cell clusters overlying focally disrupted ME cell layers

3a & 3b: BP1. 3a: 100X; 3b is a higher magnification of 3a, 300X.

3c & 3d: MMP-26 (brown) + SMA (red). 3c: 100X; 3d is a higher magnification of 3c, 300X

3e. BP1; 3f. MMP-26; 3g. cytokeratins 5 & 8; 3h. cytokeratins AE1/AE/3; 200X

Arrows identify non-immunoreactive cell clusters.

Figure 4. The expression of c-erb-B2 in cell clusters overlying focally disrupted ME cell layers.

4a & 4b: BP1& SMA (red) + c-erb-B2 (brown). 4a: 150X; 4b is a higher magnification of 4a, 400X

4c & 4d: MMP-26 & SMA (red) + c-erb-B2 (brown); 4d is a higher magnification of 4c, 400X.

Arrows identify c-erb-B2 positive cell clusters.

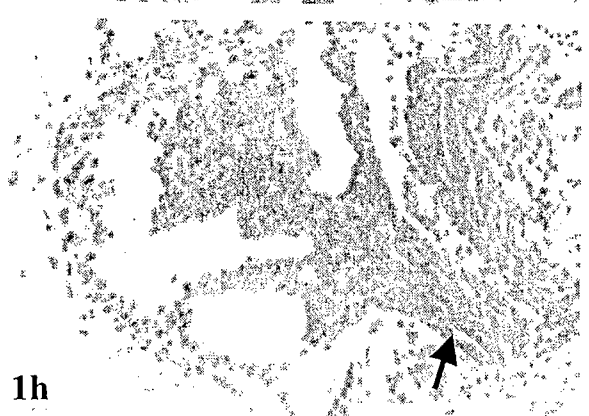
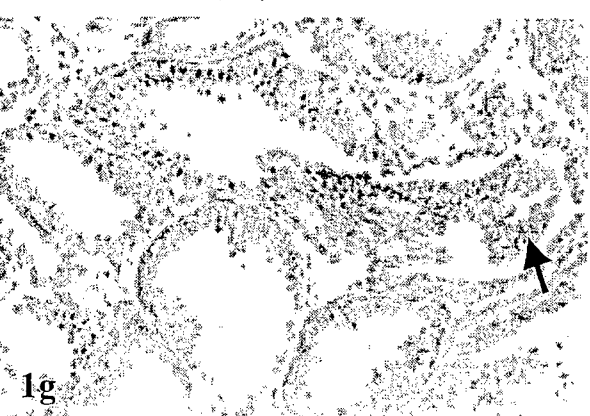
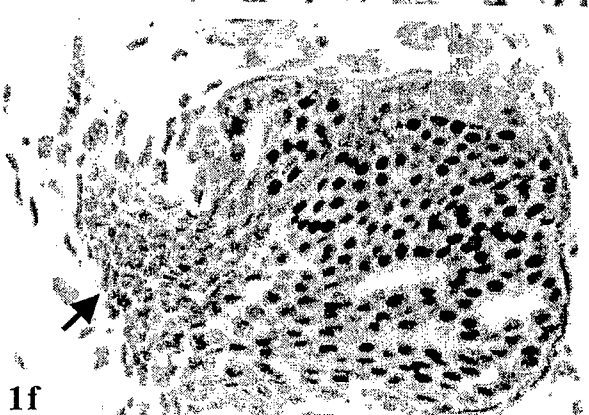
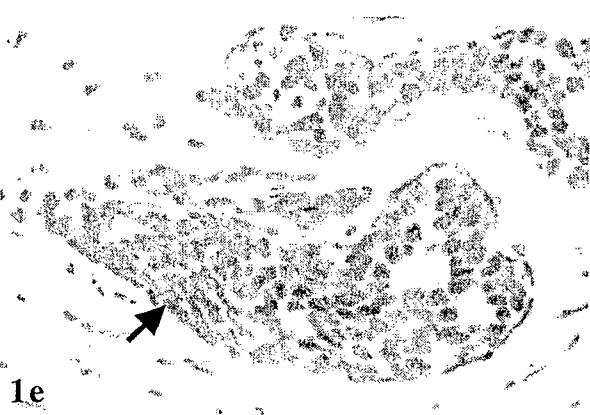
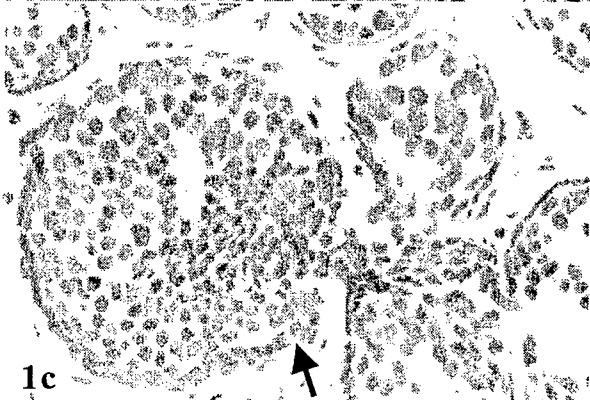
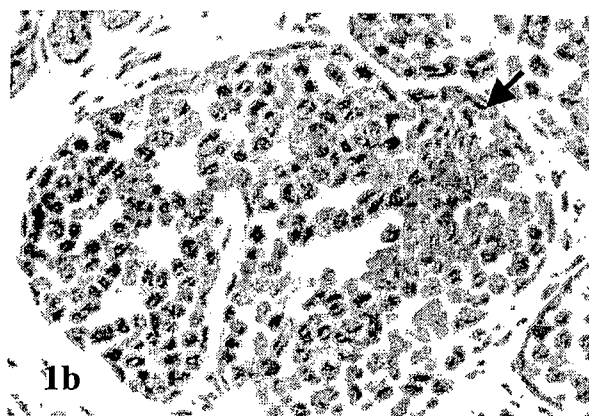
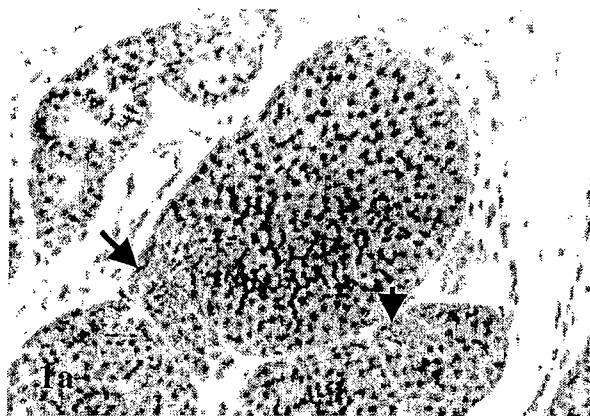
Figure 5. Localization of ER negative cell clusters within blood vessels-like structures

5a – 5f. ER, Ki-67, cyclin A (brown) + SMA (red). 200X

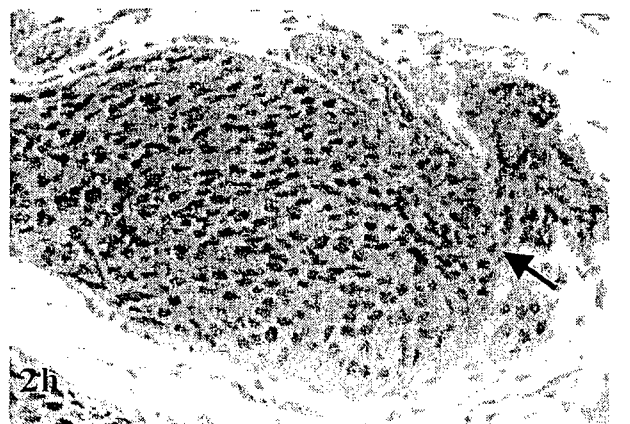
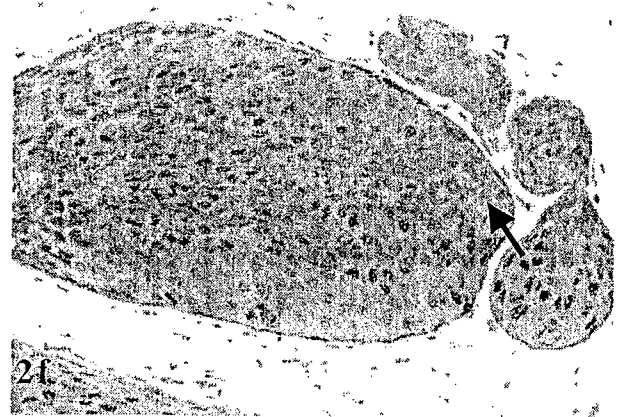
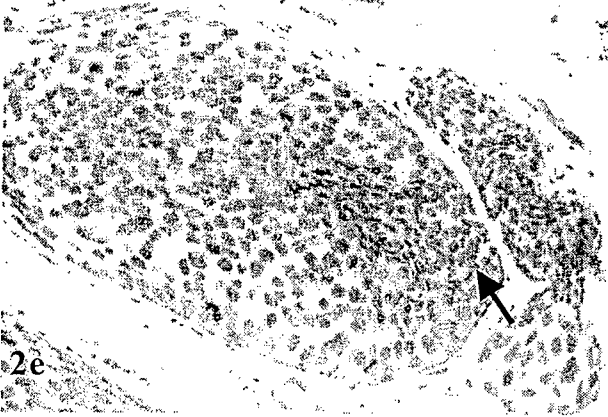
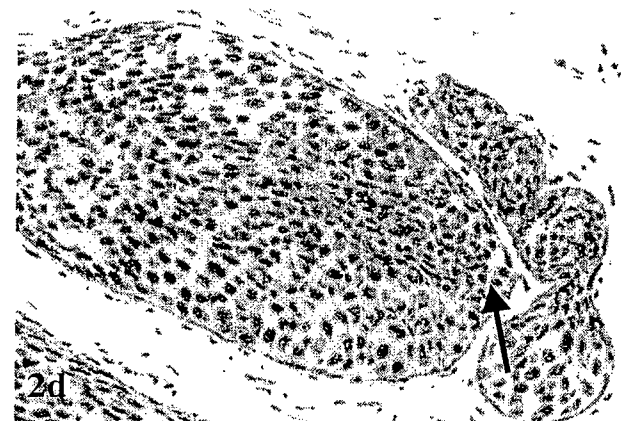
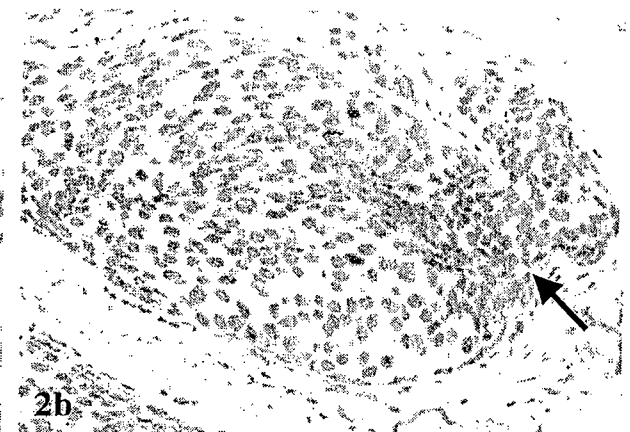
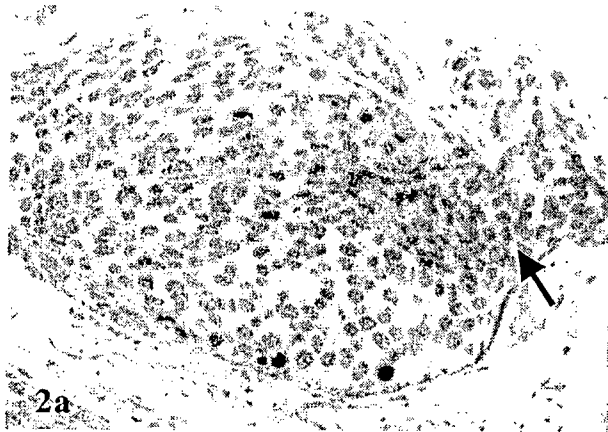
5g . A adjacent (but discontinues) of 5f, cytokeratin 8 (red) + p63 (brown)

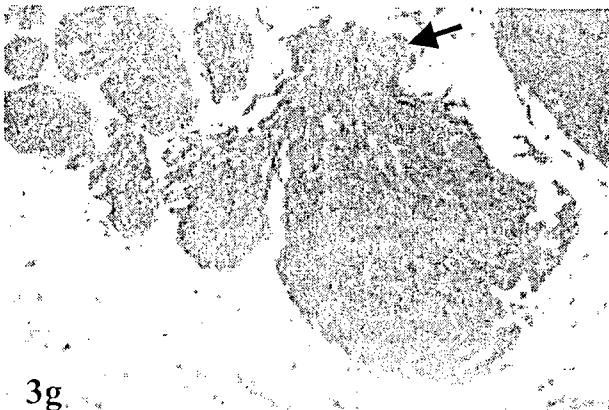
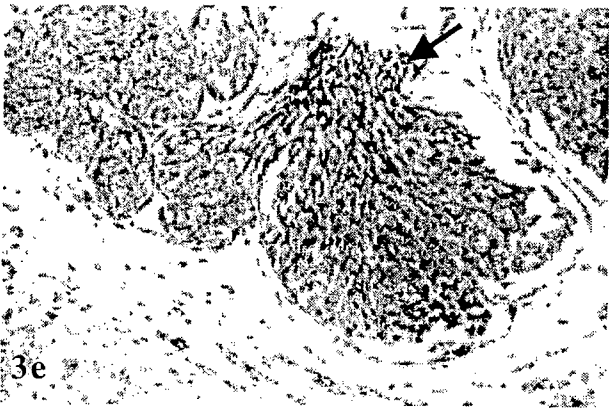
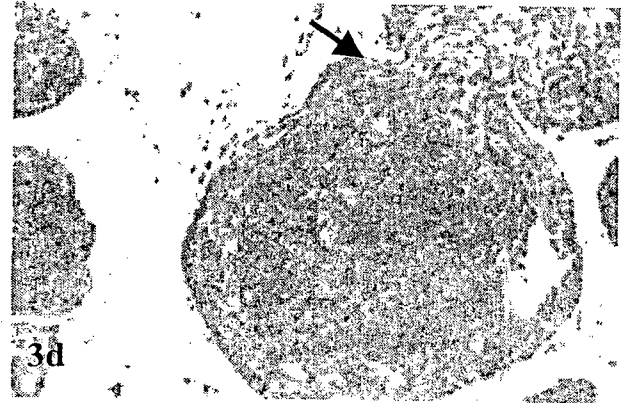
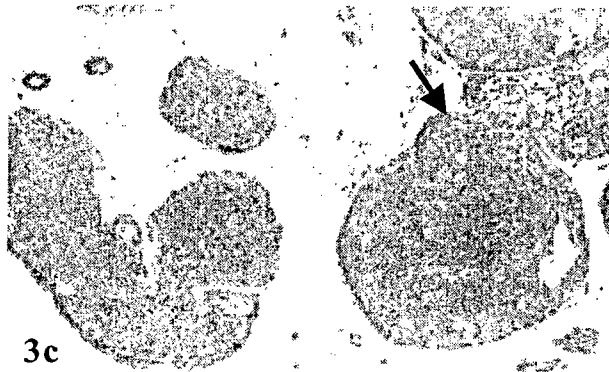
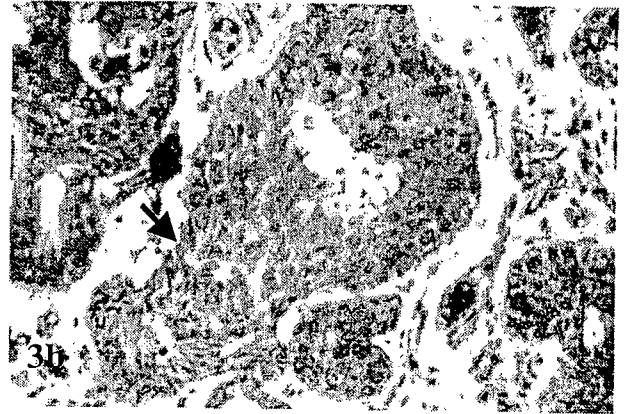
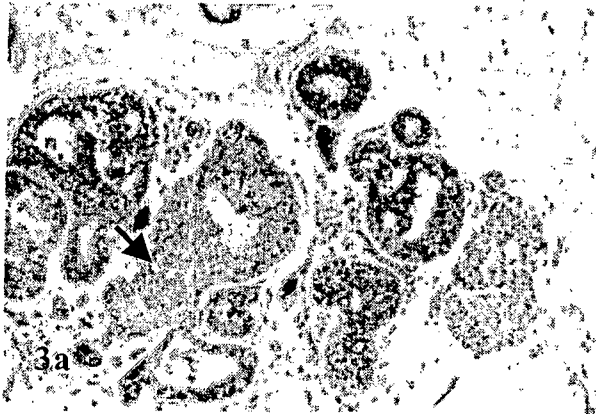
5h. The adjacent section of 5g, cytokeratin 8 (red) + CD31 (brown)

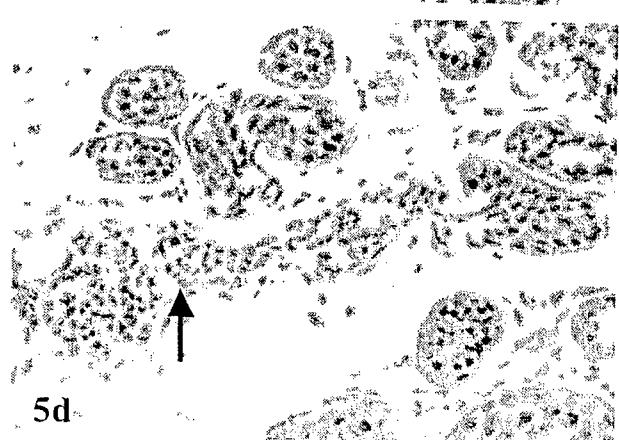
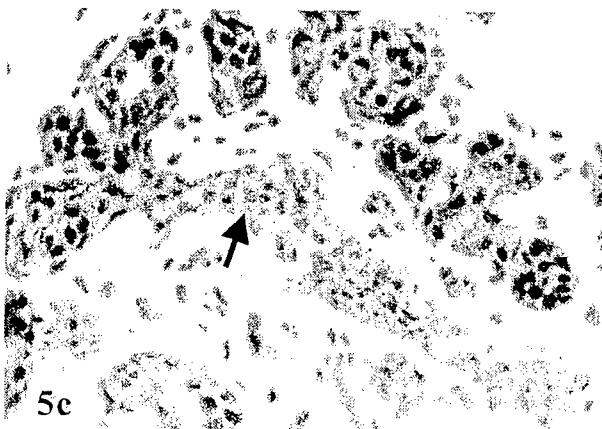
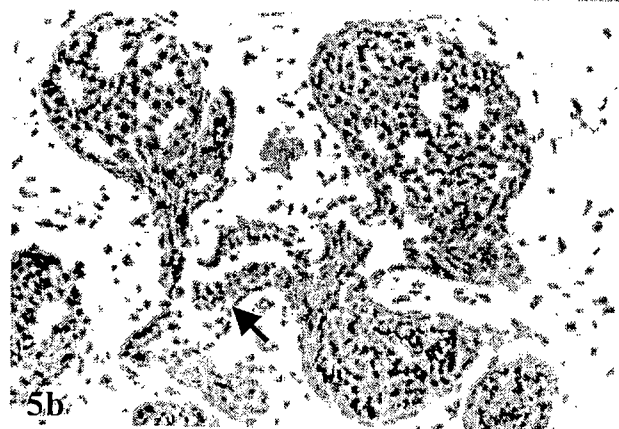
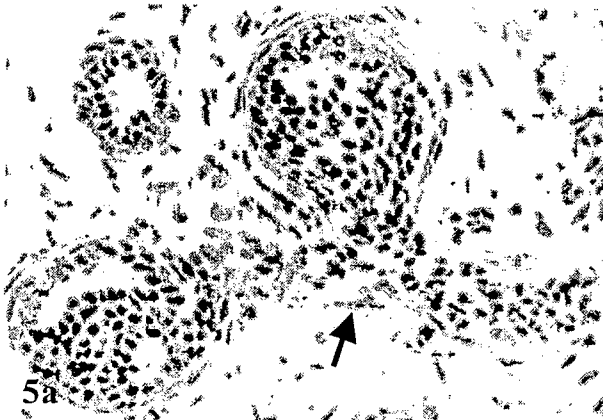
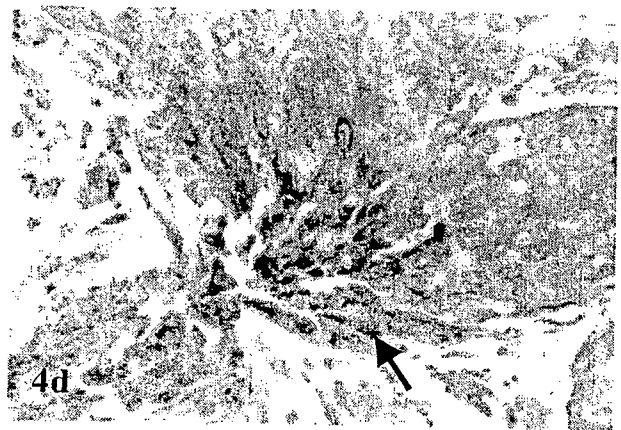
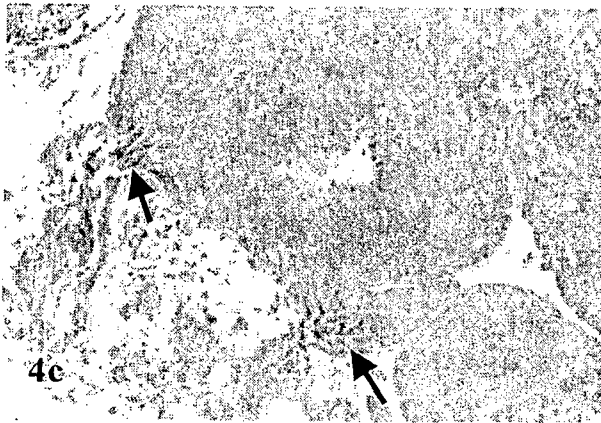
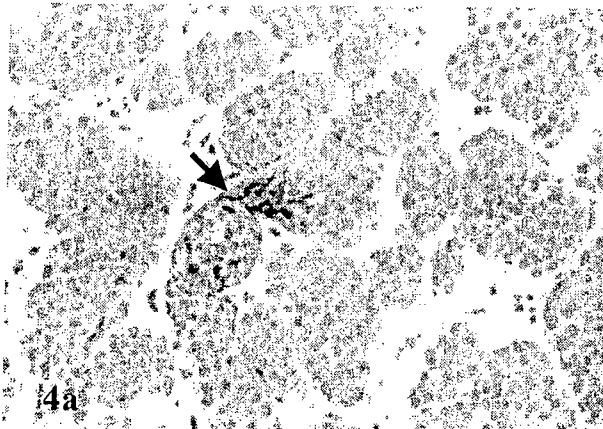
Arrows identify tube-like structures. Thin arrows identify the ME cell layers. Note that cells within these tube-like structures have a non-cohesive or “floating” appearance.











# **The significance of focal myoepithelial cell layer disruptions in breast tumor invasion: Implications from MMPI trials and our recent studies**

Yan-gao Man<sup>1</sup>, MD., PhD., Qing-xiang Amy Sang<sup>2</sup>, PhD.

<sup>1</sup>Department of Gynecologic and breast Pathology, Armed Forces Institute of Pathology and American Registry of Pathology, Washington DC

<sup>2</sup>Department of Chemistry and Biochemistry, Florida State University, Tallahassee, FL

## Address of corresponding author:

Qing-xiang Amy Sang, PhD.

Dept. of Chemistry and Biochemistry

Florida State University

Tallahassee, FL

Tel: 850-644-8683

Yan-gao Man, MD., PhD

Dept. of Gynecologic and Breast Pathology

Armed Forces Institute of Pathology

Washington DC 20306-6000

Tel: 202-782-1612; Fax: 202-782-3939

The opinions and assertions contained herein represent the personal views of the authors and are not to be construed as official or as representing the views of the Department of the Army or the Department of Defense.

## **Summary**

The normal human breast epithelium and the stroma are physically separated by the basement membrane and a layer of myoepithelial cells, whose degradations are an absolute pre-requisite for breast tumor invasion. It has been generally accepted that the degradation of the basement membrane is attributed, primarily, if not solely, to an over-production of proteolytic enzymes by the tumor or stromal cells, while the cause and early sign of myoepithelial cell layer degradations are elusive. Our recent studies revealed that a subset of non-invasive breast tumors contained focal disruptions in their myoepithelial cell layers. Focal disruptions in myoepithelial layers were associated with substantial immunohistochemical and genetic alterations in the overlying tumor cells, including the loss of estrogen receptor expression, a significantly higher frequency of loss of heterozygosity, and a significantly higher expression of cell cycle and invasion related genes. Focal ME layer disruptions were also associated with a significantly higher rate of leukocyte infiltration and cell proliferation at or near the focal disruptions. These and other findings have promoted the introduction of a novel hypothesis that a localized death of myoepithelial cells and subsequent immunoreactions might be a direct trigger factor for myoepithelial layer disruptions and subsequent tumor invasion.

## **I. Introduction**

The epithelium of normal human breasts and *in situ* breast tumors is physically separated from the stroma by both the myoepithelial (ME) cell layer and basement membrane, whose degradation is an absolute pre-requisite for tumor invasion and metastasis. A generally accepted hypothesis for the direct cause of basement membrane degradations and tumor invasion has been attributed primarily, if not solely, to the over-production of proteolytic enzymes by the tumor or stromal cells (Goldfarb and Liotta, 1986). This hypothesis alone, however, may not reflect the complete intrinsic mechanisms of these events for three main reasons: [1] The ME cell layer is a normal structural constituent, which should not be the target of the host's own enzymes; [2] Neither the normal cellular kinetics nor the dynamic alterations of ME cells during tumor invasion have been elucidated; [3] Although results from *in vitro* tests and animal models have clearly demonstrated that protease inhibitors could effectively inhibit or prevent tumor invasion, results from protease inhibitor-based clinical trials have been very disappointing (Coussens et al., 2002; Matrisian et al., 2003).

Based on these reasons, this article attempted to elucidate the biologic and clinic profiles of ME cells based on previously published reports, and to assess the potential significance of ME cells in tumor progression and invasion. In addition, this article attempted to present several unique findings from our recent studies, on the correlation between the structural integrity in ME cell layers and the genetic and immunohistochemical profiles in adjacent tumor cells. These unique findings and other supportive data have led to the introduction of a novel hypothesis that the ME cell layer and basement membrane degradations and subsequent tumor invasion are triggered by a localized ME cell death and resultant leukocyte infiltration and immunoreactions. The rationale and speculated steps for our hypothesis are summarized and discussed.

## **II. The normal distribution, morphology, and functions of myoepithelial cells**

The normal human breast consists of two major components, the epithelium and stroma. The epithelium contains two cell types: the ME cells and luminal cells, which compose both the secretory lobules and branching ducts. ME cells are inter-positioned between the luminal cells and basement membrane, attaching to them by desmosomes and hemidesmosomes, respectively (Tsubura et al., 1988; Slade et al., 1999; Jolicoeur et al., 2002). The basement membrane is composed of a group of fibrous proteins embedded in a hydrated polysaccharide gel, forming a continuous lining surrounding ME cells (Nerlich, 1995; Miosge, 2001). ME cells are joined by intercellular junctions and adhesion molecules, forming a continuous layer that encircles the entire duct system, and a discontinuous layer or a basket-like structure that covers a vast majority of the cells at terminal duct-lobular units and lobules. Both the ME layer and basement membrane are normal structural constituents, physically separating the epithelium from the stroma (Fig 1).

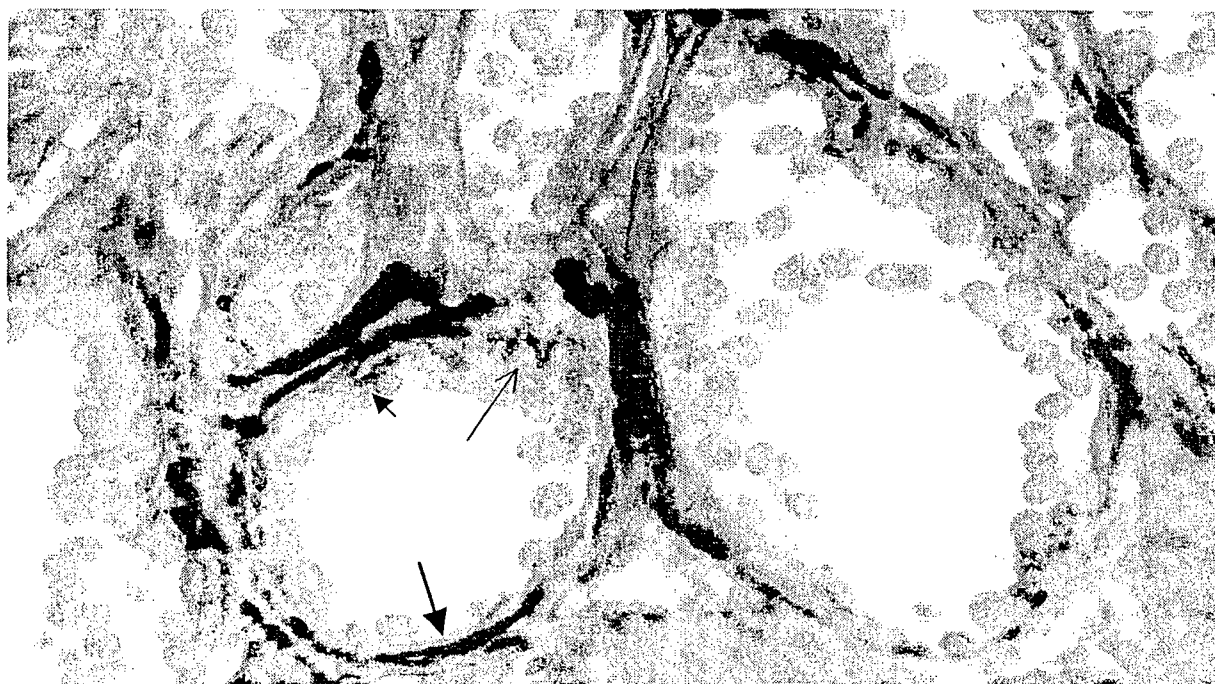


Fig 1. The architectural relationship of the basement membrane, ME cells, and epithelial cells. A paraffin section double immunostained for ME cells and basement membrane with anti-smooth muscle actin (red) and collagen IV (brown) antibodies. The arrow identifies the basement membrane, a thin arrow for a ME cell, and a arrow head for a epithelial cell.



In clear-cut normal breast tissues, ME and epithelial cells are roughly equal in number, and ME cells are generally of cuboid or spindle shape with pale cytoplasm and nuclei. The number and morphology of ME cells, however, vary substantially at different stages of tumor evolution. In hyperplastic and *in situ* lesions, ME cells are often substantially attenuated or stretched out with scanty or no distinct cytoplasm (Fig 2), morphologically resembling smooth muscle cells of small blood vessels and fibroblasts. In invasive lesions and a rare benign lesion, microglandular adenosis, ME cells are not appreciable or occasionally found in residual normal tissues trapped in these lesions. Under an electromicroscope, ME cells contain a large amounts of both micro-filaments, the unique structural constitute of smooth muscle cells, and intermediate filaments, the unique structural constitute of epithelial cells (Murad and Haam, 1986).

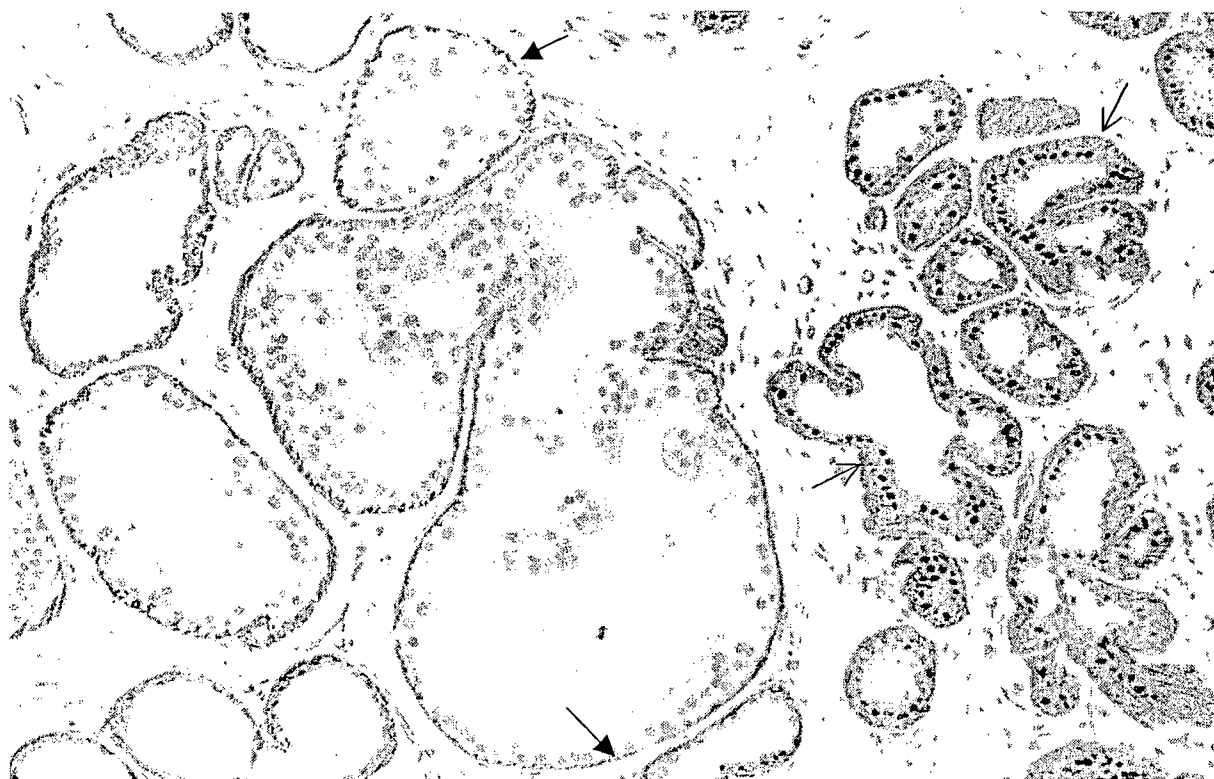


Fig 2. The morphology and ratio of ME cells to epithelial cells vary at different tumor stages. A paraffin section double immunostained for estrogen receptor (black) and smooth muscle actin (red). The ME cell layers in the *in situ* tumorous ducts are attenuated (arrows), compared to those in the normal ducts (thin arrows).



This architectural feature confers the ME cells and basement membrane two essential biological and clinical functions. First, as the normal epithelial component is devoid of blood vessels and lymphatic ducts and totally depends on the stroma for its metabolism and survival needed materials, the ME cells and basement membrane are the nature structural barriers that directly mediate the communications between these two cellular components. Second, cells of *in situ* tumors have to first pass through the ME cell layer, then, the basement membrane, to physically reach the stroma. In another word, the degradation of both the ME cell layer and basement membrane is an absolute pre-requisite for tumor invasion (Fig 3).

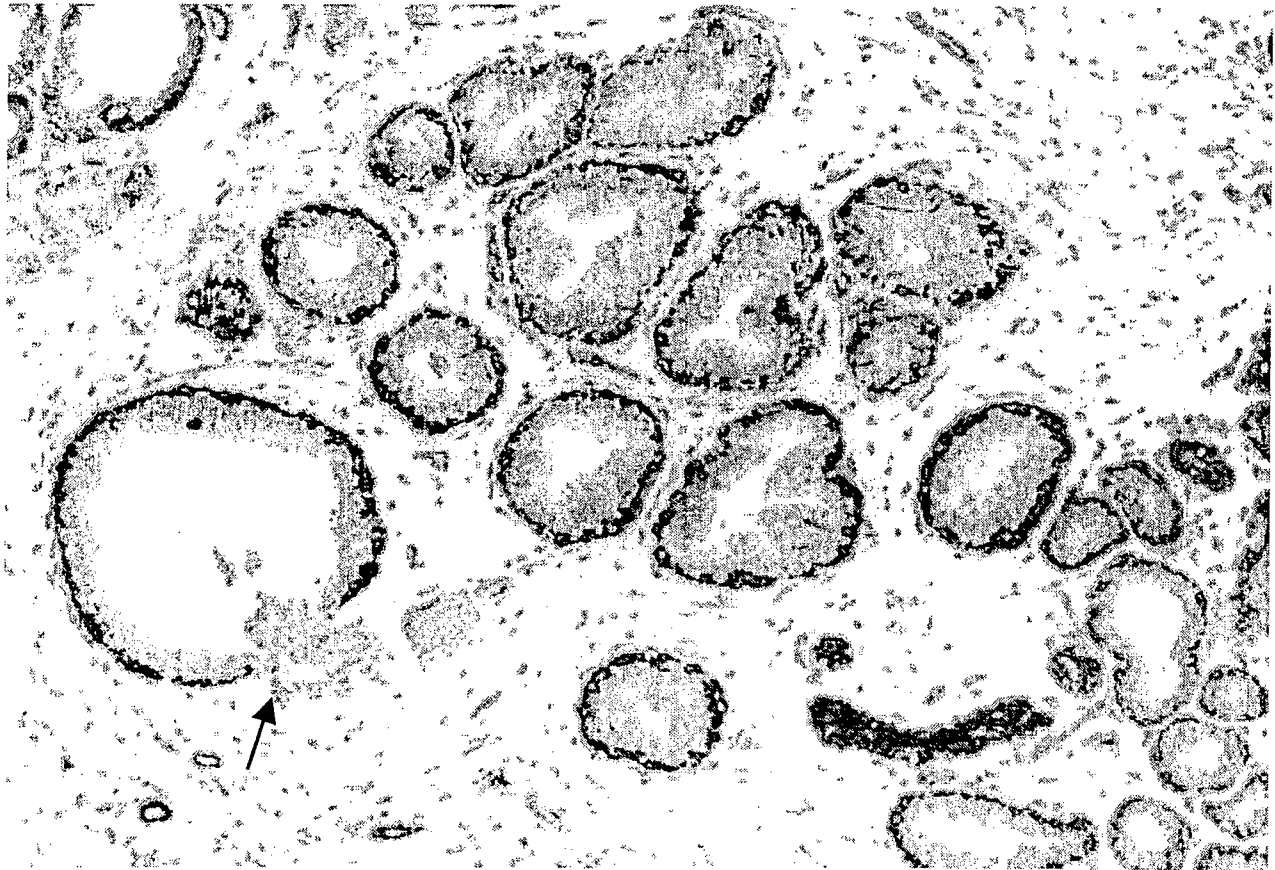


Fig 3. The degradation of both the ME cell layer and basement membrane is needed for invasion. A paraffin section immunostained for smooth muscle actin plus collagen IV (red). Note that the ME cell layer and basement membrane in one duct is focally disrupted and the epithelial cells are in direct contact with the stroma (a arrow).

In addition to these passive functions, recent studies have revealed that ME cells might also possess the following active or “voluntary” functions.

1. Production of tumor suppressor proteins

A number of tumor suppressor proteins, including maspin, Wilms' tumor 1, p63, p73, and 14-3-3Sigma have been detected exclusively or preferentially in ME cells (Sternlicht et al., 1997; Zhang et al., 2003; Yang et al., 1999; Yamamoto et al., 2001; Simpson et al., 2004). In vitro and/or in vivo studies have demonstrated that these proteins have significant inhibitory functions on tumor growth and invasion (Sternlicht et al., 1997; Yang et al., 1999; Simpson et al., 2004).

2. Paracrine down-regulation of matrix metalloproteinase (MMP) expression

It has been speculated that ME cells may modulate breast tumor invasion by controlling the expression of MMP in both tumor and surrounding fibroblasts. To explore this possibility, a recent study quantitatively compared the MMP expression levels in breast cancer cell lines and fibroblasts co-cultured with and without ME cells purified from normal breasts (Jones et al., 2003). Results revealed that both cancer cells and fibroblasts co-cultured with the ME cells had a significantly lower MMP expression level, compared to those without ME cells, and that the reduction of MMP expression was accompanied by a reduced invasion (Jones et al., 2003).

3. Turnover of extracellular matrix (ECM)

While most of the ECM-degradation enzymes found in the breast are manufactured by the stromal cells, several such enzymes, including a recently described angiogenesis-related matrix metalloproteinase, MMP-19, are reported to be produced by normal ME cells (Djonov et al., 2001). These ECM degradation enzymes produced by the ME cells are expected to participate in the turnover of ECM (Djonov et al., 2001; Gudjonsson et al., 2002).

4. Regulation of normal development

During the normal development, a number of growth factors and their corresponding receptors, including the epidermal growth factor, basic fibroblast growth factor and its receptor, Tcf transcription factors, and transforming growth factors, are differentially expressed in the luminal and ME cells (Moller et al., 1989; Deugnier, 1999; Gomm et al., 1997; Roose et al., 1999). A perturbed expression of these and other related molecules in the ME cells led to abnormal morphogenesis and development of the breast (Deugnier, 1999; Gomm et al., 1997).

#### 5. Establishment and stabilization of the polarity of the bilayer epithelial structure

In the tissue cultures, the luminal cells alone could form acinus-like structures, while with a reversed polarity (Gudjonsson et al. 2002). The addition of ME cells from the normal breasts could establish and stabilize a correct polarity, whereas ME cells from breast tumors failed to correct the reversed polarity, suggesting that ME cells play important roles in establishment and stabilization of the bilayer epithelial structure cultures, the luminal cells alone could form acinus-like structures, while with a reversed polarity (Gudjonsson et al. 2002).

#### 6. Steroid hormone metabolism

A recent study assessed the mRNA expression and enzymatic activity of steroid sulfatase (STS) in human breast ME and MCG-7 cells, and the effects of 17-beta estradiol on the activity of STS (Tobacman et al. 2002). The study revealed that the sulfatase activity was about 120 times greater in the ME than in the MCF-7 cells, and that exposure to 17-beta estradiol was associated with 70% reduction of the sulfatase activity in the MCF cells, while 9% increase in ME cells, suggesting a potential role of ME cells in converting hormone precursors into active steroid hormones (Tobacman et al. 2002).

### **III. Exclusively or preferentially expressed bio-molecules in myoepithelial cells**

Currently, there are more than a dozen of commercially available antibodies that can be used for immunohistochemistry in formalin-fixed, paraffin-embedded sections, to elucidate the molecules reported to be exclusively or preferentially present in ME cells. Based on their compositions, subcellular localizations, and potential functions, these molecules can be roughly classified into two groups.

*a. Structure-specific proteins (related to microfilaments and intermediate filaments)*

1. Smooth muscle actin (SMA)

SMA is one of microfilamentous contractile polypeptides and presents in the cells with myogenous features. In human breast tissues, SMA immunostaining is present in the cytoplasm of about 95% of the ME cells in the normal ducts and lobules, as well as in non-invasive breast lesions (Bose et al., 1999; Joshi et al., 1996). The invasive lesions and a very rare benign lesion, microglandular adenosis, are devoid of SMA immunoreactivity, due to the lack of ME cells surrounding these lesions. A false positive SMA staining is not uncommon, due to the cross immunoreactivity with smooth muscle cells of small blood vessels and myofibroblast cells of the stroma that are often adjacent to the invasive components.

2. Smooth muscle myosin heavy chain (SMMHC)

SMMHC is a cytoplasmic structural protein that is a major component of the contractile apparatus of smooth muscle cells. This protein is specific for the early development of smooth muscle. It is also a myoepithelium-associated protein, heavily present in the ME cells of normal and benign breast tissues, and has been reported to be a very useful marker in differentiation between noninvasive and invasive breast lesions (Yoshida, 1998; Dabbs and Gown, 1999).

3. Calponin

Calponin, a calmodulin, binds tropomyosin and F-actin and is thought to be involved in the regulation of smooth muscle contraction. The expression of calponin is restricted to smooth muscle cells, and has also been demonstrated in human breast ME cells. It is a useful marker in differentiation between ME cells and spindle cells of the stroma, and non-invasive and invasion lesion (Damiani et al., 1999; Dabbs and Gown, 1999). However, Calponin staining in ME cells may be occasionally discontinuous or absent in *in-situ* ductal lesions (Ohyabu et al., 1998).

#### 4. H-caldesmon (HCD)

HCD is a cytoskeleton-associated actin-binding protein. In human breast tissues, HCD is predominantly expressed in ME cells, while a high level of HCD expression is also often seen in smooth muscle cells of small blood vessels (Miettinen et al., 1999; Batistaton et al., 2003).

#### 5. P-cadherin

p-cadherin, like the E-cadherin, is a  $\text{Ca}^{2+}$ -dependent cell adhesion molecule with a fundamental role in the maintenance of the integrity of multicellular structures and the phenotype of epithelial cells (Shimoyama et al., 1989). In breast tissues, p-cadherin is preferentially expressed in ME cells of normal ducts, lobules, and sclerotic lesions (Jarrard et al., 1997). However, p-cadherin is also occasionally seen in a portion of tumor cells of hyperplasias and *in situ* carcinomas (Soler et al., 1999).

#### 6. Cytokeratins 5, 7, 14, and 17

Cytokeratins 5, 7, 14, and 17 are a group of cellular structural proteins in epithelial cells and cells with epithelioid features (Moll et al., 1982). In human breast tissues, these molecules are predominantly present in myoepithelial cell layer (Wetzels et al., 1989, 1991;). CK-17 is also related early skin development and wound repairing (McGowan and Coulumbe, 1998).

#### *b. Non-structure-restricted molecules*

### 1. Maspin

Maspin, or mammary-specific serpin, is a tumor suppressor protein, which belongs to the serine proteinase inhibitor family (Maass et al., 2000; Zhang et al., 2000). It is present in both breast and prostate glands. In the breast, maspin is predominantly a soluble cytoplasmic protein that is consistently detectable in normal human ME cells and ME-derived tumors (Maass et al., 2002; Reis-Filho et al., 2001). The expression of maspin decreases with increasing malignancy of the breast tumors (Maass et al., 2002; Reis-Filho et al., 2001). Both in vitro and in vivo studies have shown that maspin has significant inhibitory functions on tumor growth and invasion (Maass et al., 2000; Zhang et al., 2000).

### 2. Wilms' tumor 1 (WT-1)

WT-1 functions as a transcription factor regulating gene expression in a similar fashion as the p53 (Scharnhorst et al., 2001). The expression of WT-1 in the breast appears to correlate with the behavior and progression of breast tumors (Fabre et al., 1999). Our previous study showed that WT-1 expression was also consistently detectable in ME cell, and that the level of WT-1 expression was inversely correlated with breast tumor progression (Man et al., 2003).

### 3. p63 and p73

p63 is a nuclear protein that shares a significant amino acid identity with the p53 protein in the transactivation domain, the DNA binding domain, and the oligomerization domain. The expression of p63 in the breast is exclusively detectable in the nuclei of ME cells, and neither the stromal fibroblasts nor vascular smooth muscle cells shows p63 immunostaining (Barbareschi et al., 2001). p63 is believed to be critical for maintaining the progenitor cell populations that are necessary to sustain epithelial development and morphogenesis (Yang et al., 1999). p73 is also a

an homologue of p53, and is believed to have a similar function and distribution as p63 (Yamamoto, et al., 2001).

#### 4. 14-3-3Sigma

This is a recently introduced novel ME cell marker (Simpson et al., 2004). This protein was reported to be consistently present in benign and pre-invasive breast lesions, and might also to a novel prognostic factor (Simpson et al., 2004).

#### 5. Neuropilin-1 (NRP-1)

NRP -1 is a recently identified specific receptor for vascular endothelial growth factor (Stepheson et al., 2002; Fakhari et al., 2002). The ME cells in both hyperplastic and neoplastic lesions displayed a higher level of NRP-1 expression than those in the normal breast, and NRP-1 expression is also detectable in the vascular smooth muscle and endothelial cells (Stepheson et al., 2002; Fakhari et al., 2002).

#### 6. CD 10

CD10 is a 100kD cell surface metalloendopeptidase named neprilysin, which inactivates a variety of biologically active peptides. This protein was initially classified as a common acute lymphoblastic leukemia antigen. Subsequent studies have shown that CD10 was consistently positive in ME cells of all normal breast tissue, whereas the number of ME positive cells and the intensity of the immunostaining were substantially reduced in distended ducts and ductal adenomas (Moritani et al., 2002; Iwaya et al., 2002; Yaziji et al., 2000).

#### 7. S100

S100 is an EF-hand  $\text{Ca}^{2+}$  -binding protein, originally isolated from neural tissues. S100 is consistently present in human breast ME cells, but is also often expressed in some luminal epithelial cells (Gillett et al., 1990; Dwarakanath et al., 1987; Lunde et al., 1987).

## 8. Other important molecules

A number of growth factors, growth factor receptors, and other biologically important molecules have also been reported to be present in ME cells (Moller et al., 1989; Deugnier., 1999; Gomm et al., 1997; Roose et al., 1999), while the clinic significance is unknown.

## **IV. ME cell lesions, morphologic and immunohistochemical alterations**

Compared to epithelial lesions, ME cells lesions are very rare, which prevents a detailed biological and clinical profiling of this entity. Morphologically, ME cell lesions can be roughly classified into three categories.

### 1. Myoepitheliosis

This lesion is characterized by a mild proliferation of ME cells within and around ducts. The proliferating cells are of spindle or cuboid shape, often distending or occluding the involved ducts. These ME cells can be easily differentiated from the involved ductal epithelial cells by immunohistochemical staining with antibodies to microfilaments and intermediate filaments related molecules, as well as epithelial specific antigen (ESA), as the former are uniformly reactive to all microfilaments-related antibodies, while the later are uniformly reactive to ESA.

### 2. Adenomyoepithelioma

This lesion is characterized by extensive proliferation of ME cells. Morphologically, these proliferating cells can be divided into spindle cell, tubular, and lobulated variants. The common feature of these variants is the formation of solid masses that distend or occluded the duct structures. Similar to myoepitheliosis, these hyperplastic lesions can be easily differentiated from epithelial cells by immunohistochemical staining with antibodies to microfilaments and intermediate filaments related molecules, as well as epithelial specific antigen (ESA).



### 3. Myoepithelial carcinoma

This lesion is rare, accounting for less than 1% of the breast malignancies. Based on published reports, the most commonly seen type of this lesion is of spindle cell type. This lesion is believed to be generally not clinically aggressive, while examples of metastases from pure ME carcinoma have been reported (Tavassoli, 1991; Schurch et al., 1985; Thorner et al., 1986).

Immunohistochemically, above ME cell markers have been routinely used in the clinic for elucidation of ME cells in differentiation between *in situ* and invasive tumors. Among these, SMA is most frequently used and is considered to be very reliable. We and others, however, have repeatedly noticed that about 4-6% of morphologically distinct ME cells in H & E stained sections fail to show SMA immunostaining (Bose et al., 1999; Joshi et al., 1996). In an attempt to further characterize these SMA negative cells, one of our recent studies assessed the H & E and SMA immuno-stained sections from 175 breast cancer patients, and identified 3 cases that harbored ducts, which displayed morphologically distinct ME cell layers in H & E sections, while showed no SMA immunostaining in  $\geq 1/3$  or the entire ME cell layer (Zhang et al., 2003). Additional 8 consecutive sections from each of these cases were stained for SMA with a black chromogen, and the same ducts with SMA negative ME cells in each of the 8 sections were photographed. Then, each section was re-stained for one of 8 additional markers that are supposed to exclusively or preferentially expressed in ME cells, with a red chromogen. The same duct with SMA (-) cells in each of the 8 sections were re-examined for the expression of other markers. Results showed that SMA negative ME cells in two cases also failed to display immunoreactivity for other markers, including Calponin, CD10, smooth muscle myosin-heavy chain (SMMHC), maspin, Wilms' tumor-1, and cytokeratins 5, 14, and 17 (CK5, 14, and 17).

SMA negative ME cells in one case, however, showed distinct immunoreactivities for maspin, CK5, 14, and 17 (Fig 4).

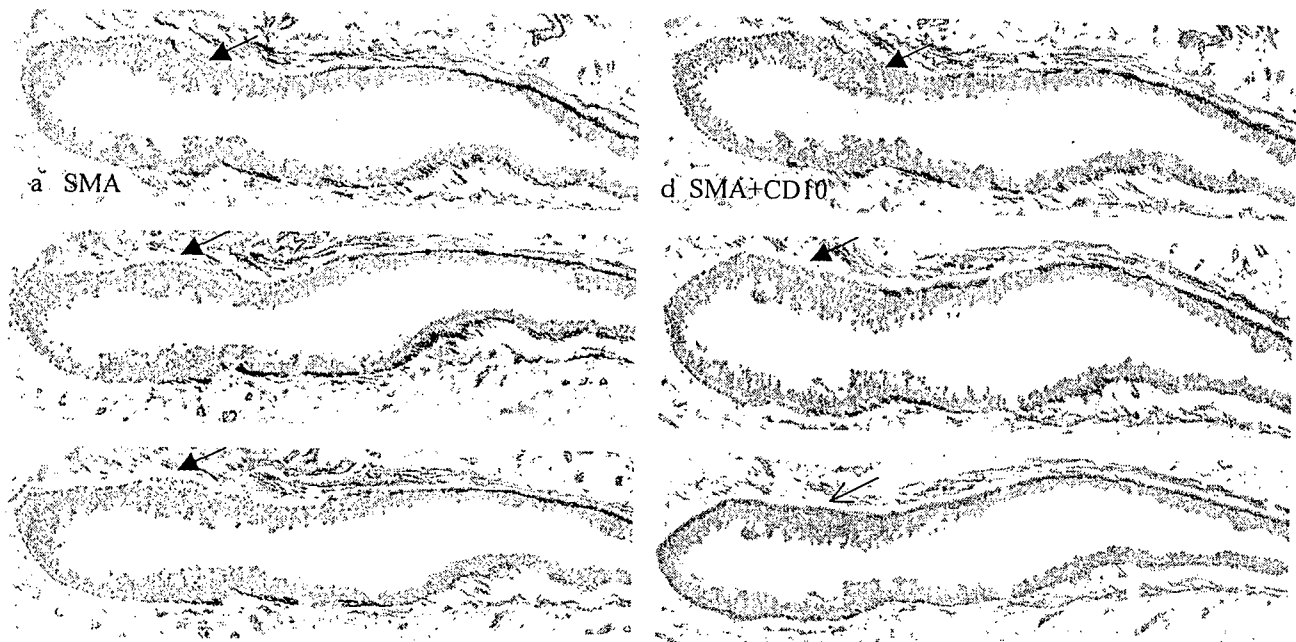


**Fig 4.** The absence of the expression of multiple ME phenotypic markers  
Consecutive sections were double immunostained for smooth muscle actin (brown) plus a panel of additional ME cell markers. Note that about 1/3 of the ME cell layer in a duct is devoid of SMA expression, as well as several other markers, including SMMHC, calponin, CD10, and WT-1 (a-e, arrows). These ME cells, however, are positive for CK 5 (f, a thin arrow), maspin, CK 14, and 17 (not shown).

#### **V. Impacts of ME cell alterations on adjacent epithelial cells**

While attempting to identify the early sign of ME layer disruptions and precursor of invasive breast lesions, we have recently carried out a number of studies, focusing on the correlation between the structural integrity in ME cell layers and the immunohistochemical and genetic profiles in adjacent epithelial cells. Our studies have revealed, for the first time, several lines of evidence, suggesting that the structural integrity of ME cells directly impact epithelial cells' biologic presentations and tumor progression and invasion process.

1. Focal ME layer disruptions and loss of ER expression in overlying cells are correlated events.

In 5,698 duct cross sections from 220 patients with estrogen receptor (ER) positive, *in situ* breast tumors, we detected a total of 405 focal ME cell layer disruptions, defined as the absence of ME cells resulting in a gap equal to or greater than the combined size of 3 ME cells (Man et al., 2003). Of these, 350 (86.4%) were overlaid by clusters of cells with no or substantially reduced ER expression, in a sharp contrast to adjacent cells within the same duct, which showed strong ER immunoreactivity and overlaid a non-disrupted ME cell layer (Fig 5; Table 1).

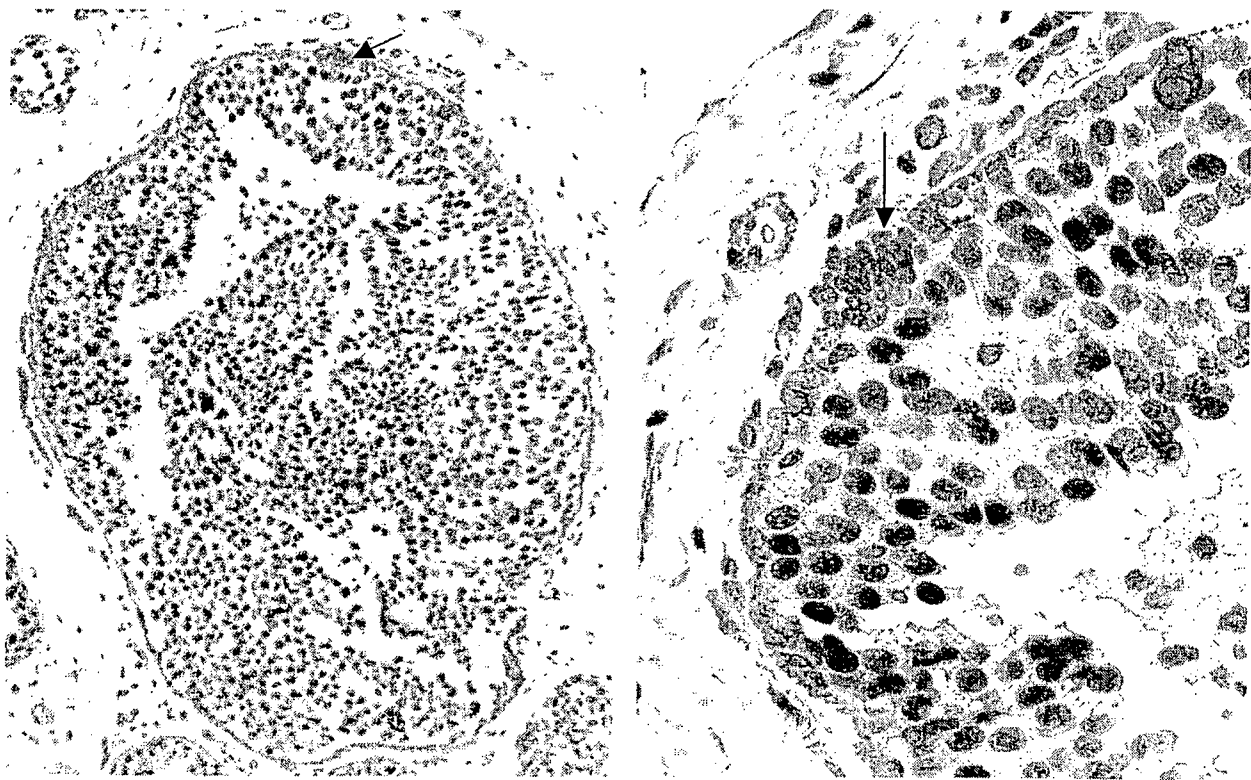


Fig 5. Focal disruptions in ME cell layers and loss of ER expression in overlying tumor cells. A paraffin section double immunostained for ER (black or brown) and SMA (red). Arrows identify focal ME disruptions and overlying ER negative cell clusters.

Table 1. Frequency of ME cell layer disruptions and the status of ER expression

Total sections	Total disruptions	ER (-) clusters	ER (+) clusters	p
5,698	405(7.1%)	305(86.4%)	55(13.6%)	< 0.01

2. Cells in ducts with and without focal ME disruptions have different proliferation rates.

Compared to those in morphologically comparable ducts without focal ME layer disruptions, cells in ducts with focally disrupted ME layers with or without ER negative clusters also had a significantly higher ( $p < 0.01$ ) proliferation rate, 18.2% versus 3.6% and 19.9% versus 4.4%, in two separate studies (Man et al., 2002; Man et al., 2002), using immunohistochemical staining for Ki-67 (Fig 6).

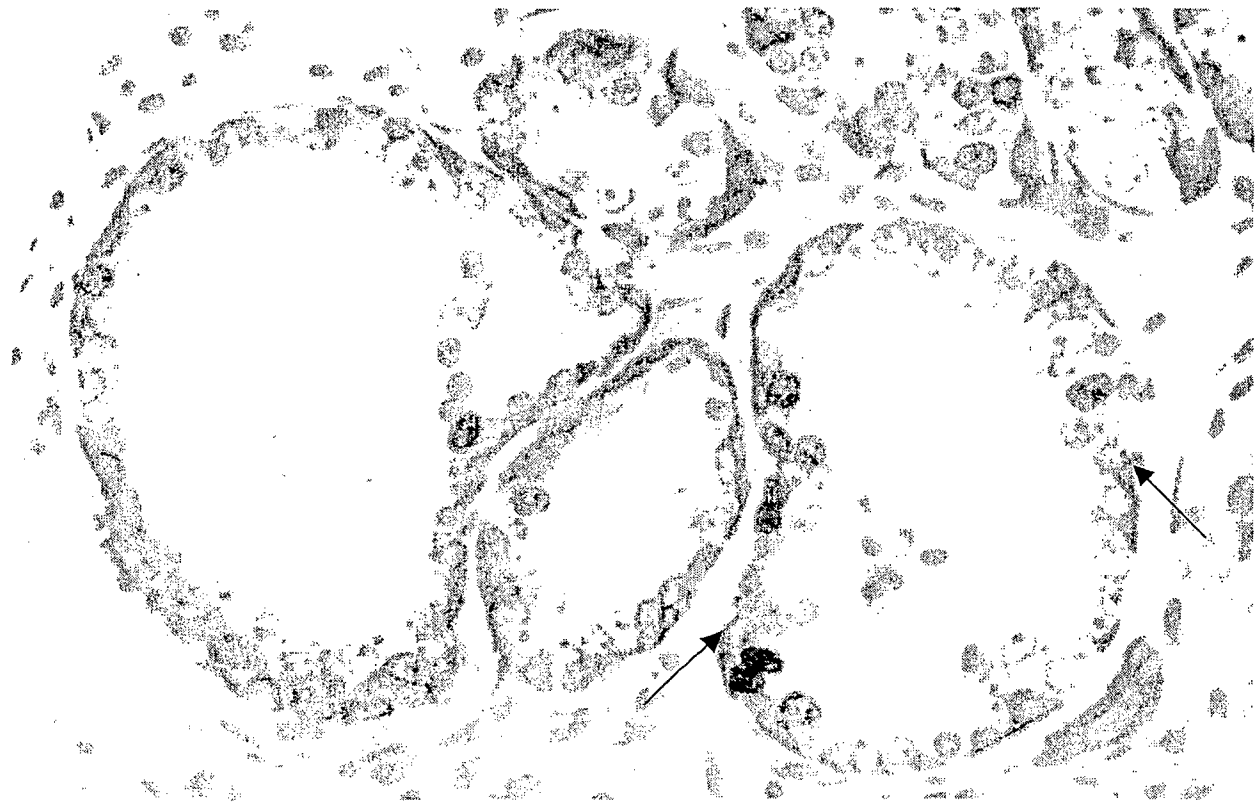


Fig 6. Cells in ducts with and without focal ME cell layer disruptions show a different proliferation rate

A paraffin section double immunostained for Ki-67 (brown) and SMA (red). Note that more Ki-67 positive cells are seen in a duct with focally disrupted ME cell layer (arrows), compared to adjacent ducts without focal ME cell layer disruptions.

3. Compared to their adjacent ER positive counterparts within the same duct, microdissected ER negative cells had a substantially higher frequency and different pattern of loss of heterozygosity at multiple chromosomal loci, including those harboring tumor suppressor genes fragile histidine triad and Wilms' tumor 1 (Man et al., 2002; Man et al., 2003) (Fig 7).

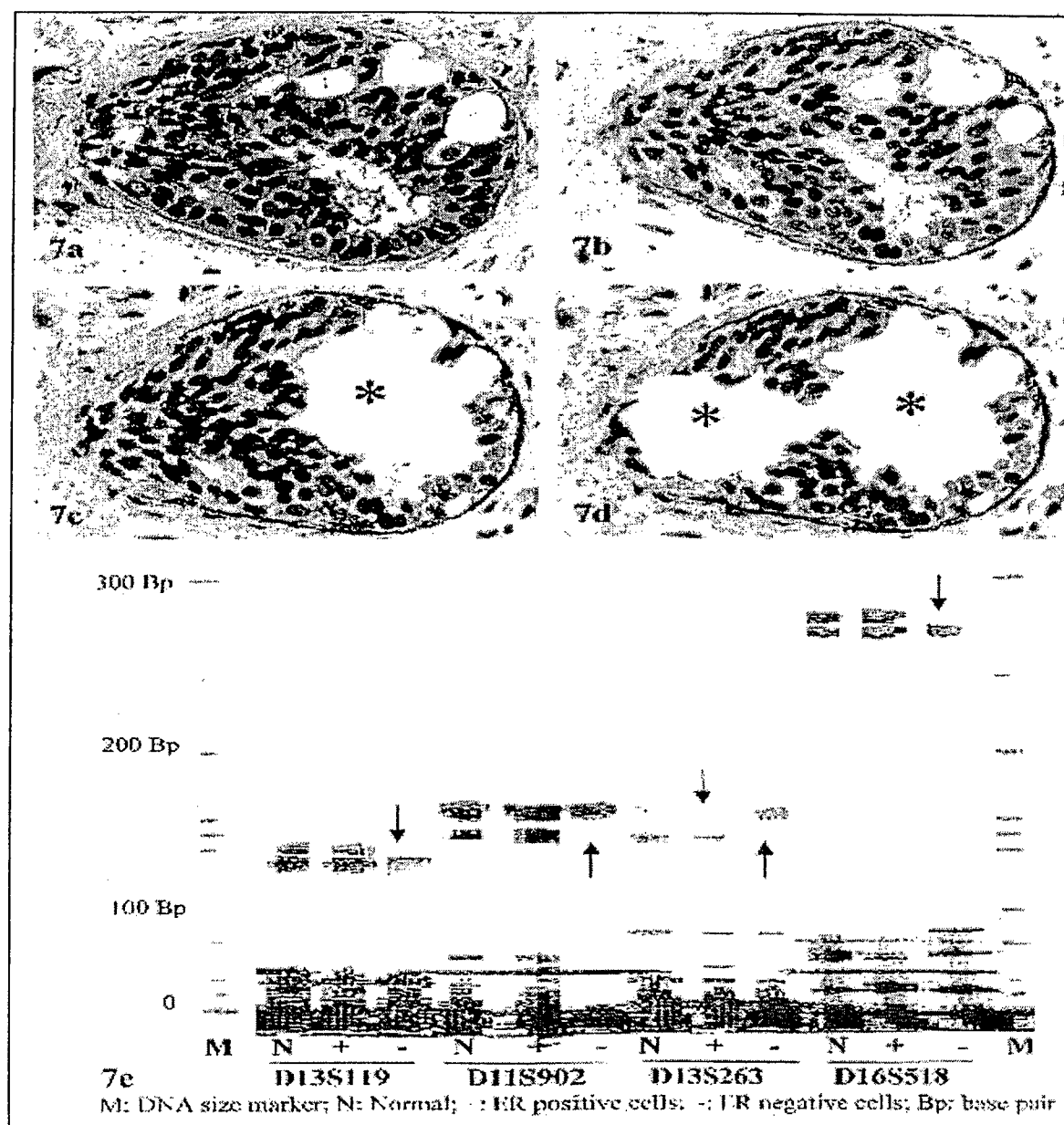


Fig 7. Comparison of the frequency and pattern of LOH in ER (+) and ER (-) cells. Sections were double immunostained for ER (brown) and SMA (red), and ER (+) and (-) cells were separately microdissected and assessed for LOH. Asterisks identify dissected cells. Arrows identify LOH.

4. Cell clusters overlying focally disrupted ME layers had a significantly higher frequency and level of mRNA expression in proliferation, apoptosis, invasion, and metastasis related genes, compared to their adjacent counterparts within the same duct (Man et al., 2004).

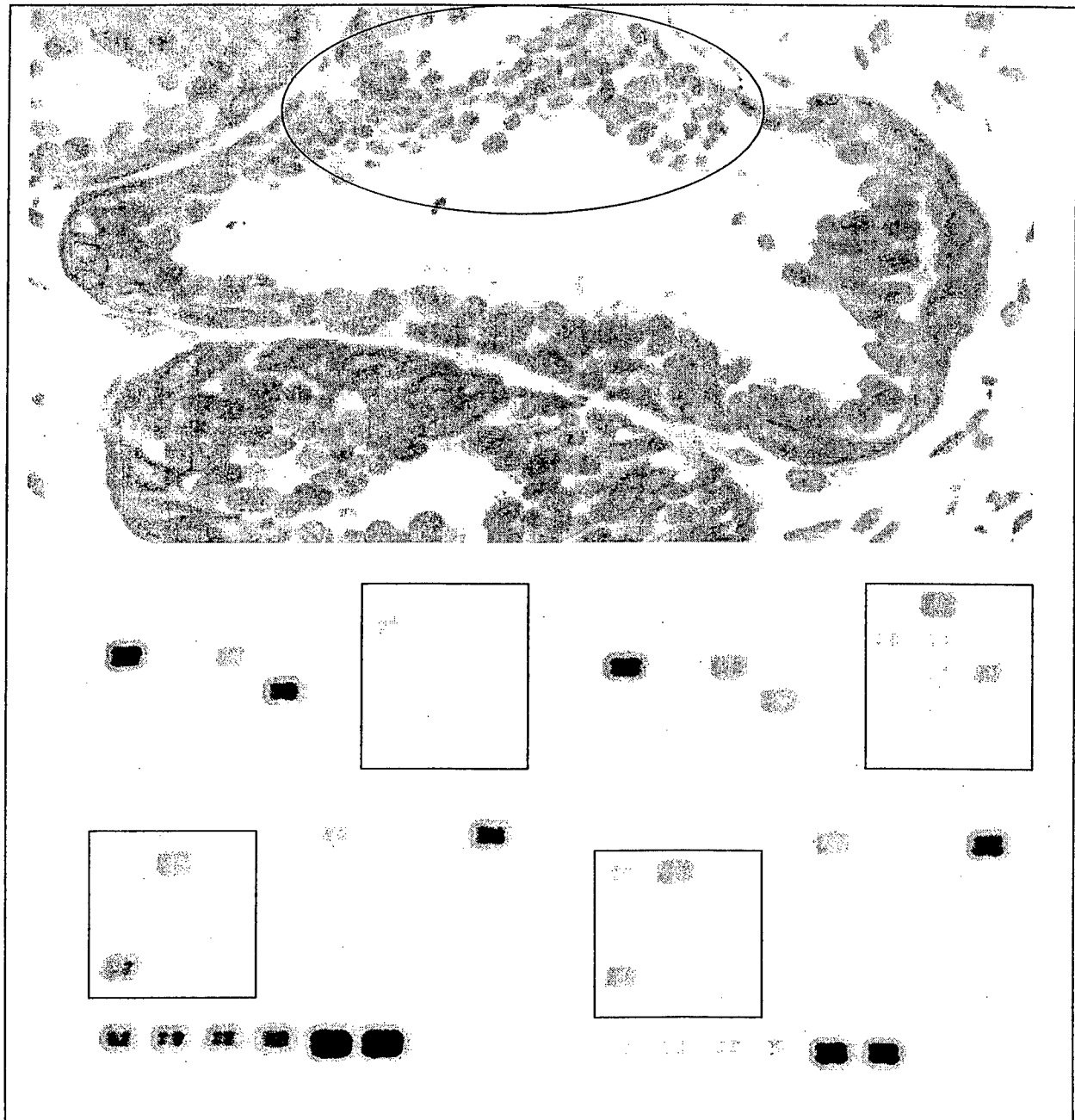


Fig 8. Comparison of the frequency and level of mRNA expression in ER (+) and ER (-) cells. Frozen sections were double immunostained for ER (brown) and SMA (red). ER (+) and (-) cells were separately microdissected for cDNA arrays. Cycles identify dissected ER (-) cells and differentially expressed mRNAs.

**Table 2. Comparison of the frequency and level if mRNA expression in ER (+) and (-) cells**

Gene group	Gene name	Higher in ER (-)	Higher in ER (+)	Equal in both	Case number
Adhesion	CD44	13	4	1	18
	CDH1	13	4	3	20
	MUC18L	5	5	2	12
Angiogenesis	EGFR	5	6	1	12
	IFNA1	10	5	2	17
	TNF	5	9	6	20
Apoptosis	BAX	9	4	0	13
	CASP9	9	5	5	19
	CFLAR	10	5	1	16
Cell cycle	CDC25A	9	1	7	17
	CDKN2A	10	4	2	16
	RAD53	9	1	2	12
Inv & metastasis	NME4	10	4	6	20
	TIMP1	6	6	3	15
Signal transduct	NFKB1	11	6	3	20
Total		134(54.3%)	69(27.9%)	44(17.8%)	247
p	< 0.01				

As macrophages and leukocytes contain digestive enzymes capable of degrading both the BM and damaged host cells, our recent studies assessed the possible roles of these cells in ME cell layer disruptions and tumor invasion. A total of 23 DCIS containing ducts with focally disrupted ME cell layers were selected from 94 such cases identified in our previous studies.

Two consecutive sections from each case were double immunostained, one with leucocyte common antigen (LCA) plus smooth muscle actin (SMA); the other with Ki-67 plus SMA. Ducts lined by  $\geq 50$  epithelial (EP) cells and distinct ME cell layers were examined. Our studies have revealed, for the first time, several interesting phenomena that have not been reported in the English literature:

1. Ductal tumors with and without ME disruptions have different rates of leukocyte infiltration.

A total of 191 duct cross-sections were found to contain focal ME cell layer disruptions; of which, 186 (97.4%) were with and 5 (2.6%) were without leukocyte infiltration. Of 207 morphologically similar sections without ME disruptions, 46 (22.2%) were with and 161 (77.8%) were without leukocyte infiltration (Yousefi et al., 2004; Man et al., 2004) (Fig 9).

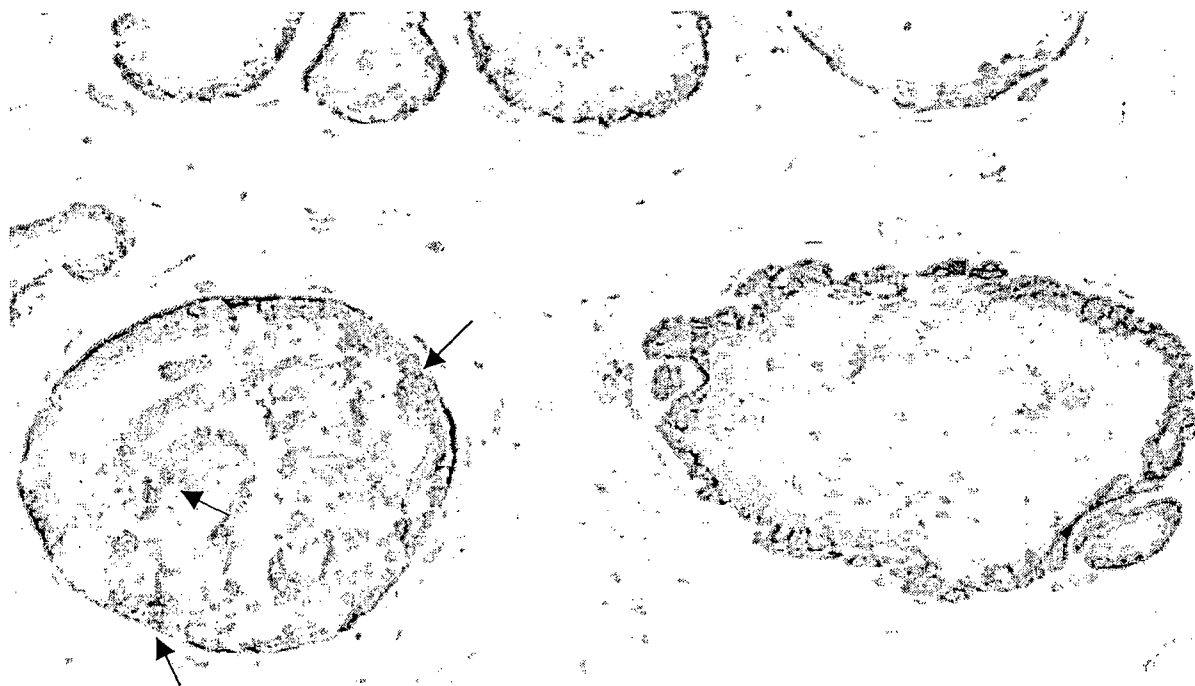


Fig 9. Ducts with and without focal ME layer disruptions have a different frequency of leukocyte Infiltration

The section was double immunostained with SMA (red) and leucocyte common antigen (brown). Note that the duct on the right has an intact ME cell layer with no leukocyte infiltration, while the duct on the left has a disrupted ME layer with multiple leukocytes (arrows).



**Table 3. Frequencies of white blood cell infiltration in mammary ducts with and without focal myoepithelial cell layer disruptions**

	Section number	With WBC	Without WBC	P
Disrupted	191	186 (97.4%)	5 (2.6%)	< 0.01
Non-disrupted	207	46 (22.6%)	161 (77.4%)	

2. A vast majority of the proliferating cells and clusters of multiple proliferating cells are located at or near focally disrupted ME layers.

Ki-67 positive cells in ducts with focally disrupted ME cell layers were generally subjacent to disruptions, and over 30 clusters of multiple proliferating cells were seen directly overlying or near focally disrupted ME cell layers (Fig 10). In contrast, Ki-67 positive cells in ducts without ME disruptions were scatteringly distributed over the entire EP compartment.

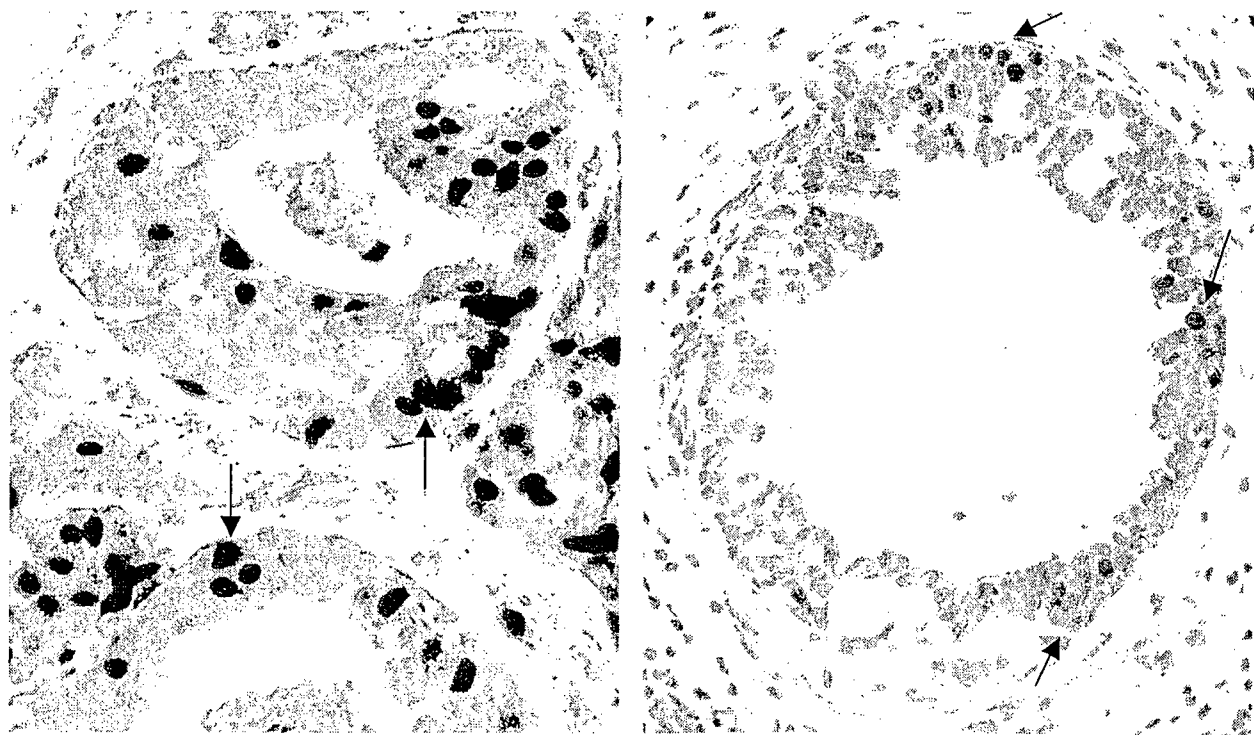


**Fig 10. Localization of proliferating cells in ducts with focally disrupted ME cell layers**  
The section was doubled immunostained for SMA (red) and Ki-67 (black or brown). Note that a vast majority of the Ki-67 positive cells are located near the ME disruptions (arrows).

3. ME cells surrounded by or adjacent to leukocytes often show distinct morphologic alterations.

Compared to their counterparts that are at a distance to the leukocytes, ME cells surrounded by or adjacent to leukocytes often show distinct morphologic alterations, including the loss of SMA immunostaining, the fragmentations and focal disruptions of the cell layer (Fig 11).

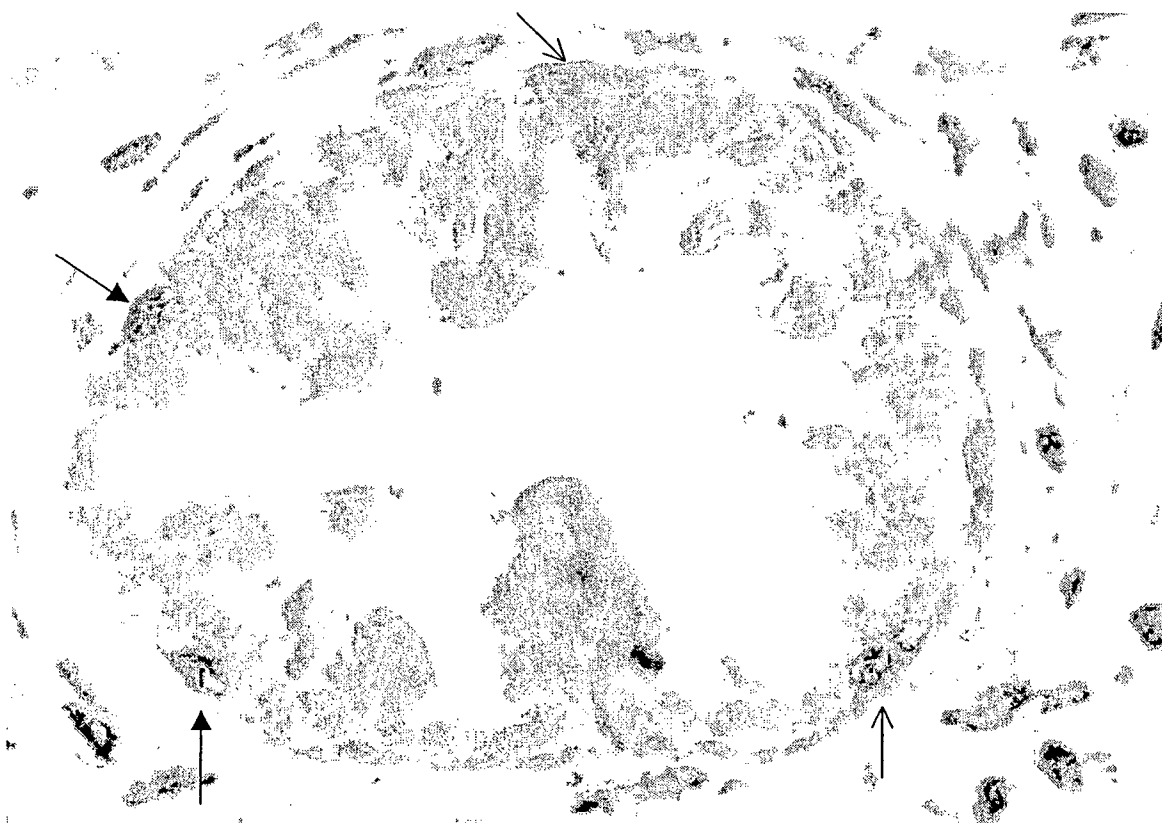


Fig 11. Correlation of focal ME cell layer disruptions and leukocyte infiltration

The section was double immunostained for SMA (red) and leukocyte common antigen (brown). Note that leukocytes are located at or near the focal ME disruptions (arrows). The ME cells near leukocytes generally show loss of SMA immunostaining (thin arrows).

The ME cells in focally disrupted ME layers generally have a substantially lower proliferation rate, compared to these in non-disrupted layers. Our recent studies in human prostate tumors, using the same approach, revealed very similar changes (Man et al., 2004).

## **VI. Our hypothesized mechanism for ME cell layer degradations and tumor invasion**

The mechanism(s) for focal ME layer disruptions and formation of ER negative cell clusters is unknown, but is likely to result from a localized ME cell death and leukocyte infiltration and resultant responses, based on the following reasons. First, no morphologically distinct ME cells are detectable at the disruptions in multiple consecutive sections in all cases, indicating the physical absence of ME cells. Second, our previous studies have shown that the frequency of focal ME cell layer disruptions is independent of the size, length, and architecture of ducts and acini (Man et al., 2003), suggesting that the disruption is unlikely induced by mechanic forces, such as an elevated pressure in the lumen and an increased cell number. Third, our previous studies have shown that 97.4% of the ducts with focal ME disruptions showed leukocyte infiltration, compared to 22.2% ( $p < 0.01$ ) in morphologically similar ducts without focal ME cell layer disruptions (Man et al., 2004). Fourth, ME cells surrounded by or adjacent to leukocytes often showed distinct morphological alterations. Fifth, both the ME and prostate basal cells of focally disrupted layers seem to have a substantially lower proliferation rate, compared to those with intact ME and basal layers (Man et al., 2004).

Our speculation is further supported by several lines of evidence. Increasing data have shown that a variety of external and internal insults could specifically impact the physical and functional status of the ME cells. A wide variety of proteolytic enzymes produced by tumor or stromal cells could substantially impact the physical integrity of the basement membrane, which might subsequently impact the functions of the ME cells (Goldfarb and Liotta, 1986; Mignati et al., 1986). A number of chemical compounds or reagents could specifically target the ME cells. For example, exposure to lambdacarrageenan could specifically result in filament disassembly and loss of the ME cells, while exposure to oxytocin could substantially enhance the rate of ME

cell proliferation and differentiation (Tobacman, 1997; Sapino et al., 1993). In addition, the human nature immuno-surveillance system could specifically or non-specifically target the ME cells. It has been well documented that leukocyte infiltration into tumor tissues is a common event, and that the number of leukocytes within tumor tissues is linearly increased with tumor progression (Ben-Hur et al., 2002; Harmeiy et al., 1998). The increase of leukocytes is particularly evident during the progression of DCIS to infiltrating ductal carcinoma, in which up to a four-fold increase of lymphoid infiltration has been reported (Ben-Hur et al., 2002; Harmeiy et al., 1998). The extent of the increased macrophages in tumor tissues has been found to correlate with a worse prognosis and a significantly higher mortality rate (Ben-Hur et al., 2002; Harmeiy et al., 1998). Also, patients with lymphocyte infiltration at the tumor edge were found to have a noticeable poorer short-term prognosis, compared to those with lymphocyte infiltration in other locations (Hartveil, 1998). More importantly, it has been well elucidated that leukocytes are capable of freely crossing through both the basement membrane and ME cell layer, and that leukocytes contain a number of digestive enzymes that can effectively degrade both the basement membrane and altered host cells (Zhang et al., 1998; Steadman et al., 1993; Heck et al., 1990; Nzula et al., 2004).

Based on these findings, we propose that a localized ME cell death and resultant immunoreactions are the triggering factor for disruptions in ME cell layers, the formation of ER negative cell clusters, and subsequent stromal and vascular invasion. Our hypothesized main processes are the following:

1. The ME cells belong to a self-renewal population, which normally undergoes proliferation to replace aged or injured ME cells.

2. An external or internal insult, such as a localized trauma or the exposure to lambda-carrageenan, directly disrupts the structural integrity of the ME cell layers or impairs the normal replacement process, resulting in a cluster of damaged or dying ME cells.
3. The damaged or dying ME cells lose their capability of manufacturing tumor suppressor proteins, and subsequently result in the loss of the paracrine regulation on the adjacent tumor cells.
4. The degradation products of dying ME cells attract macrophages and leukocytes, which migrate to the injured site and interact with altered ME cells.
5. Macrophages and leukocytes release digestive enzymes, leading to the physical destruction of altered ME cells and basement membrane, resulting in a focal disruption or gap that allows direct communications between the tumor and stromal cells.
6. The focal disruption or gap results in a focally increased permeability for metabolism- and growth-related molecules to overlying and adjacent cells.
7. The altered micro-environment leads to variable consequences in overlying tumor and adjacent ME cells, depending on the nature of these cells: [1] If the overlying and adjacent cells are fully differentiated, no substantial alteration may be detectable; [2] If the cells are partially differentiated, a limited or mild increase in cell proliferation might be seen, which might lead to a localized stromal invasion; [3] If they are primitive stem cells, an extensive cell proliferation might be seen, which may lead to the formation of new structures with normal morphology and functions; [4] If they are mutated stem cells, a series of events that markedly differ from both primitive stem cells mediated and differentiated progenitors mediated proliferation may take place. Previous studies have shown that a mutated stem cell is the common cellular origin of teratocarcinomas,

epithelial cancers, and blood vessels and lymphatic ducts (Sell and Pierce, 1994; Trosko and Chang, 2001).

8. The newly formed cell clusters undergo differentiation, releasing invasion-associated molecules, which trigger angiogenesis, tissue remodeling, and increasing production of growth factors in the stroma, providing a favorable environment for tumor cell growth (Rudolph and Matrisian, 1998; Matriasia et al., 2003; Moinfar et al., 2000; Man et al., 2002; Man et al., 2003; Man et al., 2004).
9. The interactions between tumor and stromal cells lead to further degradation of ME layers and basement membrane, and a deeper and wider migration of the newly formed cell clusters.
10. The above processes could potentially or even equally (to in situ ductal carcinoma) occur in normal breast tissues and hyperplastic lesions, which may lead to a direct invasion. These processes may also a trigger factor for the progression of the tumor stages.

## **VII. Potential implications of our hypothesis**

It is not known, however, whether or to what extent our hypothesis reflect the intrinsic mechanism of ME cell disruptions and the formation of these ER negative tumor cell clusters for three main reasons: [1] our data are limited, extracted from a small sample size, which might not reflect the real status in the general population; [2] the underlined mechanism(s) and detained processes for each of our hypothesized steps has not be elucidated. However, given the facts that: [1] The disruption of the ME cell layer is an absolute pre-requisite for tumor invasion; [2] Cells overlying focally disrupted ME cells are morphologically, immunohistochemically, and genetically different from their adjacent counterparts within the same duct; [3] Focal ME cell

---

layer disruptions and leukocyte appear to be correlated events, our hypothesis might have important scientific and clinical implications. In the scientific field, our hypothesis may open a new window for the exploration of the mechanism of ME cell layer disruptions and tumor invasion. Our hypothesis might also be useful in reconciliation of the conflicting reports regarding the immunohistochemical and genetic profiles of the breast lesions, as our findings clearly implicate that those conflicts are likely to result from the presence or absence of ME cell layer disruptions, and the differences in the nature and growth pattern of the cells overlying or adjacent to the disruptions. In the clinical field, our hypothesis might be beneficial for the early detection and treatment of breast tumors. As genetic alterations determine the scope and extent of, as also precede, biochemical and morphologic changes, microdissection of these ER negative cell clusters and their adjacent ER positive counterparts for genetic and biochemical comparisons could potentially lead to the identification of specific molecules associated with the early events of ME cell layer disruptions, tumor invasion and metastasis. The development of antibodies or chemical reagents to target these cells might provide a more effective and less toxic means to block tumor invasion at the very early stage. Also, microdissection of these ER negative cell clusters in frozen tissues for tissue culture may lead to the establishment of useful cell lines that benefit stem cell researches. More importantly, as our studies suggest that leukocytes and other immuno-surveillance related cells might be direct trigger factors for breast tumor progression and invasion, and that invasion could potentially occur from normal or hyperplastic lesions, the development of new strategies and approaches to deal with these issues may have direct impacts on patients' prognosis (Herbert, 2004).

### VIII. Conclusions

The ME cell and basement membrane are inter-positioned between the epithelium and the stroma, normally only permitting the exchange of small molecules between these two cellular components. Due to this architectural feature, the disruption of both the ME cell layer and basement membrane is absolutely needed for the progression of ductal carcinoma *in situ* to the invasive status. In addition to this passive function as a nature structural barrier, ME cells have been found to possess several active or “voluntary” functions, including the production of tumor suppressors, paracrine down-regulation of matrix metalloproteinase (MMP) expression, and participation in steroid hormone metabolism. Like the luminal cells, ME cells exclusively or preferentially express a number of proteins, and subject to a variety of pathological alterations. Focal disruptions in the ME cell layers are associated with the emergence of unusual cell clusters overlying disruptions and displaying several unique features, including [1] the loss of estrogen receptor expression; [2] a significantly higher proliferation rate; [3] a significantly higher or different pattern of LOH; [4] a significantly higher frequency and level of mRNA expression in cell cycle, apoptosis, and invasion related genes, compared to their adjacent counterparts with the same duct. Focal ME layer disruptions are also correlated with a significantly higher leukocyte infiltration, and a higher rate of cell proliferation at or near the disruptions. Together, these and other findings have promoted the introduction of a novel hypothesis that focal ME cell layer disruptions, leukocyte infiltration, and emergence of ER negative cell clusters might be correlated events, representing an early sign of ME degradations and formation of a biologically more aggressive cell clone that is in the process on invasion. This novel hypothesis appears to be useful in reconciliation of the conflicting reports regarding the heterogeneous genetic and



immunohistochemical profiles of the breast lesions, and lead to the development of more effective and specific approaches for breast cancer detection, treatment, and prevention.

### **Acknowledgment**

Supported in part by DOD grants DAMD17-01-1-0129 and DAMD17-01-1-0130 to YGM and DOD grant DAMA17-02-1-0238, NIH grant CA78646, American Cancer Society grant F01FSU-1 to QXAS.

### **References**

- Barbareschi M, Pecciarini L, Cangi MG, Macri E, Rizzo A, Viale G, and Doglioni CW (2001) p63, a p53 homologue, is a selective nuclear marker of myoepithelial cells of the human breast. *Am J Surg Pathol* 25, 1954-1060
- Batistatou A, Stefanou D, Arkoumani E, and Agnantis NJ (2003) The usefulness of p63 as a marker of breast myoepithelial cells. *In Vivo* 17, 573-576
- Ben-Hur H, Cohen O, Schneider D, Gurevich P, Halperin R, Bala U, Mozes M, and Zusman I (2002) The role of lymphocytes and macrophages in human breast tumorigenesis: an immunohistochemical and morphometric study. *Anticancer Research* 22(2B), 1231-1238.
- Bose S, Derosa CM, and Ozzello L (1999) Immunostaining of type IV collagen and smooth muscle actin as a aid in the diagnosis of breast lesions. *Breast J* 5, 194-201.
- Coussens LM, Fingleton B, and Matrisian LM (2002) Matrix metalloproteinase inhibitors and cancer: trial and tribulations. *Science* 295 (5564), 2387-2392.
- Dabbs DJ and Gown AM (1999) Distribution of calponin and smooth muscle myosin heavy chain in fine-needle aspiration biopsies of the breast. *Diagn Cytopathol* 20, 203-207.
- Deugnier MA, Farado MM, Rousselle P, Thiery JP, and Glukhova MA (1999). Cell-extracellular matrix interactions and EGF are important regulators of the basal mammary epithelial cell phenotype. *J Cell Sci* 112, 1035-1044.
- Djonov V, Hogger K, Sedlacek R, Laissure J, and Draeger A (2001) MMP-19: cellular

- localization of a novel metalloproteinase within normal breast tissue and mammary gland tumors. *J Pathol* 195, 147-155.
- Dwarakanath S, Lee AK, Delellis RA, Silverman ML, Frasca L, and Wolfe HJ (1987) S-100 Protein positivity in breast carcinomas: a potential pitfall in diagnostic immunohistochemistry. *Hum Pathol* 18, 1144-1148.
- Fabre A, McCabb AH, O'Shea D, Broderick D, Keating G, Tobin B, Gorey T, and Dervan PA. (1999) Loss of heterozygosity of the Wilms' tumor suppressor gene (WT-1) in in-situ and invasive breast carcinoma. *Hum Pathol* 1999,30(6):661-5.
- Fakhari M, Pullirsch D, Abraham D, Paya K, Hofbauer R, Holzfeind P, Hofmann M, and Aharinejad S (2002) Selective upregulation of vascular endothelial growth factor receptors neuropilin-1 and -2 in human neuroblastoma. *Cancer* 94, 258-263.
- Gerald W, Sussman J, True L (1987) Actin-positive myoepithelial cells characterize breast disease. *Lab Invest* 56, 27a.
- Gillett CE, Bobrow LG, and Millis RR (1990) S100 protein in human mammary tissue—immunoreactivity in breast carcinoma, including Paget's disease of the nipple, and value as a marker of myoepithelial cells. *J Pathol* 160, 19-24
- Goldfarb RH and Liotta LA (1986) Proteolytic enzymes in cancer invasion and metastasis. *Semin Thromb Hemost* 12: 294-307.
- Gomm JJ, Browne PJ, Coope RC, Bansal GS, Yiangou C, Johnston CL, Mason R, and Coombes RC (1997) A paracrine role for myoepithelial cell-derived FGF2 in the normal human breast. *Exp Cell Res* 234, 165-173.
- Gudjonson T, Ronnov-Jessen L, Villadsen R, Rank F, Bissell MJ, and Peterson OW (2002) Normal and tumor-derived myoepithelial cells differ in their ability to interact with luminal breast epithelial cells for polarity and basement membrane deposition. *J Cell Sci* 115, 39-50.
- Harmey JH, Dimitriadis E, Kay E, Redmond HP, and Bouchier-Hayes D (1998) Regulation of macrophage production of vascular endothelial growth factor (VEGF) by hypoxia and transforming growth factor beta-1. *Ann Surg Oncol* 1998; 5, 271-278.
- Hartveil F (1998) Breast cancer: poor short-term prognosis in cases with moderate lymphocyte infiltration at the tumor edge: a preliminary report. *Oncol Rep* 5, 423-426.
- Heck LW, Blackburn WD, Irwin MH, and Abrahamson DR (1990) Degradation of basement membrane laminin by human neutrophil elastases and cathepsin G. *Am J Pathol* 136, 1267-1274.
- Herbert BS (2003) Advances in breast cancer therapy and chemoprevention: Current strategies and new approaches. *Cancer Therapy* 1, 363-371

- Iwaya K; Ogawa H, Izumi M, Kuroda M, and Mukai K (2002) Stromal expression of CD10 in invasive breast carcinoma: a new predictor of clinical outcome. *Virchows Arch* 440(6), 589-93.
- Jarrard DF, Paul R, van Bokhoven A, et al (1997) P-cadherin is a basal cell-specific epithelial marker that is not expressed in prostate cancer. *Clin Cancer Res* 3, 2121-2128.
- Jolicoeur F, Seemayer TA, Gabbiani G, et al (2002) Multifocal, nascent, and invasive myoepithelial carcinoma(malignant myoepithelioma) of the breast: an immunohistochemical and ultrastructural study. *Int J Surg Pathol* 10, 281-291.
- Jones JL, Shaw JA, Pringle JH, and Walker RA (2003). Primary breast myoepithelial cells exert an invasion-suppressor effect on breast cancer cells via paracrine down-regulation of MMP expression in fibroblasts and tumor cells. *J Pathol* 201, 562-572.
- Joshi MG, Lee AK, Pedersen CA, Schnitt Camus MG, and Hughes KS (1996) The role of immunohistochemical markers in the differential diagnosis of proliferative and neoplastic lesions of the breast. *Mod Pathol* 9, 57-62.
- Lunde S, Nesland JM, Holm R, and Johannessen JV (1987) Breast carcinomas with protein S-100 immunoreactivity. An immunocytochemical and ultrastructural study. *Pathol Res Pract* 182, 627-631.
- Maass N, Hojo T, Zhang M, Sager R, Jonat W, and Nagasaki K (2000) Maspin-a novel protease inhibitor with tumor suppressing activity in breast cancer. *Acta oncol* 39,931-934.
- Man YG, Tai L, Barner R, Vang R, Saenger JS, Shekitka KM, Bratthauer GL, Wheeler DT, Liang CL, Vinh TN, and Strauss BL (2003) Cell clusters overlying focally disrupted mammary myoepithelial cell layers and adjacent cells within the same duct display different immunohistochemical and genetic features: implications for tumor progression and invasion. *Breast Cancer Res* 5, R231-241.
- Man YG, Shekitka KM. Saenger JS, Tai L, Bratthauer GL, Chen PY, and Tavassoli FA (2002) Focal loss of estrogen receptor (ER) expression in ER positive ductal intraepithelial neoplasia is associated with disruption of the immediate subjacent myoepithelial cell layer. *Mod Pathol* 15(1),42A, 162.
- Man YG, Saenger JS, Strauss B, Vang RS, Bratthauer GL, Chen PY, and Tavassoli FA (2002) Focal alterations of p27 expression and subjacent myoepithelial cell layer disruptions are correlated events in ER (-) ductal intraepithelial neoplasia. *Proceedings of Department of Defense Breast Cancer Research Program Meeting*. 1, P9,14.
- Man YG, Strauss B, Saenger JS, Tai L, Bratthauer GL, Chen PY, and Tavassoli FA (2002). Genetic alterations in ER (-) mammary epithelial cells overlying focally disrupted myoepithelial cell layers. *Proceedings of Department of Defense Breast Cancer Research Program Meeting*. 1, P9,15.

- Man YG, Vang RS, Saenger JS, Strauss B, Bratthauer GL, Chen PY, and Tavassoli FA (2002). Co-expression of maspin and wilms' tumor 1 proteins in mammary myoepithelial cells---implication for tumor progression and invasion. Proceedings of Department of Defense Breast Cancer Research Program Meeting. 1, P9,16.
- Man YG, Shekitka KM, Bratthauer GL, and Tavassoli FA (2002) Immunohistochemical and genetic alterations in mammary epithelial cells overlying focally disrupted myoepithelial cell layers. Breast Cancer Res Treat 76 (sup 1), S143, 569.
- Man YG, Saenger JS, Vang RS, Barner R, Wheeler D, Martinez A, and Mulshine JL (2003) Identification of invasive precursor cells in normal and hyperplastic breast tissue. Proceedings of the American Association for Cancer Research. Cancer Res, volume 44, 68, 357.
- Man YG, Vang RS, Saenger JS, Strauss BL, Barner R, Wheeler DT, Liang CY, Bratthauer GL, and Mannion C (2003) Development and progression of mammary ductal tumors appear to be mediated by surrounding myoepithelial cells. Mod Pathol 16(1), 39A-40A.
- Man YG, Mattu R, Zhang R, Yousefi M, Sang QXA, and Shen T (2003) A subset of normal and hyperplastic appearing mammary ductal cells display invasive features. Breast Cancer Res Treat 82 (supplement 1), S141.
- Man YG, Zhang R, Mattu R, Shen T, and Sang QXA (2003) A subset of mammary epithelial cells overlying focally disrupted myoepithelial cell layers shows an unusual immunostaining pattern for proliferation -related proteins. Breast Cancer Res Treat 82 (supplement 1), S163-164.
- Man YG, Zeng X, Shen T, Vang R, Barner R, Wheeler DT, Vihn T, Liang CY, and Strauss BL (2004) Cell clusters overlying focally disrupted myoepithelial cell layers and their adjacent counterparts within the same duct display a different pattern of mRNA expression. Mod Pathol 17, 40-41A.
- Man YG, Barner R, Vang R, Wheeler DT, Liang CY, Vihn T, Bratthauer GL, and Strauss BL (2004). Non-smooth muscle restricted proteins exclusively or preferentially expressed in mammary myoepithelial cells: a programmed or induced phenomenon? Mod Pathol 17, 40A.
- Man YG, Berg PE, Barner R, Vinh TN, Wheeler DT, Liang CY, and Strauss BL (2004). Morphologically similar normal and hyperplastic mammary ductal cells associated with and without malignant lesions have a different immunohistochemical profile. Cancer Detection & Prevention, 2004 Symposium Volume, S-137.
- Man YG, Shen T, Zhao YG, and Sang QX (2004) Morphologically comparable prostate acini

- and ducts with and without a focal basal cell layer disruption have a different cell proliferation rate: Implications for tumor invasion. *FASEB* 18(5): A1183.
- Man YG, Shen T, Zhao YG, and Sang QX (2004) Focal prostate basal cell layer disruptions and leukocyte infiltration are correlated events: Implications for basal cell layer degradation and tumor invasion. *Cancer Detection & Prevention*, 2004 Symposium, S51-52.
- Matrisian LM, Sledge GW Jr, and Mohla S (2003) Extracellular proteolysis and cancer: meeting summary and future directions. *Cancer Res* 63, 6105-6109.
- McGowan KM and Coulombe PA (1998) Onset of keratin 17 expression coincides with the definition of major epithelial lineages during skin development. *J Cell Biol* 143(2),469-86.
- Miettinen MM, Sarlomo-Rikala M, Kovatich AJ, and Lasota J (1999) Calponin and h-caldesmon in soft tissue tumors: consistent h-caldesmon immunoreactivity in gastrointestinal stromal tumors indicates traits of smooth muscle differentiation. *Mod pathol* 12, 756-762
- Mignatti P, Robbins E, and Rifkin DB (1986) Tumor invasion through the human amniotic membrane: Requirement for a proteinase cascade. *Cell* 47,487-498.
- Milis AA, Zheng B, Wang XJ, Vogel H, Roop DR, and Bradley A (1999) p63 is a p53 homologue required for limb and epidermal morphogenesis. *Nature* 398, 708-713.
- Miosge N (2001) The ultrastructural composition of basement membrane in vivo. *Histol Histopathol* 16,1239-1248.
- Moinfar F, Man YG, Arnould L, Bratthauer GL, Ratschek M, and Tavassol FA (2000) Concurrent and independent genetic alterations in the stromal and epithelial cells of mammary carcinoma: Implications for tumorigenesis. *Cancer Res* 60, 2562-2566.
- Moll R, Franke WW, Schiller DL, Geiger B, and Krepler R (1982) The catalog of human cytokeratins: Patterns of expression in normal epithelia, tumors and cultured cells. *Cell* 31,11-24.
- Moller P, Mechttersheimer G, Kaufmann M, Moldenhauer G, Momburg F, Mattfeldt T, and Otto HF (1989) Expression of epidermal growth factor receptor in benign and malignant primary tumours of the breast. *Virch Arch A Pathol Anat Histopathol* 414, 157-164.
- Moritani S, Kushima R, Sugihara H, Bamba M, Kobayashi T, and Hattori T (2002) Availability of CD10 immunohistochemistry as a marker of breast myoepithelial cells on paraffin sections. *Mod Pathol* 2002;15(4):397-405.
- Murad TM and von Haam E (1986) Ultrastructure of myoepithelial cells in human mammary gland tumor. *Cancer* 21, 1137-1149.

- Nerlich A (1995) Morphology of basement membrane and associated matrix proteins in normal and pathological tissues. *Veroff Pathol* 145:1-139.
- Nzula S, Going JJ, and Stott D (2003) The role of B lymphocytes in breast cancer: a review and current status, *Cancer Therapy* 1, 81-91.
- Ohyabu I, Takasaki T, Akiba S, Nomura S, Enokizono N, Sagara Y, Hiroi J, Nagai R, and Yoshida H (1998) Immunohistochemical studies on expression of human vascular smooth muscle myosin heavy chain isoforms in normal mammary glands, benign mammary disorders and mammary carcinomas. *Pathol Int* 48, 433-439
- Reis-Filho JS, Milanezi F, Silva P, and Schmitt FC (2001) Maspin expression in myoepithelial tumors of the breast. *Pathol Res Pract* 197,817-21.
- Roose J, Huls G, van Beest M, Moerer P, van der Horn K, Goldschmeding R, Logtenberg T, and Clevers H (1999) Synergy between tumor suppressor APC and the beta-catenin-Tcf4 target Tcf1. *Science* 285, 1923-1926
- Rudolph-Owen LA and Matrisian LM (1998) Matrix metalloproteinases in remodeling of the normal and neoplastic mammary glands. *J Mammary Gland Biol Neoplasia* 3, 177-189.
- Scharnhorst V, van der Eb AJ, and Jochemsen AG (2001) WT1 proteins: functions in growth and differentiation. *Gene* 273(2):141-61.
- Schurch W, Potvin C, and Seemayer TA (1985) Malignant myoepithelium (myoepithelial carcinoma) of the breast: An ultrastructural and immunohistochemical study. *Ultrastruct Pathol* 8, 1-11.
- Sell S, Pierce GB (1994) Maturation arrest of stem cell differentiation is a common pathway for the cellular origin of teratocarcinomas and epithelial cancers. *Lab Invest* 70, 6-22.
- Shimoyama Y, Yoshida T, and Terada M (1989) Molecular cloning of a human Ca<sup>2+</sup>-dependent cell-cell adhesion molecule homologous to mouse placental cadherin: its low expression in human placental tissues. *J Cell Biol* 109, 1787-1794.
- Simpson PT, Gale T, Reis-Filho JS, Jones C, Parry S, Steele D, Cossu A, Bodroni M, Palmieri G, and Lakhani SR (2004) Distribution and significance of 14-3-3sigma, a novel myoepithelial marker, in normal, benign, and malignant breast tissue. *J Pathol* 202, 274-285.
- Slade MJ, Coope RC, Gomm JJ, and Coombes RC (1999) The human mammary gland basement membrane is integral to the polarity of luminal epithelial cells. *Exp Cell Res* 247, 267-278.
- Soler AP, Knudsen KA, Salazar H, et al (1999) P-cadherin overexpression in breast carcinoma indicates poor survival. *Cancer* 86, 1263-1272.

- Steadman R, Irwin MH, St John PL, et al (1993) Laminin cleavage by activated human neutrophils yields proteolytic fragments with selective migratory properties. *J Leukoc Biol* 53,354-365
- Stepheson JM, Banerjee S, Saxena NK, Cherian R, and Banerjee SK (2002) Neuropilin-1 is differentially expressed in myoepithelial cells and vascular smooth muscle cells in preneoplastic and neoplastic human breast: a possible marker for the progression of breast cancer. *Int J Cancer* 101,409-414.
- Sternlicht MD and Barsky SH (1997) The myoepithelial defense: a host defense against cancer. *Med Hypotheses* 48, 37-46.
- Sugano I, Nagao K, Matsuzaki O, Ide G, and Toyota N (1981) Immunohistochemical studies on myoepithelial changes in breast tumors. *Acta Pathol Jpn* 31, 35-44.
- Tavassoli FA (1991) Myoepithelial lesions of the breast: myoepitheliosis, adenomyoepithelioma, and myoepithelial carcinoma. *Am J Surg Pathol* 15, 554-568
- Thorner PS, Kahn HJ, Baumal R, Lee K, and Moffatt W (1986) Malignant myoepithelioma of the breast: An immunohistochemical study by light and electron microscope. *Cancer* 57, 745-750.
- Tobacman JK (1997) Filament disassembly and loss of mammary myoepithelial cells after exposure to lambda-carrageenan. *Cancer Res* 57, 2823-2826.
- Tobacman JK, Hinkhouse M, and Khalkhali-Ellis Z (2002) Steroid sulfatase activity and expression in mammary myoepithelial cells. *J Steroid Biochem Mol Biol* 81, 65-68.
- Trosko JE and Chang CC (2001) Role of stem cells and gap junctional intercellular communications in human carcinogenesis. *Radia Res* 155, 175-180.
- Tsubura A, Shikata N, Inui T, Morii S, Hatano T, and Oikawa T (1988) Immunohistochemical localization of myoepithelial cells and basement membrane in normal, benign and malignant human breast lesions. *Virchows Arch* 413,133-139.
- Wetzels RH, Kuijpers HJ, Lane EB, Leigh IM, Troyanovsky SM, Holland R, Van Haelst UJ, and Ramaekers FC (1991) Basal cell-specific and hyperproliferation-related keratins in human breast cancer. *Am J Pathol* 138(3),751-63.
- Wetzels RH, Holland R, Van Haelst UJ, Lane EB, Leigh IM, and Ramaekers FC (1989) Detection of basement membrane components and basal cell keratin 14 in noninvasive and invasive carcinomas of the breast. *Am J Pathol* 34(3),571-9.
- Yamamoto T, Oda K, Miyazaki K, Ichiyotani Y, Takenouchi Y, Kamei T, Shirafuji N,

- Nimura Y, Hamaguchi M, and Matsuda S (2001) p73 is highly expressed in myoepithelial cells and in carcinomas with metaplasia. *Int J Oncol* 19, 271-276.
- Yang A, Schweitzer R, Sun D, Kaghad M, Walker N, Bronson RT, Tabin C, Sharpe A, Caput D, Crum C, and McKeon F (1999) p63 is essential from regenerative proliferation in limb, craniofacial and epithelial development. *Nature* 398, 714-718
- Yaziji H, Gown AM, and Sneige N (2002) Detection of stromal invasion in breast cancer: the myoepithelial markers. *Adv Anat Pathol* 7,100-9.
- Yoshida H (1998) Immunohistochemical studies on expression of human vascular smooth muscle myosin heavy chain isoforms in normal mammary glands, benign mammary disorders and mammary carcinomas. *Pathol Int* 48, 433-439.
33. Yousefi M, Mattu R, Gao C, and Man YG (2004) Mammary ducts with and without focal myoepithelial cell layer disruptions show a different frequency of white blood cell infiltration and growth pattern: Implications for tumor progression and invasion. *AIMM*, In press
- Zaika AI, Kovalev S, Marchenko ND, and Moll UM (1999) Overexpression of the wild type p73 gene in breast cancer tissues and cell lines. *Cancer Res* 59, 3257-3263.
- Zhang R, Man YG, Vang RS, Saenger JS, Barner R, Wheeler D, Liang CY, Vinh TN, and Bratthauer GL (2003) A subset of morphologically distinct mammary myoepithelial cells lacks corresponding immunophenotypic markers. *Breast Cancer Res* 5, R151-156.
- Zhang R, Man YG, Strauss BL, Vang RS, Saenger JS, Barner R, Wheeler D, and Liang CY (2003) A subset of morphologically identifiable mammary myoepithelial cells lacks expression of corresponding phenotypic markers. *Mod Pathol* 16(1) 52A.
- Zhang XD, Schiller GD, Gill PG, and Coventry BJ (1998) Lymphoid cell infiltration during cancer growth: a syngeneic rat model. *Immunol Cell Biol* 76,550-555.
- Zhang M, Volpert O, Shi YH, et al (2000) Maspin is an angiogenesis inhibitor. *Nature Medicine* 6, 196-199.
- Zhao YG, Xiao AZ, Park HI, Newcomer RG, Yan M, Man YG, Heffelfinger SC, and Sang QX (2004) Endometase in human breast carcinoma, selective activation of progelatinase B and inhibition by tissue inhibitors of metalloproteinases-2 and -4. *Cancer Res* 64, 590-598.



**Expression of BP1, a homobox gene, correlates with progression and invasion of mammary ductal carcinoma**

Yan-gao Man\*, MD., PhD, Sidney W. Fu# PhD., Joseph J. Pinzone#, MD., Arnold M. Schwartz<sup>+</sup>, MD., PhD., Samuel J. Simmens<sup>++</sup>, PhD, Patricia E. Berg#, PhD.

\*Department of Gynecologic and Breast Pathology, Armed Forces Institute of Pathology, and  
#Department of Biochemistry and Molecular Biology, <sup>+</sup>Department of Pathology, and  
<sup>++</sup>Epidemiology and Biostatistics, The George Washington University Medical Center, Washington DC.

Address of corresponding author:

Patricia E. Berg, Ph.D.

Department of Biochemistry and Molecular Biology

George Washington University Medical Center

2300 Eye Street, NW

Washington DC 20037

USA

Tel: 202-994-2810; Fax: 202-994-8974

The opinions and assertions contained herein represent the personal views of the authors and are not to be construed as official or as representing the views of the Department of the Army or the Department of Defense.

## Abstract

The BP1 gene is a member of the homeobox gene superfamily of transcription factors that are essential for early development. Our recent studies revealed that the human homeobox gene BP1 mRNA is expressed in 80% of breast infiltrating ductal carcinoma (IDC). This study attempted to elucidate the immunohistochemical profile of BP1, to determine (1) whether the expression of BP1 protein correlated with breast tumor progression and invasion; (2) whether BP1 was co-localized with c-erb-B2, a well-defined onco-protein. Paraffin sections from normal reduction mammoplasties (n=34) and a variety of *in situ* and invasive mammary tumors (n=270) were immunostained with a polyclonal antibody to BP1, and double immunostained for BP1 and c-erb-B2 or Ki-67. The number of BP1 positive cells and the intensity of BP1 immunoreactivity linearly increased with the advance of the hypothetical tumor stages, normal→ hyperplasia→ *in situ*→ invasive. In cases with co-existing normal, hyperplasia, *in situ*, and invasive lesions, the invasive lesions consistently showed the highest number of BP1 positive cells and highest intensity of BP1 immunostaining, followed by *in situ* tumor cells. Double immunostaining revealed that BP1 was co-localized with c-erb-B2 in all c-erb B2 positive *in situ* and invasive tumor cells examined, and that BP1 positive cells had a substantially higher proliferation rate than their morphologically similar counterparts without BP1 expression. Together, these findings suggest that BP1 is an important upstream factor in an oncogenic pathway, and that expression of BP1 may reliably reflect or directly contribute to tumor progression and/or invasion.

## Introduction

BP1 is a member of the homeobox gene superfamily of transcription factors that are essential for early development. Our recent studies, however, revealed that BP1 mRNA was detectable in 80% of breast infiltrating ductal carcinoma (IDC), whereas it was undetectable in 5 of 6 matched normal controls, as measured by RT-PCR (1). Our studies also revealed that BP1 expression was significantly higher in estrogen receptor (ER) negative than in ER positive breast tumors, 100% versus 73% ( $p = 0.03$ ), and in African Americans than in Caucasians, 89% versus 57% ( $p = 0.04$ ) (1).

The exclusive or preferential expression of BP1 in IDC, in ER negative tumors, and in African American women, if confirmed on a larger scale, could have a number of scientific and clinical implications. First, as has been well documented, ER negative tumors have a significantly more aggressive clinical behavior and worse prognosis, compared to ER positive tumors (2-4), the expression of BP1 may reliably reflect or directly contribute to the aggressiveness of those breast tumors. Consequently, the development of therapeutic approaches to specifically manipulate BP1 expression might provide a more effective treatment option for ER negative tumors. Second, our previous studies in leukemia have revealed that BP1 has oncogenic properties, including as a modulator of cell survival (5 and unpublished data), suggesting that the high percentage (80%) of BP1 expression in IDC might also correlate with breast tumor invasion. The development of invasive breast cancers is believed to result from a progressive, multistep process that is initiated by the sequential dysregulation of specific biomolecules (6-7). The elucidation of the immunohistochemical profile and kinetics of BP1 expression during different stages of tumor progression may indicate whether BP1 is one of those biomolecules. This, in turn, could facilitate the early detection of breast tumor invasion.

Third, the significantly higher frequency of BP1 expression in the tumors of African American than in Caucasian women suggests that the development and progression of breast tumors among different genetic cohorts might be initiated and regulated by different molecular and/or biochemical mechanisms.

Based on these observations, the goal of this study is to elucidate the immunohistochemical profile of BP1 expression in order to determine whether the expression of BP1 protein correlates with breast tumor progression and/or invasion. In addition, as our previous studies have suggested that BP1 possesses oncogenic properties (5), this study attempted to assess whether BP1 is co-localized with c-erb-B2, a well-defined onco-protein with known functions (10-11).

## **Materials and Methods**

Formalin-fixed, paraffin-embedded human breast tissues from reduction mammoplasties (n=34) of individuals with no family history of breast cancer, no mammographic and histological breast abnormalities, and from patients with a wide variety of *in situ* and invasive breast lesions (n=270) were retrieved from the files of The Armed Forces Institute of Pathology. Consecutive sections at 4-5  $\mu$ m thickness were made and placed on positively charged microscopic slides. The first and last sections from each case were stained with hematoxylin and eosin for morphological classification, based on our published criteria (12).

A polyclonal antibody against the BP1 peptide was made from rabbit (Research Genetics, Huntsville, AL). The biotinylated secondary antibody, ABC detection kits (avidin-proxidase and Avidin-alkaline-phosphatase), diaminobenzidine (DAB) chromogen kit, and normal serum

were purchased from Vector (Burlingame, CA, USA). The AP-red chromogen kit was obtained from Zymed (San Francisco, CA, USA). A background block solution was from Cell Marque (Hot Springs, AR, USA). The antigen retrieval solution and Tris-buffered saline (TBS) were purchased from Biocare Medical, LLC (Walnut Creek, CA, CA).

Before application to experimental cases, several methods were used to verify the specificity and sensitivity of the BP1 antibody. First, the BP1 antibody was pre-absorbed with the BP1 peptide at different concentrations before incubation with the sections. Second, the BP1 antibody was diluted to different concentrations and incubated with consecutive sections from multiple types of breast tumors, and from tissue culture cells with different levels of BP1 expression. Third, the primary antibody was substituted with PBS or normal serum, or the secondary antibody was omitted from the immunostaining sequence. Also, several technical approaches, including treating the tissue sections with different antigen unmasking protocols, incubating the sections with the primary antibody at different temperatures, and elucidating the antigen-antibody complex with different detection systems, were used to identify the optimal immunostaining condition. After a series of pre-tests, a pre-treatment at 80 °C for two hours, an overnight incubation of the primary antibody at 4 °C, and elucidation of the antigen and antibody complex with avidin-alkaline phosphatase were found to yield the best results. This approach was subsequently used for BP1 immunostaining of the tissue sections. The intensity of BP1 immunostaining, scored according to routine guidelines (15-16), linearly increased with the increase of the BP1 antibody concentration.

Ducts and acini lined by  $\geq 40$  epithelial cells were examined for BP1 expression. A given cell was considered BP1 positive if distinct chromogen coloration was consistently seen in its cytoplasm or nucleus in at least two duplicates of the same immunostaining procedure. A

given case was considered BP1 positive if over 5% of its entire cell population showed distinct BP1 immunoreactivity. The intensity of BP1 immunostaining was scored according to the routine guideline (12).

To assess the possibility that the level of BP1 expression might increase with advance of the hypothesized tumor stages (normal→ hyperplasia→ *in situ* tumor→ invasive tumor), two approaches were used. First, the BP1 expression status (the percentage of positive cases, the number of positive cells, and the intensity of the immunostaining) among cases at each stage was statistically compared. Second, in cases with co-existing normal, hyperplasia, *in situ*, and invasive lesions, the expression status in each histologic component was statistically compared. :

To assess the pattern of BP1 expression among cancer subtypes, the BP1 positive cell number and intensity among common and several uncommon histologic subtypes, including pregnancy-associated, bilateral, apocrine and male (the cells of which are regulated mainly by androgen) breast cancers were compared. To assess the potential co-localization of BP1 and c-erb B2 (Vector, Burlingame, CA, USA), a set of three consecutive sections from each of 15 previously identified c-erb B2 positive cases were immunostained for BP1 and c-erb-B2, and double immunostained for BP1 plus c-erb B2, respectively, using our published protocols (13-14). To assess the potential correlation between BP1 expression and cell proliferation, sections from morphologically similar lesions with and without BP1 expression were double immunostained for BP1 and Ki-67.

## Results

To assess the possibility that the level of BP1 expression might increase with advance of the tumor stages, several approaches were used. First, the percentages of BP1 positive cases among normal (n=34), hyperplasia (n=70), *in situ* (n=100) and invasive (n=100) were statistically compared. Among the normal reduction mammoplasties, 30 (88.2%) were completely devoid of BP1 immunostaining, and 4 (11.8%) contained BP1 positive cell clusters (Fig 1), which accounted for about 1-3% of the total cell population (Table 1A), and consequently were regarded as BP1 negative. Among 70 hyperplastic lesions, 15 (21.4%) were BP1 positive. Of the 100 *in situ* breast tumors, including cribriform, papillary, male, apocrine, and pregnancy-associated (n=20 for each type), 46 (46%) were BP1 positive. We examined 100 invasive tumors, including ductal (n=91) and lobular (n=9) types; 81 (81%) were BP1 positive. There was a significant increase in the number of BP1 positive cases as histological types became more aggressive ( $p < .0001$ ).

In each histological type, ducts and acini were examined for BP1 expression. Fifteen cases with a large number of morphologically distinct ducts or invasive foci lined by  $\geq 40$  epithelial cells were selected from each stage, and the BP1 expression status was examined in each. A given cell was considered BP1 positive if distinct chromogen coloration was consistently seen in its cytoplasm or nucleus in at least two duplicates of the same immunostaining procedure. A duct or invasive focus was considered BP1 positive if multiple (at least 4-5) BP1 immuno-reactive cells were seen in a given structure.

Of 193 ducts analyzed in normal reduction mammoplasties, 17 (8.9%) were BP1 positive (Table 1B). In hyperplasia, 67 of 374 ducts (17.9%) were BP1 positive. In those cases, BP1 positive ducts were frequently distributed as clusters with a defined boundary with the adjacent

BP1 negative ducts (Fig 5). In *in situ* tumors, 325 ducts were assessed; 101 (31%) were BP1 positive. BP1 positive *in situ* tumor cells were generally basally located, often with some BP1 negative cells near the ductal lumen (Fig 6). Of 121 invasive foci analyzed, 95 (78.5%) were BP1 positive. Thus the number of BP1 positive ducts also increased with tumor aggressiveness ( $p < .0001$ ).

The frequency of BP1 positivity was also examined in 82 cases with co-existing normal, hyperplasia, *in situ*, and invasive components. The frequencies of BP1 expression were 18.3%, 32.9%, 47.5%, and 82.9%, respectively ( $p < .0001$ ) (Table 1C).

The potential co-localization of BP1 and c-erb-B2 was examined using a set of three consecutive sections from each of 15 previously identified c-erb-B2 positive cases. Immunostaining for BP1 and c-erb-B2, and double immunostaining for BP1 plus c-erb-B2, respectively, was performed using our published protocols (13-14). Double immunostaining revealed that BP1 was co-localized with c-erb-B2 in a subset of the tumor cells in each of the 15 c-erb-B2 positive tumors, and that the number of cells with co-localized BP1 and c-erb-B2 increased with the progression from an *in situ* to invasive status (Fig 9). BP1 was also co-localized with c-erb-B2 in clusters of normal and hyperplastic appearing cells in two cases (Fig 10). BP1 positive cells, however, were far greater in number than c-erb-B2 cells (Fig 11).

To measure the rate of cell proliferation, sections from 20 morphologically similar *in situ* and invasive tumors with ( $n=10$ ) and without ( $n=10$ ) BP1 expression were double immunostained for Ki-67 and BP1. The cell proliferation rate in 3-5 morphologically similar ducts from each case was calculated, and the rates among cases in each category were averaged and statistically compared. Ductal cells with BP1 expression had a significantly higher rate of cell proliferation, 3.4% versus 7.2% ( $p < .0001$ ) (Table 1D).



To assess the pattern of BP1 expression among cancer subtypes, the BP1 positive cell number and intensity among common and several uncommon histologic subtypes, including pregnancy-associated, bilateral, apocrine and male (the cells of which are regulated mainly by androgen) breast cancers were compared, as mentioned above. Of particular interest was the observation that myoepithelial cells were BP1 positive in pregnancy-associated breast cancer, in contrast to non-pregnancy associated breast cancer, where the epithelial cells were BP1 positive. The reason for this difference in localization is unknown.

### Discussion

Our current study reveals that expression of BP1 protein linearly increases with the advance of the hypothetical tumor stages (normal→ hyperplasia→ *in situ*→ invasive), from a few randomly distributed BP1 positive cell clusters in normal controls to the vast majority of cells in 83% of the invasive tumors showing distinct BP1 immunoreactivity. Compared to normal, hyperplastic, and *in situ* lesions, invasive lesions also consistently showed the highest number of BP1 positive cells, and the highest intensity of BP1 immuno-reactivity (Fig 7). This was even more apparent in cases with co-existing normal, hyperplastic, *in situ*, and invasive components (Fig 8).

In the majority of cases, distinct BP1 immunoreactivity was preferentially present in the epithelial cells, and was occasionally observed in myoepithelial cells and leukocytes. A vast majority of the stromal elements, including fibroblasts, leukocytes, and smooth muscle cells were devoid of BP1 expression (Fig 1).

Double immunostaining revealed that BP1 is co-localized with c-erb-B2 in a subset of the tumor cells in each of 15 c-erb-B2 positive tumors, and that the number of cells with co-localized

BP1 and c-erb-B2 increases with the progression from an *in situ* to invasive status. BP1 maps near erb B2, and we speculate they may be co-amplified (Fu et al, NAR). Future studies will examine whether there is a direct relationship between expression of these two genes.

Not only is BP1 aberrantly expressed in breast tumors, it is also expressed in 63% of the bone marrows (BM) of acute myeloid leukemia (AML) patients, including 81% of pediatric and 47% of adult patients, as well as in 32% of pediatric T-cell acute lymphocytic leukemia patients. In contrast, BP1 mRNA is barely if at all detectable in normal BM and PHA-stimulated T cells.

Together, our current and past findings suggest that BP1 may be an important upstream factor in an oncogenic pathway. While the specific role(s) of BP1 in breast tumor development and progression has not been defined, it appears to be specifically involved in blocking the normal process of the programmed cell death (apoptosis), facilitating the formation and expansion of a biologically more aggressive cell clone, since: (i) Our previous studies have shown that ectopic expression of BP1 in the leukemia cell line K562 substantially increased the clonogenicity (5), suggesting that BP1 is capable of sustaining or facilitating a deregulated cell proliferation, which has been regarded as a direct cause of malignancy (17-18). (ii) Abrogation of BP1 expression in K562 cells causes apoptosis (unpublished data). (iii) Breast cancer cells expressing BP1 have a significantly higher cell proliferation rate, compared to their morphologically comparable counterparts without BP1 expression (see Fig 12). (iv) BP1 positive cells are generally distributed as distinct clusters or foci with a well-defined boundary to adjacent BP1 negative cell clusters, or even as a well-defined ductal segment that is connected to BP1 negative cells at its both ends (see Fig 3), consistent with the typical feature of a clonal proliferation and expansion (19).

The preferential cytoplasmic localization of BP1 was at first unexpected since BP1 can act as a transcription factor. However, it is known that homeotic proteins can be transported to the cytoplasm and secreted, then taken up by other cells (xx). This would be a new role for BP1, one with important implications if true.

BP1 expression frequency and pattern among different cancer subtypes are very similar. Even in male and apocrine breast carcinomas, whose cells are regulated mainly by androgen, the frequency of BP1 expression and distribution of BP1 positive cells are not noticeably different from those of other cancer subtypes. It has been noted, however, that distinct BP1 expression is detectable in a subset of myoepithelial cells exclusively or preferentially associated with pregnancy-associated breast carcinomas. This finding is of interest, as it suggests that BP1 expression is inducible, and BP1 may be detectable in other tumor types. This possibility is under investigation.

The biological effects of BP1 expression in tumors are under investigation. Our previous studies have shown that BP1 over-expression correlates with the activation of cyclin D1 (xx), a cell proliferation-related protein encoded by a proto-oncogene, PRAD-1/cyclin D1 (22-23). Dysregulation of cyclin D1 occurs in about 50% of breast tumors; about 20% are due to amplification, and the rest are of unknown causes (xx). In addition, BP1 may regulate, directly or indirectly, genes involved in other pathways. In particular, we have evidence that BP1 expression confers anti-apoptotic properties on MCF7 cells when challenged with  $\text{TNF}\alpha$ , an apoptotic-inducing agent. Separately or collectively, these events could confer a growth advantage and the ability to escape apoptosis on a cell population, which not only would facilitate the formation of a biologically more aggressive cell clone and expansion by clonal proliferation, but also could promote progression from one stage to the other. On the other

hand, the deprivation of BP1 might be able to stop or reverse these processes. Thus, BP1 expression may serve as a marker for early detection of breast cancer, while the manipulation of BP1 expression may have significant value in its treatment.

### Acknowledgments

Supported by in part by DOD grants DAMD17-01-1-0129 and DAMD17-01-1-0130 (YGM), NIH grant CA91149 (PEB) and a grant from the Susan B. Komen Foundation (PEB).

### References

1. Fu SW, Schwartz A, Stevenson H, Pinzone JJ, Davenport GJ, Orenstein JM, Gutierrez P, Simmens SJ, Abraham J, Poola I, Stephan DA, Berg PE. Correlation of expression of BP1, a homeobox gene, with estrogen receptor status in breast cancer. *Breast Cancer Res*. 2003; 5:R82-87
2. Schmitt FC: Multistep progression from an oestrogen-dependent growth towards an autonomous growth in breast carcinogenesis. *Eur J Cancer* 1995, 31A: 2049-2052.
3. Clarke R, Brunner N, Katzenellenbogen BS: Progression of human breast cancer cells from hormone-dependent to hormone-independent growth both in vitro and in vivo. *Proc. Natl Acad Sci USA* 1989, 86:3649-3653.
4. Sheikh MS, Garcia M, Pujol P, Fontana JA, Rochefort H: Why are estrogen receptor negative breast cancers more aggressive than the estrogen receptor positive breast cancers ? *Invasion Metastasis* 1994-95,14:329-336.
5. Haga SB, Fu S, Karp JE, Ross DD, Williams DM, Hankins WD, Behm F, Ruscetti FW, Chang M, Smith BD, Becton D, Raimondi SC, Berg PE. BP1, a new homeobox gene, is frequently expressed in acute leukemias. *Leukemia* 2000; 14: 1867-1875
6. Schedin P, Elias A. Multistep tumorigenesis and the microenvironment. *Breast Cancer Res* 2004; 6: 93-101
7. Takami K, Yana I, Kurahashi H, Nishisho I. Multistep carcinogenesis in colorectal cancers. *Southeast Asian J Trop Med Public Health* 1995; 26(supplement 1): 190-196

8. Man YG, Martinez A, Avis IM, Hong SH, Cuttitta F, Venzon DJ, Mulshine JL. Phenotypically different respiratory epithelial cells with hnRNP A2/B1 over-expression display similar genetic alterations. *Am J Respir Cell Mol Biol* 2000; 23:636-645
9. Mayeda A, Munroe SH, Caceres JF, Krainer AR. Function of conserved domains hnRNA A1 and other hnRNP A/B proteins. *EMBO J* 1994; 13: 5483-5495
10. Bezwoda WR. C-erb-B2 expression and response to treatment in metastatic breast cancer. *Mod Oncol* 2000, 17: 22-28
11. Kaptain S, Tan LK, Chen B. Her-2/neu and breast cancer. *Diagn Mol Pathol* 2001; 10: 139-152
12. Tavassoli FA, Man YG. Morphofunctional features of intraductal hyperplasia, atypical hyperplasia, and various grades of intraductal carcinoma. *The Breast J* 1995; 1:155-162.
13. Man YG, Ball WD, Culp AJ, Hand AR, Moreira JE. Persistence of a perinatal cellular phenotype in the ducts of adult glands. *J Histochem Cytochem* 1995; 43(12):1203-1215
14. Man YG, Tavassoli FA. A simple epitope retrieval method without the use of microwave oven or enzyme digestion. *Appl Immunohistochem* 1996; 4(2):139-141
15. Tsuda H, Sasano H, Akiyama F, Kurosumi M, Hasegawa T, Osamura RY, Sakamoto G. Evaluation of interobserver agreement in scoring immunohistochemical results of HER-2/neu (c-erb B-2) expression detected by Hercep Test, Nichirei Polyclonal antibody CB11 and TAB250 in breast carcinoma. *Pathol Int* 2002; 52: 126-134
16. Birner P, Oberhuber G, Stani J, et al. Evaluation of the United States Food and Drug Administration approved scoring and test system of HER-2 protein expression in breast cancer. *Clin Cancer Res* 1001; 7: 1669-1675
17. Pan H, Yin C, Van Dyke T. Apoptosis and cancer mechanism. *Cancer Surv* 1997; 29:305-327
18. Pierce GB, Speers WC. Tumors as caricatures of the process of tissue renewal: prospects for therapy by directing differentiation. *Cancer Res* 1996; 48:1990-2004.
19. Man YG, Ball WD, Marchetti L, Hand AR. Contributions of intercalated duct cells to normal parenchyma of submandibular glands of adult rats. *Anat Rec* 2001; 263:202-214.
20. Linke SP, Sengupta S, Khabie N, Jeffries BA, Buchhop S, Mista S, Henning W, Pedoux R, Wang XW, Hofseth LJ, Yang Q, Garfield SH, Sturzbecher HW, Harris CC. P53 interacts with hRAD51 and hRAD54, and directly modulates homologous recombination. *Cancer Res* 63: 2596-2605
21. Subramanian D, Griffith JD. Interactions between p53, hMSH2-hMSH6 and HMG I(Y) on

Holloday junctions and bulged bases. *Nucleic Acids Res* 2002; 30: 2427-2434

22. Bartkova J, Lukas J, Strauss M, Bartek J. The PRAD-1/cyclin D1 oncogene product accumulates aberrantly in a subset of colorectal carcinomas. *Int J Cancer* 1994; 58: 568-573
23. Gillertt C, Fantl V, Smith R, Fisher C, Bartek J, Dickson C, et al. Amplification and overexpression of cyclin D1 in breast cancer detected by immunohistochemical staining. *Cancer Res* 1994; 54: 1812-1817.
24. Chase MB, Fu S, Haga SB, Davenport G, Stevenson H, Do K, Morgan D, Mah AL, Berg PE. BP1, a homeodomain-containing isoform of DLX4, represses the beta-globin gene. *Mol Cell Biol* 2002; 22: 2505-2514
25. Man YG, Berg PE, Strauss BL. Increasing BP1 expression correlates with progression and invasion of male breast and prostate tumors. *Cancer Detect Prev* 2004 Symposium Volume S149

**Table 1. Percentages of BP1 positive cases among normal and different breast lesions**

Histological Type	Numbers of Cases	BP1 Positive	P
Normal	34	0*	< 0.001
Hyperplasia	70	15 (21.4%)	
<i>In situ</i>	100	46 (46.0%)	
Invasive	100	81 (81.0%)	

\*4 (11.8%) contain BP1 (+) cell clusters, but only in 1-3% of the total cells.

**Table 2. Numbers of BP1 (+) ducts and foci among normal and different breast lesions**

Histological Type	Number of ducts & foci	BP1 positive (%)	P
Normal	193	17 (8.8%)	< 0.001
Hyperplasia	374	67 (17.9%)	
<i>In situ</i>	325	101 (31.1%)	
Invasive	121	95 (78.5%)	

### 3. BP1 expression in 82 cases with co-existing normal and different breast lesions

Tissue components	BP1 positive (%)	P
Normal	15 (18.3%)	< 0.001
Hyperplasia	27 (32.9%)	
<i>In situ</i>	38 (46.3%)	
Invasive	68 (82.9%)	

**Table 4. Cell proliferation rates in morphologically similar BP1 (+) and (-) cells**

Cell Type	Cells counted	Ki-67 positive (%)	P
BP1 positive	5,000	360 (7.2%)	< 0.001
BP1 negative	5,000	170 (3.4%)	